University of Southern Queensland
Faculty of Engineering and Surveying

# Analysis of Engine Performance using Palm Oil Methyl Ester

A dissertation submitted by

Cheah, Siew Lee

in fulfilment of the requirements of

**Courses ENG4111 and 4112 Research Project**

towards the degree of

**Bachelor of Engineering (Mechatronic)**

Submitted:28th October, 2004

# ABSTRACT

The project aims to investigate and simulate the palm oil methyl ester flow through the fuel injection system and the viscosity effect on the engine. The nozzle designs were simulated in 2-D and 3-D using FLUENT and the engine performance analyzed using Matlab. The validity of the simulation cannot be tested due to the lack of experimental facilities. The simulated results show that the best design for a nozzle is by using smaller holes size or nozzle with large *L/D* ratio where turbulent flow are well developed inside the nozzle. The best engine performance for palm oil methyl ester operates at the engine speed of 2000 rpm to 2500 rpm. The overall analysis has shown that palm oil methyl ester has potential as an alternative fuel in conventional combustion engine.

University of Southern Queensland

Faculty of Engineering and Surveying

# ENG4111 & ENG4112 *Research Project*

## Limitations of Use

The Council of the University of Southern Queensland, its Faculty of Engineering and Surveying, and the staff of the University of Southern Queensland, do not accept any responsibility for the truth, accuracy or completeness of material contained within or associated with this dissertation.

Persons using all or any part of this material do so at their own risk, and not at the risk of the Council of the University of Southern Queensland, its Faculty of Engineering and Surveying or the staff of the University of Southern Queensland.

This dissertation reports an educational exercise and has no purpose or validity beyond this exercise. The sole purpose of the course pair entitled "Research Project" is to contribute to the overall education within the student's chosen degree program. This document, the associated hardware, software, drawings, and other material set out in the associated appendices should not be used for any other purpose: if they are so used, it is entirely at the risk of the user.

**Prof G Baker**
Dean
Faculty of Engineering and Surveying

# Certification

I certify that ideas, designs and experimental work, results, analyses and conclusions set out in this dissertation are entirely my own effort, except where otherwise indicated and acknowledged.

I further certify that the work is original and has not been previously submitted for assessment in any other course or institution, except where specifically stated.

**Cheah, Siew Lee**

**Student Number: 0050012463**

_____

Signature
Date :28th October 2004

# DEDICATION

…to my mom, dad, family, Dr.Sai-Cheong Fok, Dr.Talal F. Yusaf, and friends…

# ACKNOWLEDGEMENT

First of all, I would like to express my sincere appreciation and gratitude to my project supervisors, Dr. Sai-Cheong Fok and Dr. Talal F.Yusaf for their valuable advice, guidance and willingness to share their expertise. Throughout this long period, they had given me best supports, which help a lot on my completion of the project.

Secondly, I wish to send my appreciation to Dr. Nigel Hancock, my final year project's examiner for his time to grade my thesis.

I would like to express my gratitude and sincere thanks to Mr. Chris Snook for allowing me to take this project. It has been part of my personal goal to get involve in a project that enables me to develop and analyze the performance of engine using palm oil methyl ester, a chance I never had previously.

I would like to mention the staff of Engineering Faculty, especially to Ms. Suhaila as she has given me hundreds of suggestions. Thanks to her.

I would also like to thank my friends and contacts in industry. Mr. Chew, a project engineer from GALVAN Automation Pte Ltd, has shared his views regarding the parameter on engine performance with me in hundreds of discussions. Mr. Adran from PETRONAS Sdn Bhd ,Mr. Vincent Chu, engineer from CSC Sdn. Bhd. and Mr. Edwin Chua, engineer from C.H Engineering who have shared their views regarding palm oil with me in hundreds of discussions.

They have discussed their field of expertise, allowing me to expand my horizons and keep on top of new developments.

Last but not least, I would like to thank all my friends, who have worked together with me, giving me moral support and ideas to complete my final year project .Without them, this project cannot be accomplished in a good manner and on time.

Regards,
CHEAH SIEW LEE
University of Southern Queensland,
Faculty of Engineering and Surveying
October 2004.

# TABLE OF CONTENTS

**CHAPTER 2**

**Literature Review**



**CHAPTER 3**

**Chemical and Physical Properties of fuel**



**CHAPTER 4**

**Engine Performance**

# LIST OF TABLES

# LIST OF FIGURES

# NOMENCLATURE

| | |
|---|---|
| $\theta$ | Crank angle |
| $\theta_b$ | Burn duration in degrees crank angle |
| $\theta_1$ | Crank angle at reference |
| $\theta_s$ | Crank angle for the start of combustion |
| $\mu$ | Viscosity |
| $\rho$ | Density (kg/m3) |
| $\Phi$ | Equivalence ratio |
| $\omega$ | Reference angle |
| A | Area of cylinder |
| bmep | Brake mean effective pressure |
| C | Blowby constant |
| $D_{iv}$ | Diameter of the inlets valves |
| F | Actual Fuel to Air ratio |
| f | Residual mass fraction |
| fmep | Frictional loss mean effective pressure |
| $F_s$ | Stoichiometric Fuel to Air ratio |
| h | Heat transfer coefficient |
| H | Chemical symbol for hydrogen |
| h | Heat transfer coefficient of the burnt gas |
| imep | Indicated mean effective pressure |
| $imep_c$ | Mean effective pressure associated with manifold losses |
| $K_p$ | Constant used to demonstrate an expression |
| m | Mass of gas |
| $n_c$ | Number of cylinders |
| $n_{iv}$ | Number of inlet valves per cylinder |
| P | Pressure in the cylinder |
| $p_a$ | Atmospheric pressure |
| $p_{e,g}$ | Pressure in the exhaust manifold |

$p_{i,g}$ Pressure in the inlet manifold

$P_m$ Motoring pressure

$P_{max}$ Maximum pressure in the cylinder

$P_r$ Reference pressure

$\dot{Q}$ Rate of heat transfer

$\dot{Q}_b$ Rate of heat transfer from the burnt gas

$\dot{Q}_s$ Rate of heat transfer through the surface of the cylinder

$\dot{Q}_u$ Rate of heat transfer from the unburnt gas

$R_{1,2,3}$ Constants used in the calculation of the NO formed

t Time

$T_s$ Temperature of the cylinder surface

$T_w$ Temperature of the cylinder wall

u Velocity component due to piston motion and pressure in the cylinder

u Specific internal energy

$u_b$ Specific internal energy of the burnt gas

$u_u$ Specific internal energy of the unburnt gas

U Total internal energy of the control volume

V Volume of the gas in the cylinder

$V_s$ Swept volume

$v_b$ Specific volume of the burnt gas

$v_p$ mean piston speed

$v_{1\text{-}14}$ Volumetric fraction of chemical elements

x Mass fraction burnt

$p_o$ Pressure, velocity, and area at section 1

$p_T, A_T$ Pressure, velocity and area at section 2 (throat)

$T_o$ Inlet temperature

$C_D$ Discharge coefficient of venturi

$m_{real}$ Mass flow rate of air

$d_o$ Orifice diameter

$n$ number of orifices

$\gamma$ Pressure ratio

$p_2$ Pressure at the tip of the gas inlet

$\rho f$ Density of POME

$V_f$ Velocity of the POME

$C_{Df}$ Discharge coefficient

$m_a$ Mass flow rate of air (kg/s)

$m_f$ Mass flow rate of fuel (kg/s)

$v_a$ Air intake velocity, m/s

$v_f$ POME intake velocity, m/s

$l_a$ Diameter of air intake, m

$l_f$ Diameter of POME intake, m

$n$ Number of holes

$\dot{m}$ Mass flow rate

$u_j$ $j^{th}$ Cartesian of the instantaneous velocity

$\rho$ Fluid density

ρ Static pressure

$\tau_{ij}$ Viscous stress tensor

$f_j$ Body force

| | |
|---|---|
| $\mu$ | Fluid dynamic viscosity |
| $\delta_{ij}$ | Kronecker deltas |
| $J_{ij}$ | Total diffusive mass flux for species ai |
| $h_i$ | Enthalpy for species ai |
| $S_a$ | Additional sources due to surface reaction, radiation, and liquid spray |
| $q_j$ | $j$ component of the heat flux |
| K | Thermal conductivity |
| H | Total enthalpy |
| $k$ | Von Karman's constant (= 0.419) |
| E | Empirical constant (= 9.81) |
| $M$ | Dynamic viscosity of the fluid |
| $y$ | Distance from point to the wall |
| u | Perturbation velocities about the mean velocities U |
| v | Perturbation velocities about the mean velocities V |
| w | Perturbation velocities about the mean velocities W |
| k | Dissipation rate of turbulent kinetic energy |
| D | Turbulent kinetic energy |
| $C_\mu$ | Constant, normally 0.09 |
| $L$ | Inlet height or diameter |
| $\dot{m}_{pq}$ | Mass transfer between primary phase $q$ and secondary phase $p$ |
| $\frac{\partial}{\partial t}$ | Material time derivative |
| $R$ | The bubble radius |

| | |
|---|---|
| $p_v$ | The pressure of vaporization |
| $\rho_q$ | The density of the liquid |
| $n$ | The number of bubbles per unit volume |
| $\psi$ | Specific gravity |
| $ip$ | Input Power |
| $Q_{net,v}$ | Lowe calorific value of fuel |
| τ | Torque |
| P | Load |
| N | Engine speed in RPM |
| $bp$ | Break Power |
| A | Area of Piston |
| L | Length of stroke |
| n | number of cylinders |
| $sfc$ | Specific fuel consumption |
| $\eta_{BT}$ | Break thermal efficiency |
| $bhp$ | Break Horse Power |
| $\Delta H_c$ | Heating of combustion |
| $H_f^\circ$ | Net enthalpy change |
| $h_f^\circ$ | Enthalpy formation |
| $\Delta h$ | Specific heat change |
| $M_{fuel}$ | Molecular weight of fuel |

# ABBREVIATIONS

| | |
|---|---|
| A/F | Air to Fuel Ratio |
| AFV | Alternative Fuel vehicle |
| BDC | Bottom Dead Centre |
| BTX | Xylene |
| C | Carbon |
| CDF | Conventional Diesel Fuel |
| CFD | Computational Fluid Dynamics |
| CO | Carbon Monoxide |
| $CO_2$ | Carbon Dioxide |
| CPO | Crude Palm Oil |
| H | Hydrogen |
| HC | Hydrocarbon |
| kW | Kilowatt |
| NO | Nitric Oxide |
| $NO_x$ | Nitrogen Oxide |
| $N_2$ | Nitrogen Gas |
| N | Nitrogen |
| O | Oxygen |
| PM | Particulate matters |
| POME | Palm Oil Methyl Ester |
| PORIM | Palm Oil Research Institute Malaysia |
| RPM | Revolution per Minute |

| | |
|---|---|
| S | Sulphur |
| $SO_2$ | Sodium Oxides |
| TDC | Top Dead Centre |
| THC | Total Hydrocarbon |
| TG | Triglyceride |

# CHAPTER 1

# INTRODUCTION

## 1.1 INTRODUCTION

Gasoline and diesel are considered as conventional fuel. Alternative fuel (AF) vehicle can be considered as any vehicle using non conventional fuel. In Malaysia, the research into AF has been carried out by many organizations such as PORIM and PETRONAS. One of the main AF studied is Palm Oil Methyl Esters (POME). This is because Malaysia has a large quantity of palm oil.

POMES produced by PORIM and PETRONAS have similar fuel properties as the petroleum diesel. Over the past few years, POME had been extensively tested as a diesel

substitute in a wide range of cabs, buses, and trucks. In these studies, it was found that POMES could affect the performances of the engines.

One of the factors that can affect engine performance using POMES involves the fuel injection system. The penetration of the POME spray into the compressed charge of air depends upon the following factors; the length of the nozzle orifice, the diameter of the orifice outlet, the nature of the fuel and the pressure of the fuel. To understand the engine performance, the modelling of nozzle in the fuel injection system is critical. In this project, Computational Fluid Dynamic (CFD) FLUENT software is used to investigate the flow behaviour of POME in the nozzle of fuel injector.

## 1.2 THE PRESENT WORK

### 1.2.1 Project background and Objectives

Fuel is injected into the combustion chamber of the engine through the nozzle of the fuel injection system. The penetration of the spray into the combustion chamber depends upon factors such as the length of the nozzle orifice, the diameter of the orifice outlet, the viscosity of the fuel and the pressure of the fuel. The design of the nozzle may ultimately affect the fuel flow behaviour and the engine performance.

The main objective of this project is to investigate the effect of the fuel injection system on the flow behaviour of POME. In this project, the Computational Fluid Dynamic (CFD) FLUENT software will be used. A 2-D CFD model will be developed using FLUENT to investigate the nozzle design and the effect of the viscosity of POME on the

flow behaviour. This will provide a clear picture of the swirl ratio and the degree of turbulence associated with POME. The associated heat and fuel performance will be calculated using a Matlab program. The result of the simulation study can be used to design better fuel injection system for the engine using POME as an AF.

### 1.2.2 Project Methodology

The first part concerns the familiarization with the material and organization. This involves literature reviews on the historical background of using palm oil as an alternative fuel in Malaysia and CFD simulation.

The second part of the study is to compare the chemical and physical properties of palm oil methyl ester and conventional diesel fuel. This is achieved through gathered data. The third part contains the theoretical study and calculation of fuel performance. The calculation will be performed using Matlab. A 2-D CFD simulation model will be developed through GAMBIT and analyse through FLUENT. Different types of nozzle design will be developed in 3-D using GAMBIT. The Matlab program and CFD simulation will be done concurrently.

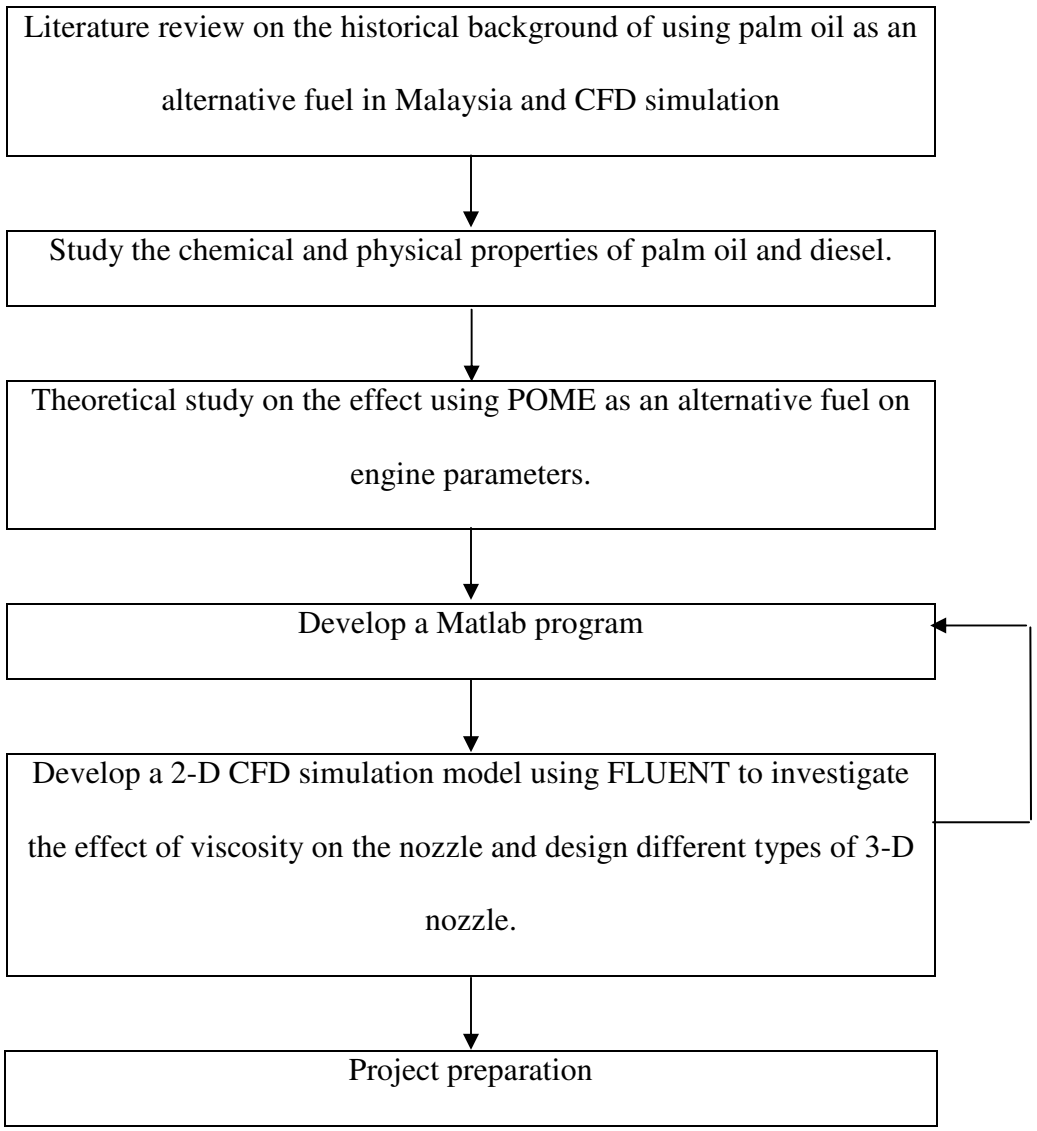


Figure 1.1 Project Methodology Flowchart

## 1.2 OUTLINE OF THE REPORT

Chapter 1 introduces the project description, objective and methodology. This chapter gives an overview of the project. Chapter 2 stresses on the historical background of palm oil and CFD simulation. Chapter 3 studies the chemical and physical properties of palm oil, and diesel. This will help to study the comparison between different fuels. The theoretical study on the effect of using palm oil as an alternative fuel on engine parameters will be discussed in chapter 4. This theoretical study will lead to the design of fuel injector in chapter 6. CFD software is summarized in chapter 5. The analysis on the simulation of CFD and Matlab is discussed in chapter 7 and project is concluded in chapter 8.

# CHAPTER 2

# LIRERATURE REVIEWS

## 2.1 INTRODUCTION

The oil palm, or ***Elaeis guineensis***, originated in West Africa and was introduced to Malaysia in about 1870 as an ornamental plant. The current crop in Malaysia is a cross of the *dura and pisifera* varieties known as *tenera*, all belonging to the *E. guineensis* species. By 1917, it was being cultivated on a commercial scale. Currently, palm oil tree production occurs on about three million hectares (Mha), which is well over one-third of Malaysia's total cultivated area (M.A Faud, A.R.Rohana & B.G. Chua 1997,p.125).

Palm oil is one of the seventeen major oils and fats produced and traded in the world today. In Malaysia, oil palm is the ‘golden crop’. There is great confidence that it will

continue contributing significantly to the increase in the global oils and fats trade. In the meantime, the Malaysian palm oil statistics remain impressive.

Malaysia's crude palm oil (CPO) production is forecasted to range between 13.5 million and 13.6 million tonnes in 2004, slightly above 2003 output of 13.4 million tonnes (The Star 28 July. 2004 , p.10). The production of crude palm oil (CPO) in 2003 increased by about 12.1%, from 1.4 million tonnes to 13.35 million tonnes compared with 11.91 million tonnes in 2002. Exports of palm oil have increased by 12.5% or 1.36 million tonnes to 12.25 million tonnes from 10.89 tonnes in 2002.

The increase was due to the expansion in matured planted area, weather conditions, constant sunshine, and rainfall distribution throughout the year. The fresh fruit bunches yield per hectare increased by 5.7% to 18.99 tonnes from 17.97 tonnes. However, the oil extraction rate fell by 0.8%.

The increase in total export value was impressive, soaring by RM6.50 billion to RM26.15 billion compared to RM19.64 billion in 2002. The end of the year stock level of palm oil was 2.5% higher .The average CPO price increased by RM181 to RM1, 544 as compared to 2002. Table 2.1 gives the summary of the performance of Malaysian Palm Oil Industry.

Table 2.1 Performance of Malaysian Palm Oil Industry (*MPOB 2003*)

| | 2002 | 2003 | Diff (%) |
|---|---|---|---|
| Planting (Hectares)Area | 3,670,243 | 3,790,636 | 3.3 |
| Production (Tonnes) | 11,909,298 | 13,354,769 | 12.1 |
| Exports(Tonnes) | 10,886,259 | 12,248,303 | 12.5 |
| Closing stocks(Tonnes) | 1,136,444 | 1,165,109 | 2.5 |
| Imports(Tonnes) | 402,507 | 460,633 | 14.4 |
| Export Revenue (RM Million) | 15,002.0 | 19,854.1 | 32.3 |
| Total Revenue (RM Million) | 19,644.5 | 26,148.0 | 33.1 |
| Prices (RM/Tonne) | 1,363.50 | 1,544.00 | 13.2 |
| Oil Extraction Rate (%) | 19.91 | 19.75 | -0.8 |
| Fresh Fruit Bunches Yields (Tonnes/Hectare) | 17.97 | 18.99 | 5.7 |

### 2.1.1 Palm oil fuel research

Malaysia is trying to introduce palm oil as an alternative to diesel. This is because the country is the world leader in the production of palm oils. It is also the largest exporter of edible oils. Malaysia was the first, to use palm oil as fuel in vehicles in a field trial programme in 1983 .The results was promising and lead to more experimental work. Research on the use of palm oil as a diesel fuel alternative had been conducted at PORIM (the Palm Oil Research Institute of Malaysia), the University of Technology Malaysia (UTM), the University of Malaya (UM) , PROTON (National Automobile Industry of Malaysia) and Castrol Malaysia Sdn. Bhd.

Palm oil fuel was obtained by blending with other oil fuels in Thailand. In 1982, the Primary Energy Investigation Unit of the James Cook University, Queensland, Australia

carried out work on the thermal efficiency of palm oil and its product as a ignition fuel in engine. At the same time, an investigation was done on palm oil fuel at the National Chemical Laboratories for Industries; Japan.

There is cooperation between the University of Surrey and University of Technology Malaysia (UTM) to investigate the performance, emission, and carbon deposits in stationary diesel engines. Various studies on combustion parameters such as spray characteristics and the ignition delay of palm oil fuel has been carried out in the University of Leeds (S.M Sapuan , H.H. Masjuki & A.Azlan 1996,p.48).

### 2.1.2 Development of Biodiesel

Malaysia currently accounts for 51 % of world palm oil production and 62% of world exports, and therefore also for 8% and 22% of the worlds total production and exports of oils and fats. Malaysia produced approximately 12.4 million tonnes of palm oil in 2003 (*The Malaysian Palm Oil Promotion Council (MPOPC) 2003*).

Since the oil crisis in 1970's, there was an effort in seeking a new substitute for fuel. In addition, environmentally aware consumers are also concerned with the emission from vehicles using conventional diesel oil. As the biggest producer and exporter of palm oil and palm oil products, Malaysia has an important role to play in fulfilling the growing global need and innovative usage of oils and fats in general.

### 2.1.3 Environmental, Economical, Social, and Political Considerations

It is envisaged that POME could be used as an energy source for transportation. This is one of the highest energy consumption sectors in Malaysia. Transportation is also a major contributor to air pollution. The major environment pollution from transportation systems is caused by the emission from the exhaust of diesel engine. The conventional diesel fuel used in the diesel engine contains a higher amount of particulate matters (PM) and harmful gases such as Nitric Oxide (NO), Nitrogen Oxide ($NO_x$), Nitrogen Gas ($N_2$), Sodium Oxides ($SO_2$) etc. These gases are the main causes of greenhouse effect and acid rains. It is partly the resolute to reduce air pollution that has encouraged intensified search for alternative sources of energy that are both renewable and environment friendly.

POME has been identified as a potential source of energy that can substitute diesel. It has been tested in wide range of vehicles and the result was promising. POME has low sulphur content and almost biological decomposable. The combustion of POME leads to a near balanced $CO_2$ cycle and a favourable reduction in greenhouse effects. It is due to these characteristics that PORIM has listed palm oil as an available and important alternative fuel. This is a truly benign fuel substitute especially for diesel engine.

Since the 1970s, Malaysia's economy has gone through a major transformation. From one based mainly on exporting palm oil, it has evolved into one of the most diversified economies in Southeast Asia. The economics of POME very much depend on world prices of palm oil, methanol, glycerol and crude petroleum oil (or diesel). In the early

nineties, the unfavourable economics have inhibited development work of palm oil as diesel substitutes (Masjuki & Bharuddin 1993, p.108). There is the prediction that the cost of palm oil will decrease due to the current excess on the market. The future cost of producing palm oil for fuel within developing countries will depend on local factors such as land and the cost of labour (S.M Sapuan , H.H. Masjuki & A.Azlan 1996,p.51).

The cost of palm oil production could be offset by the profit if palm oil can make a marginal contribution as an alternative additive fuel. With the depletion of global fuel reserves, POME will contribute future wealth to the nation. Nevertheless, due to the current excess of palm oil in the market, there will be fluctuation of world market price. This makes it difficult to assess the economic viability and availability of palm oil compared to CDF (Schafer 1995,p.75).

Economic comparisons of palm oil and mineral oil are very difficult to make as it varies from country to country. Picken et al (1986) had outlined the factors that affect the cost, which include:

(a) Local cost of mineral oil and refining cost per litre;

(b) Annual cost of a unit area of land for cultivation;

(c) Fuel used in cultivation and harvesting of land per unit area;

(d) Fuel used as fertilizer on land per unit area;

(e) Labour cost in cultivation of unit area;

(f) Cost of processing vegetable oil per litre;

(g) Transport and distribution costs per litre;

(h) Diesel oil equivalent of oil produced per unit area;

(i) Taxation system;

(j) And value of residue after oil extraction per unit area

Besides economical consideration, one of the social advantages of using palm oil as a fuel in Malaysia is that the local community can largely control the fuel price and supply. In Malaysia, the supply of petroleum-based fuels depended mainly on external factors (Lowry et al 1990,p.97) and this could be undesirable. This is because the locals have the view that if the costs of palm oil and petroleum fuel are similar, they would prefer to spend the money within the community to promote local employment rather than on foreign imports (S.M Sapuan , H.H. Masjuki & A.Azlan 1996,p.51). Furthermore, urban air pollution has become a politically sensitive issue; substitution of POME for diesel fuel in the transportation sector can have a substantial impact on lowering smog-forming emissions.

The flow effects of the fuel in the injection system can influence the efficiency of POME in automobiles. The flow of POME through the fuel injector is important because of the effects on the spray and the atomization process can decisively affect the economical use of the fuel. In an effort to minimize fuel costs, increase reliability**,** and obtain environmental and social benefits, there is a need to examine the types of nozzle design and their effects on the performance of the engine.

## 2.2 PALM OIL METHYL ESTER (POME)

### 2.2.1 POME as an additive to CDF

Malaysia produces about 13.6million tonnes of palm oil in 2004(The Star 28 July. 2004, p.10). This is one of the reasons why PORIM investigates the effects of POME on engines. The results of these studies indicated that the adoption of the emulsification approach between CDF and POME could produce viscosity and surface tension reduction, which yielded better combustion of fuel.

POME as CDF substitute is well acceptable as the two have similar characteristics. POME has advantages over CDF in several aspects, including environmental friendly, technically and economically feasibility. Table 2.2 gives the typical composition of CDF.

Table 2.2 Percentages Composition of Conventional Diesel Fuel (Heywood 1988,p.74)

| Element | Composition (%) |
|---|---|
| Carbon ,C | 83.0 – 87.0 |
| Hydrogen, H | 10.0 – 14.0 |
| Nitrogen, N | 0.1 – 2.0 |
| Oxygen, O | 0.05 – 1.50 |
| Sulphur, S | 0.05 – 6.00 |

## 2.3 CFD ON NOZZLE

A thorough understanding of the dynamics of flow is important in the future development of engine with high-performance. Modelling nozzle flow is complicated; this investigation will use two-dimensional and three-dimensional models of nozzle flow to observe the effects of nozzle parameters.

The flow characteristics of the injected fuel at the nozzle are crucial. Viscosity of POME is the most significant of all liquid properties in the design because it can vary over an extreme range. Liquid viscosity resists surface formation. The nozzle may produce a mass of filaments if the viscosity is great enough; liquid viscosity is extremely sensitive to temperature and is a major effect on the spray characteristics.

The design and the flow characteristics will be analysed through CFD to predict the transfer of heat, chemical reaction, and fluid flow behaviour etc. CFD is based on the fundamental governing equations of fluid dynamics - the continuity, momentum and energy equation. It is a powerful tool to carry out numerical experiment. This project uses the Computational Fluid Dynamic software – FLUENT.

### 2.3.1 General Considerations of Nozzles

Fuel injector nozzles play an important role in the delivery and atomization of fuel in diesel engines. Nozzles are very small and the fuel flow is very fast, making experimental observation very difficult. The internal flow through diesel fuel injector nozzles is very

important for reducing emissions, although the nature of the connection between the injector and emissions appears to be quite complicated (Montgomery [1]).

The typical nozzle is roughly 0.2 mm diameter and the fluid is moving at several hundred meters per second making experimental measurements of the flow difficult. Studying real fuel injectors is also difficult because the nozzle geometry is often some variant of the plain orifice. This problem can be overcome with CFD by using a variety of geometries to make some practical observations. The results could further our understanding of fuel injector flow.

The penetration of the spray into the compressed charge of air depends on the following factors; the length of the nozzle orifice, the diameter of the orifice outlet, the nature of the fuel and the pressure of the fuel. The best atomizing results appear to be obtained by decreasing the ratio of the orifice length to its diameter (Arthur W.Judge 1967,p.1021). This means that the higher the pressure of fuel, the better will be the atomization effect. Other design aspects that have to be taken into account include the impact region extension (*De*), cone angle (*CL*) and flow stabiliser (*L*) and exit orifice (*d*). Figure 2.1 shows the nozzle geometry depicting these considerations.

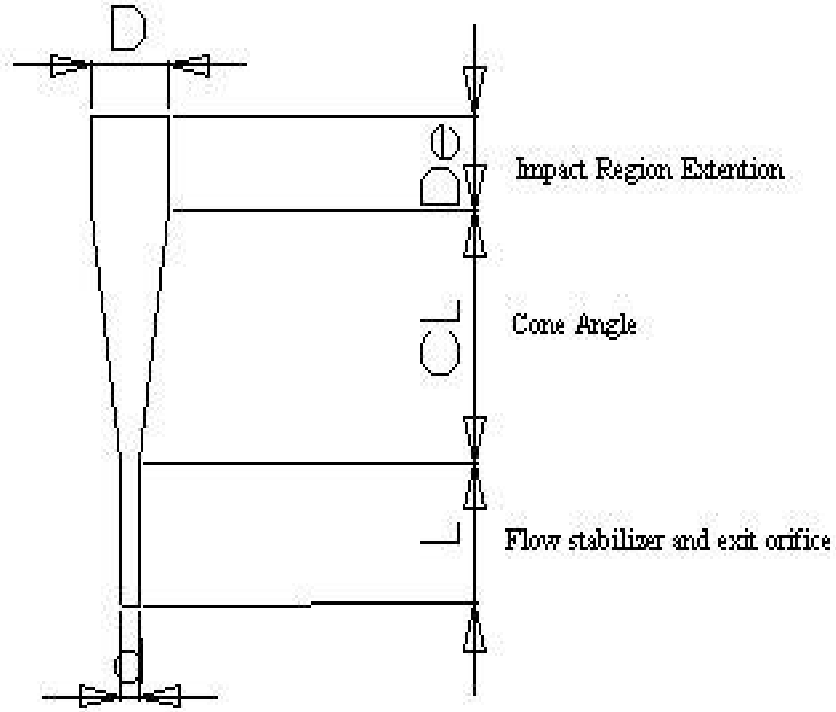


Figure 2.1 Nozzle geometry

# CHAPTER 3

# CHEMICAL AND PHYSICAL PROPERTIES OF PALM OIL METHYL ESTER AND DIESEL

## 3.1 INTRODUCTION

The properties of POME and CDF are very similar and POME is well acceptable as a CDF substitute. Furthermore, POME has advantages over CDF. This chapter summarizes the chemical compositions of palm oil.

## 3.2 PRODUCTION OF POME

Biodiesel is a generic name for fuels obtained by transesterification of a vegetable oil. In oleo chemical industry, crude palm oil is converted to methyl esters through direct

esterification of fatty acids or transesterification of triglyceride. PORIM has developed a process that converts crude palm oil into methyl ester, which is used as a CDF substitute (Choo, Ma & Y. Barison 1995,p.3).

The processes consist of two steps: (a) esterification of the free fatty acids present in the oil into methyl ester, followed by (b) transesterification of neutral glycerides mixture into methyl ester without going through the washing stage. Figure 3.1 shows the transesterification process. The esterification is carried out at 200°C -250°C under pressure (Choo, Ma & Y. Barison 1995,p.3). Methanols are used to deactivate lipase enzymes. Most crude palm oil are triglycerides (TGs; triglyceride = TG). Chemically, TGs are the triacylglyceryl esters of various fatty acids with glycerol (Ulf Schuchardt & Ricardo Serchelia 1997; Rogério Matheus Vargas 1997,p.199).

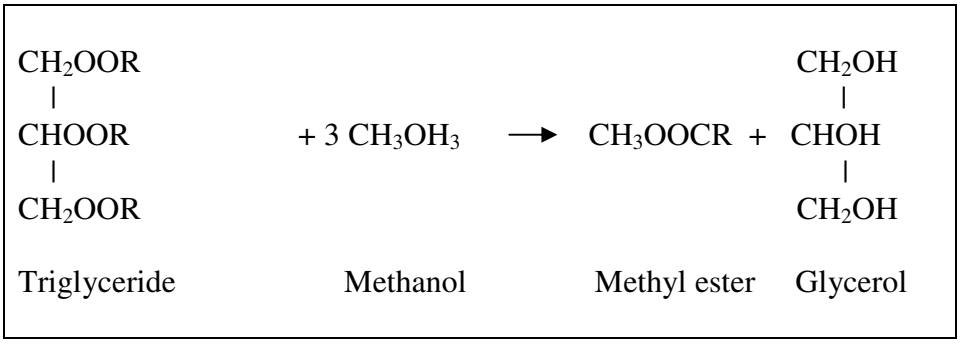


Figure 3.1 Structure of triglycerides and principle of the transesterification reaction (Shown for methyl esters; R = $(CH_2)$ x $CH_3$ or unsaturated rests according to the fatty acids)

## 3.3 CHEMICAL PROPERTIES OF POME

The fatty acid composition of palm oil contains larger amounts of saturated fatty acid such as palmitic acid and small amount of myristic and stearic acid. It contains 40% of mono unsaturated oleic acid and 10 % of polyunsaturated acid. Table 3.1 shows the component of POME.

Table 3.1 Component of POME (S.M Sapuan, H.H Masjuki & A.Azlan 1997,p.47; Choo, Ma& Y. Barison 1995,p.16)

| | Component | Chemical equation | Percentage |
|---|---|---|---|
| Saturated | Myristic Acid C14:0 | $CH_3(CH_2)_{12}CO_2H$ | 1 |
| | Palmitic Acid C16:0 | $CH_3(CH_2)_{14}CO_2H$ | 45 |
| | Stearic Acid C18:0 | $CH_3(CH_2)_{16}CO_2H$ | 4 |
| Mono unsaturated | Oleic Acid C18:1 | $CH_3(CH_2)_7CH=CH(CH_2)_7CO_2H$ | 40 |
| Poly unsaturated | Linoleic Acid (ω6) C18:2 | $CH_3(CH_2)_4=CHCH_2CH=CH(CH_2)_7CH CO_2H$ | 10 |

Free glyserol in free fatty acid methyl ester may cause a problem in the fuel system. Compared to petroleum, the reactivity of the free fatty acid methyl ester palm oil is high with different chemical structure and subjected to oxidation. This may lead to corrosion of the engine (Schindlbauer, 1998,p.200). Table 3.2 shows the typical composition of POME.

Table 3.2 Typical compositions POME (Schäfer 1995,p.202)

| Element | Composition (%by mass) | Formula | Molecular Weight (g/mole) |
|---|---|---|---|
| Carbon, C | 76.3 | 18.0 | 283.7 |
| Hydrogen, H | 12.4 | 34.9 | 283.7 |
| Oxygen, O | 11.3 | 2 | 283.7 |

## 3.4 PHYSICAL PROPERTIES OF POME AND CDF

POME has similar properties to those of petroleum diesel (Table 3.3). It has a higher cetane number than diesel fuel (Table 3.4) and is commonly used in direct injection diesel engines without modifications (Ma 1993,p.3). The viscosity of the fluid changes with temperatures – increasing as temperature is decreased, and decreasing as the temperature is increased. At normal atmospheric condition, the viscosity of POME is ten times higher than that CDF.

According to de Almeida et al (2002), POME have been heated to a temperature of 100 °C in order to reduce its viscosity to a comparable value of CDF (Talal F. Yusaf et al, 2002,p.2). Elsbett engine manufacturer has successfully demonstrated that the viscosity of the POME can be reduced by incorporating a heating device in the diesel engine (Yusof Basiron & Ahmad Hitam, 1992,p.6). POME has very much improved volatility properties, does not contain gummy substances with high pour point, 16° C, and can be used in tropical countries like Malaysia.

The cetane number of POME is 50. The cetane index 50 for palm oil fuel is slightly lower than that of 53 for CDF. Ma et al used POME blended with diesel fuel in an automobile diesel engine and compared its performance and emission with diesel fuel .It was found that the cetane rating was higher for POME compare to diesel oil (Table 3.4)

Table 3.3 Properties of Malaysian Diesel and Palm Oil Methyl Ester (H. Masjuki & Baharuddin 1993,p.35)

| Property | Conventional Diesel Fuel (CDF) | Palm Oil Methyl Ester (POME) |
|---|---|---|
| Specific gravity ASTM D 1298 (°F) | 0.8330 at 60.0 ° | 0.8700 at 74.5 ° |
| Sulphur content (% Wt) IP 242 | 0.10 | 0.04 |
| Viscosity at 40 °C (cST) ASTM D445 | 4.0 | 4.5 |
| Pour Point (°C) ASTM D 97 | 15.0 ° | 16.0 ° |
| Distillation D 86 (°C)<br>I.B.P.<br>10%<br>20%<br>50%<br>90%<br>F.B.P. | <br>228.0<br>258.0<br>270.0<br>298.0<br>376.0<br>400.0 | <br>324.0<br>330.0<br>331.0<br>334.0<br>343.0<br>363.0 |
| Final recovery (%) | - | 98.0 |
| Cetane Index ASTM D 976 | 53 | 50 |
| Gross heat of combustion (KJ/kg) ASTM D 2382 | 45800 | 40135 |
| Flash Point (°C) ASTM D 93 | 98 | 174 |
| Conradson carbon residue (% Wt.) ASTM D 189 | 0.14 | 0.02 |
| Calorific value (kJ/kg) | 46800 | 41300 |

Table3.4 Cetane numbers of POME, CDF and their blends (H. Masjuki & Baharuddin 1993,p.11)

| Blends | | Cetane number ASTM D 613 |
|---|---|---|
| Palm Oil Methyl Ester (%) | Diesel (%) | |
| 100 | 0 | 62.4 |
| 0 | 100 | 37.7 |
| 5 | 95 | 39.2 |
| 10 | 90 | 40.3 |
| 15 | 85 | 42.3 |
| 20 | 80 | 44.3 |
| 30 | 70 | 47.4 |
| 40 | 60 | 50.0 |
| 50 | 50 | 52.0 |
| 70 | 30 | 57.1 |

## 3.5 EMISSION CHARACTERISTIC OF POME

In Malaysia, the exhaust gases from vehicles using fossils fuel contain various kind of harmful pollutant such as carbon monoxide (CO), carbon dioxide ($CO_2$), hydrocarbon (HC) , sulfur dioxide ($SO_2$), aromatic hydrocarbon and smoke particulate. The use of fossils fuel such as benzene, toluene, ethyl benzene and xylene (BTX) affects human health (Hitam,T.S.Tang & Y. Barison 1998,p.1). If this issue is not addressed, it will destroy our environment and life.

In order to reduce the hazardous emission gases from the vehicles, renewable fuels have to be developed and introduced. POME as a vegetable oil based fuel does not contribute $CO_2$ to the atmosphere and assists the new growth for plants (H.S. Sii, H. Masjuki & A.M. Zaki 1995,p.3). Some vegetable blended with other fuel such as diesel reduces

smoke, exhaust odours and provides less engine wear problem. POME can also work as a substitute to reduce sulphur emission and aromatic. Vegetable oil is also oxygenated so there is no eye irritation. In addition, diesel can have more complete combustion with vegetable oil than any other fossil fuel. The combination can be handled as diesel oil due to high flash point (H.S. Sii, H. Masjuki & A.M. Zaki 1995,p.906)

A study by T.S Tang, Ahmad Hitam and Yusof Barison from PORIM using Elsbett engine showed that a engine can undergone a long term trial using POME. The exhaust emissions result from tests showed that there is reduction of emission when diesel was substituted with palm oil (T.S.Tang,Hj.Ahmad Hitam & Y. Barison 1995,p.4). It was found that the contents of hydrocarbon, carbon monoxide, carbon dioxide, particulate, and nitrogen oxide of the exhaust from diesel fuel were 0.13, 0.82, 1.47, 0.14, 1.12 g/km respectively. Whereas, those from palm oil fuel were 0.09, 1.48, 0.04, and 1.04 g/km respectively. Comparing this two sets data, using palm oil as fuel seemed to reduce the hydrocarbon, particulate, and nitrogen oxide. The results are summarized in Table 3.5 and Figure 3.2.

Table 3.5 Content of emission from Elsbett engine using CDF and CPO (T.S.Tang, Hj.Ahmad Hitam & Y. Barison 1995,p.13)

| Emissions (g/km) | CDF | CPO | Deviation (%) |
|---|---|---|---|
| Hydrocarbon (HC) | 0.13 | 0.09 | -29.70 |
| Carbon Monoxide(CO) | 0.82 | 0.84 | 2.45 |
| Carbon Dioxide ($CO_2$) | 1.47 | 1.48 | 1.2 |
| Particulate | 0.14 | 0.04 | -47.20 |
| Nitrogen Oxide ($NO_x$) | 1.12 | 1.04 | -7.59 |

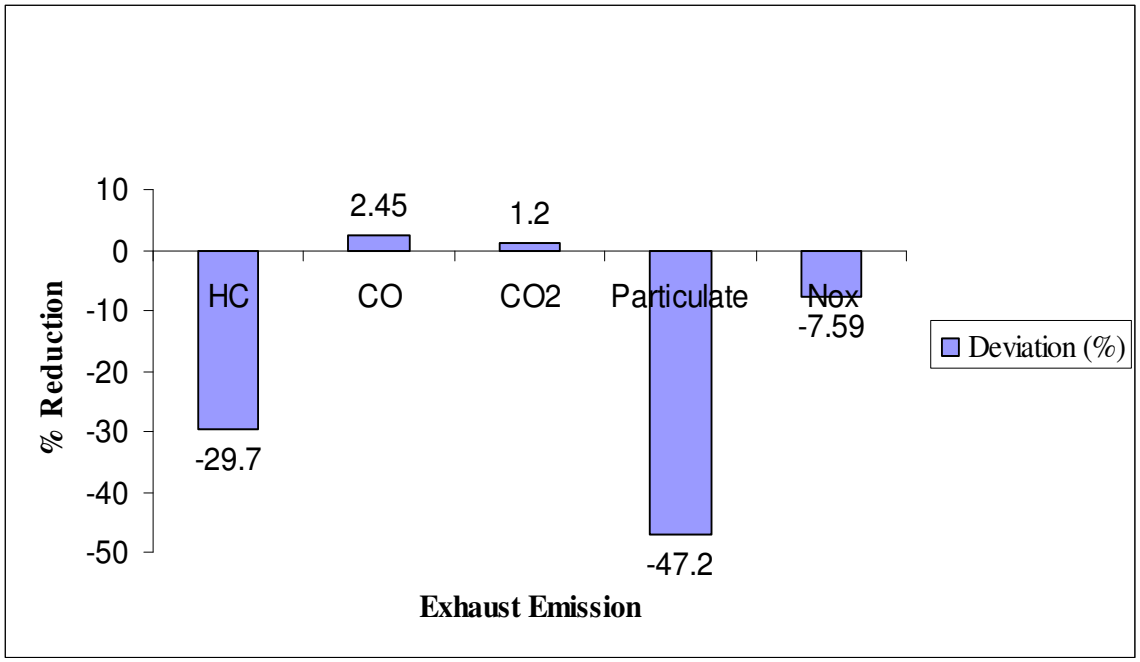


Figure 3.2 Percentage reduction of Exhaust Emission using Palm Oil

(T.S.Tang,1995)

# CHAPTER 4

# ENGINE PERFORMANCE

## 4.1 INTRODUCTION

This chapter investigates the engine performance through simulation. The parameters that were being simulated are given in Table B.1 in Appendix B. These parameters and engine specification calculated using Matlab, a popular software package for modelling and the analysis of data. The overall results obtained using the Matlab routines are compared to results from available experimental data.

## 4.2 THEORETICAL CALCULATION AND MATLAB

The mass flow rate, torque, input power, brake power, brake mean effective pressure, specific fuel consumption, break thermal efficiency and the relationship between pressure and time will be investigated. From theoretical calculations, the graphs of mass flow rate versus engine speed, specific fuel consumption versus engine speed, torque versus engine speed, break thermal efficiency versus engine speed and pressure versus time are obtained.

### 4.2.1 Major equations used for Matlab Programme

#### 4.2.1.1 Engine Performance Equations

Engine torque is measured by the dynamometer. The engine is clamped on a test bed and the shaft is connected to the dynamometer rotor. The torque can be found as follow:

$$\tau = \frac{P}{\omega} \text{ or } \tau = \frac{60P}{2\pi N} \tag{4.1.1}$$

Where:

$P$ = Power (kW)

$N$ = Angular Speed (rev/s)

$\tau$ = Torque (Nm)

Input power is given by the

$$ip = \dot{m} Q_{net,v} \tag{4.1.2}$$

Where:

$ip = \text{InputPower}(kW)$

$Q_{net,v}$ is the lower calorific value of the fuel.

For CDF ,$Q_{net,CFD} = 45000kJ/kg$,

POME, $Q_{net,POME} = 41300kJ/kg$,

The mass flow rate is calculated by multiplying the volumetric flow rate with density of the fuel

$$\dot{m} = \frac{V}{t} \text{ x } 1 \text{ x } 10^{-3} \text{ x } \rho_{water} \text{ x } \psi \qquad (4.1.3)$$

Where:

$\dot{m}$ = Mass Flow Rate of Fuel ($kg/s$)

$V$ = Volume Flow Rate of Fuel ($cm^3/s$)

$\rho_{water}$ = Density of Water ($kg/cm^3$)

$\psi$ = Specific gravity ($kg/cm^3$)

0.833 $kg/cm^3$ and 0.899 $kg/cm^3$ for CFD and POME respectively

Torque depends on the engine size and good engine designs have maximum break mean effective pressure. The break mean effective pressure are dependent on break power and is expressed as

$$bp = \frac{2\pi N\tau}{60 \text{ x } 10^3} \tag{4.1.4}$$

$$bmep = \frac{2bp}{ALNn} \tag{4.1.5}$$

Where:

$bp$ = Break Power ($kW$)

$bmep$ = Mean Effective Pressure (kPa)

n = number of cylinder

$A$ = Area of engine bore ($m^2$)

$L$ = Length of stroke (m)

The break fuel consumption is measured as a flow rate:

$$bsfc = \frac{\dot{m}}{bp} \tag{4.1.6}$$

With break power and input power, the efficiency of the engine can be calculated using

$$\eta_{BT} = \frac{bp}{ip} \text{x} 100\% \tag{4.1.7}$$

(Refer to Appendix D.1 for Matlab scripts)

#### 4.2.1.2 Derivative of Pressure with respect to Crank Angle

In an engine, the crank angle $\theta$ changes with time. The relationship between pressure and time will be investigated as the crank angle changes. The graph of $\frac{dP}{d\theta} vs.\ \theta$ is obtainable by solving the following equations:

$$\frac{dP}{d\theta} = \frac{k-1}{V}\left[Q_{in}\frac{df}{d\theta} - \frac{hA}{w}\left(T_g - T_w\right)\frac{\pi}{180}\right] - k\frac{P_{in}}{V}\frac{dV}{d\theta} \tag{4.1.8}$$

$$\frac{dV}{d\theta} = \frac{V_d}{2}\sin\theta\left[1+\cos\theta(R^2-\sin^2\theta)^{-1/2}\right] \tag{4.1.9}$$

$$V = \frac{V_d}{r-1} + \frac{V_d}{2}\left[R+1-\cos-(R^2-\sin^2\theta)^{1/2}\right] \tag{4.2.0}$$

$$f = 1-e^{\left(-a\left[\frac{(\theta-\theta^\circ)}{D\theta}\right]\right)^n} \tag{4.2.1}$$

$$\frac{df}{d\theta} = \frac{(1-f)na}{\Delta\theta}\left[\frac{(\theta-\theta^\circ)}{\Delta\theta}\right]^{n-1} \tag{4.2.3}$$

$$A = \frac{\pi B^2}{2} + \frac{\pi BS}{2}\left[R+1-\cos\theta+\left(R^2-\sin^2\theta\right)^{1/2}\right] \tag{4.2.4}$$

From the characteristics of the pressure versus time graph, the maximum pressure can be obtained. Different types of graph $\left(\frac{dP}{d\theta} vs.\ \theta\right)$ are produced at different compression ratio.

It is assumed that the cylinder content behaves as an ideal gas. The mean cylinder gas temperature is obtained using the following expression:

$$T_g = \left[\frac{(r-1)V_d}{r}\right]\frac{P_{in}VMRu}{\rho} \tag{4.2.5}$$

The specific gas constant R is calculated from the mean gas composition estimated from the initially trapped mass and the amount of fuel burned at the current crank angle.

$$Q_{in} = P_1 V_d \tag{4.2.6}$$

The Nusselt number, defined as:

$$\begin{aligned} Nu &= \frac{hB}{K} \\ &= x\left[\rho Sp\frac{B}{\mu}\right]^b \end{aligned} \tag{4.2.7}$$

All the above equation are obtained from *Ref.* [*4*]

(Refer to Appendix D.2 for Matlab scripts)

#### 4.2.1.3 Derivation of heat release rate

The net heat release rate is determined by applying the first law of thermodynamic.

$$\frac{dQ_{net}}{d\theta} = \frac{C}{r}\left( P\frac{dV}{d\theta} + V\frac{dP}{d\theta} - \frac{PV}{m}\frac{dm}{d\theta}\right) + P\frac{dV}{d\theta} \tag{4.2.8}$$

$$\frac{dQ_w}{d\theta} = A\left( a_c \frac{K}{B}\mathrm{Re}\left(T_w - T_g\right) + r\left(T_w{}^4 - T_g{}^4\right)\right) \tag{4.2.9}$$

The Reynolds number, defined as

$$\mathrm{Re} = \frac{4\dot{m}}{\pi\mu_g B} \tag{4.2.10}$$

The gross heat release rate, provides the actual rate of energy release, is then obtained by,

$$\frac{dQ_{gross}}{d\theta} = \frac{dQ_{net}}{d\theta} - \frac{dQ_w}{d\theta} \tag{4.2.11}$$

Where the heat loss rate $\frac{dQ_w}{d\theta}$ (negative from gas to walls) is obtained from Eq. (4.2.12) using the heat transfer model of Annand [12].

$$\frac{dQ_w}{d\theta} = A(a_c \lambda \mathrm{Re}^b (T_w - T_g) + c_r (T_w{}^4 - T_g{}^4) \tag{4.2.12}$$

$$\dot{m} = e^{\left(\frac{-C(\theta+\pi)}{w}\right)} \tag{4.2.13}$$

$$\frac{dm}{d\theta} = \frac{-C\dot{m}}{w} \tag{4.2.14}$$

Where:

$h$ = heat transfer coefficient

$K$ = Thermal conductivity = 0.15 W/m.K

$x$ = varies from 0.35 to 0.8 for normal combustion = 0.6

$Sp$ = mean piston speed

= $2Sw$

$\mu$ = Dynamic viscosity

= $7 \times 10^5$ kg/ms

$w$ = speed of the piston

$P_1$ = Atmospheric pressure

$Q_{in}$ = Overall heat input ($J/rev$)

$k$ = $\frac{C_p}{C_v}$ = 1.4 (air)

$R$ = $\frac{1}{R_c}$ l is connecting rod

$R_c$ is crank radius

$r$ = compression ratio

$V_d = \frac{\pi B^2 S}{4}$

B is bore

S is stroke

$V_d$ is swept volume

$R = \frac{V_d + V_c}{V_c}$ , $V_c$ is clearance volume

$f$ = fraction of heat added

$\theta$ = Crank angle

$\theta^o$ = Angle of the start of the heat addition

$\Delta\theta$ = Burn duration

$a$ = 5

$b$ =0.7

$n$ = 3

$A$ = surface area of the cylinder

$T_g$ = average gas temperature

$M$ = Molar mass of the fuel per air mixture

$Ru$ = universal gas constant

$\rho$ = Density of the fuel per air mixture

$C$ =0.8 */s* (constant)

All the above equation are obtained from *Ref.* [*4*]

(Refer to Appendix D.2 for Matlab scripts)

## 4.3 ENGINE PERFORMANCE

### 4.3.1 Fuel's Power Performance

The engine specification were used according to a stationary Perkins diesel engine model 4-108V. The direct injection has the following specifications: 4 strokes, 4 cylinders, bore 79.5mm, stroke 88.9mm, compression ratio 22, and 32 kW rated power output at 4000 rpm.

The performance of POME and CDF are compared at a fixed throttle opening within the speed range from 1000 to 3000 rpm .The results obtained show two distinct trends when speed is below or above 2000 rpm. The results under standard operation condition with CDF and POME are shown in Table C.1 and Table C.2 respectively in Appendix C.

Specific fuel consumption is one of the best indicators of engine performance in terms of efficiency. Theoretically specific fuel consumption is initially high due to the pumping work, increase magnitude of friction and increase relative heat transfer which reduce the fuel conversion efficiency (Heywood 1989,p.125).

Figure 4.1 shows specific fuel consumption for emulsion of POME compared to CDF. The trend shows maximum fuel consumption at the range of 1800 to 2000 rpm. Below the range, the fuel consumption of POME is higher compared to CDF. The flow rate decreased as the speeds goes beyond 2000 rpm. The effects are due to the relationship of volumetric fuel injection system, fuel density, viscosity, and heating value. The

consumption of POME-CDF mixtures was higher than CDF and increased as mixture increase.

This result is comparable with the results by Talal et al, 1999 and Masjuki et al, 1998 where the rate of fuel delivery to engine speed was affected by specific gravity and viscosity of fuel. In general, emulsions of POME and CDF have similar characteristics.

Figure 4.2 shows the brake fuel consumption (BSFC) of POME compare to CDF. At low speed, BSFC of POME is greater than CDF. As the speed increases, the BSFC of POME becomes lower compare to CDF at 2200 to 2500 rpm. However, BFSC increased for both fuel at high speed. This indicates good combustion of POME at the high-speed range.

The engine torque versus speed for POME and CDF are shown in Figure 4.3. The torque reaches maximum for both fuels within the range speed of 1800 to 2000 rpm. However, the torque produced by POME is higher compare to CDF in general. The torque produced by POME-CDF was higher when the percentage of POME increased. Torque reduced as the speed increase for both fuels.

Brake power was calculated with respect to torque and engine speed. The brake power as a function of speed is shown in Figure 4.4.It is obvious that POME required greater brake power compare to CDF. The brake power is at the peak when speed is within the range of 1800 to 2200 rpm for CDF, and 2000 to 2400 rpm for CDF. The torque and brake power produced by both fuels are comparable. At speed above 2000 rpm, the brake power was

higher when POME-CDF was increased. According to Talal F. Yusaf et al, 1999, the POME-CDF mixtures could produce higher power than CDF .This is due to the lower calorific value. This result also matches with the result by Masjuki et al, 1998.

Figure 4.5 shows the efficiency in percentage vs. speed. The result for POME shows that the efficiency is not constant and fluctuates between the speeds of 2000 to 2800 rpm. The POME efficiency is greater than CDF within this range. For CDF, it is at the transient state and start to drop when the speed is beyond 2000 rpm. The efficiencies for POME-CDF are comparable with CDF. These results agreed with those from Masjuki et al, 1998 where they found the brake power reduces as the engine speed increases and this affect the low efficiency.

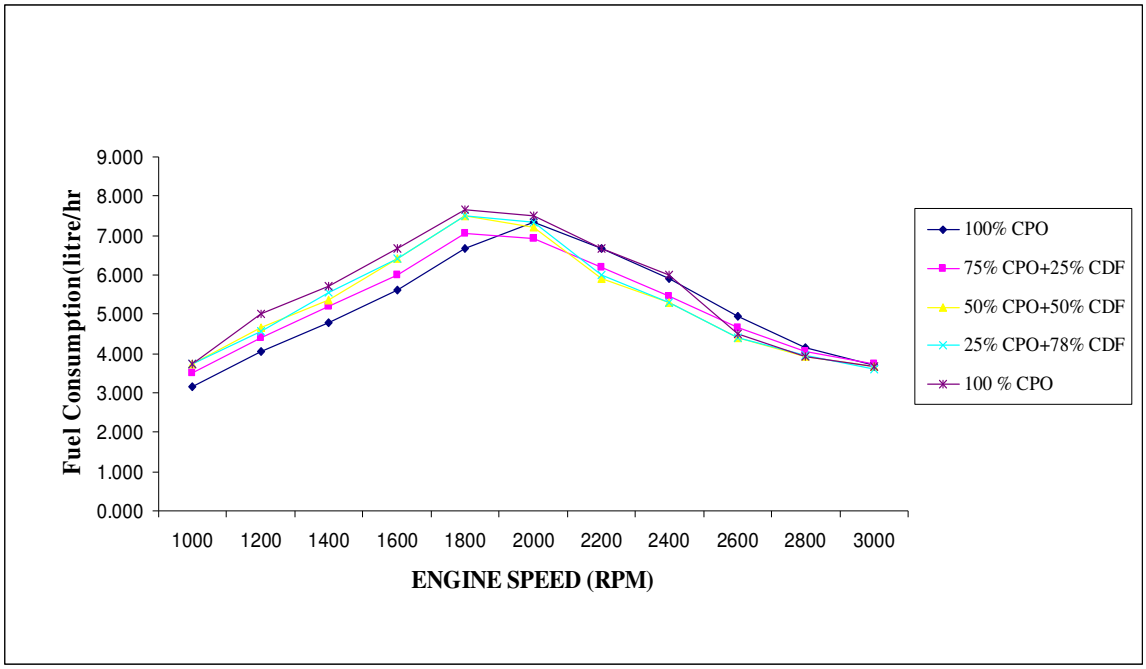


Figure 4.1 Fuel Consumption as a Function of Engine Speed (Talal F. Yusaf et. al, 1999)

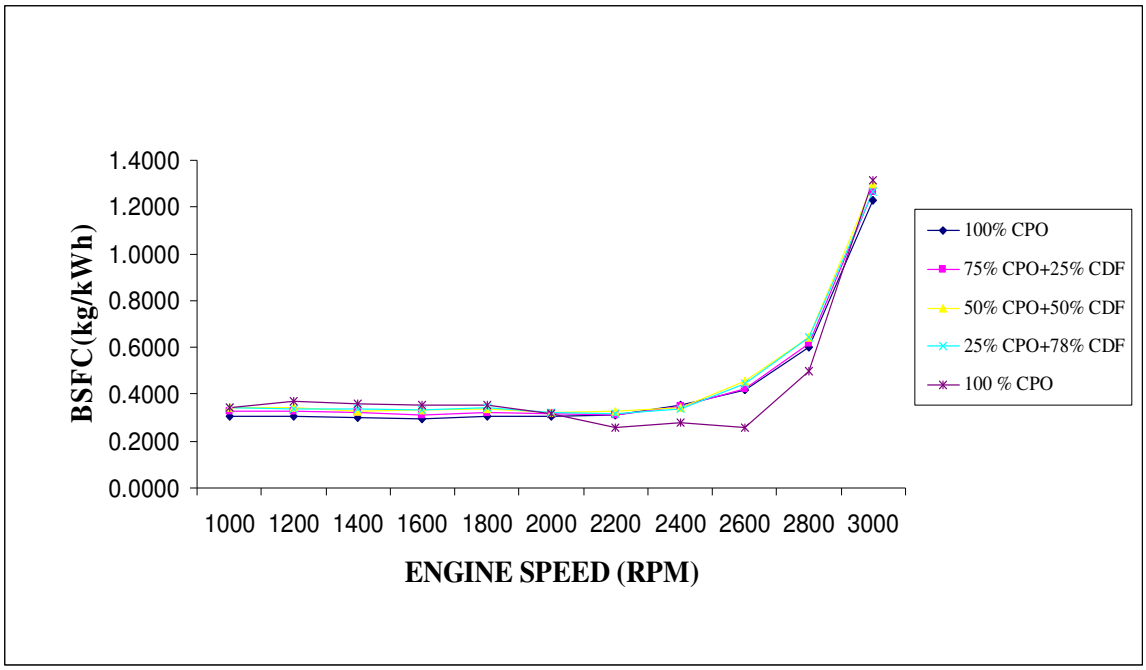


Figure 4.2 Brake Specific Fuel Consumption as a Function of Engine Speed (Talal F. Yusaf et. al, 1999)

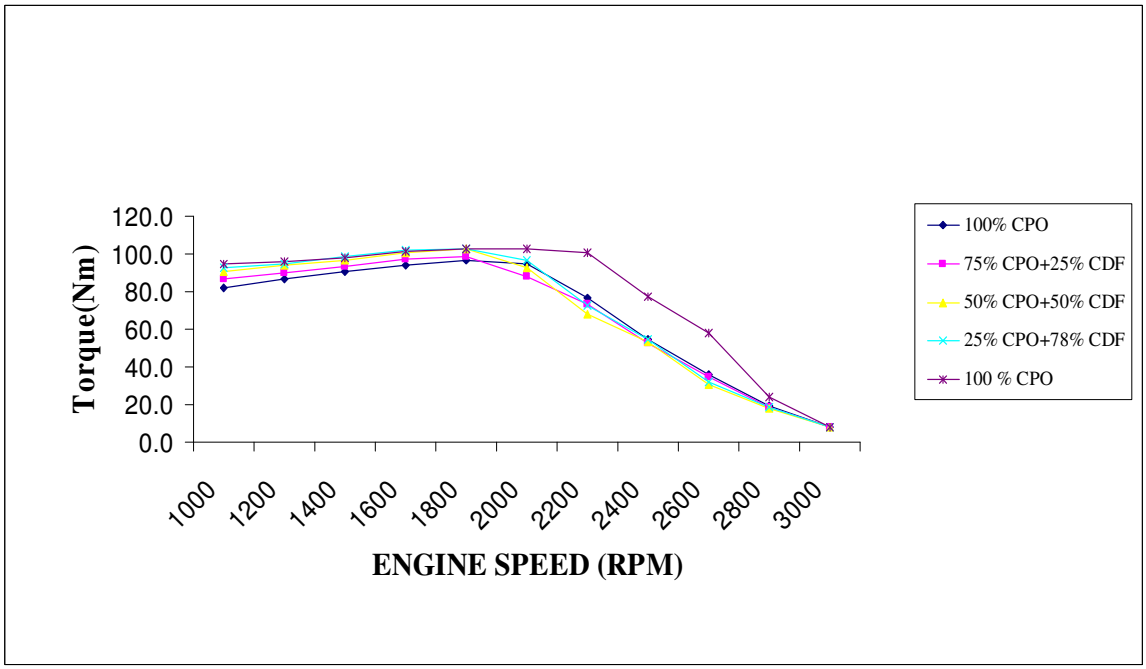


Figure 4.3 Torque as a Function of Engine Speed (Talal F. Yusaf et. al, 1999)

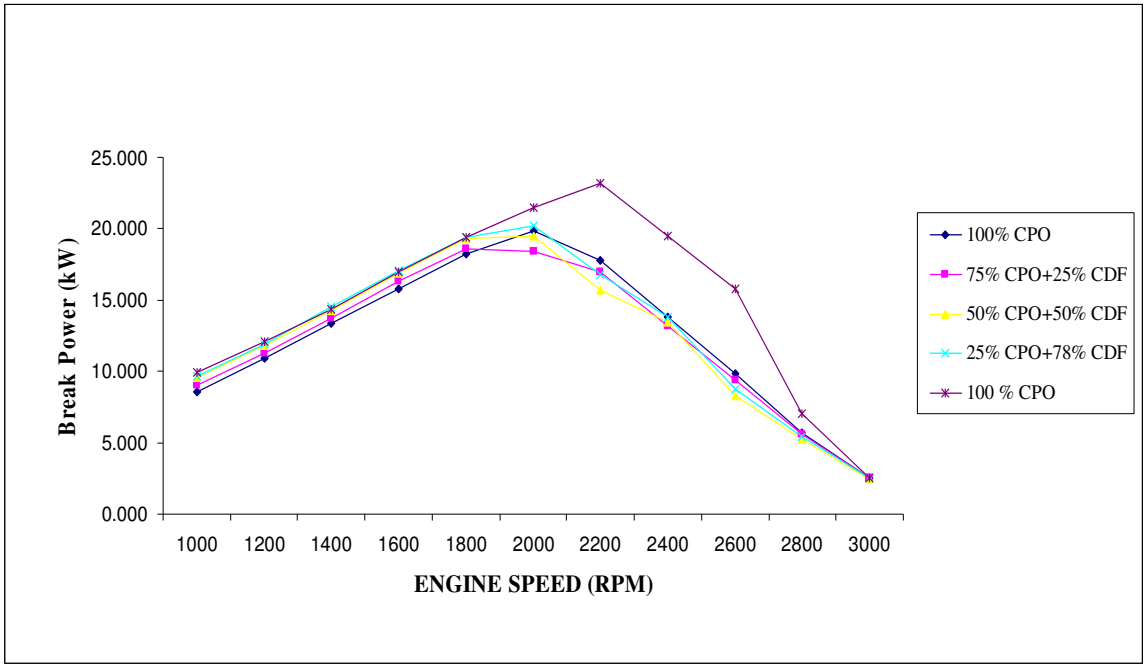


Figure 4.Brake Power as a Function of Engine Speed (Talal F. Yusaf et. al, 1999)

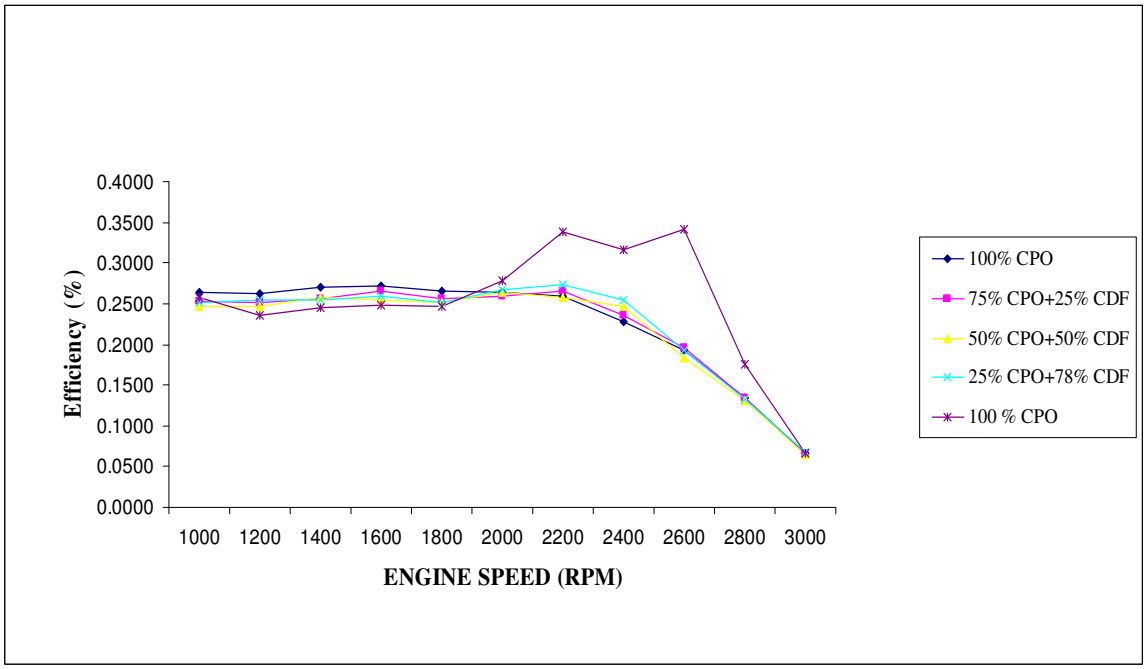


Figure 4.5 Efficiency as a Function of Engine Speed (Talal F. Yusaf et. al, 1999)

## 4.4 EMMISION GAS

Major environmental pollution from transportation systems is caused by the emission from the exhaust of diesel engine. The CDF used in the diesel engine contains higher amount of particulate matters (PM) and harmful gases such as nitrogen oxide ($NO_x$), carbon monoxide (CO) etc. These causes damage to the environment.

POME has been used for research over the past few years in a wide range of engines. The exhaust gas was found to be much cleaner. It contained comparable nitrogen oxide ($NO_x$) but less carbon monoxide. The emission effects were studied by El-Awad et al (1999). The engine was running within the range of 1000 to 3000 rpm with three crude palm oil (CPO) mixtures containing 25%, 50% and 75% of CPO by volume. The engine also ran with 100% CPO and CDF for comparison. The data obtained are given in Table C.3 to C.7 Appendix C.

### 4.4.1 Carbon Monoxide

The presence of carbon monoxide indicates that the combustion of fuel is incomplete. The experiment results were obtained from Talal F Yusaf et al. Figure 4.6 shows the fraction of carbon monoxide (CO) in the exhaust gas. At speed of 1800 rpm, it was found that the maximum CO emission from 100% CDF was approximately 2500 ppm. At speed below 2000 rpm, all CPO-CDF mixtures produced much higher percentages of CO in the exhaust gas compared with 100% CDF. CO emissions from the CPO-CDF mixtures were comparable to 100% CDF at high speed. This could be due to the presence of oxygen in

CPO, which helps to achieve better combustion. These results show that CPO is more environmentally friendly in all sense.

### 4.4.2 Oxygen

Air-fuel mixing cannot be perfect even though the combustion is complete. There is always the possibility of some $O_2$ appearing in the exhaust gas. Figure 4.7 shows the percentage of $O_2$ in the exhaust under different engine speeds. For all fuels, the percentage of $O_2$ passes through its minimum value within the speed range of 1800 to 2000 rpm. This minimum value indicates that the air fuel ratio is closest to the stoichiometric value (H.S. Sii, H. Masjuki & A.M. Zaki 1995,p.906). At low speed, all CPO-CDF mixtures showed lower $O_2$ percentage in the exhaust compared to 100% CDF. These results show that the higher the concentration of CPO in the mixture, the lower is the percentage of $CO_2$ in the exhaust. A good combustion of the 25% and 50% CPO-CDF mixtures in the high-speed range has made up for the low fuel consumption so that the fuel's brake power was comparable to CDF. There lowered the $O_2$ content in the exhaust for 75% CPO-CDF to CDF for all engine speeds (Talal F. Yusaf & El-Awad, 1999,p.4).

### 4.4.3 Nitrogen Oxides

Figure 4.8 shows the $NO_x$ emitted versus engine speed. The result shows different trends for low and high engine speeds. In the low-speed range, all CPO-CDF mixtures emitted lower $NO_x$ levels compared to 100% CDF, with the 75% CPO mixture producing the lowest $NO_x$ level. In the high-speed range, the $NO_x$ emissions of CPO-CDF mixtures were comparable to that of pure 100% CDF .However, 75% CPO-CDF mixture produced

higher level of $NO_x$ emissions. The emissions could probably be due to higher temperature and an extended delay period (Talal F. Yusaf & El-Awad 1999,p.4).

### 4.4.4 Exhaust gas Temperature

A high exhaust gas temperature can be taken as the combustion temperature. The gas analyser measures the difference ($T^*$) between the temperature of the exhaust gas ($T_g$) and the ambient atmospheric temperature ($T_a$) i.e. $T^* = (T_g - T_a)$. From the experimentation results, Figure 4.9 shows that $T^*$, the temperature for 100% CDF and all CPO-CDF mixtures reached their peak values at engine speeds lower than 1800 rpm. The 50% CPO mixture produced higher exhaust gas temperatures compared to 100% CDF at low engine speed. The 75% CPO-CDF mixture produced higher exhaust gas temperatures compare to CDF for all engine speeds. The exhaust gas temperature of 25% CPO mixture was comparable to CDF in the low speed range. (Refer Figure 4.9)

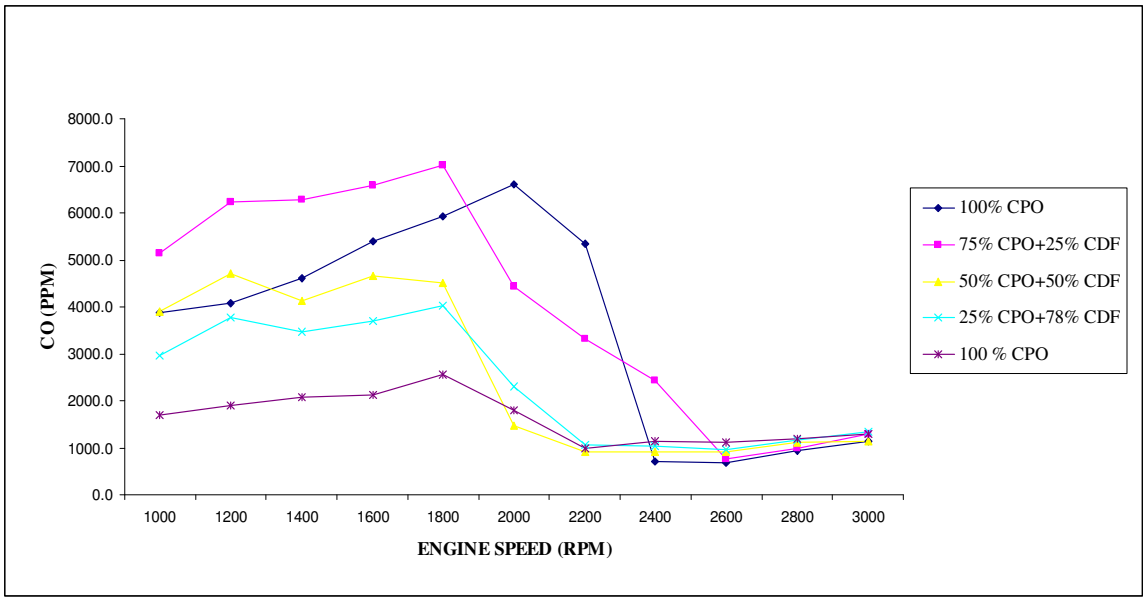


Figure 4.6 Carbon Monoxide vs. Engine Speed (Talal F. Yusaf et. al, 1999)

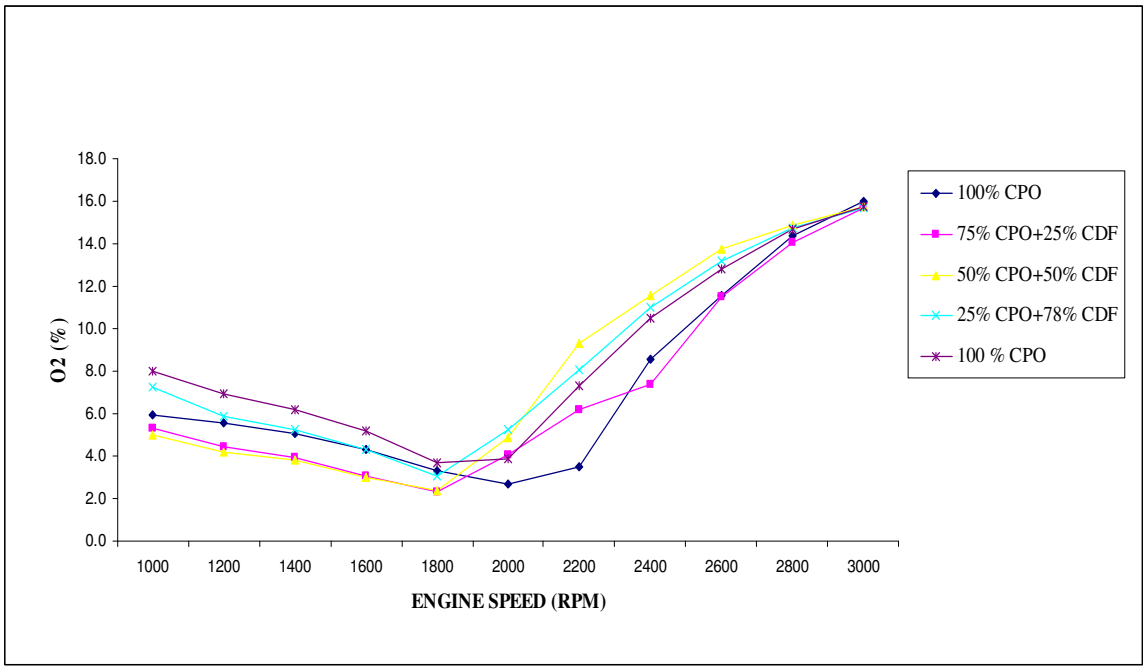


Figure 4.7 Oxygen vs.Engine Speed (Talal F. Yusaf et. al, 1999)

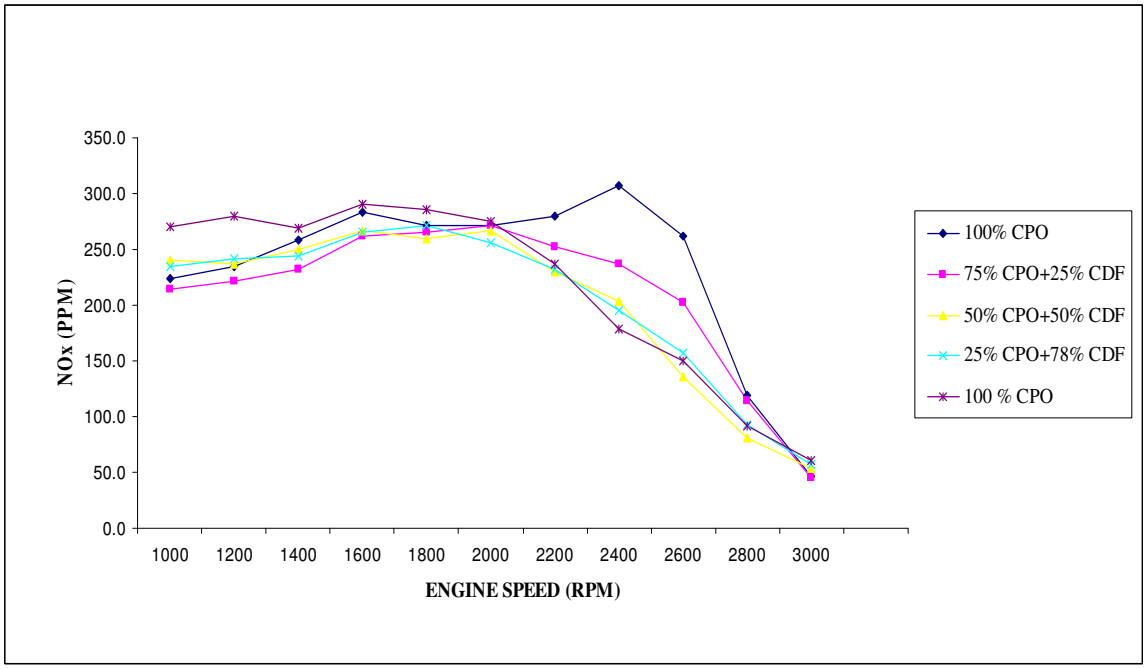


Figure 4.8 Nitrogen Oxide vs. Engine Speed (Talal F. Yusaf et. al, 1999)

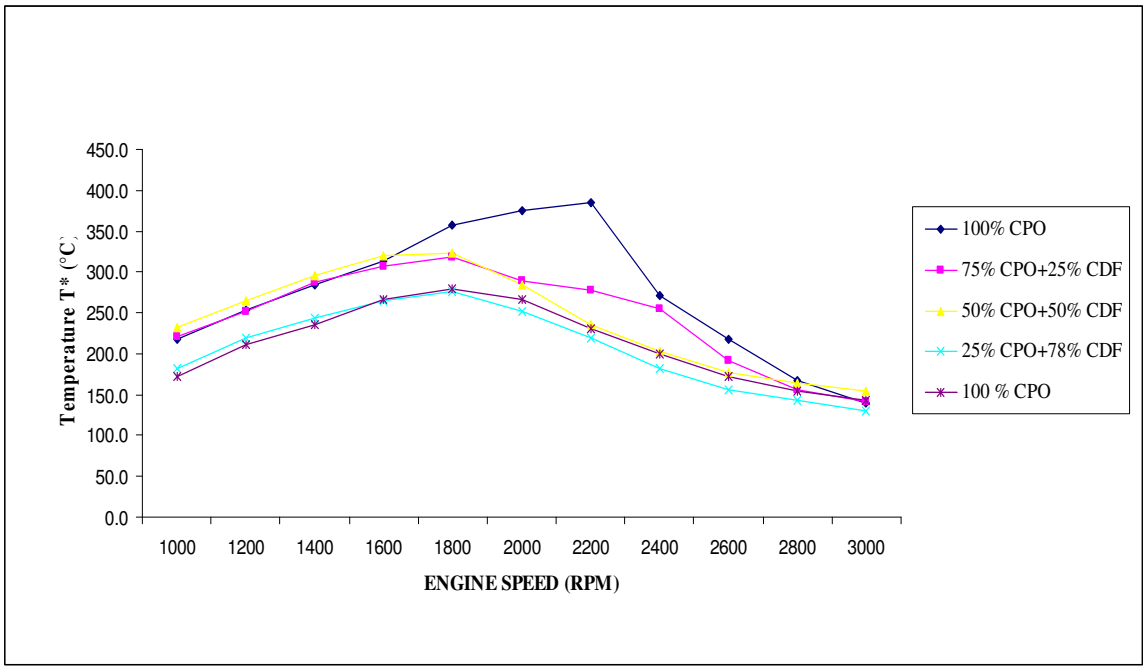


Figure 4.9 Temperature T* vs. Engine Speed (Talal F. Yusaf et. al, 1999)

# CHAPTER 5

# COMPUTATIONAL FLUID DYNAMICS

## 5.1 INTRODUCTION

CFD is a sophisticated analysis technique that enables the analyst to predict transfer of heat, chemical reaction, and fluid flow behaviour etc. CFD is based on the fundamental governing equations of fluid dynamics - the continuity, momentum and energy equation. It is a powerful tool to carry out numerical experiments. This project uses the Computational Fluid Dynamic – FLUENT software package.

The process of utilizing FLUENT can be summarized in Figure 5.1. Firstly, the geometry and grid is created using GAMBIT. TGrid can be used to generate a 2D triangular, 3D tetrahedral or 2D and 3D hybrid volumes mesh from an existing boundary mesh. Another

alternative of creating grids for FLUENT is using ANSYS (Swanson Analysis Systems, Inc.) or I-DEAS (SDRC); or MSC/ARIES, MSC/PATRAN or MSC/NASTRAN (all from MacNeal-Schwendler Corporation). PreBFC and GeoMesh are the names of FLUENT pre-processors that were used before the introduction of GAMBIT.

Once a grid has been read into FLUENT, all remaining operations are performed within the solver. These include setting the boundary conditions, defining fluid properties, and material properties, executing the solution, refining the grid, viewing and post-processing the results. The procedure using FLUENT can be summarized as in Figure 5.1;

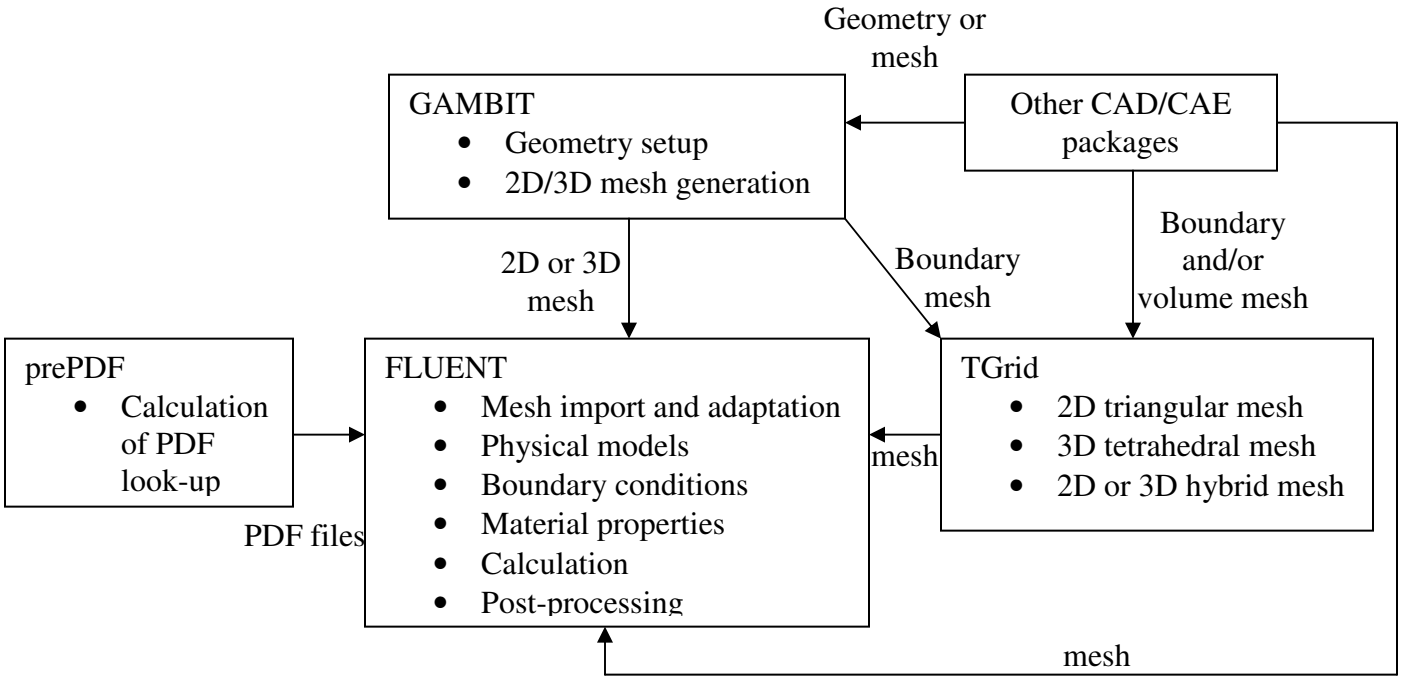


Figure 5.1 CFD flowcharts

## 5.2 APPLICATION OF CFD

CFD is a useful tool in performing theoretical experimentation. It solves all problems concerning fluid flows such as incompressible and compressible flow, Newtonian or non-Newtonian flow, swirl, transfer of heat, in viscid, laminar and turbulent flow, radiation, mixing, chemical reaction, spray models etc.

CFD can be applied to solve industrial flow problems due to rapid growth of powerful computer resources and the development of CFD software packages. In engineering applications, it is much cheaper to use CFD than conventional design process. In CFD simulation, we can simulate different set of parameters for the same design without any additional cost. This reduces the time and cost of experimental work.

## 5.3 VALIDATION OF CFD

Validation of a code is important in assessing its usefulness before applying to a practical application. This could involve comparison of present computational data with other published experimental or computational data. The simplest situation is considered for validation before the work is extrapolated to the more complex phenomena.

The sources for simple validation work should be reliable and accurate. In this research, validation has been limited and hence, well-judged assumptions are used for prediction. These validation techniques are generally qualitative.

## 5.4 MESH GENERATION

The local flow characteristics of high speed liquids are not necessarily parallel to the flow of direction. Therefore, it is pertinent to use unstructured triangular grids. The commercial mesh generation package GAMBIT is used. GAMBIT uses the Delaunay triangulation automatic mesh generation technique, with an advancing front method. All the meshes are axi-symmetric in two and three-dimensions. The advantages of Delaunay triangulation are that no point is contained in the circum-circle of any triangle and it maximises the minimum angle for all triangular elements, which is a requirement for good quality finite elements, i.e. the mesh has a low skewness.

The mesh is generated by applying points along the boundaries of geometry with certain stretching function. The geometry is made of edges and faces. It was found that geometries, which had interiors that were made of multiple faces, performed better in calculation. This was due to the increase in versatility of the stretching function that minimised a large cell volume jumps within the domain.

The mesh can be modified as a function of the solution. Post solution adaptation is undertaken in FLUENT. First, the individual cells are marked for refinement based on an adaptation function, which is created from the solution data. Next, the cell is refined based on these adaptation marks. The mesh is adapted by the hanging node technique, whereby the cells marked for refinement are iso-tropically subdivided. Figure 5.2 shows an example of this technique.

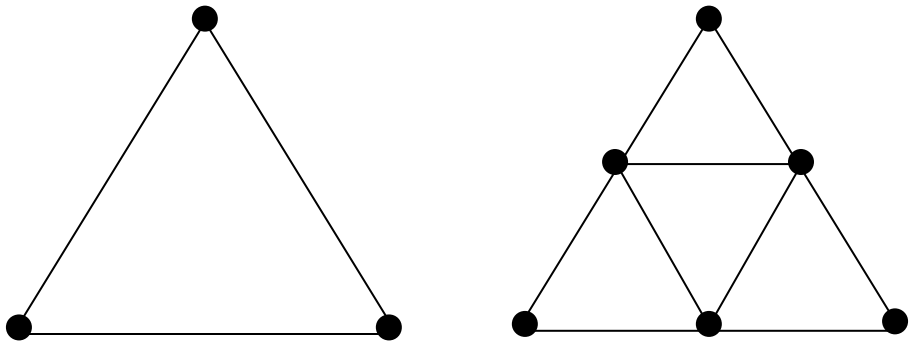

Figure 5.2 Method of Hanging Node Adaptation

The adaptation function is used under the assumption that the greatest error occurs in high-gradient regions. The equi-distribution adaptation technique used multiplies the undivided Laplacian of the solution variable by a characteristics length scale. The length scale is the square root of the cell volume. The introduction of this length scale permits resolution of both strong and weak disturbances, increasing the potential for more accurate solutions. The gradient function has the following form:

$$\left|e_i\right| = \left(A_{cell}\right)^{\frac{r}{2}} \left|\nabla^2 f\right| \tag{5.4.1}$$

Where $e_i$ is the error indicator, $A_{cell}$ is the cell area, r is the gradient volume weight and $\nabla^2 f$ is the undivided Laplacian of the desired field variable, $f$ .

## 5.5 GOVERNING EQUATION

In the CFD methodology, fluid flows are stimulated by numerical solving partial differential equations that govern the transport of flow quantities also known as flow variables. These variables include mass, momentum, energy, turbulent quantities, and species concentrations. In designing the POME- nozzle, the basic governing equations that will be used are the conservation of mass, momentum and energy equations.

### 5.5.1 Continuity Equation

In any fluid flow, the equation for conservation of mass, or continuity equation, can be written as follows:

$$\frac{\partial \rho}{\partial t} + \frac{\partial}{\partial xj}\left(\rho u_j\right) = \dot{m} \tag{5.5.1}$$

Where $u_j$ is the $j^{th}$ Cartesian of the instantaneous velocity, $\rho$ is the fluid density and $\dot{m}$ represents the rate of mass generation in the system. This equation is valid for incompressible as well as compressible flows.

### 5.5.2 Momentum Equation

The law of conservative of momentum states that

$$\frac{\partial}{\partial t}\left(\rho u_i\right) + \frac{\partial}{\partial xi}\left(\rho u_i u_j\right) = -\frac{\partial \rho}{\partial x_i} + \frac{\partial \tau_{ij}}{\partial x_i} + \rho f_i \tag{5.5.2}$$

Where ρ is the static pressure, $\tau_{ij}$ is the viscous stress tensor and $f_j$ is the body force.

For Newtonian fluids:

$$\tau_{ij} = \mu\left(\frac{\partial u_i}{\partial x_j} + \frac{\partial u_j}{\partial x_i}\right) - \frac{2}{3}\mu\left(\frac{\partial u_k}{\partial x_k}\right)\delta_{ij} \qquad (5.5.3)$$

Where $\mu$ is the fluid dynamic viscosity and $\delta_{ij}$ is the Kronecker deltas.

Substitute equation (5.5.3) into (5.5.2) results in the Navier –Strokes Equation

$$\frac{\partial}{\partial t}(\rho u_i) + \frac{\partial}{\partial x_j}(\rho u_i j_i) + \frac{\partial}{\partial x_j}\left\{\mu\frac{\partial u_i}{\partial x_i} + \frac{\partial u_j}{x_i} - \frac{2}{3}\mu\frac{\partial \mu_k}{\partial x_k}\delta_{ij}\right\} + \rho f_i \qquad (5.5.4)$$

**6.5.3 Energy Equation**

The energy equation governs the enthalpy balance. For CFD, the static enthalpy is used. Conservation of energy is described by

$$(\rho h) + \frac{\partial}{\partial x_j}(\rho u_j h) = -\frac{\partial q_j}{\partial x_j} + \frac{\partial \rho}{\partial \rho} + u_j\frac{\partial \rho}{\partial x_j} + \tau_{ij}\frac{\partial u_i}{\partial x_j} - \frac{\partial}{\partial x_i}(J_{ij}h_i) + S_a \qquad (5.5.5)$$

Where $J_{ij}$ is the total diffusive mass flux for species ai, $h_i$ is the enthalpy for species ai, $S_a$ stands for additional sources due to surface reaction, radiation and liquid spray and $q_j$ is the $j$ component of the heat flux. Fourier's Law is employed to model the heat flux

$$q_k = -K\frac{\partial T}{\partial x_j} \tag{5.5.6}$$

Where K is the thermal conductivity. This equation is only true for incompressible flow at low March number. The total enthalpy of the energy equation is fully conservative and is recommended for high-speed compressible flows. The total enthalpy H is defined as

$$H = h + \frac{u_j u_j}{2} \tag{5.5.7}$$

The governing equation for *H* can be obtained by adding the fluid kinematics energy equation to the static enthalpy equation:

$$\frac{\partial}{\partial t}(\rho H) + \frac{\partial}{\partial x_j}(\rho u_j H) = \frac{\partial}{\partial x_j}\left(K\frac{\partial T}{\partial x_j}\right) + \frac{\partial \rho}{\partial t} + \frac{\partial}{\partial x_i}(\tau_{ij} u_j) - \frac{\partial}{\partial x_j}(J_{ij} h_i) + S_a + \rho f_i u_i \tag{5.5.8}$$

### 5.5.4 Reynolds (Ensemble) Averaged Equation

The fundamental equations of fluid dynamics that have been introduced are applicable to Newtonian fluid under steady or transient, incompressible or compressible, laminar, transitional or turbulent conditions. The non linearity of Navier-Strokes equations, coupled with the complexity of the boundary conditions, make it impossible to obtain analytical solution for all but limited number of flows. In Reynolds averaging, the

solution variables in the instantaneous Navier-Stokes equations are decomposed into the mean (ensemble-averaged or time-averaged) and fluctuating components. If the Navier-Strokes equations are averaged over time, the average equations are yielded. Reynolds Averaging can be defined as

$$\phi = \tilde{\phi} + \phi'' where \tilde{\phi} = \frac{\overline{\rho\phi}}{\overline{\rho}} \tag{5.5.9}$$

Applying the equation (5.5.8) into (5.5.1), the averaged continuity equation developed is

$$\frac{\partial \overline{\rho}}{\partial t} + \frac{\partial}{\partial x_j}\left(\overline{\rho}\tilde{u}_j\right) = \overline{\dot{m}} \tag{5.5.10}$$

(Refer to Appendix E for other relevant conditions)

## 5.6 DISCRETIZATION METHOD

The method contains settings that control the discretization of the convection terms in the solution equations. It is a numerical method to solve the above equation by discretization of the partial Differential Equations on a computational grid, the formation of a set algebraic equations and the solution of the algebraic equations.

FLUENT allows choosing the discretization scheme for the convection terms of each governing equation. The numerical method yields a discrete solution of the flow field, which is comprised of the values of the flow variables at the grid points. One of the most important terms that need to be discretized is convection. Second-order accuracy is automatically used for the viscous terms.

The mathematical code uses a control-volume-based technique to convert the governing equations to algebraic equations that can be solved numerically. It consists of integrating the governing equations about each control volume.

For example, take an unknown scalar quantity $\phi$, and integrate it for an arbitrary control volume *V*:

$$\oint \rho\phi v.dA = \oint \Gamma_\phi \nabla\phi.dA + \int_V S_\phi dV \qquad (5.6.1)$$

Where:

$\rho$ = density

$v$ = velocity vector= $u\hat{i} + v\hat{j}$

$A$ = surface area

$\Gamma_\phi$ = diffusion coefficient for $\phi$

$\nabla\phi$ = gradient of $\phi = \left(\frac{\partial\phi}{\partial x}\right)\hat{i} + \left(\frac{\partial\phi}{\partial y}\right)\hat{j}$

$S_\phi$ = source of $\phi$ per unit volume

When the above equation is applied to the control volume or cells in the computational domain, the discretization yields:

$$\sum_f^{N_{forces}} v_f \phi_f A_f = \sum_f^{N_{forces}} \Gamma_\phi \left(\nabla_\phi\right)_n A_f + S_\phi V \qquad (5.6.2)$$

Where:

$N_{forces}$ = number of faces enclosing cell

$\phi_f$ = value of $\phi$ convected through face

$v_f$ = mass flux through the face

$A_f$ = area of face $f$ , $|A| = \left|A_x\hat{i} + A_y\hat{j}\right|$

These equations can be applied readily to unstructured, multi-dimensional meshes. Each discrete scalar value of $\phi$ is stored in the cell centre. The cell face values $\left(\phi_f\right)$ required for the convection terms in the equations are interpolated from the cell centres by means

of an upwinding scheme. In up winding, the face value $\phi_f$ is derived from quantities in the cell upstream, or upwind, relative to the direction of the normal velocity $v_n$. The diffusion terms in the equations are all central differenced.

### 5.6.1 Upwinding

Due to the computational domain, the initialised values are quite different from those expected in the final solution after the iteration process has begun. For this reason, first order upwinding scheme is utilised until a more realistic solution is achieved, afterwhich a more accurate second order upwinding scheme could be implemented.

### 5.6.2 First Order Scheme

When first order accuracy is desired, quantities at cell faces are determined by assuming that the cell-centre values of any field variable represent a cell-average value and hold throughout the entire cell; the face quantities are identical to the cell quantities. Thus when first –order upwinding is utilised, the face value $\phi_f$ is set equal to the cell-centre value of $\phi$ in the upstream cell.

### 5.6.3 Sequential Discretization

The solver can cope with both steady and unsteady state fluid dynamic scenarios. For blunt-body work, the steady state equations are implemented, i.e. the time marching continues until a steady state solution is reached. Implicit equations are able to accomplish this.

### 5.6.4 Steady State Implicit

An Euler implicit discretization in time of the governing equations is combined with Newtonian-type linearization of the fluxes to produce the following linearized system in delta form:

$$\left[ D + \sum_{j}^{N_{force}} S_{j,k} \right] \Delta Q^{n+1} = -R^{n} \tag{5.6.3}$$

The centre and off-diagonal coefficient matrices $D$ and $S_{j,k}$ are given by:

$$\begin{aligned} D &= \frac{V}{\Delta t}\Gamma + \sum_{j}^{N_{force}} S_{j,i} \\ S_{j,k} &= \left( \frac{\partial F_j}{\partial Q_k} - \frac{\partial G_j}{\partial Q_k} \right) \end{aligned} \tag{5.6.4}$$

$R^n$ and $\Delta t$ are defined in Equations (5.6.5) and (5.6.7) in Appendix D.

## 5.7 PHENOMENA SIMULATED

### 5.7.1 Turbulent flow

This problem involves the use of turbulence model, which generally requires the solution of additional transport equations. $k$-$\varepsilon$ transport equation is used because it over predicts turbulent viscosity in regions of flow separation and stagnation. The model transport equation for k is derived from the exact equation. Three quantities - turbulent kinetic energy, K, dissipation rate, D and the length scale are very important in specifying the

turbulence characteristics at the inlet. If K and D are specified, the value for L will be ignored. It is sometimes more convenient to provide a length scale instead of a value for dissipation rate. In the derivation of the $k$-$\varepsilon$ model, it was assumed that the flow is fully turbulent, and the effects of molecular viscosity are negligible. The turbulent kinetic energy can be calculated as follows;

$$k = \frac{1}{2}\left(u^2 + v^2 + w^2\right) \tag{5.7.1}$$

Where u, v, w = perturbation velocities about the mean velocities U,V,W respectively. After determining k, the dissipation rate of turbulent kinetic energy D can be determined using the following formula:

$$D = \frac{C_\mu^{3/4} k^{3/2}}{0.014L} \tag{5.7.2}$$

Where

$C_\mu$ = constant, normally 0.09

$L$ = inlet height or diameter

**5.7.2 Incompressible**

Flow speeds for problems can range from low speed subsonic to transonic and supersonic. In the incompressible flow, the density of fluids is either constant or calculated as a function of temperature and/or species mass fractions, where the mass

fractions are the values you entered as an inlet condition. The inlet total pressure and the static pressure, $p_s$, are related to the inlet velocity via Bernoulli's equation:

$$p_o = p_s + \frac{1}{2}\rho v^2 \tag{5.7.3}$$

### 5.7.3 Inlet boundaries

The conditions needed to specify the inlet boundaries are fixed velocity conditions where the flow solver determines the mass flow rate applied to each of the boundary using specification such as pressure, temperature and fluid property density.

### 5.7.4 Outlet boundaries

The fixed pressure outlet boundary conditions allow both inflow and outflow to be satisfied in the domain. It is important to provide realistic values of turbulence quantities and temperature at these boundaries because these values are used to evaluate diffusion at the boundary.

## 5.8 COMPUTATIONAL RESOURCES

All the numerical simulations described in this thesis have been executed on an Intel Pentium III machine. It has a 500 MHz CPU clock speed and 520MB of RAM. Benchmarking tests have shown that the configuration is capable of executing 670 mega floating point per seconds (MFLOPS). The operating system is Windows XP based.

The preceding calculations especially RAM, for the computational domain are not complicated. The important attribute is the floating-point capability. This function dictates iterative speed and solvable flow component capacity. Its FLOPS rating is not the highest currently available but it is dedicated and of comparable rating to a shared CPU supercomputer. All calculations are run in serial on a single processor.

The typical CPU times for the blunt body calculations are between 1 to 2 hours depending upon the Mach number. For low-density ratio, each time step takes approximately 1 1/2 hour CPU times. For high-density ratio, each step can take up to 3 hours CPU time due to the need for a low CFL number to maintain solver stability.

## 5.9 CONCLUDING REMARKS

The FLUENT solver has the ability, through its numerical modules, to model all the important characteristics at high speed. The main feature is its coupled handling of the governing equations that allows density variation and the incorporation of the ideal gas law. The solver is able to cope with the numerical anomalies caused by large gradients and discontinuities.

The method of mass fraction prediction is similar to the concentration technique. It does not predict atomisation, but is useful in prediction of mixture dependent on phenomena such as combustion.

The other important factors that effect the computation of compressible flow have been considered. The most important of these are dilatation dissipation and the Mach number round off problem.

The discretization and time marching techniques used, whilst being well suited to the type of flow scenarios, are also computationally economic. This means that high cell density grids can be used to resolve large gradients and capture the numerical calculations. The time scales used for calculations can be quite realistic and not a hindrance to the user's progress. The schemes are suitably computationally efficient.

The mesh generation technique is suitable for flows that have more than one direction. All this leads to a code that has potential to solve the dynamics and characteristics of the nozzle. The deciding factors on its successful application will depend on how it is applied, the boundary conditions set, initial estimation of flow properties and the construction of the mesh around important flow features.

# CHAPTER 6

# FUEL INJECTOR (NOZZLE)

## 6.1 FUEL INJECTION STYSTEM

### 6.1.1 Characteristic of fuel injector system

The fuel injection system supplies fuel to the diesel engine. The low pressure part of the fuel injection system consists of the fuel tank, fuel filter, pump, overflow valve and fuel lines as shown in Figure 6.1. The characteristics of the fuel injection system consists of metering, timing, rate control, atomization and distribution.

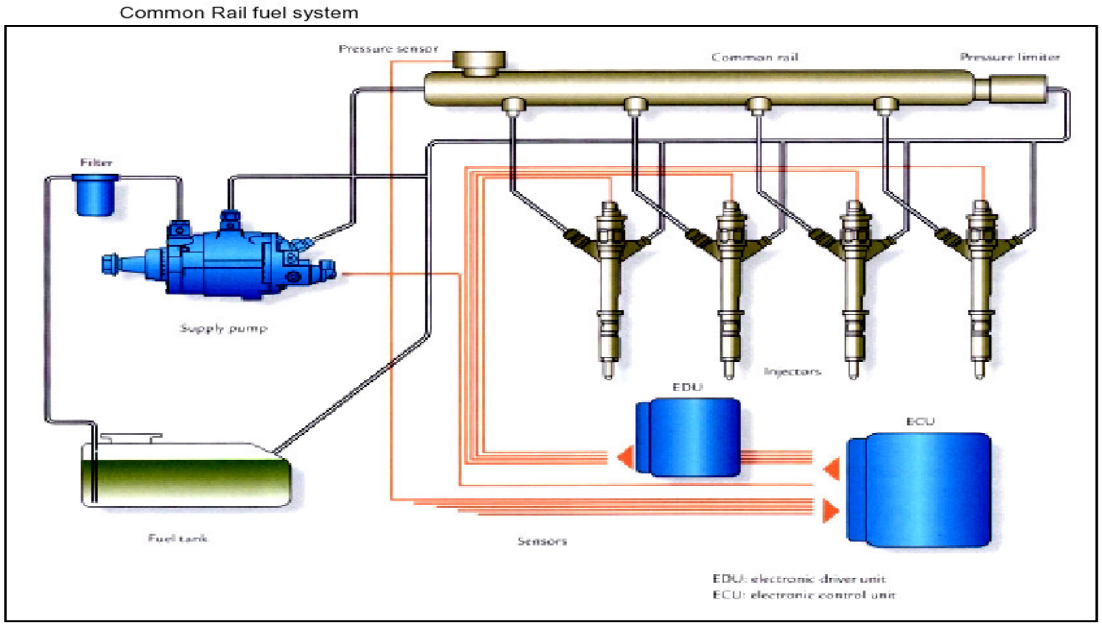


Figure 6.1 Fuel injection system

### 6.1.2 Main Function of Fuel Injection

Fuel injection offers many advantages. For example:

a) Increase in volumetric efficiency will increase the power and torque. This is due to lower gas velocities in the intake manifold, as it need not be heated to promote vaporization when fuel droplets are smaller.

b) Improvement in the mixture control of air and fuel resulting in better thermal efficiency.

c) Lower exhaust emissions because during starting, atomization is independent on crank speed.

d) The distribution is independent of vaporization and fuel volatility and this result in more fuel tolerant.

e) Elimination of short circuit fuel turbo since injection can be timed.

(Colin R. Ferguson 1986,p.314)

The purpose of injector is to distribute and mix the fuel with the surrounding air. The engine load is controlled by the amount of fuel injected and is changed through modification of injection duration. The number of holes and their sizes in the injector tips affect the injection duration. For a fixed pressure, the amount of fuel per cylinder can be increased by decreasing the hole size in the injector tip.

The quality of POME injection is judged by factors such as:

(a) Spray Angle;

(b) Spray Penetration;

(c) Droplet distribution;

(d) and Droplet size

Other parameters, which influenced combustion rate and emissions, are:

(a) Spray influence on turbulent mixing rates;

(b) Turbulence in the injector nozzle holes;

(c) Effects of injection rate shape;

(d) Effects of cavitation in the holes;

(e) Effects of spatial distribution within the spray;

(f) And Effects of coupling between spray parameters and droplet vaporization

Proper injector design can help to decrease the combustion duration and reduce hydrocarbon and smoke emissions. All these will eventually result in improvements to fuel economy (Colin R. Ferguson 1986,p.316).

## 6.2 NOZZLE DESIGN

Methods of distribution the fuel can be improved by the means of proper nozzle design. A thorough understanding of the dynamics of flows is important in the future development of engine with high-performance. Modelling nozzle flow is complicated; this investigation will use two-dimensional and three-dimensional models of nozzle flow to observe the effects of nozzle parameters and flow properties on the engine performance.

The knowledge of the flow characteristics of the injected fuel at the nozzle is a key issue. Viscosity of POME is the most significant of all liquid properties in the design because it can vary over an extreme range. Liquid viscosity resists surface formation. Nozzle may produce a mass of filaments if the viscosity is great enough; liquid viscosity is extremely sensitive to temperature and affects the spray characteristics.

The most important consideration in this thesis is the nozzle design. Different types of nozzles will behave differently. The internal geometry is the most important aspect as it holds the liquid. Three aspects for design are taken into account. First, the exit orifice ($d$), secondly, the volume of liquid contained in the nozzle ($V_{noz}$) and lastly the half cone angle of the geometry. The nozzle holder is the test tank that sets the outer dimensions.

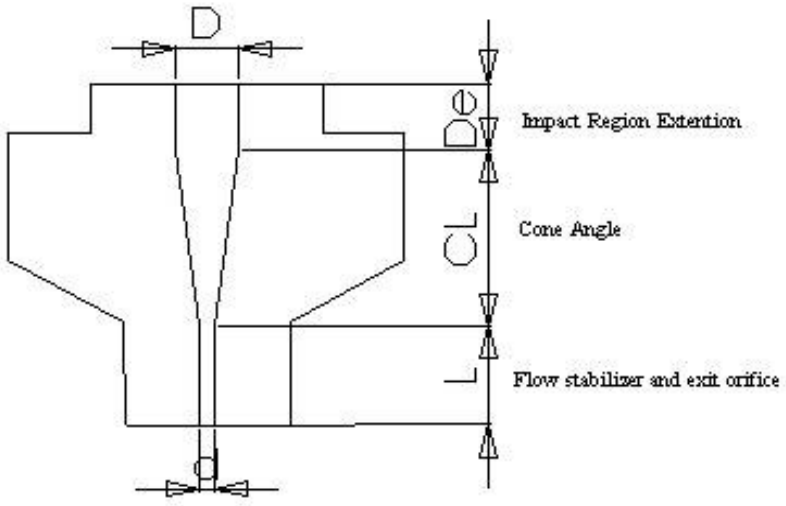


Figure 6.2 Schematic of nozzle internal geometry

The nozzle geometry is composed of three sections as shown in Figure 6.2.

### 6.2.1 Impact region extension.

This is the beginning of the nozzle geometry and it is set by the diameter of the pressure relief section, being 8.2mm (*D*).After this, there is a small length of straight section .This allows the projectile time to transfer all its momentum into the liquid before stopping. It was found from early nozzle design that if this section was not included (i.e. *De*=0), the speeds were low. This is due to the fact that the projectile could not instantaneously transfer its momentum to the liquid; therefore, little time is required (Sam Zakrzewski 2002).

### 6.2.2 Cone Angle

This section contains most of the volume of liquid and has the largest influence on the speed of the jet (Sam Zakrzewski 2002,p.25). It consists of a linear gradient converging from the entrance orifice (*D*) to the exit orifice diameter (*d*). It is known as a straight cone. The converging geometry acts as a venturi and accelerates the liquid as it moves towards the exit orifice (Mustafa Kamal 2000,p.21).The ratio between the *D* and *d* determines the liquid velocity. The convergence also acts as buffer to stop the progress of the projectile.

### 6.2.3 Flow Stabiliser and exit orifice

This region is a length of straight section with the diameter of the exit orifice (*d*). Its purpose is to streamline the accelerated fluid into a more uniform velocity field. The instabilities from the cone angle section are not propagated into the jet flow.

## 6.3 DESIGN CONSIDERATION

The most important consideration is the ratio of entrance orifice diameter to exit orifice diameter (*D:d*). Since the speed of the jet will be subsonic with respect to the liquid, it is a reasonable assumption to ignore the density fluctuations and assume that the flow through the nozzle is incompressible for a first order design. The conservation of continuity can be applied and jet velocities estimated using

$$A_D v_D = A_d v_d \tag{6.3.1}$$

The discharge coefficient ($C_D$) for this nozzle design is estimated at 0.68, which is acceptable for this type of conical nozzle.

The volume of the POME contained in the nozzle must be considered. When the projectile hits the packet, it must transfer all its momentum in an even repeatable manner. The mass of POME $(m_{POME})$ to mass projectile $(m_{\text{Proj}})$ ratio has a large influence on this consideration. If $(m_{POME})$ is larger than $(m_{\text{Proj}})$ the projectile is likely to bounce back. The ratio must be optimised to produce desired speed.

The cone angle $(\alpha)$ within the nozzle geometry is crucial. For a step angle, the jet is more likely to be faster. The liquid will find it harder to escape as it is pressed up against a steeper wall. The pressure in the liquid will increase at a greater rate and when finally released will produced a faster jet. The steeper wall is more likely to incur a reflected shock in the POME. This influences the jet generation characteristics.

The flow stabiliser acts as a minimal but significant effect on the jet speed and it also influences the shape and characteristics of the emerging jet. The important consideration is the ratio exit orifice diameter *d* to the flow stabiliser length (*L/d*). The larger the *L/d* ratio, the more stabilised the flow becomes and discontinues are not propagated into the flow. If *L/d* is large, friction will impede the jet speed. As indicated before, if *L/d* is too low, jet characteristics become inconsistent.

A limitation of nozzle is that the overall length of the nozzle $(De + CL + L)$ is constant for each design. This means that each of the three design considerations is dependent on each other. For constant *CL*, *De* will increase as *L* decreases and vice-versa. For constant *CL, L* and *De,* $\alpha$ will decrease as d increase (Mustafa Kamal 2000,p.5).

A number of nozzle designs are utilised with varying dimensions in order to generate the speed of the flow. Table 6.1 shows an outline of this.

Table 6.1 Various nozzle designs tested in 2-D

| Design No. | D(mm) | De(mm) | $\alpha$ | CL(mm) | L(mm) | d(mm) |
|---|---|---|---|---|---|---|
| D1 | 8.2 | 10 | 9.772 | 18 | 6 | 2 |
| D2 | 8.2 | 12 | 10.965 | 16 | 6 | 2 |
| D3 | 8.2 | 10 | 9.834 | 15 | 9 | 3 |
| D4 | 8.2 | 12 | 11.310 | 13 | 9 | 3 |

## 6.4 TYPES OF DESIGN

The types of nozzle design are the major concern in the project. Different types will behave differently. Two types of design under consideration are shown in Figure 6.3. The design varies on the size of holes, length of mixer over throat diameter (*L/D*), and the number of holes.

In solid stream nozzle, the liquid is pressed through around the hole, forming a solid stream. The flow rate is very sensitive to the edge shape, which can be sharp or round.

The solid nozzle can nearly achieve the maximum theoretical flow rate when designed with the correct liquid approached channel and radius. The maximum outlet velocity and subsequent impact on target surface can be achieved with this type of nozzle.

If the orifice is not properly shaped, a reduction in width of the resultant solid stream occurs; i.e. the diameter of the stream is not as large as the diameter of the orifice. A properly shaped orifice will produce a solid stream whose diameter equals the diameter of the orifice.

3-D models for two-nozzle designs having the same dimension were created. Designs are done only at the tip of the nozzle. Figure 6.3a shows nozzle with sharp edge with 45° taper while nozzle with rounded edge is shown in Figure 6.3b.

Figure 6.3 Different types of design on nozzle

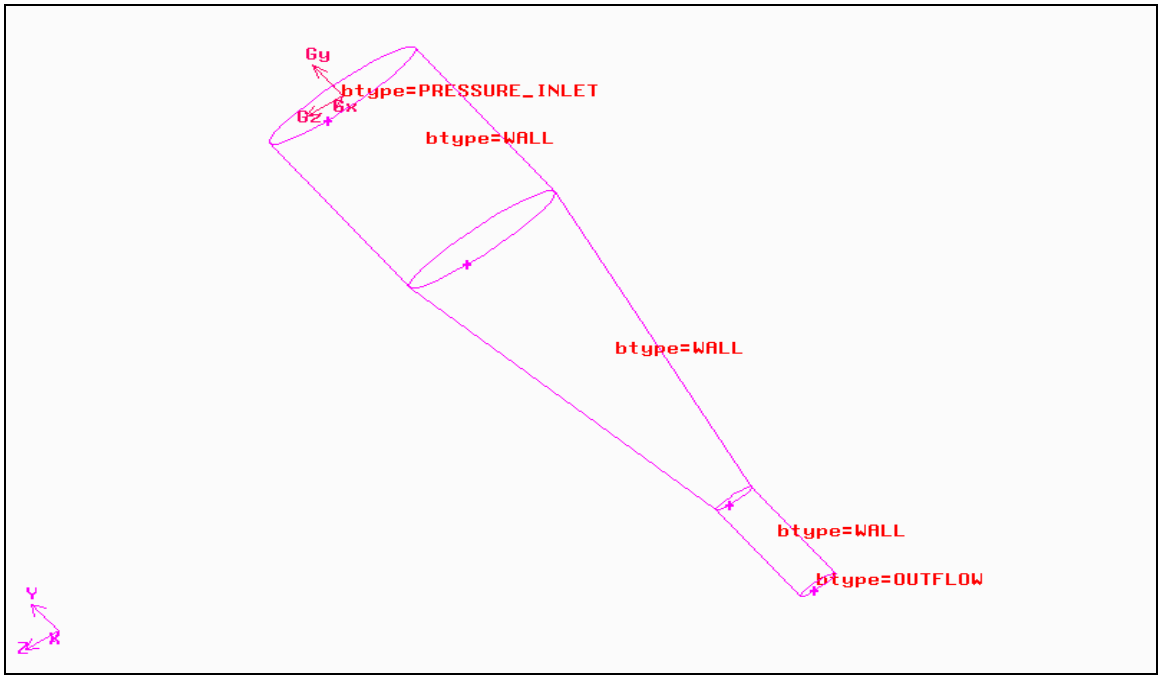


Figure 6.3a Sharp edge with taper

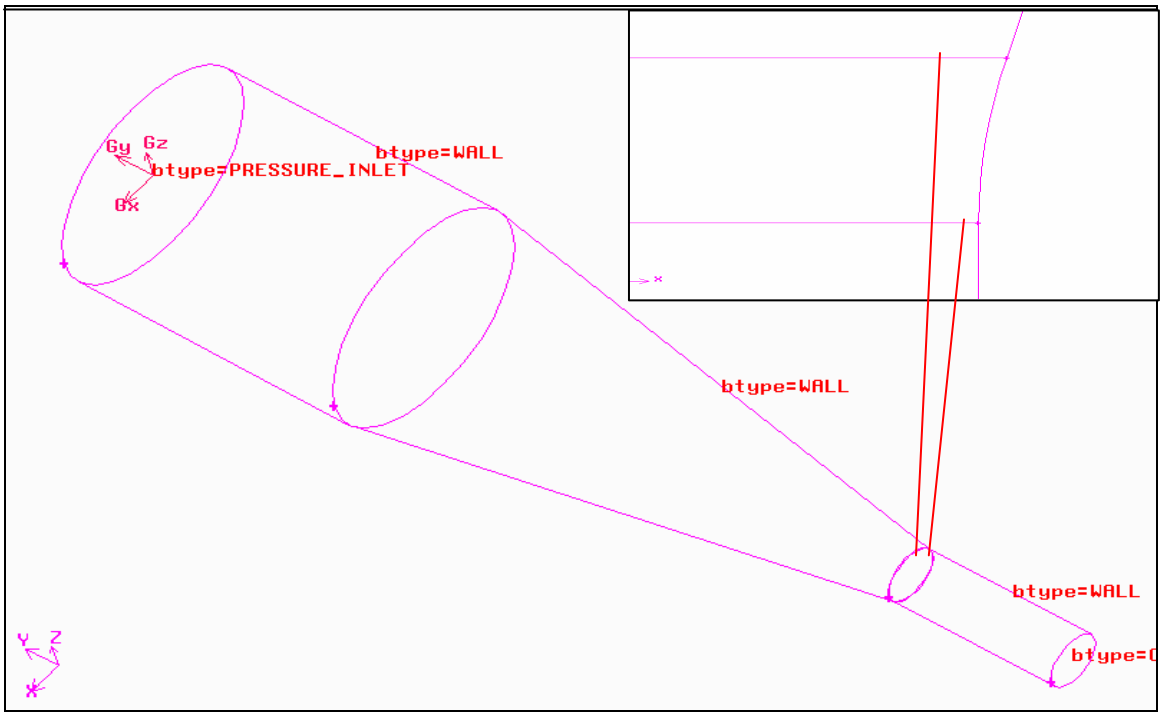


Figure 6.3b Rounded edge

## 6.5 THEORETICAL CALCULATION

For the ideal flow, the stagnation temperature, and pressure, $T_o$ and $p_o$ are related to the conditions at other locations in the mixer by the steady flow energy equation:

$$T_o = T + \frac{V^2}{2c_p} \tag{6.5.1}$$

and the isentropic relation

$$\left(\frac{T}{T_o}\right) = \left(\frac{p}{p_o}\right)^{\frac{\gamma-1}{\gamma}} \tag{6.5.2}$$

By introducing the Mach number $M = V/a$ where $a$ is the sound speed $\left(= \sqrt{\gamma RT}\right)$, the following equations are obtained;

$$\frac{T_o}{T} = 1 + \frac{\gamma-1}{2} M^2 \tag{6.5.3}$$

$$\frac{p}{p_o} = \left(1 + \frac{\gamma-1}{2} M^2\right)^{\frac{\gamma}{\gamma-1}} \tag{6.5.4}$$

The mass flow rate $\dot{m}$ is

$$\dot{m} = \rho A V \tag{6.5.5}$$

Assuming ideal gas flow, the above relations for $p$ and $T$ can be arranged as

$$\frac{\dot{m}_{ideal}\sqrt{\gamma R T_o}}{A p_o} = \gamma M \left(1 + \frac{\gamma - 1}{2} M^2\right)^{\frac{-(\gamma+1)}{2(\gamma-1)}} \tag{6.5.6}$$

or

$$\frac{\dot{m}_{ideal}\sqrt{\gamma R T_o}}{A p_o} = \gamma \left(\frac{p}{p_o}\right) \frac{1}{\gamma} \left\{ \frac{2}{\gamma - 1} \left[ 1 - \left(\frac{p}{p_o}\right)^{\frac{(\gamma-1)}{\gamma}} \right] \right\}^{\frac{1}{2}} \tag{6.5.7}$$

For given values of $p_o$ and $T_o$, the maximum mass flow occurs when the minimum throat velocity equals the velocity of sound. This condition is called chocked or critical flow. When the flow is chocked the pressure at the throat, $p_T$ is related to the stagnation pressure $p_o$ as follows:

$$\frac{p}{p_T} = \left(\frac{2}{\gamma + 1}\right)^{\frac{\gamma}{\gamma-1}} \tag{6.5.8}$$

This ratio is called the critical pressure ratio. For $(p_T / p_o)$ less than or equal to the critical pressure ratio,

$$\frac{\dot{m}_{ideal}\sqrt{\gamma R T_o}}{A p_o} = \gamma \left(\frac{2}{\gamma - 1}\right)^{\frac{(\gamma+1)}{2(\gamma-1)}} \tag{6.5.9}$$

The critical pressure ratio is 0.528 for $\gamma = 1.4$ and 0.546 for $\gamma = 1.3$

For a real gas flow, the discharge coefficient is introduced. For sub-critical flow, the real mass flow rate is given in terms of conditions at the minimum area or throat by

$$\dot{m}_{ideal} = \frac{C_d A_T p_o}{\sqrt{RT_o}} \gamma^{\frac{1}{2}} \left( \frac{2\gamma}{\gamma+1} \right)^{\frac{(\gamma+1)}{2(\gamma-1)}} \tag{6.5.10}$$

$$A_T = \pi d_o{}^2 n / 4 \tag{6.5.11}$$

Where:

$p_o$ = pressure at section 1

$p_T, A_T$ = pressure and area at section 2 ( throat)

$T_o$ = inlet temperature

$C_D$ = discharge coefficient of venturi

$m_{real}$ = mass flow rate of air

$d_o$ = orifice diameter

$n$ = number of orificies

$\gamma$ = pressure ratio

For the POME

$$\frac{p_1}{\rho f} - \frac{p_2}{\rho f} = \frac{V_f{}^2}{2} \tag{6.5.12}$$

Where:

$p_1$ = POME pressure

$p_2$ = pressure at the tip of the gas inlet

$\rho f$ = density of POME

$V_f$ = velocity of the POME

The mass flow rate of POME is given by

$$m_{xpome} = A_T V_f \rho_f$$

$$= A_T \left(2\rho_f (p_1 - p_2)\right)^{\frac{1}{2}} \tag{6.5.13}$$

$$m_{pomereal} = C_{Df} A_T \left(2\rho_f (p_1 - p_2)\right)^{\frac{1}{2}} \tag{6.5.14}$$

Where $C_{Df}$ is the discharge coefficient at the tip of the POME gas inlet

The air-fuel ratio can be calculated as:

$$A/F = m_{air} / \left(m_{pomereal} + m_{diesel}\right) \tag{6.5.15}$$

The above equations are only valid for a 3–D model. For the 2-D simplified model, the design is based on this following equation;

$$\frac{m_a}{m_f} = A/F \qquad (6.5.16)$$

Where:

$m_a$ = mass flow rate of air (kg/s)

$m_f$ = mass flow rate of fuel (kg/s)

$A/F$ = air –fuel ratio

## 6.6 CONCLUDING REMARKS

The important factors in generating a liquid jet of a certain speed have been illustrated with respect to the design of the internal nozzle geometry. The nozzle geometry has been refined and the mass of POME to mass projectile ratio has been found to influence the jet speed. The ratio in this case has been increased to unity value.

# CHAPTER 7

# RESULTS AND DISSCUSSION

## 7.1 INTRODUCTION

The parameters for the simulation are given in Table B.1 in Appendix B. These parameters and engine specification are used in the Matlab simulation. The simulation on the nozzle with different designs can be found in Figure F.1 to F.5 at Appendix F. The simulation is model in 2-D while the nozzle designs are 3-D. The flow characteristic of the injected fuel at the nozzle is a key issue. From the figures, the flow stream develops turbulent flow.

## 7.2 ENGINE PERFORMANCE

The result shows that there are two distinct trends for the engine when the speed is below or above 2000rpm.In terms of efficiency, specific fuel consumption is one of the best indicators of engine performance. In theory, specific fuel consumption will be high because of the pumping work, increase friction and heat transfer. These will reduce the efficiency of fuel consumption (Heywood 1989, p.105).

The specific fuel consumption for emulsion of POME compared to CDF is shown in Figure 7.1. There is a pattern showing that, between the range of 1800 n 2000 rpm, the fuel consumption is at it's maximum ;under that specific range, the fuel consumption of POME is relatively higher than CDF .As the speeds goes higher than 2000 rpm, the flow rate decreased. The relationship of volumetric fuel injection system, fuel density, viscosity, and heating value caused the above effects.

This result is comparable with the results by Talal et al, 1999 and Masjuki et al, 1998 where the rate of fuel delivery to engine speed was affected by specific gravity and viscosity of fuel. In general, emulsions of POME and CDF have similar characteristics.

Figure 7.2 shows the brake fuel consumption (BSFC) of POME compare to CDF. At low speed, BSFC of POME is greater than CDF. As the speed increases, BSFC of POME becomes lower compare to CDF at 2200 to 2500 rpm. However, BFSC increased for both fuels at high speed. This indicates good combustion of POME at the high-speed range.

Figure 7.3 shows the engine torque vs. speed for POME and CDF. The torque decreases as the engine speed increased. As the engine speed increases, the high initial torque will decrease. The maximum torque is reached for both fuels for speeds ranging from 1800-2000rpm. However POME produces a higher torque compared to CDF. Generally the torque reduces for every increase of speed. These apply to both fuels.

Brake power was calculated with the values of torque and engine speed. Figure 7.4 shows the brake power as a function of speed. From the figure, it shows that POME required a higher amount of brake power. For CDF, the brake power reached the maximum value for speed from 1800 to 2200 rpm. The torque and brake power produced by both fuels are comparable to each other

Brake thermal efficiency is the percentage ratio of the output and the input. In the simulation performed, the input is calculated with the values of fuel consumed and time taken. Figure 7.5 shows the efficiency in percentage vs. speed. When input power decreases, the efficiency of the engine increases. The POME graph illustrates that the efficiency varies and fluctuates between the speeds of 2000 to 2800 rpm. POME proves to be more efficient than CDF in this range. For CDF, the efficiency starts to drop when the speed decreases below 2000 rpm. We can also say that engine efficiency is proportional to combustion efficiency. To improve the thermal efficiency for braking, other factors such as input power, specific fuel consumption and exhaust temperatures need to be calibrated to their respective optimum values .


Figure 7.1 Fuel Consumption vs. Speed at 32kW load

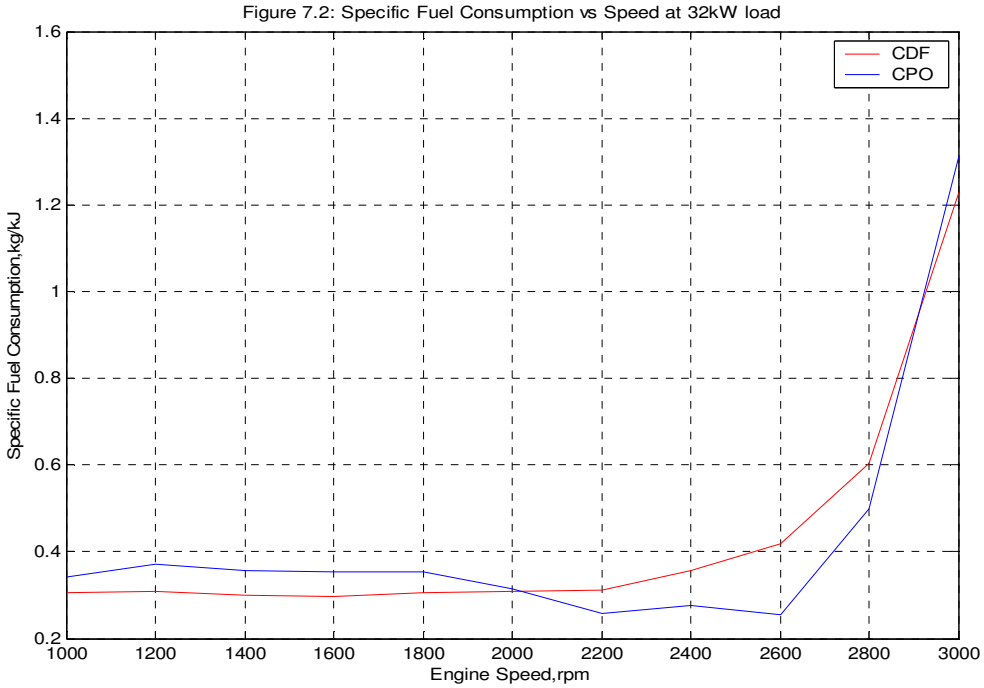


Figure 7.2 Specific Fuel Consumption vs. Speed at 32kW load

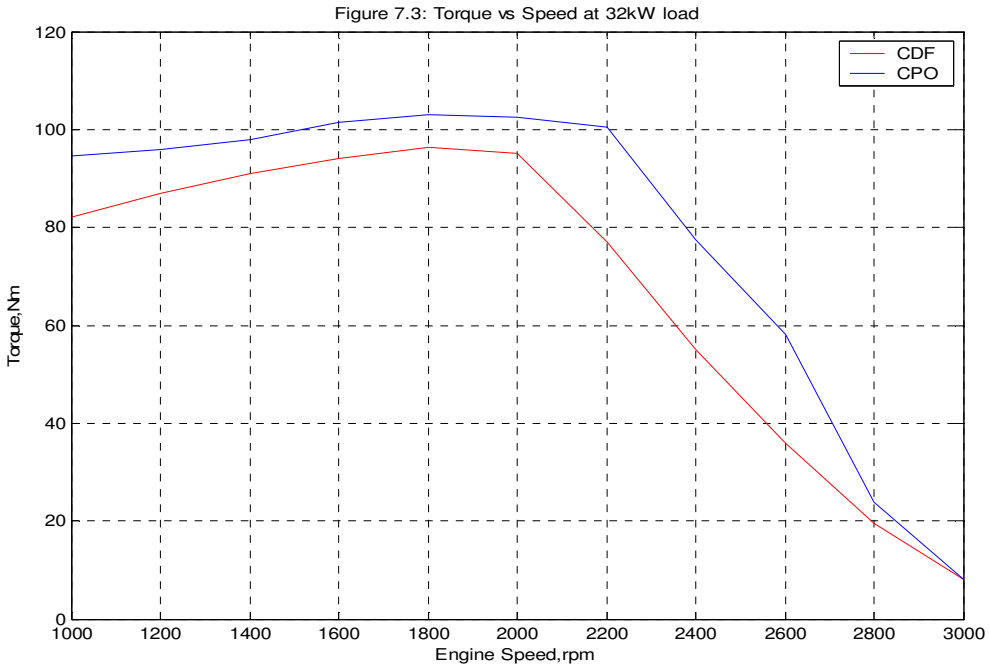


Figure 7.3 Torque vs. Speed at 32kW load

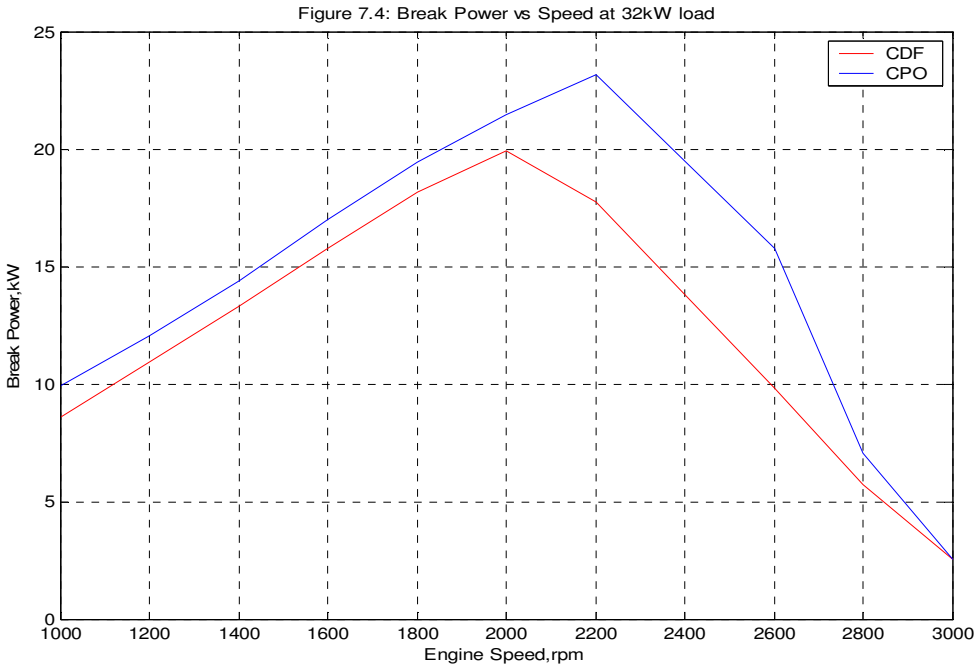


Figure 7.4 Brake Power vs. Speed at 32kW load

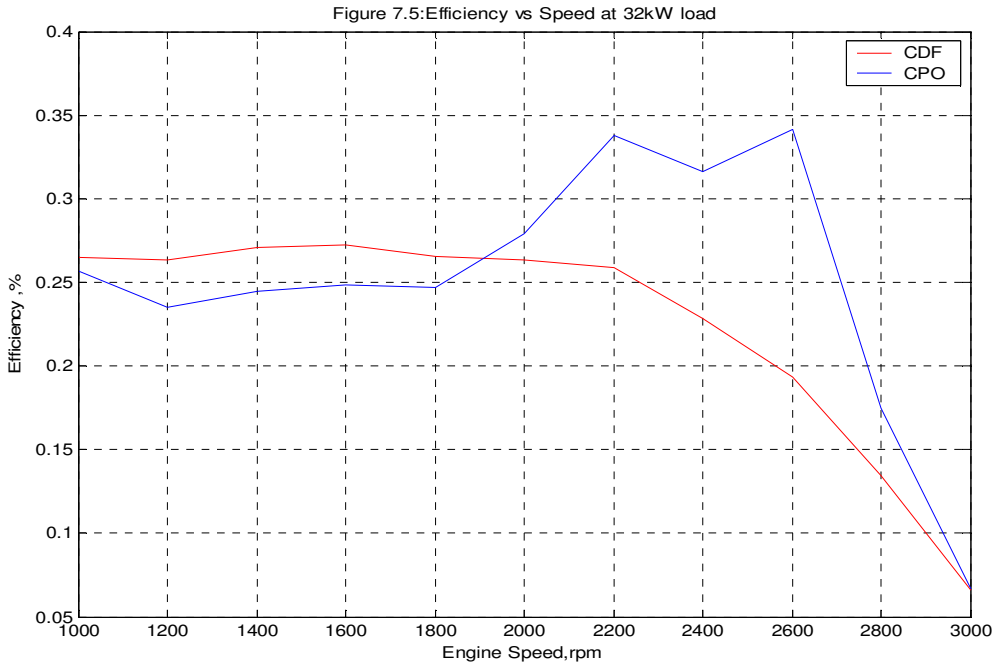


Figure 7.5 Efficiency vs. Speed at 32kW load

## 7.3 DERIVATIVE OF PRESSURE AND HEAT NET RESPECT TO CRANK ANGLE

The output here refers to the results of the program after evaluating the different conditions of different fuels. Below are the comparison graphs of $\frac{dP}{d\theta}$ versus θ for POME and CDF.

The output for CDF and POME:

SPECIFY THE ENGINE CHARACTERISTICS (POME)

Ratio of connecting rod to crank radius R=2.998888

Swept volume in m=0.000446

Compression ratio=13.397601

Overall heat input in Joule/rev=892.627236

Heat transfer coefficient in W/m^2.K=0.379421

SPECIFY THE ENGINE CHARACTERISTICS (DIESEL)

Ratio of connecting rod to crank radius R=2.998888

Swept volume in m=0.000446

Compression ratio=12.157840

Overall heat input in Joule/rev=892.627236

Heat transfer coefficient in W/m^2.K=0.379421

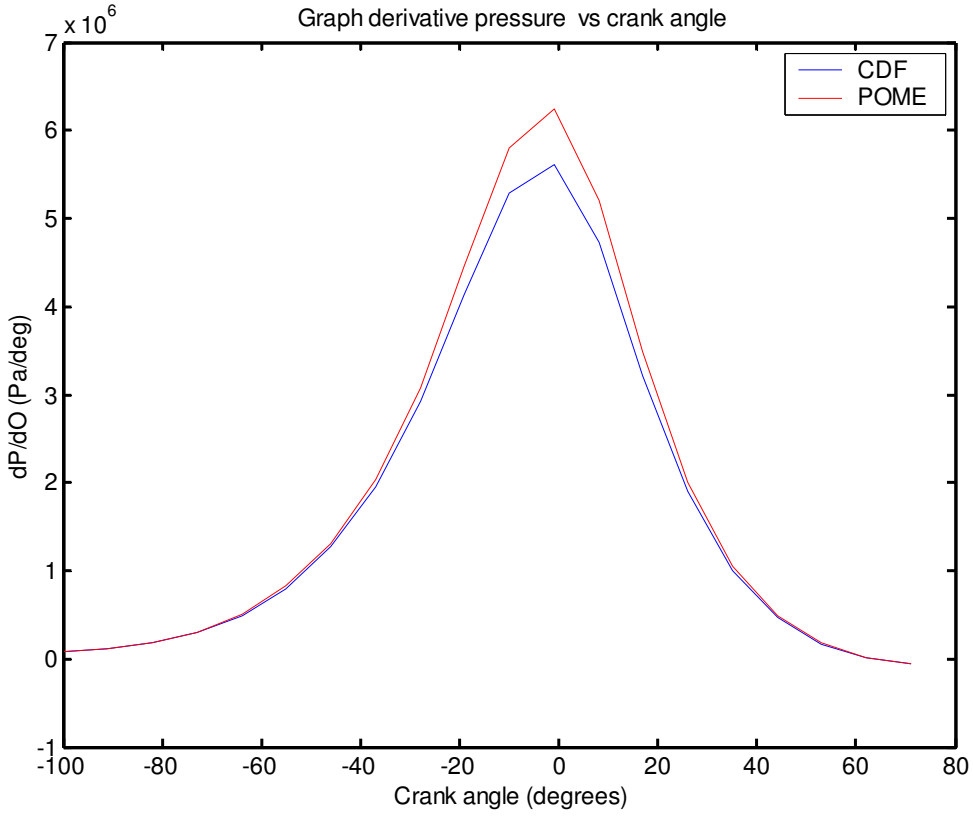


Figure 7.5 Graph derivative pressures vs. crank angle

Assumptions are made whereby cylinder charge is considered to behave as an ideal gas and no variation of cylinder mass due to blowby is considered. The engine used has a low blowby rate (C) in the order of 0.7% of the intake mass flow rate.

Below are the comparison graphs of $\frac{dQ_n}{d\theta}$ versus θ for POME and CDF.

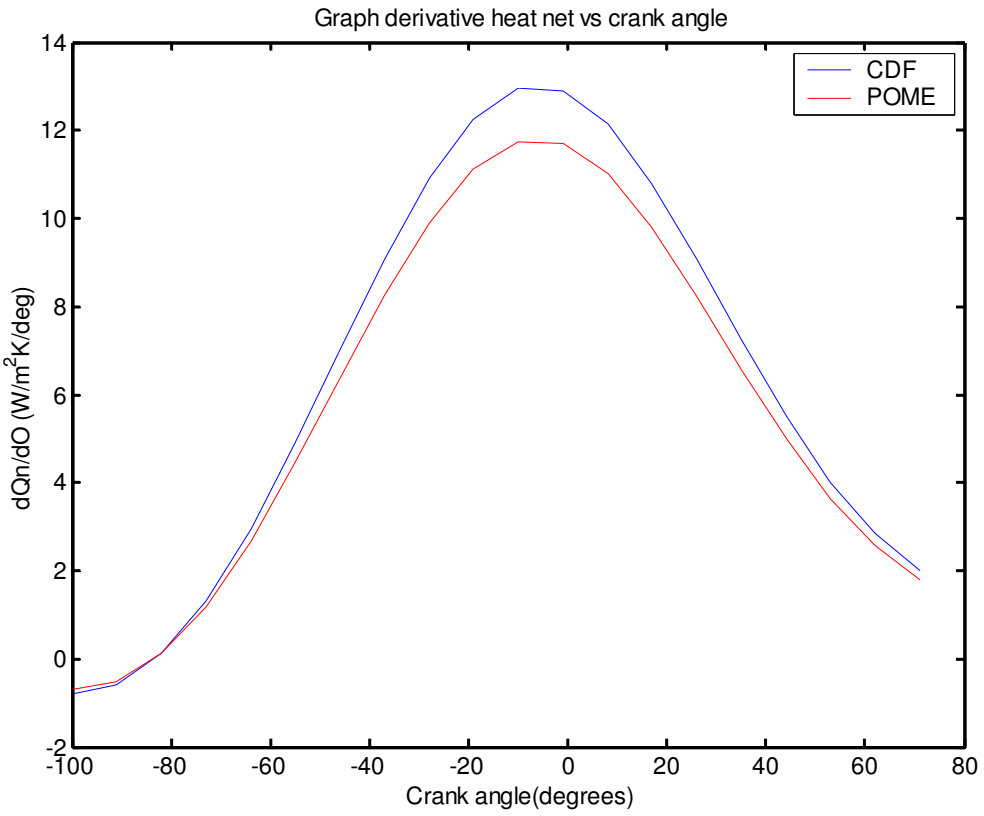


Figure 7.6 Graph derivative heat net vs. crank angle

Figure 7.5 shows the results of derivative pressures as a function of crank angle for POME and CDF. The area under the curve is the same. There is no effect on the cylinder pressure for both POME and CDF. This is model dependent; no worse case by assuming the system to be homogeneous.

Notice that POME fuel in the charge affects the value of the cylinder pressure compared to the one under normal CDF operation. Cylinder pressure under CDF fuel operation diverges from the respective values under POME operation. The lower cylinder pressures observed under POME fuel operation during the compression stroke are the result of the

lower specific heat capacity. During the initial stages of combustion, a similar effect is observed.

The total heat release curves in Figure 7.6 show that during the second phase of diffusion combustion, the total heat net rate under POME fuel operation is slightly lower compared to the CDF fuel operation. However, the effect on the cylinder pressure is small in the expansion stroke.

The characteristic of the system at each compression ratio is justified through investigation of the insertion of plates, modifying the piston groove and modifying the connecting rod. This is done by modifying the bore, stroke, connecting rod, and crank radius in the engine specification. Different types of graph ($\frac{dP}{d\theta}$ versus $\theta$ and $\frac{dQ_n}{d\theta}$ versus θ) are produce at different compression ratio.

## 7.4 EFFECTS ON NOZZLE

### 7.4.1 Effect of length of nozzle over exit orifice diameter (*L/D*)

*L/D* is defined as the length of the nozzle over the diameter of the exit orifice. In simulation, a set of 4 *L/D ratios* are used. Figures F.9 to F.12 in appendix F show that as *L/D* increases, the turbulent flow becomes well developed inside the nozzle. Figures F.21 to F.24 in appendix F show that turbulent flow is developed almost throughout the nozzle. The swirl is only developed at the upper region, not the entire nozzle. From these figures, it can be said that increase in *L/D* gives better efficiency.

For all the above simulations, the upstream pressure was set at 170bar. The first point to note about varying *L/D* is that it has less of an effect on the discharge than corner radius, as can be seen in Figures F.21 to F.24. There is a very slight downward trend in the data. One might expect the coefficient of discharge to drop significantly with length, but the throat conditions somehow limit the flow through the nozzle.

### 7.4.2 Effect of POME Pressure

The inlet pressure affects the flow of fuel. As the pressure increases, the velocity of the flow increases. POME pressure affects the mass flow rate. In theory, the density of POME is considered to be 0.870kg/$m^{3.}$

The nozzle part of the engine can be modified to produce better result. POME has slightly different physical properties such as viscosity and density. A better atomization will result in better combustion. Atomization can be improved by increasing the injection pressure or decreasing the orifice of the nozzle. Both method will increase the velocity of the injected fuel into combustion chamber and increase the atomization level.
(Refer to Figures F.51 to F.78 in appendix F)

### 7.4.3 Flow Analysis

The results for the flow field for the designs are shown in Figures F.25 to F.28 (2D CDF), Figures F.75 to F.78 (2D POME), Figures F.42 (3D CDF) and Figures F.109 (3D POME). The figures show the streamlines and velocity vectors in a region just downstream of a sloping surface for the design with the steep slope. Note that the flow at the nozzle inlet is uniform and the boundary layers that grow from the outer and inner walls never merge.

Thus, as far as the inner wall is concerned, the outer wall creates a variable pressure gradient for its free stream flow (i.e., the flow between the two boundary layers on the two walls drives the boundary layers). Since the area between the walls decreases in general, the pressure gradient induced is a favourable one. With a favourable pressure gradient, the free stream velocity increases steadily.

# CHAPTER 8

# CONCLUSION AND RECOMMENDATION

The objective of the project is to study the engine performance using Palm Oil Methyl Ester (POME) and compared the results to a system that uses 100% Conventional Diesel Fuel (CDF). Generally, the results show that the diesel engine fuelled by POME results in different trends at high and low engine speeds.

From the results, it can be concluded that POME can be used as fuel additive in an unmodified engine. The effects of POME on the engine performance are minimal. POME shows its potential as an alternative fuel in conventional combustion engine. The analysis of palm oil in diesel engine has shown a reduction of the emission gases compared to conventional diesel system.

Designing nozzle for a POME engine is not an easy task. The current simulated results have not been validated with experimentation. The simulation indicates that the best design is a nozzle with large *L/D* ratio and smaller holes size. These parameters help the fuel flow. The project establishes the basic simulation with different fuel. This is crucial because the behaviour of the flow could vary with the boundary conditions.

Future study can be performed based on methyl ester from other vegetable oil such as coconut oil, soybean oil, sunflower oil etc. Talal et al, 1993, have done the test by using waste cooking oil methyl ester as a fuel in diesel engine. The performance and emission aspect for vegetable oil can be compared and as a result, the best alternative was chosen. Future work could also involve gathering more exhaust emission data, such as BOSCH filter set-up for Smoke Number, Hart ridge Opacity and BTX reading. Many local researchers especially from PORIM have conducted various tests on palm oil.

Many areas can be explored from this project. This includes optimization of the nozzle design. The simulation could emphasize more on the 3-D model. The number of holes is still an unresolved issue for nozzle optimization. This project only uses 1 hole with a size of 0.2mm. It will be interesting to investigate the effects as the number holes and their sizes change. Furthermore, the distribution of the holes also can be varied. The shapes of the holes may also play an most important role.

# REFERENCES

1. Abd. Halim Shamsuddin, 1989, 'Palm Oil Products and Wastes as Alternative Energy Sources', RERIC International Energy Journal, vol 11,No. 2,December 1989, pp. 25-33.

2. Ahmad Hj Hitam, and Salmah Jahis, 1995.Preliminary observations of using palm oil as fuel for cars fitted with Elsbett engine.

3. Arthur W.Judge, 1967,'SCNCER, Technical Information ', pp.1021

4. Choo Yuen May, Ma Ah Ngan, and Yusof Basiron, 1995, 'Production and Evaluation of Palm Oil Methyl Esters as Diesel Substitute', Elaeis Special Issue, November 1995, pp. 15-25.

5. Colin R. Ferguson, T. 1986, Internal Combustion Engines, Applied Thermosciences , John Wiley & Sons, New York.

6. C.W. Yu, S.Bari, and A.Ameen, 2002, 'A comparison of combustion characteristics of wast cooking oil l with diesel as fuel in a direct injection diesel engine', Proc. Instn Mech Engrs, vol 216, Part D, pp. 237-242.

7. Gurmit Singh, Lim Kim Huan, Teo Leng, David Lee Kow1999, Oil Palm and the Environment a Malaysian Perspective, Malaysian Palm Oil Grower's Council, Malaysia.

8. Heywood, J.B., 1988,Internal Combustion Engine Fundamentals , McGraw-Hill

9. H. Masjuki, A.M. Zaki, and S.M. Sapuan, 1993, 'A Rapid Test to Measure Performance, Emission and Wear of a Diesel Engine Fueled with Palm Oil Diesel', JAOCS, vol 70,No. 10,October 1993, pp. 1021-1025.

10. H. Masjuki, M.Z. Abdulmuin, H.S.Sii, 1996, 'Investigation on preheated palm oil methyl esters in the diesel engine', Proc. Instn Mech Engrs, vol 210, Part A, pp. 131-138.

11. H.H Masjuki, M.A. Kalam, M.A. Maleque, A. Kubo, and T.Nonaka,2000, 'Performance , emissions and wear characteristics of an indirect injection diesel engine using coconut oil blended fuel' , Proc. Instn Mech Engrs, vol 215 ,Part D, pp. 393-402

12. Hitam Hj. A, and Jahis S., 1995, 'Preminary Observations of using Palm Oil as Fuel for Cars fitted with Elsbett Engine', Elaeis Special Issue ,Palm Oil Research Institute on Malaysia (PORIM), pp. 92- 96.

13. Lowry et al 1990,'The main issue On Crude Oil',pp.97

14. M.A Faud, A.R.Rohana & B.G. Chua 1997,' Oil Palm and the Environment a Malaysian Perspective', Malaysian Palm Oil Grower's Council, Malaysia, pp.125

15. Masjuki Hj. Hassan , and Baharuddin Ali, 1997, 'Characteristics of Lubricants Contaminated with Palm Oil Diesel', Jurnal Institusi Jurutera Malaysia, vol 44 , pp. 35-42.

16. Mohamed M. El-Awad, and Talal F. Yusaf, 2002, 'Crude Palm Oil as a Fuel Extender for Diesel- Engines in Malaysia', pp. 1-11.

17. Picken et al ,1986 'Crude Oil as a Fuel Extender for Diesel- Engines', pp. 1-11.

18. Prof. Dr. Ronald Meyer- Piftroff, 1995, 'Biofuel: Technical, Economic and Environmental Impacts', Elaeis Special Issue, Palm Oil Research Institute on Malaysia (PORIM), pp. 1-11.

19. Schafer ,1995,'Petroleum in Malaysia',pp.75.

20. S. Bari, C.W. Yu, and T.H.Lim ,2002, 'Performance deteriotation and durability issues while running a diesel engine with crude palm oil' , Proc. Instn Mech Engrs, vol 216 ,Part D, pp. 785-792.

21. S.M. Sapuan, H. Masjuki, A. Azlan,1996, 'The use of palm oil as diesel fuel substitute', Proc. Instn Mech Engrs, vol 210 ,Part A , pp. 47-53.

22. Ulf Schuchardt[a], Richard Sercheli[a], and Rogerio MAtheaus Vargas, 1997, 'Transesterification of Vegetable Oils: a Review', J. Braz.Chem.Soc, vol 9, 1998, pp. 199-210.

# BIBLOGRAPHY


1. Abd. Halim Shamsuddin, 1989, 'Palm Oil Products and Wastes as Alternative Energy Sources', RERIC International Energy Journal, vol 11,No. 2,December 1989, pp. 25-33.

2. Advanced Simulation Technology, Inc., 2004 'CFD Nozzle Analysis', viewed 18 March 2004, < http://www.cpottersimtec.com.html>

3. Ahmad Hj Hitam, and Salmah Jahis, 1995.Preliminary observations of using palm oil as fuel for cars fitted with Elsbett engine.

4. A.H.M. Eisenga,1999 ' Application of CFD in the industry CFD for process-technological flow problems 'viewed 15 February 2004, <http://www.cyclone.nl/>

5. Alex Spataru, Alina Kulilowski-Tan, Claude Romig, and Amy Hall, 1995, 'Exhaust Emissions and Engine Performance from the use of Soya Methyl Ester Blended with ARD #2 Diesel in a 6V92TA MUI Engine', PORIM International Biofuel Conference, Palm Oil Research Institute of Malaysia, Langkawi, pp. 1- 31.

6. Antonio Zamora ,2003 'Fats, Oils, Fatty Acids, Triglycerides – Chemical Structure' viewed 8 March 2004,<http://www.scientificpsychic.com/index.html>

7. Autohaus AZ, 2002 'Fuel Pumps, Fuel Injection.' viewed 8 March 2004, <http://www.trinbagoauto.com/ >

8. Biofuel Conference, Palm Oil Research Institute of Malaysia, Langkawi, pp. 8- 10.

9. Baharuddin bin Ali, Abdul Halim, and Fuad Bin Abas, 1992, 'Development in Automobile Engine Technology', Second National Conference, Thermal Engineering and Sciences.

10. Baharuddin bin Ali, Jaya Phatap, and Masjuki Hj. Hassan ,1989, 'Characterisation of Palm Oil Diesel (POD) Open Flames', Second National Conference, Thermal Engineering and Sciences, pp. 108-118.

11. Bob Hartzler,2003 'Effect of nozzle type on spray retention and absorption' viewed 8 March 2004,< http://www.weeds.iastate.edu/>

12. Carl L. Alsberg and Alonzo E. Taylor 'The Fats and Oils: a General View' viewed 8 March 2004,< http://www.journeytoforever.org/index.html>

13. Carl Ollivier-Gooch ,2003' Intro to Computational Fluid Dynamics'viewd 22 March 2004,< http://www.mech.ubc.ca/~mech380/notes/node45.html>

14. Chhay Ty,2003 'Palm *(Elaeis guineensis*) oil and cassava foliage as feed resources for growing pigs; a review of the literature' viewed 15 March 2004, <http://www.mekarn.org/msc2001-03/theses03/chhaytylitrev.htm>

15. Choo Yuen May, Ma Ah Ngan, and Yusof Basiron, 1995, 'Production and Evaluation of Palm Oil Methyl Esters as Diesel Substitute', Elaeis Special Issue, November 1995, pp. 15-25.

16. C.K. Chang, 1992,'Designed Trends and Fuels Development for Gasoline Engines', Shell Malaysia Trading Sendirian Berhad, pp. 1-12.

17. Coanda Research and Development Corporation , 2003 'Jet and Spray Nozzle Design'viewed 8March 2004,< http://www.coanda.ca/index.html>

18. Colin R. Ferguson, T. 1986, Internal Combustion Engines, Applied Thermosciences , John Wiley & Sons, New York.

19. C.W. Yu, S.Bari, and A.Ameen, 2002, 'A comparison of combustion characteristics of wast cooking oil l with diesel as fuel in a direct injection diesel engine', Proc. Instn Mech Engrs, vol 216, Part D, pp. 237-242.

20. Datuk Dr. Yusof Basiron, 2004 'Overview of The Malaysian Oil Palm Industry 2003' viewed 15 March 2004, < http://www.mpod.com.my>

21. Dean R. Eklund,1994 'Fuel/Air Mixing in a Scramjet Combustor' viewed 8 March 2004, < http://www.nas.nasa.gov/>

22. Dennis R. Gardisser, Robert E. Wolf, John Slocombe, and Bryan W. Shaw, UniversityNozzle Types for Boom Sprayer Application of Crop Protection Products' viewed 15 March 2004, <http://www.uaex.edu/Other_Areas/publications/default.asp>

23. Dott.Roberto Varese, 1995, 'Integrated production of Bio-Diesel Esters and Glycerol',SVECO, pp. 1-10.

24. David Schmidt,2000 'The Cavalry Page' viewed 8 March 2004, <http://www.erc.wisc.edu/~dschmidt/index.html>

25. Expenditures and Activities of Cairns Group Countries Malaysia , viewed 8 March 2004, <http://www.fas.usda.gov/>

26. Fitrian A and Isrr Ardiansyah,2003 'Palm Oil - Search continues for sustainable resource development' viewed 8 March 2004, <http://www.ecologyasia.com/index.htm>

27. Fuel Injection Data Bryce-Berger Type Coding Information , viewed 8 March 2004, <http://www.oldengine.org/members/diesel/Injection/front.htm>

28. Fuel Injection Systems , viewed 8 March 2004, <http://www.mentor.com/mentorsearch/>

29. Forman A. Williams 1994, Combustion Theory, 2nd edition, Addison Wesley, Priceton University, United State of America.

30. FOSFA International ,2001 'Palm Kernel Oil' viewed 15 March 2004, , viewed 8 March 2004, <http://www.fosfa.org/index.htm >

31. Full Cone Nozzle Selection , viewed 8 March 2004, < http://www.fluidproducts.com/nozzleindex.htm >

32. Gurmit Singh, Lim Kim Huan, Teo Leng, David Lee Kow1999, Oil Palm and the Environment a Malaysian Perspective, Malaysian Palm Oil Grower's Council, Malaysia.

33. H.H Masjuki, M.A. Kalam, M.A. Maleque, A. Kubo, and T.Nonaka,2000, 'Performance , emissions and wear characteristics of an indirect injection diesel engine using coconut oil blended fuel' , Proe Instn Mech Engrs, vol 215 ,Part D, pp. 393-402.

34. Hj Masjuki, M.Z.Abdulmuin, and H.S.Sii, 1995, 'Investigation of Palm Oil Diesel Emulsion as Fuel Extender for Diesel Engine', PORIM International.

35. Hitam Hj. A, and Jahis S., 1995, 'Preminary Observations of using Palm Oil as Fuel for Cars fitted with Elsbett Engine', Elaeis Special Issue ,Palm Oil Research Institute on Malaysia (PORIM), pp. 92- 96.

36. Hj. Ismail Hashim 1992, 'Energy and the Environment', Second National Conference, Thermal Engineering and Sciences, pp. 1-12.

37. H. Masjuki, M.Z. Abdulmuin, H.S.Sii, 1996, 'Investigation on preheated palm oil methyl esters in the diesel engine', Proe Instn Mech Engrs, vol 210, Part A, pp. 131-138.

38. H. Masjuki, A.M. Zaki, and S.M. Sapuan, 1993, 'A Rapid Test to Measure Performance, Emission and Wear of a Diesel Engine Fueled with Palm Oil Diesel', JAOCS, vol 70,No. 10,October 1993, pp. 1021-1025.

39. Holley Fuel Injection Terms & Definitions , viewed 8 March 2004, <http://www.holley.com/hioctn/HomePage/TofC.html>

40. H. S. Bean., 1991 'Nozzle Flowmeter Calculation for Liquids. ISO-5167 equation.' viewed 8 March 2004, < http://www.lmnoeng.com/>

41. Husna Kassim , Mariani Osman , and Hamzah Abdul Hamid,1995, 'Biofuel : Impact on Environment', PORIM International Biofuel Conference, Palm Oil Research Institute of Malaysia, Langkawi, pp. 1-17.

42. ljaya , 2001 'Dynamic analysis of the combustion cycle' viewed 15 March 2004, < http://www.oscillatorengine.com/index.htm>

43. Ismail B. Celik, Allen E. Badeau Jr., Andrew Burt and Sherif Kandil,2000 'A Single Fluid Transport Model For Computation of Stratified Immicible Liquid- Liquid Flows' viewed 8 March 2004,< http://www.wvu.edu.com>

44. J. Chomiak, A.K. Gupta , and D.G. Lilley 1989,Energy & Engineering Science Series, Abacus Press/ Gordon & Breach Science Publishers, Billings & Son Ltd, Worcester, United Kingdom.

45. Jim Coal Josh ,2003 'Madisons Convert program Fundamentals of 4 Stroke/Cycle Piston Engine Performance'viewed 14 Jan 2004 , <http://home.att.net/~jroal/perftheory.htm>

46. John Roach, 2003 'Vegetable Oil—The New Fuel?' viewed 8 March 2004, <http://news.nationalgeographic.com/index.html>

47. Lewa Pardomuan ,2001 'Malaysia launches palm-fuel burning, seeks more clients' viewed 8 March 2004, < http://forests.org/ >

48. Long Term Benefits from Oil Palm Biomass , viewed 8 March 2004, < http://forests.org/>

49. Low Emissions Fuel Injector , viewed 8 March 2004, < http://www.cfdrc.com/>

50. Malaysia Palm Oil at Glance , viewed 8 March 2004, <http://www.mpopc.org.my/abtegfu2.htm#The Palm Oil Industry - A Brief Introduction>

51. Malaysia's Palm Oil Registration and Licensing Authority provides statistics and prices, viewed 8 March 2004, < http://161.142.157.2/home2/home/p77.htm>

52. Masjuki Hj. Hassan , and Baharuddin Ali, 1997, 'Characteristics of Lubricants Contaminated with Palm Oil Diesel', Jurnal Institusi Jurutera Malaysia, vol 44 , pp. 35-42.

53. Masjuki Hj. Hassan, and Baharuddin bin Ali,1989, 'Effects of Engine Lubricants on The performance Cylinder Engine', Second National Conference, Thermal Engineering and Sciences, pp. 29-38.

54. Maria da Grada Carvalho, Woodrow A. Fiveland, F.C. Lockwood , and Christos Papadopoulous 1999, Clean Combustion Technologies Part A, Gordon & Breach Science Publishers.

55. Maria da Grada Carvalho, Woodrow A. Fiveland, F.C. Lockwood , and Christos Papadopoulous 1999, Clean Combustion Technologies Part B, Gordon & Breach Science Publishers

56. Mark Bellis,1999 'Vegetable Oil and Biodiesel' viewed 8 March 2004, <http://www.veggievan.org/ >

57. Matthew Ryan 2000 'Deflection, breakdown and impact of a liquid jet in an air crossflow', viewed 14 Jan 2004,<http://www.CFDjetresearch.htm>

58. Mohd Ariffin, and Baharuddin bin Ali 1992, 'Alternative Automotive Fuels for Malaysia', Second National Conference, Thermal Engineering and Sciences.

59. Mohamed M. El-Awad, and Talal F. Yusaf, 2002, 'Crude Palm Oil as a Fuel Extender for Diesel- Engines in Malaysia', pp. 1-11.

60. M. Pourkashanian ,1997 'Theoretical and experimental investigations into low NOx oxy-fuel burner design' viewed 8 March 2004, <http:///fuel%20injection/lnox.html#top>

61. ONERA,2001 'CARS Technique Applied to Dynamic Flames and Turbulent Jets' viewed 15 March 2004,< http://www.onera.fr/english.html>

62. Palm Oil Industry in Malaysia viewed 15 March 2004, <http://www.malaysiainformation.com/index.htm>

63. Paul Grimshaw,1998 ' Selecting Correct Fuel Injectors for B21F Engines' viewed 8 March 2004,< http://www.telusplanet.net/Volvo_Books/home.html>

64. Prof. Dr. Ronald Meyer- Piftroff, 1995, 'Biofuel: Technical, Economic and Environmental Impacts', Elaeis Special Issue, Palm Oil Research Institute on Malaysia (PORIM), pp. 1-11.

65. Reuters, 2002 'Malaysian palm oil futures steadier at close' viewed 15 March 2004,< http://wardsauto.com/home/index.htm>

66. Richard E. Klabunde, Ph.D.,2004 'Cardiovascular Physiology Concepts-Turbulent Flow' viewed 8 March 2004, <http://www.cvphysiology.com/index.html>

67. ROMCONVERT,2003 'An experimental and analytical study of engine fuel spray atomization quality' viewed 15 March 2004, < http://romconvert.kappa.ro/home-e.html>

68. Robert Iseli, 1998 'Oil Palm - Palm Oil' viewed 8 March 2004, <http://www.agua.ch/index.html>

69. Robert W. Weeks and John J. Moskwa,2000 'Engine and Control System Models' viewed 8 March 2004,< http://www.simcar.com/literature/sae950417/sae950417.htm>

70. S. BAri, C.W. Yu, and T.H.Lim ,2002, 'Performance deteriotation and durability issues while running a diesel engine with crude palm oil' , Proc. Instn Mech Engrs, vol 216 ,Part D, pp. 785-792.

71. S.M. Sapuan, H. Masjuki, A. Azlan,1996, 'The use of palm oil as diesel fuel substitute', Proc. Instn Mech Engrs, vol 210 ,Part A , pp. 47-53

72. Sophie Labrousse / Etienne Poitrat,1998 'Biofuels for transport : Environmental impact of Rape Methyl Ester (Life Cycle Analysis)' viewed 8 March 2004, <http://www.eeci.net/>

73. Spray Nozzle , viewed 8 March 2004,< http://www.fluidproducts.com/>

74. Stan Spak, 2001 Bulletin, 'Malaysia: Palm Oil Situation and Outlook' vol 14, no. 15, viewed 8 March 2004, item: SSN 1494-1805 AAFC No. 2081/E.

75. The Malaysian Palm Oil Board annual statistics for crude palm oil , viewed 8 March 2004, <http://porim.gov.my/>

76. The Palm Oil Refiners Association of Malaysia ,viewed 8 March 2004, <http://www.poram.org.my/main.html>

77. The Scottish Crop Research Institute, 'Triacylglycerols- Structure , Composition and Analysis' viewed 8 March 2004,< http://www.lipid.co.uk/infores/>

78. Thomas Bouché, Michael Hinz, Detlef Hieber, Helmut Tschöke ,2003 'Effect of Different Vegetable Oil Properties on Combustion and Pollution Formation in a DI Diesel Engine' viewed 8 March 2004, < http://www.wtz.de/>

79. Tom Benson,2004 'Density' viewed 8 March 2004, <http://www.lerc.nasa.gov/WWW/K-12/index.html>

80. T.S.Tang, Hj. Ahmad Hitam, and Yusof Basiron ,1995, 'Emission of Elsbett Engine using APlm Oil Fuel', PORIM International Biofuel Conference, Palm Oil Research Institute of Malaysia, Langkawi, pp. 1-26.

81. Turbine and Nozzle Effects on Emissions , viewed 8 March 2004, <http://www.grida.no/climate/ipcc/aviation/020.htm>

82. Turns S.R 1996, An Introduction to Combustion: Concepts and Applications, McGraw-Hill, New York.

83. Twidell , J. & Weir, T. 1986, Renewable Energy Resources, E and F N Spon Ltd, University Press, Cambridge.

84. Ulf Schuchardt[a], Richard Sercheli[a], and Rogerio MAtheaus Vargas, 1997, 'Transesterification of Vegetable Oils: a Review', J. Braz.Chem.Soc, vol 9, 1998, pp. 199-210.

85. Universal Nozzle Calculator , viewed 8 March 2004, <http://www.pveng.com/index.htm>

86. W. Addy Majewski,2002 'Biodiesel' viewed 8 March 2004, <http://www.DieselNet.com.>

87. William J. Devenport ,1998'Compressible Aerodynamics Calculator' viewed 8 March 2004, < http://www.aoe.vt.edu/~devenpor/aoe3114/calch.html>

88. Zakrzewski, Sam ,2002 ' A Numerical and Experimental Investigation of High-Speed Liquid Jets - Their Characteristics and Dynamics' viewed 15 February 2004,< http://www.library.unsw.edu.au/~thesis/adt-NUN/uploads/approved/adt-NUN20021108.042745/public/01front.pdf>

89. Zulkifli Idris,1999 'Effluent Related Fee in the Palm Oil Industry of Malaysia' viewed 8 March 2004, < http://www.unescap.org/drpad/vc/index.htm>

90. 2003'Country Brief Analysis: Malaysia' viewed 8 March 2004, <http://www.eia.doe.gov/>

# APPENDIX A

## PROJECT SPECIFICATION

University of Southern Queensland

FACULTY OF ENGINEERING AND SURVEYING

**ENG 4111/4112 Research Project**
**PROJECT SPECIFICATION**

FOR: **CHEAH, Siew Lee**

TOPIC: ANALYSIS ON ENGINE PERFORMANCE USING PALM OIL METHYL ESTER

SUPERVISORS: Dr. Fok Sai Cheong (USQ) and
Dr. Talal Yusaf (UNITEN)

ENROLMENT: ENG 4111-S1, D, 2004
ENG 4110-S2, D, 2004

PROJECT AIM: The project aims to investigate the palm oil flow through the engine and the viscosity effects on the fuel injection system when palm oil and methyl ester are used.

PROGRAMME: **Issue A, 20 March 2004**

1. A Literature review on the historical background of using palm oil as an alternative fuel in Malaysia.

2. Study the chemical and physical properties of palm oil, gasoline and diesel. This will help to study the comparison of different fuel.

3. Theoretical study on the effect of using palm oil as an alternative fuel on engine parameters including heat transfer, combustion and emission, theory related to turbulent flow and viscosity.

4. Develop a Matlab program to calculate the heat and mass transfer in the combustion chamber using palm oil.

5. Develop a 2-D CFD simulation model using FLUENT to investigate the effect of viscosity on the fuel injection system (notably the nozzle). This will give a clear picture on the swirl ratio and the degree of turbulent with the new fuel.

6. A 2D CFD model will be developed to correlate the palm oil viscosity with different fuel tank temperature. Analytical calculation will be used for verification purposes.

AGREED:

_____(Student)_____,_____(Supervisors)

___/___/___ ___/___/___ ___/___/___

# APPENDIX B

## ENGINE SPECIFICATION

Table B.1 Engine Specification

| | |
|---|---|
| Make | Perkins |
| Engine Model | 4-108V |
| Working Cycle | Four Stroke Diesel |
| Bore | 79.5mm |
| Stroke | 88.9mm |
| Maximum Rated Speed | 4000rpm |
| Compression Ratio | 22:1 |
| Firing Order | 1-3-4-2 |
| Piston Clearance | 1.0-1.2mm |
| Operating Fuel Injection Pressure | 175 bar |

# APPENDIX C

Table C.1: Engine performance of 100% Conventional Diesel Fuel

| No | Engine Speed (RPM) | Torque (Nm) | Brake Power (kW) | Time (50 ml) | Fuel Consumption ( litre/hr) | SFC (kg/kWh) | Bmep (bar) | Thermal Efficiency ( ht ) |
|---|---|---|---|---|---|---|---|---|
| 1 | 1000 | 82.0 | 8.587 | 57 | 3.158 | 0.3063 | 5.7586 | 0.2647 |
| 2 | 1200 | 87.0 | 10.933 | 45 | 4.045 | 0.3082 | 6.1098 | 0.2631 |
| 3 | 1400 | 91.0 | 13.342 | 38 | 4.800 | 0.2997 | 6.3907 | 0.2706 |
| 4 | 1600 | 94.0 | 15.750 | 32 | 5.625 | 0.2975 | 6.6013 | 0.2726 |
| 5 | 1800 | 96.5 | 18.190 | 27 | 6.667 | 0.3053 | 6.7769 | 0.2656 |
| 6 | 2000 | 95.0 | 19.897 | 25 | 7.347 | 0.3076 | 6.6716 | 0.2637 |
| 7 | 2200 | 77.0 | 17.740 | 27 | 6.667 | 0.3130 | 5.4075 | 0.2591 |
| 8 | 2400 | 55.0 | 13.823 | 31 | 5.902 | 0.3556 | 3.8625 | 0.2280 |
| 9 | 2600 | 36.0 | 9.802 | 37 | 4.932 | 0.4191 | 2.5282 | 0.1935 |
| 10 | 2800 | 19.5 | 5.718 | 44 | 4.138 | 0.6028 | 1.3694 | 0.1345 |
| 11 | 3000 | 8.0 | 2.513 | 49 | 3.711 | 1.2300 | 0.5618 | 0.0659 |

Table C.2: Engine performance of 100% Palm Oil Methyl Ester

| No | Engine Speed (RPM) | Torque (Nm) | Brake Power (kW) | Time (50 ml) | Fuel Consumption ( litre/hr) | SFC (kg/kWh) | Bmep (bar) | Thermal Efficiency ( ht ) |
|---|---|---|---|---|---|---|---|---|
| 1 | 1000 | 94.5 | 9.896 | 48 | 3.750 | 0.3407 | 6.6365 | 0.2569 |
| 2 | 1200 | 96.0 | 12.064 | 36 | 5.000 | 0.3726 | 6.7418 | 0.2349 |
| 3 | 1400 | 98.0 | 14.368 | 32 | 5.714 | 0.3575 | 6.8823 | 0.2448 |
| 4 | 1600 | 101.5 | 17.007 | 27 | 6.667 | 0.3524 | 7.1281 | 0.2484 |
| 5 | 1800 | 103.0 | 19.416 | 24 | 7.660 | 0.3547 | 7.2334 | 0.2468 |
| 6 | 2000 | 102.5 | 21.468 | 24 | 7.500 | 0.3141 | 7.1983 | 0.2787 |
| 7 | 2200 | 100.5 | 23.154 | 27 | 6.667 | 0.2588 | 7.0578 | 0.3381 |
| 8 | 2400 | 77.5 | 19.479 | 30 | 6.000 | 0.2769 | 5.4426 | 0.3161 |
| 9 | 2600 | 58.0 | 15.792 | 40 | 4.500 | 0.2562 | 4.0732 | 0.3417 |
| 10 | 2800 | 24.0 | 7.037 | 46 | 3.913 | 0.4999 | 1.6855 | 0.1751 |
| 11 | 3000 | 8.0 | 2.513 | 49 | 3.673 | 1.3140 | 0.5618 | 0.0666 |

Table C.3: Gas Exhaust Data for 100% CPO

| Engine Speed | CO | SO2 | O2 | Tg | NO | Tg-Ta |
|---|---|---|---|---|---|---|
| | Min | Min | Min | | Min | Min |
| 1000 | 3865.0 | 42.5 | 6.0 | 253.0 | 224.0 | 217.5 |
| 1200 | 4074.5 | 41.5 | 5.6 | 287.0 | 234.5 | 254.0 |
| 1400 | 4600.5 | 38.5 | 5.1 | 317.0 | 258.0 | 284.0 |
| 1600 | 5405.0 | 38.0 | 4.3 | 361.0 | 283.0 | 313.0 |
| 1800 | 5923.5 | 39.0 | 3.3 | 391.0 | 272.0 | 357.0 |
| 2000 | 6620.0 | 36.0 | 2.7 | 419.0 | 272.0 | 376.0 |
| 2200 | 5344.0 | 31.0 | 3.5 | 434.0 | 279.5 | 385.5 |
| 2400 | 697.0 | 17.0 | 8.6 | 339.0 | 307.5 | 271.5 |
| 2600 | 690.0 | 21.0 | 11.6 | 269.0 | 262.5 | 217.5 |
| 2800 | 932.5 | 37.0 | 14.4 | 209.0 | 119.5 | 167.5 |
| 3000 | 1127.5 | 37.0 | 16.0 | 176.0 | 47.0 | 139.0 |

Table C.4: Gas Exhaust Data for 75% CPO+25%CDF

| Engine Speed | CO | SO2 | O2 | Tg | NO | Tg-Ta |
|---|---|---|---|---|---|---|
| | Min | Min | Min | | Min | Min |
| 1000 | 5149.0 | 41.0 | 5.3 | 239.0 | 214.0 | 220.5 |
| 1200 | 6224.0 | 41.0 | 4.5 | 252.0 | 221.5 | 251.5 |
| 1400 | 6270.0 | 37.5 | 4.0 | 301.0 | 232.0 | 288.0 |
| 1600 | 6584.0 | 35.0 | 3.1 | 320.0 | 262.5 | 306.5 |
| 1800 | 7025.0 | 37.5 | 2.3 | 343.0 | 266.0 | 319.0 |
| 2000 | 4429.5 | 29.5 | 4.0 | 342.0 | 271.5 | 288.5 |
| 2200 | 3312.5 | 21.5 | 6.2 | 371.0 | 252.5 | 278.5 |
| 2400 | 2425.5 | 19.0 | 7.4 | 345.0 | 236.5 | 255.0 |
| 2600 | 769.5 | 12.5 | 11.5 | 241.0 | 202.0 | 191.5 |
| 2800 | 980.0 | 23.0 | 14.1 | 183.0 | 114.5 | 156.5 |
| 3000 | 1294.5 | 27.0 | 15.7 | 159.0 | 45.0 | 141.5 |

Table C.5: Gas Exhaust Data for 50% CPO+50%CDF

| Engine Speed | CO | SO2 | O2 | Tg | NO | Tg-Ta |
|---|---|---|---|---|---|---|
| | Min | Min | Min | | Min | Min |
| 1000 | 3907.5 | 27.0 | 5.0 | 255.0 | 241.0 | 232.0 |
| 1200 | 4715.5 | 29.0 | 4.2 | 285.0 | 236.5 | 265.5 |
| 1400 | 4131.0 | 20.5 | 3.8 | 323.0 | 249.5 | 296.0 |
| 1600 | 4663.0 | 22.0 | 3.0 | 343.0 | 266.5 | 320.0 |
| 1800 | 4513.5 | 26.0 | 2.4 | 350.0 | 260.0 | 322.5 |
| 2000 | 1464.5 | 15.5 | 4.9 | 322.0 | 267.0 | 285.0 |
| 2200 | 915.0 | 22.0 | 9.3 | 272.0 | 229.5 | 236.0 |
| 2400 | 903.0 | 23.5 | 11.6 | 234.0 | 203.5 | 202.5 |
| 2600 | 902.5 | 21.0 | 13.8 | 209.0 | 135.5 | 176.5 |
| 2800 | 1122.0 | 27.5 | 14.9 | 198.0 | 80.5 | 163.5 |
| 3000 | 1138.0 | 29.0 | 15.7 | 191.0 | 53.0 | 155.0 |

Table C.6: Gas Exhaust Data for 25% CPO+75%CDF

| Engine Speed | CO | SO2 | O2 | Tg | NO | Tg-Ta |
|---|---|---|---|---|---|---|
| | Min | Min | Min | | Min | Min |
| 1000 | 2955.5 | 31.5 | 7.2 | 181.0 | 235.0 | 182.5 |
| 1200 | 3769.0 | 33.0 | 5.9 | 223.0 | 242.0 | 219.0 |
| 1400 | 3474.0 | 25.5 | 5.3 | 251.0 | 244.5 | 244.0 |
| 1600 | 3694.0 | 24.0 | 4.3 | 271.0 | 266.0 | 264.0 |
| 1800 | 4028.5 | 26.5 | 3.1 | 288.0 | 272.0 | 275.5 |
| 2000 | 2297.0 | 22.0 | 5.3 | 284.0 | 256.5 | 252.0 |
| 2200 | 1057.5 | 26.0 | 8.1 | 245.0 | 232.0 | 220.0 |
| 2400 | 1032.5 | 34.0 | 11.0 | 198.0 | 195.0 | 182.5 |
| 2600 | 967.5 | 27.5 | 13.2 | 172.0 | 157.5 | 156.5 |
| 2800 | 1155.5 | 32.5 | 14.8 | 159.0 | 92.5 | 143.0 |
| 3000 | 1333.0 | 41.5 | 15.7 | 150.0 | 57.5 | 130.0 |

Table C.7: Gas Exhaust Data for 100%CDF

| Engine Speed | CO | SO2 | O2 | Tg | NO | Tg-Ta |
|---|---|---|---|---|---|---|
| | Min | Min | Min | | Min | Min |
| 1000 | 1693.0 | 29.0 | 8.0 | 186.0 | 270.0 | 172.5 |
| 1200 | 1907.5 | 24.5 | 6.9 | 215.0 | 280.0 | 211.0 |
| 1400 | 2079.5 | 26.5 | 6.2 | 240.0 | 268.5 | 235.5 |
| 1600 | 2125.0 | 21.5 | 5.2 | 263.0 | 291.0 | 267.0 |
| 1800 | 2562.5 | 21.5 | 3.7 | 280.0 | 285.5 | 279.0 |
| 2000 | 1788.5 | 21.0 | 3.9 | 267.0 | 275.5 | 267.0 |
| 2200 | 985.0 | 28.0 | 7.3 | 236.0 | 237.0 | 231.0 |
| 2400 | 1148.5 | 44.5 | 10.5 | 206.0 | 178.5 | 199.5 |
| 2600 | 1105.0 | 40.0 | 12.8 | 186.0 | 150.0 | 172.5 |
| 2800 | 1178.0 | 39.0 | 14.7 | 179.0 | 92.0 | 154.5 |
| 3000 | 1298.0 | 45.0 | 15.7 | 174.0 | 61.0 | 143.0 |

# APPENDIX D

## D.1 ENGINE PERFORMANCE
## D.2 DERIVATIVE OF PRESSURE AND HEAT NET WITH RESPECT TO CRANK ANGLE

## D.1 ENGINE PERFORMANCE

**%POMEp.m**

```
p=32;              % load=32kW
w=0.01;            % 10ml
% N=[2000:500:3000];% rpm, increasement of 200 rpm
n=4;               % number of cylinders
A=0.06245;         % Area of engine bore (m2)
L=0.0889;          % Length of stroke (m)
% t=[0,2];   % time for fuel to flow in seconds
LCV=45000;         % lower calorific value of fuel (kJ/kg)
phi=0.899;         % specific gravity
```

**%CDFp.m**

```
p=32;              % load=32kW
w=0.01;            % 10ml
%N=[2000:500:3000]; % rpm, increasement of 200 rpm
n=4;               % number of cylinders
A=0.06245;         %400 Area of engine bore (m)
L=0.0889;          % Length of stroke (m)
% t=[0,2];   % time for fuel to flow in seconds
LCV=45000;         % lower calorific value of fuel (kJ/kg)
phi=0.833;         % specific gravity
```

**% POME Palm Oil Methyl Ester**

```
%mfr.m
clc
format long e
NLW=2; % normal line width
NFS=12; % normal font size
tt=cputime;
global  t  n p Qnet A L

for i=1:11;

POMEp

mdot(i)=(w/t(i))*p*0.833/3600 ; % mass flow rate (kg/h)
tq(i)=p/(2*180*N(i));          % torque(Nm)
```

```
ip(i)=mdot(i)*LCV;              % input power(kW)
bp(i)=2*180*N(i)*tq(i)/(60*10^3);% brake power(kW)
bmep(i)=2*bp(i)/A*L*N(i)*n ;    % brake mean effective pressure(bar)
bsfc(i)=mdot(i)/bp(i);          % break specific fuel consumption(kg/kJ)
Nbt(i)=(bp(i)/ip(i))*100;       % break thermal efficiency(%)

if i==11;
    break
  t(i+1)=t(i);
  N(i+1)=N(i);
end
end

CDF=input('Would you like to compare with Conventional Diesel Fuel?If yes press 1, if
no press 0:');

if CDF==1

for i=1:11;

CDFp

mdot2(i)=(w/t2(i))*p*0.899/3600 ; % mass flow rate (kg/h)
tq2(i)=p/(2*180*N(i));            % torque(Nm)
ip2(i)=mdot2(i)*LCV;              % input power(kW)
bp2(i)=2*180*N(i)*tq2(i)/(60*10^3);% brake power(kW)
bmep2(i)=2*bp2(i)/A*L*N(i)*n ;    % brake mean effective pressure(bar)
bsfc2(i)=mdot2(i)/bp2(i);         % break specific fuel consumption(kg/kJ)
Nbt2(i)=(bp2(i)/ip2(i))*100;      % break thermal efficiency(%)

if i==11;
    break
  t2(i+1)=t2(i);
  N(i+1)=N(i);
end
end

figure(1);
plot(N,mdot,'-*r',N,mdot2,'-+b');hold on;
set(gca,'FontSize',NFS);
set(gca,'LineWidth',NLW);
grid,
xlabel('Engine Speed,rpm'),
ylabel('Mass Flow Rate,kg/s'),
title('Figure 1: Mass Flow Rate vs Speed at 32kW load');
```

```
figure(2);
plot(N,bsfc,'-*r',N,bsfc2,'-+b');hold on;
set(gca,'FontSize',NFS);
set(gca,'LineWidth',NLW);
grid,
xlabel('Engine Speed,rpm'),
ylabel('Specific Fuel Consumption,kg/kJ'),
title('Figure 2: Specific Fuel Consumption vs Speed at 32kW load');

figure(3);
plot(N,Nbt,'-*r',N,Nbt2,'-+b');hold on;
set(gca,'FontSize',NFS);
set(gca,'LineWidth',NLW);
grid,
xlabel('Engine Speed,rpm'),
ylabel('Efficiency ,%'),
title('Figure 3:Efficiency vs Speed at 32kW load');

figure(4);
plot(N,tq,'-*r',N,tq2,'-+b');hold on;
set(gca,'FontSize',NFS);
set(gca,'LineWidth',NLW);
grid,
xlabel('Engine Speed,rpm'),
ylabel('Torque,Nm'),
title('Figure 1: Torque vs Speed at 32kW load');

figure(5);
plot(N,bp,'-*r',N,bp2,'-+b');hold on;
set(gca,'FontSize',NFS);
set(gca,'LineWidth',NLW);
grid,
xlabel('Engine Speed,rpm'),
ylabel('Break Power,kW'),
title('Figure 2: Break Power vs Speed at 32kW load');

else if CDF==0

figure(1);
plot(N,mdot,'-*r');hold on;
set(gca,'FontSize',NFS);
set(gca,'LineWidth',NLW);
grid,
xlabel('Engine Speed,rpm'),
ylabel('Mass Flow Rate,kg/s'),
title('Figure 1: Mass Flow Rate vs Speed at 32kW load');
```

```
figure(2);
plot(N,bsfc,'-*r');hold on;
set(gca,'FontSize',NFS);
set(gca,'LineWidth',NLW);
grid,
xlabel('Engine Speed,rpm'),
ylabel('Specific Fuel Consumption,kg/kJ'),
title('Figure 2: Specific Fuel Consumption vs Speed at 32kW load');

figure(3);
plot(N,Nbt,'-*r');hold on;
set(gca,'FontSize',NFS);
set(gca,'LineWidth',NLW);
grid,
xlabel('Engine Speed,rpm'),
ylabel('Efficiency ,'),
title('Figure 3:Efficiency vs Speed at 32kW load');

figure(4);
plot(N,tq,'-*r');hold on;
set(gca,'FontSize',NFS);
set(gca,'LineWidth',NLW);
grid,
xlabel('Engine Speed,rpm'),
ylabel('Torque,Nm'),
title('Figure 4:Torque vs Speed at 32kW load');

figure(5);
plot(N,bp,'-*r');hold on;
set(gca,'FontSize',NFS);
set(gca,'LineWidth',NLW);
grid,
xlabel('Engine Speed,rpm'),
ylabel('Break Power,kW'),
title('Figure 5:Break Power vs Speed at 32kW load');

end
end
```

## D.2 DERIVATIVE OF PRESSURE AND HEAT NET WITH RESPECT TO CRANK ANGLE

**% cap.m**

```
% parameters
a=5;
n=3;
k=1.4;          % k=Cp/Cv=1.4 for air
Ru=8.314;       % Universal gas constant
M=28.97;        % Molar mass of air in kg/kmol
p=1.1614;       % density of air in Kg/m^3 at room temperature
x=0.6;          % constant varies from 0.35 to 0.8 for normal combustion
u=7*10^5;       % dynamic viscosity in kg/ms
K=0.15;         % Thermal conductivity in W/m.K
B=0.0795;       % cylinder bore
S=0.0899;       % piston stroke
l=0.1348;       % connecting rod length
Vc=4*10^-5;  % clearance volume  (for POME:3.6*10^-5)
thetai1=-100;
theta11=180;
thetai=thetai1*pi/180; % crank angle(rad) of the start of the heat addition
thetal=theta11*pi/180; % duration of the heat addition(length of burn) in radian
Tw=200;         % cylinder wall temperature in Kelvin
w=45;           % engine speed in rad/s
C=0.8;          % blowby constant
m=200;          % mass fuel
```

**%ck1.m**

```
%ck.m
%Pressure with respect to crank angle
clc
cap
NLW=2; % normal line width
NFS=12; % normal font size

fprintf('SPECIFY THE ENGINE CHARACTERISTICS')

Rc=0.5*S;%crank radius
R=l/Rc;%ratio of connecting rod to crank radius
Vs=(3.142*B^2*S)/4;%sweept volume
r=(Vs+Vc)/Vc;%compression ratio

fprintf('\n\n');
fprintf('Ratio of connecting rod to crank radius R=%f\n',R);
fprintf('Swept volume in m=%f\n',Vs);
```

```
fprintf('Compression ratio=%f\n',r);

P1=10^(5);%atmospheric pressure
Qin=20*P1*Vs;%overall heat input;heat addition ;pg 74
fprintf('Overall heat input in Joule/rev=%f\n',Qin);

Sp=2*S*w;%mean piston speed
h=(K*x/B)*(((p*Sp*B)/u)^B);%heat transfer coefficient
fprintf('Heat transfer coefficient in W/m^2.K=%f\n',h);

theta=thetai;
for i=1:1:20;
mdot(i)=exp(-C*(theta(i)+180)/w);%mass flow rate
dm(i)=-C*mdot(i)/w;
V(i)=Vs/(r-1)+(Vs/2)*(R+1-cos(theta(i))-(R^2-(sin(theta(i)))*(sin(theta(i))))^(1/2));
dV(i)=(Vs/2)*sin(theta(i))*(1+cos(theta(i))*((R^2-sin(theta(i))^2)^(-1/2)));
f(i)=1-exp(-a*((theta(i)-thetai)/thetal)^n);%fraction of heat added
df(i)=((1-f(i))*n*a/thetal)*(((theta(i)-thetai)/thetal)^(n-1));
Tg(i)=((r-1)/(r*Vs))*((P1*V(i)*M)/(p*Ru));%average gas temperature
A(i)=(3.142*B^(2))/2 + 3.142*B*(S/2)*(R+1-cos(theta(i))+(R^2-
sin(theta(i))^2)^(1/2));%surface area of cylinder
dP(i)=((k-1)/V(i))*((Qin*df(i))-(h*A(i)/w)*(Tg(i)-Tw)*(3.142/180))-k*P1*dV(i)/V(i);
dQn(i)=(C/r)*(P1*dV(i)+V(i)*dP(i)-(P1*V(i)*dm(i))/m+P1*dV(i));
% dQw(i)=A*(((ac/(B*m))*K*Re*(Tw-Tg(i)))+r*(Tw^4-(Tg(i))^4));
% dQg(i)=dQn(i)-dQw(i);

if i==20;
   break
   end
  theta(i+1)=theta(i)+thetal/20;
  the=rad2deg(theta);
end
end

figure (1)
   plot(the,dP);hold on;
   set(gca,'FontSize',NFS);
   set(gca,'LineWidth',NLW);
   xlabel(' Crank angle (degrees)');
   ylabel(' dP/dO (Pa/rad) ');
   title (' Graph derivative pressure  vs crank angle');
   grid;
   legend('CDF','POME',1)
figure (2)
   plot(the,dQn);hold on;
   set(gca,'FontSize',NFS);
```

```
set(gca,'LineWidth',NLW);
xlabel(' Crank angle(degrees)');
ylabel(' dQn/dO (Pa/rad) ');
title (' Graph derivative heat net vs crank angle');
grid;
legend('CDF','POME',1)
```

# APPENDIX E

## WALL BOUNDARY CONDITION

**E.1 Wall Boundary Conditions**

At walls, the modified turbulent kinematic viscosity, ν, is set to zero. If mesh is fine enough, the wall shear stress is obtained from the laminar stress-strain relationship:

$$\frac{u}{u_T} = \frac{\rho u_T y}{\mu} \tag{E.1}$$

If the mesh is too coarse, it is assumed that the centroid of the wall-adjacent cell falls within the logarithmic region of the boundary layer, and the law-of-the-wall is employed:

$$\frac{u}{u_T} = \frac{1}{k} \ln E \frac{u_T y}{v} \tag{E.2}$$

Where:

$k$ = von Karman's constant (= 0.419)

E = empirical constant (= 9.81)

$\mu$ = dynamic viscosity of the fluid

$y$ = distance from point to the wall

The logarithmic law for mean velocity is known to be valid for $y^* > 30 \sim 60$. In FLUENT, the log-law is employed when $y^* > 11.225$.

### 5.6.5 Steady State Explicit

In the explicit scheme, multi-stage, time-stepping algorithm is used to discretize the time derivative. The solution is advanced from iteration n to iteration n+1 with an m-stage Runge –Kutta scheme (see Section A1) given by:

$$\begin{aligned} Q^0 &= Q^n \\ \Delta Q^i &= -\alpha_i \Delta t \Gamma^{-1} R^{i-1} \\ Q^{n+1} &= Q_m \end{aligned} \tag{E.3}$$

where $\Delta Q = Q^i - Q^n$ and *i=1,2,3,…,m* is the stage counter for the m-stage scheme. $\alpha_i$ is the multi stage coefficient for *ith* stage. The residual $R^i$ is computed from the intermediate solution $Q^i$ and is given by:

$$R^i = \sum^{N_{force}} \left( F\left(Q^i\right) - G\left(Q^i\right) \right).A - VH \tag{E.4}$$

The time step $\Delta t$ is computed from the CFL (Courant-Friedrichs-Lewy) condition (see A.2):

$$\Delta t = \frac{CFL\Delta x}{\lambda_{\max}} \tag{E.5}$$

where $\lambda_{\max}$ is the maximum of the local eigenvalues.

The maximum time step can be increased by increasing the support of the scheme through implicit averaging of the residuals with their neighbours. The residuals are filtered through a Laplacian smoothing operator:

$$\bar{R}_i = R_i + \in \sum \left( \bar{R}_j - \bar{R}_i \right) \tag{E.6}$$

This equation can be solved with the following Jacobi iteration:

$$\bar{R}_i^m = \frac{R_i + \in \sum \bar{R}_j^{m-1}}{1 + \in \sum 1} \tag{E.7}$$

Two Jacobi iterations are usually sufficient to allow doubling the time step of $\in$ =0.5

# APPENDIX F

Table F.1Design D1, D2, D3, D4 for L/D=4

| | Boundary Condition | Initial Condition |
|---|---|---|
| Velocity ,v(m/s) | 25 | 0 |
| Turbulent kinetic energy($m^2/s^2$) | 312.5 | 1 |
| Turbulent dissipation rate (D) | 7907059.858 | 1 |
| Temperature(K) | 373 | 300 |
| Gauge Total Pressure Inlet (psi) | 3674 | 0 |
| Supersonic/Initial Gauge Pressure (psi) | 1469.96 | 0 |
| Outflow rate | 1 | 1 |
| Operation Pressure (psi) | 14.696 | 1 |

Table F.2 Boundary condition for nozzle with sharp edge

| | Boundary Condition | Initial Condition |
|---|---|---|
| Velocity ,v(m/s) | 25 | 0 |
| Turbulent kinetic energy($m^2/s^2$) | 312.5 | 1 |
| Turbulent dissipation rate (D) | 7907059.858 | 1 |
| Temperature(K) | 373 | 300 |
| Gauge Total Pressure Inlet (psi) | 3674 | 0 |
| Supersonic/Initial Gauge Pressure (psi) | 1028.7 | 0 |
| Outflow rate | 1469.96 | 1 |
| Operation Pressure (psi) | 14.696 | 1 |

Table F.3 Boundary condition for nozzle with rounded edge

| | Boundary Condition | Initial Condition |
|---|---|---|
| Velocity ,v(m/s) | 25 | 0 |
| Turbulent kinetic energy($m^2/s^2$) | 312.5 | 1 |
| Turbulent dissipation rate (D) | 7907059.858 | 1 |
| Temperature(K) | 373 | 300 |
| Gauge Total Pressure Inlet (psi) | 3674 | 0 |
| Supersonic/Initial Gauge Pressure (psi) | 1028.7 | 0 |
| Outflow rate | 1469.96 | 1 |
| Operation Pressure (psi) | 14.696 | 1 |

## F.1 2D Model (CDF)

Figure F.1 Contours of Total Pressure (D1)

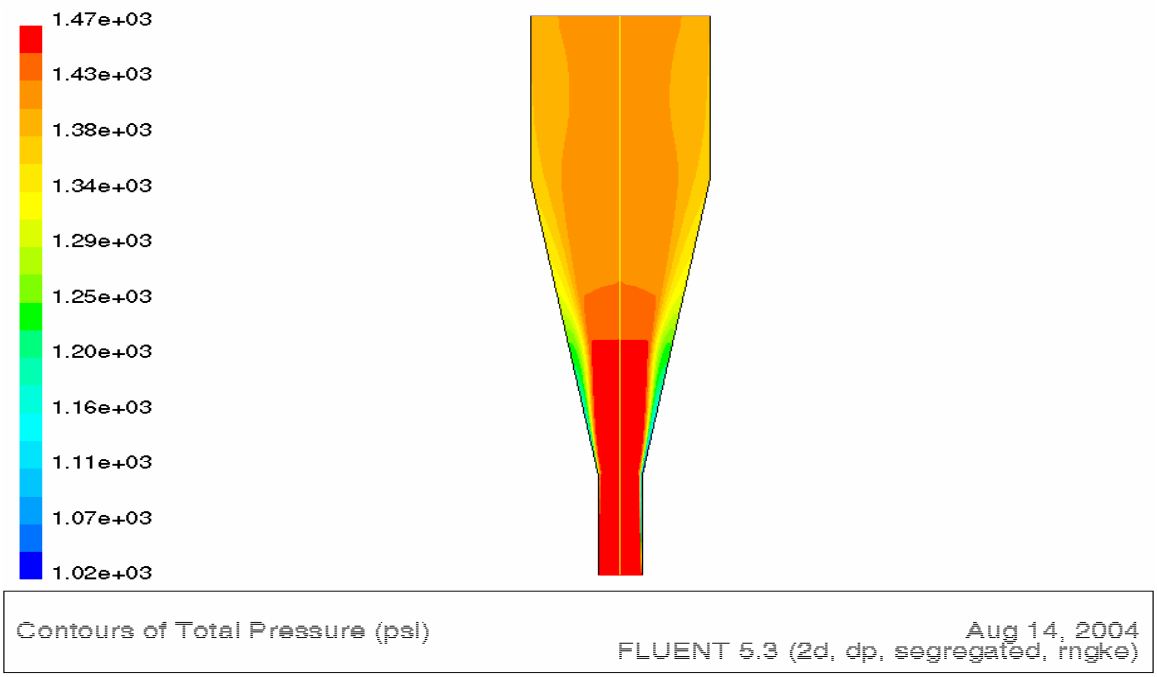


Figure F.2 Contours of Total Pressure for (D2)

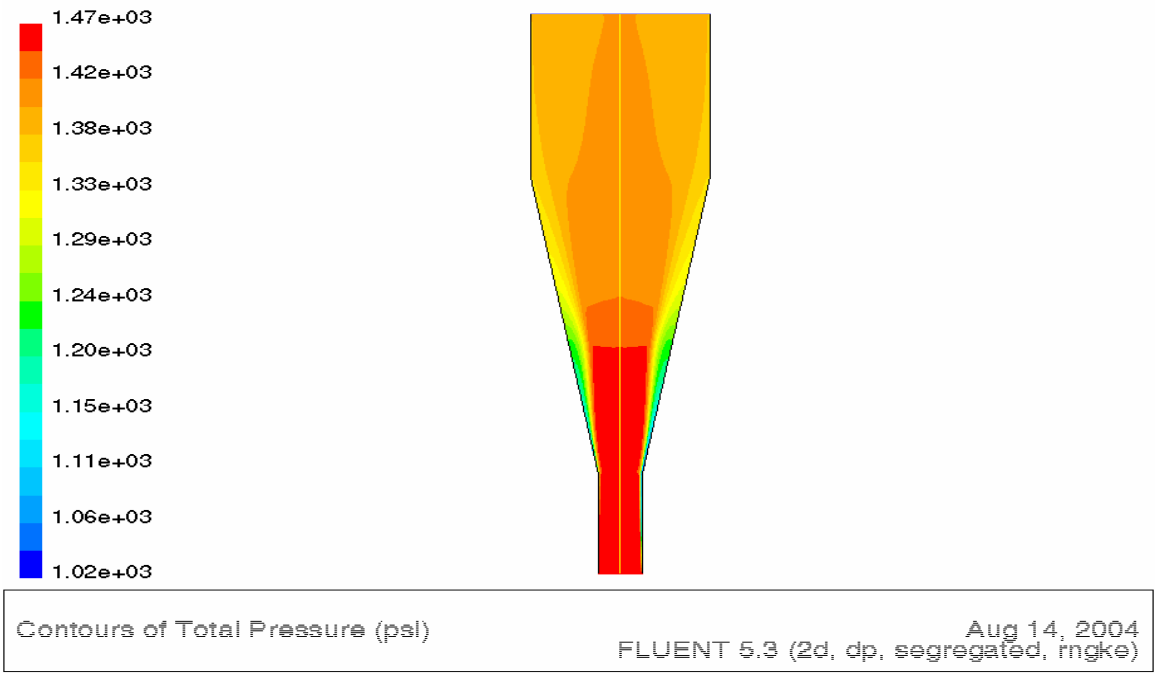

Figure F.3 Contours of Total Pressure (D3)

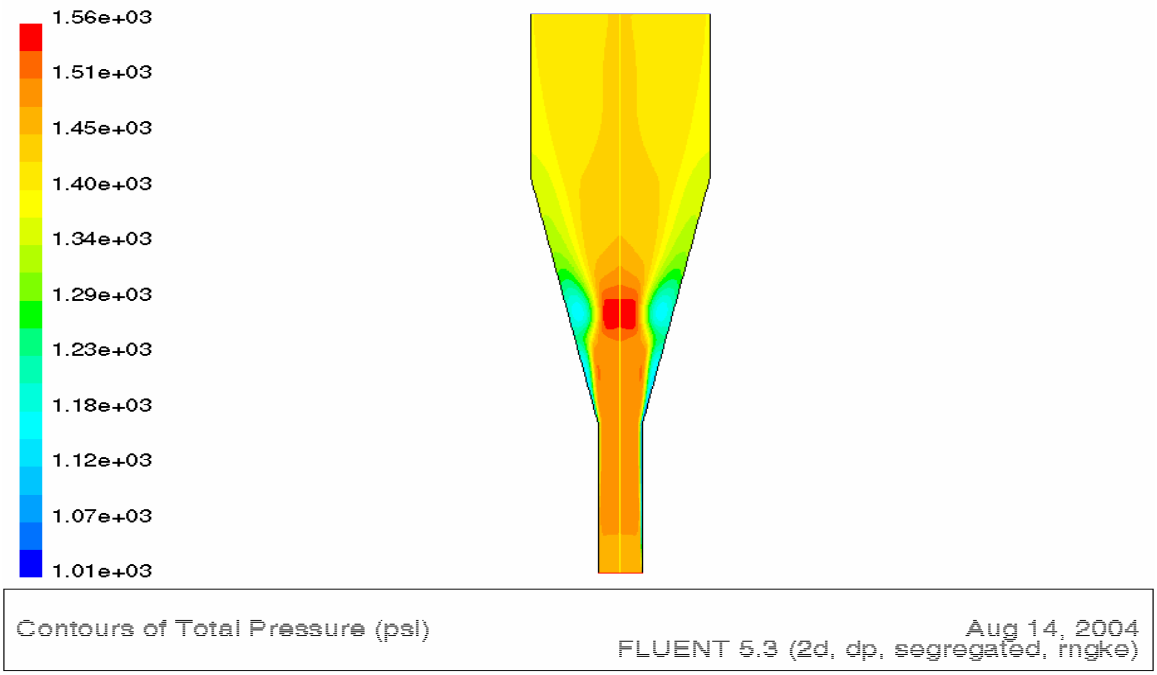


Figure F.4 Contours of Total Pressure (D4)

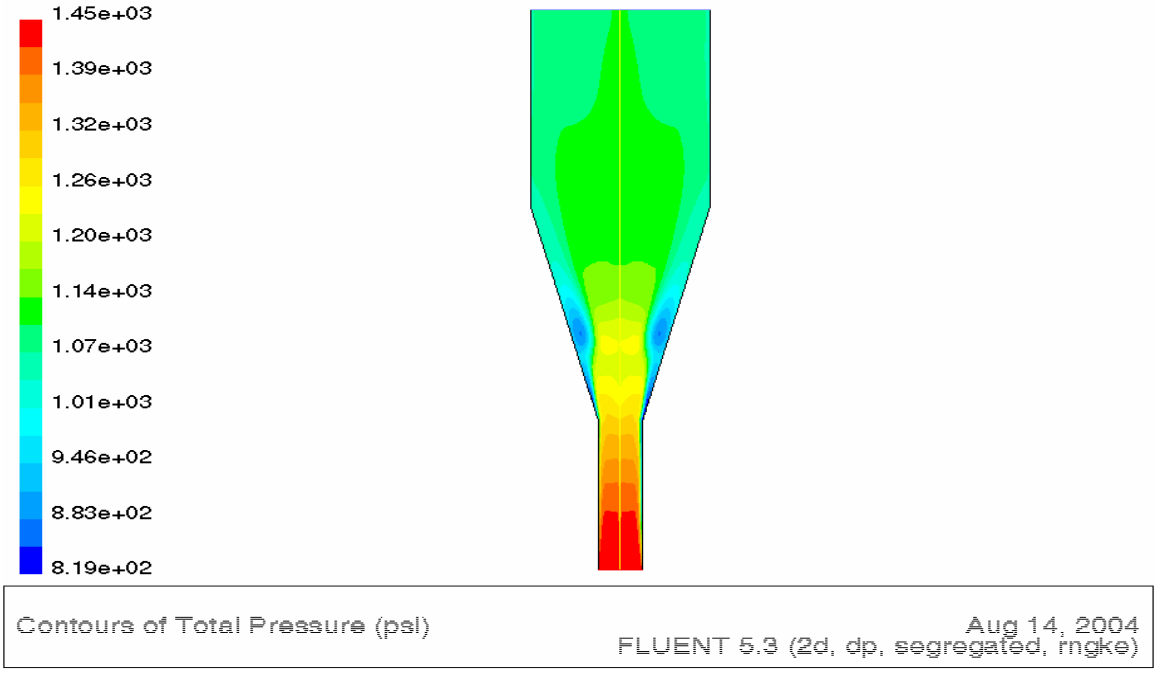

Figure F.5 Contours of Velocity Magnitude (D1)

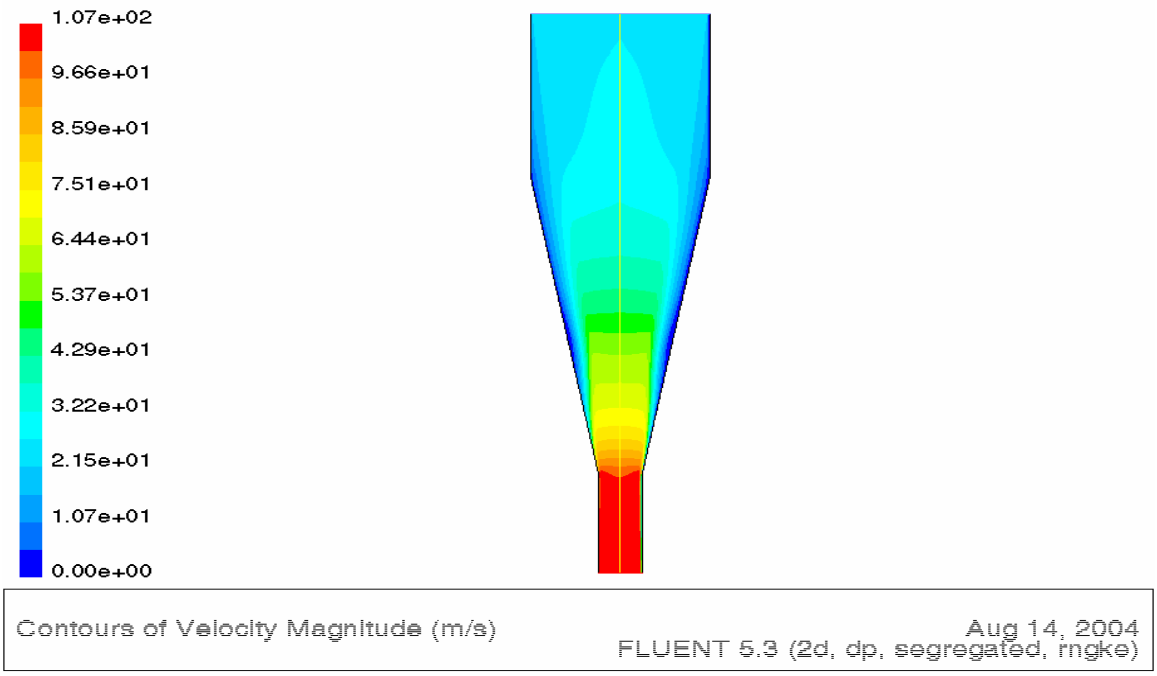


Figure F.6 Contours of Velocity Magnitude (D2)

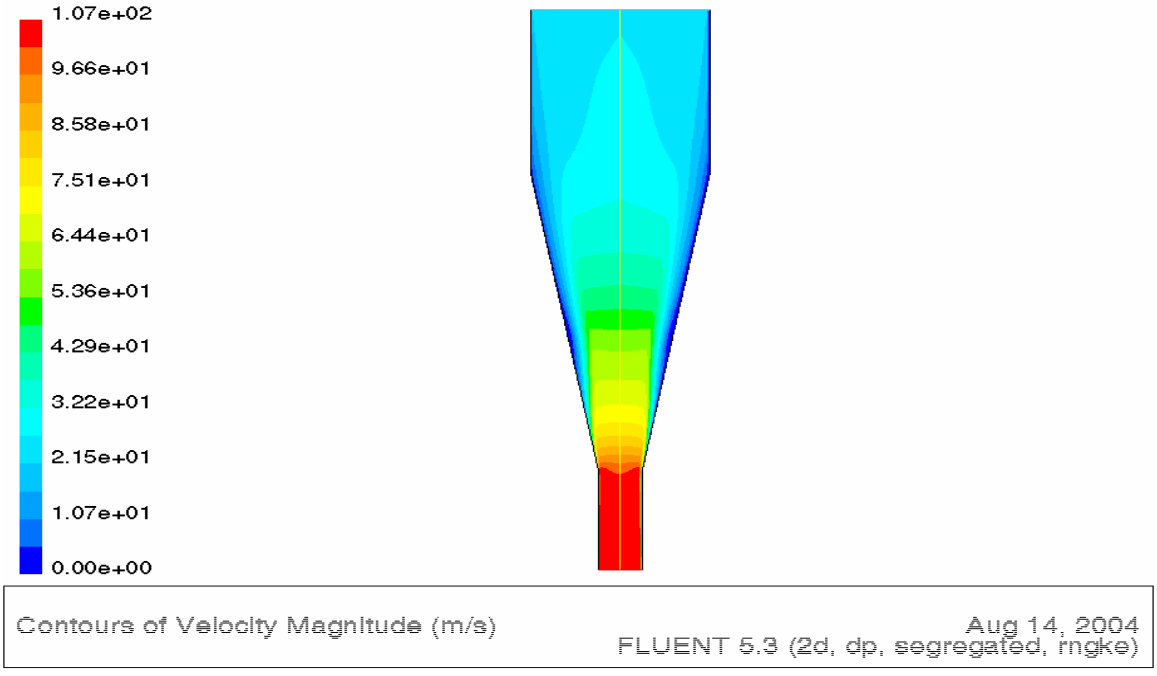

Figure F.7 Contours of Velocity Magnitude (D3)

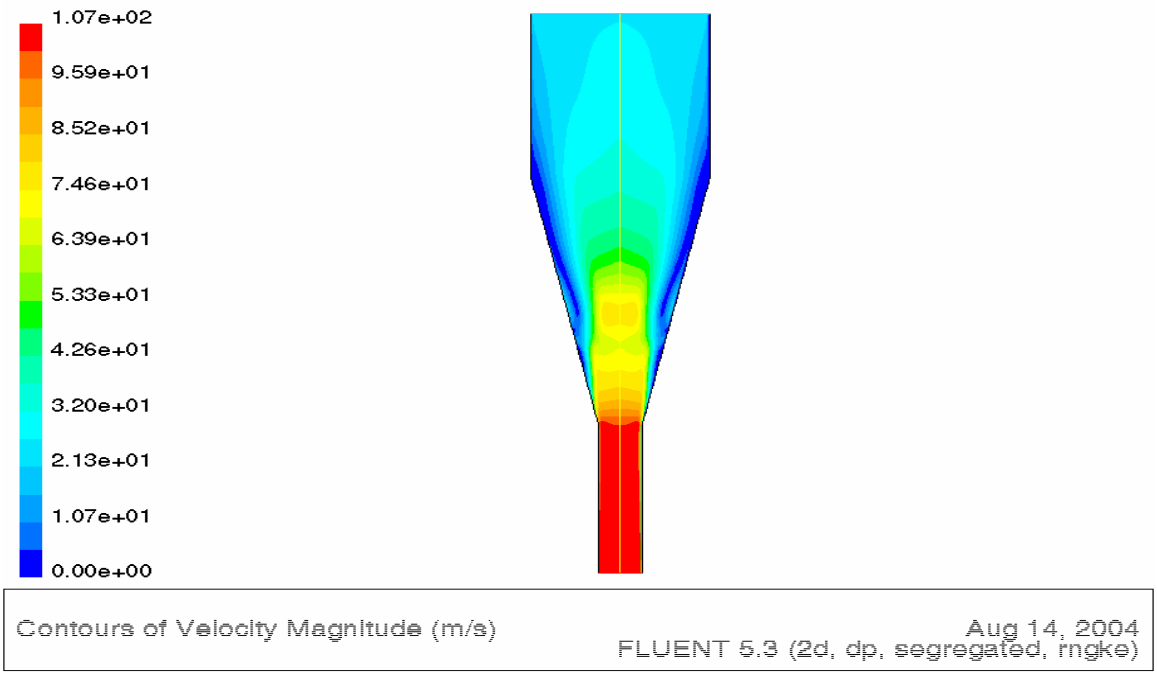


Figure F.8 Contours of Velocity Magnitude (D4)

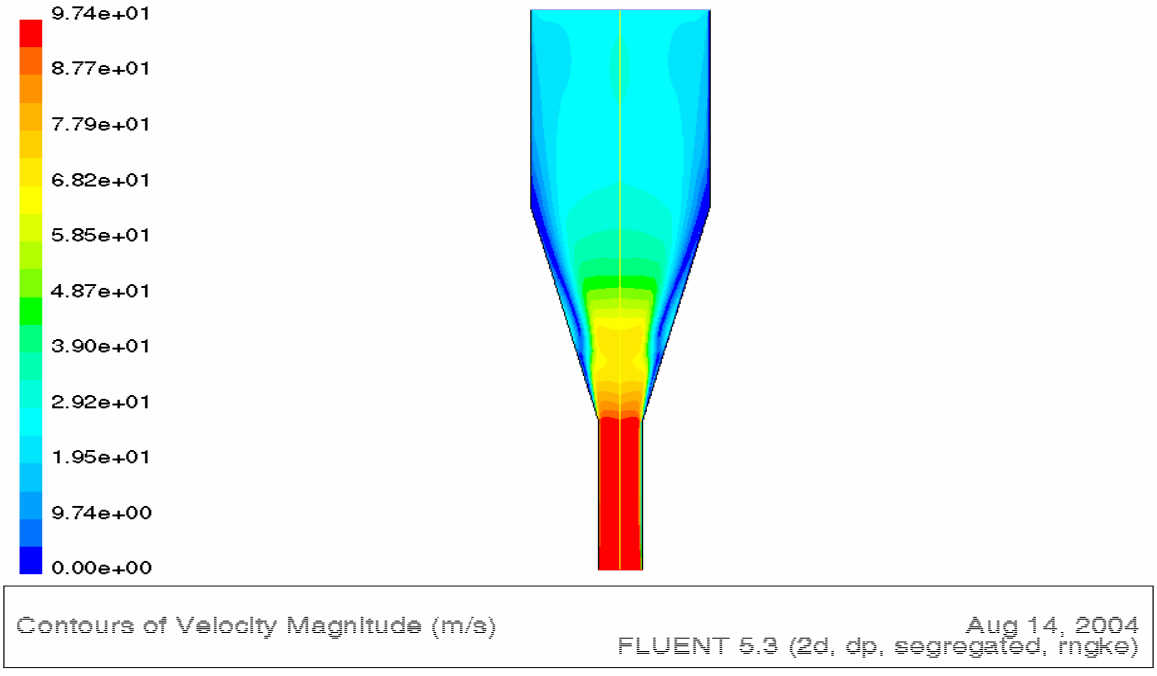

Figure F.9 Contours of Stream Function (D1)

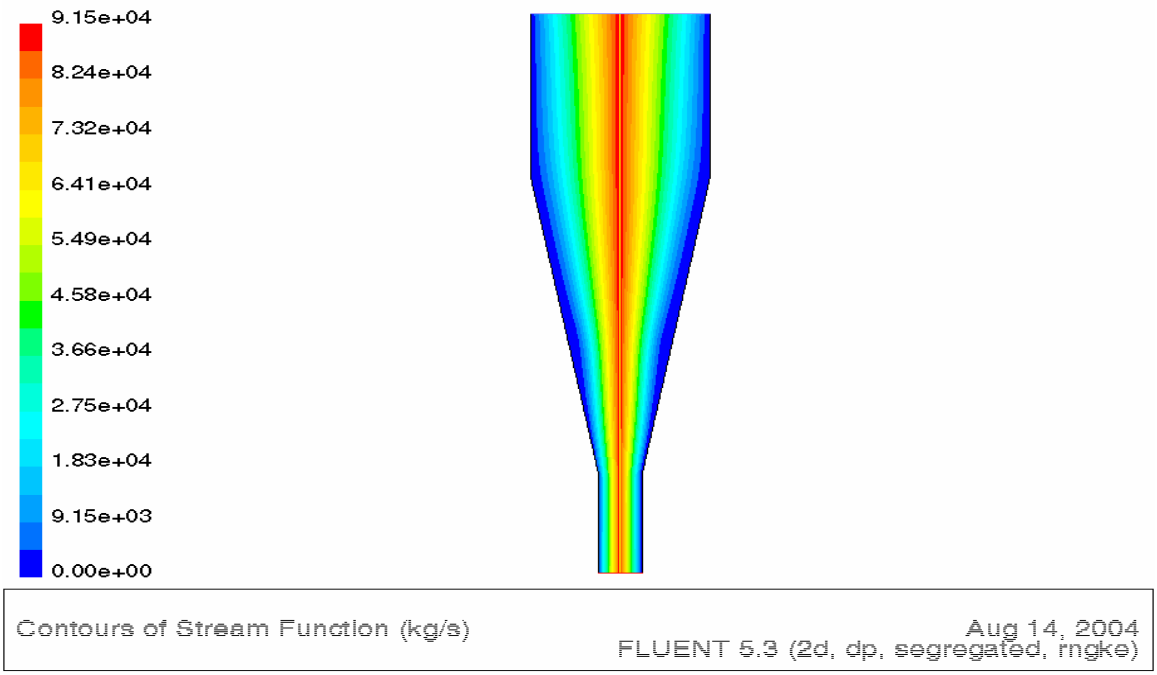


Figure F.10 Contours of Stream Function (D2)

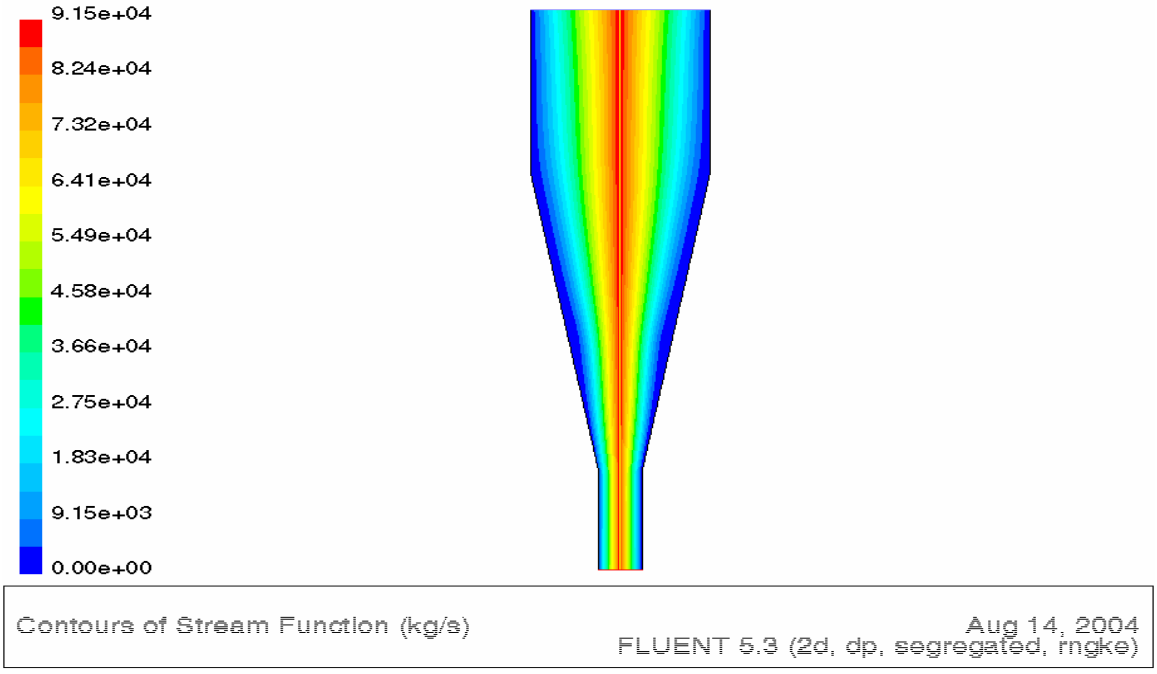

Figure F.11 Contours of Stream Function (D3)

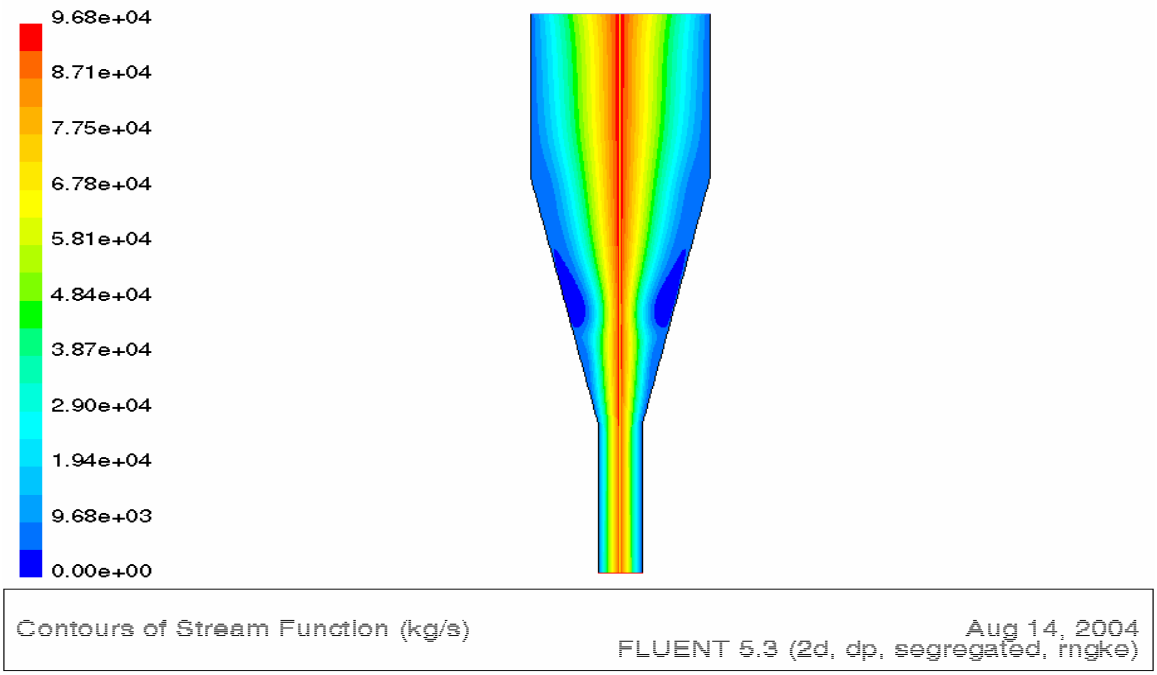


Figure F.12 Contours of Stream Function (D4)

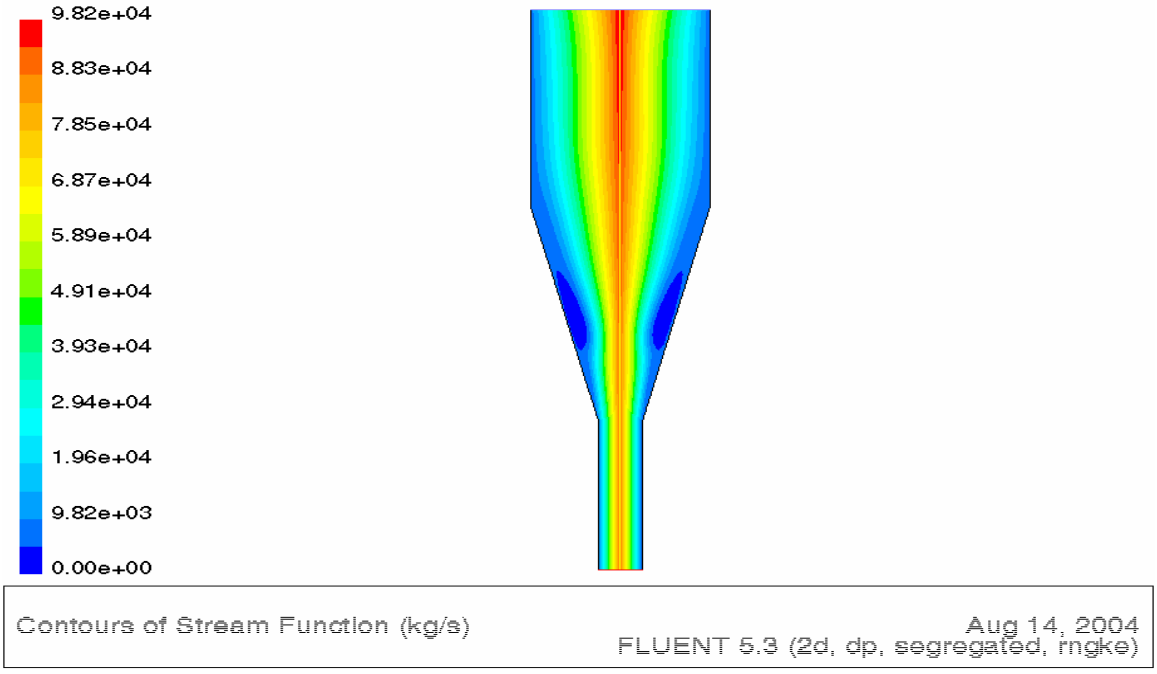

Figure F.13 Contours of Turbulent Kinetic Energy (D1)

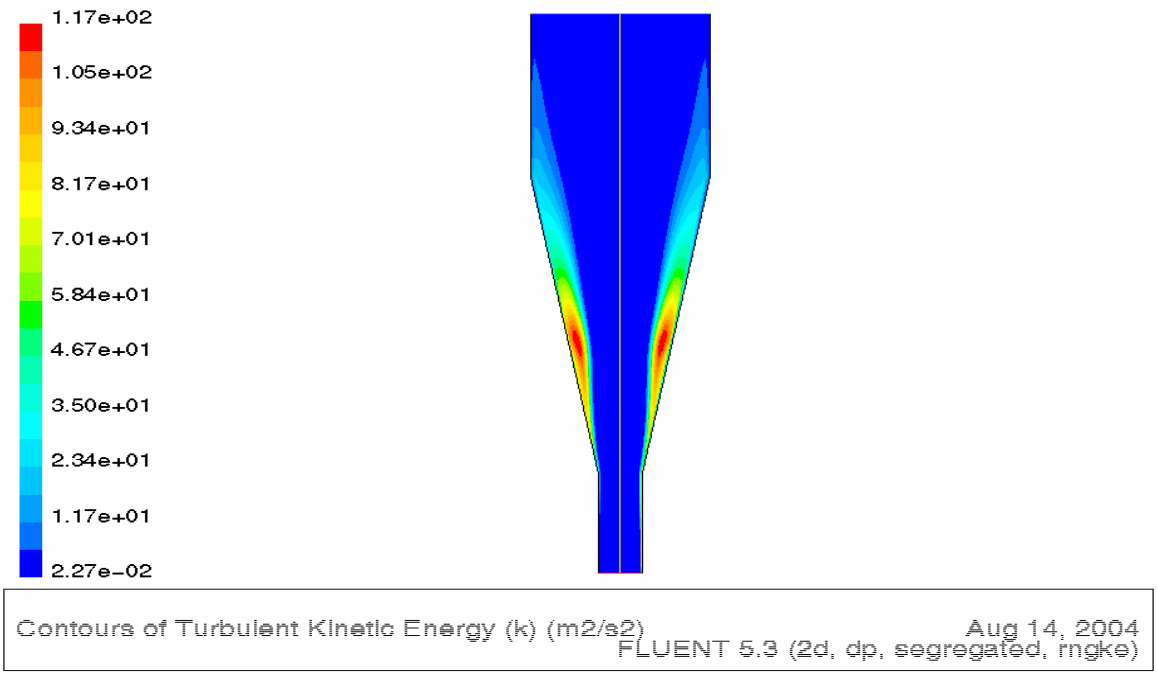


Figure F.14 Contours of Turbulent Kinetic Energy (D2)

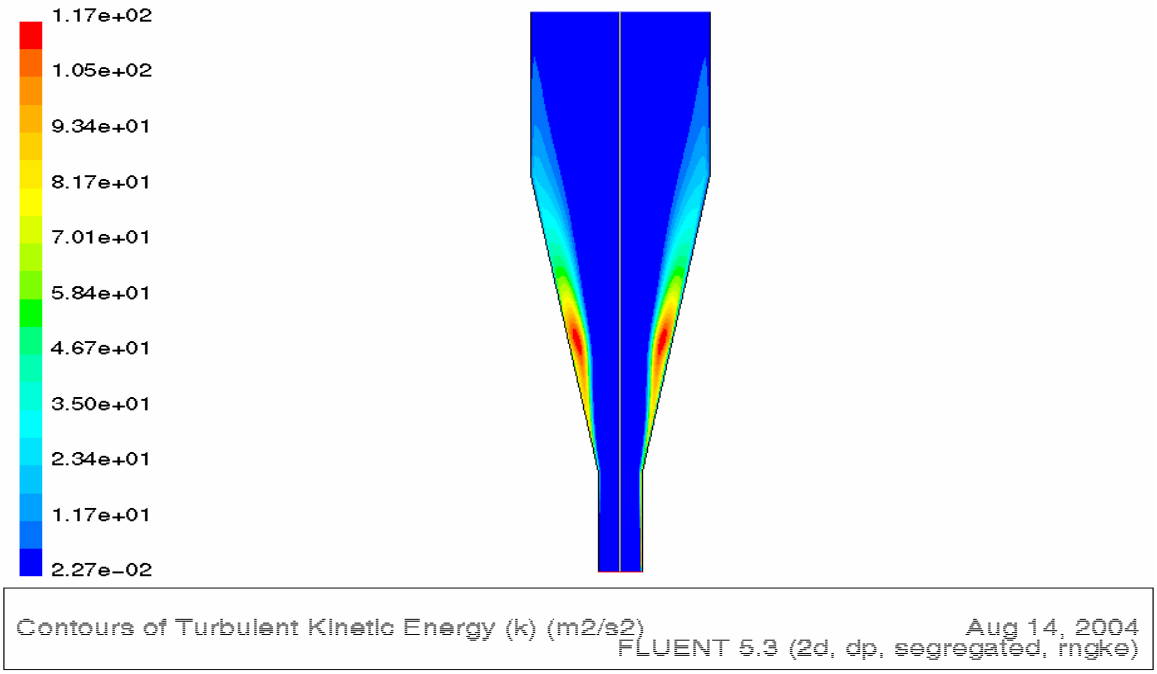

Figure F.15 Contours of Turbulent Kinetic Energy (D3)

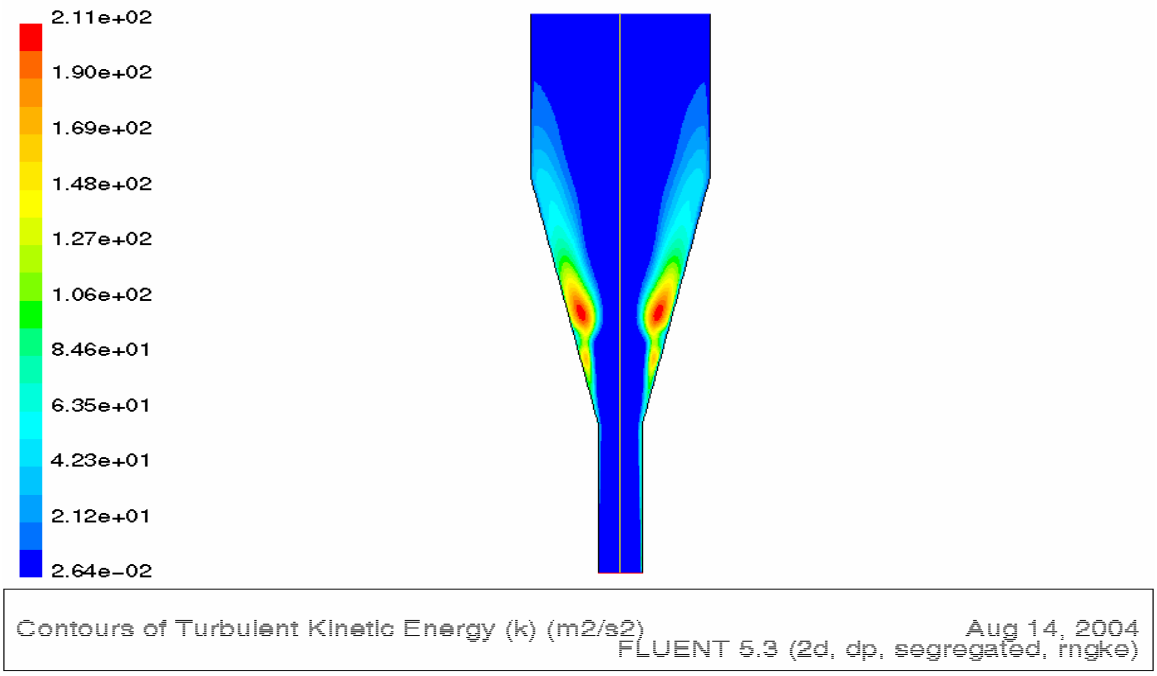


Figure F.16 Contours of Turbulent Kinetic Energy (D4)

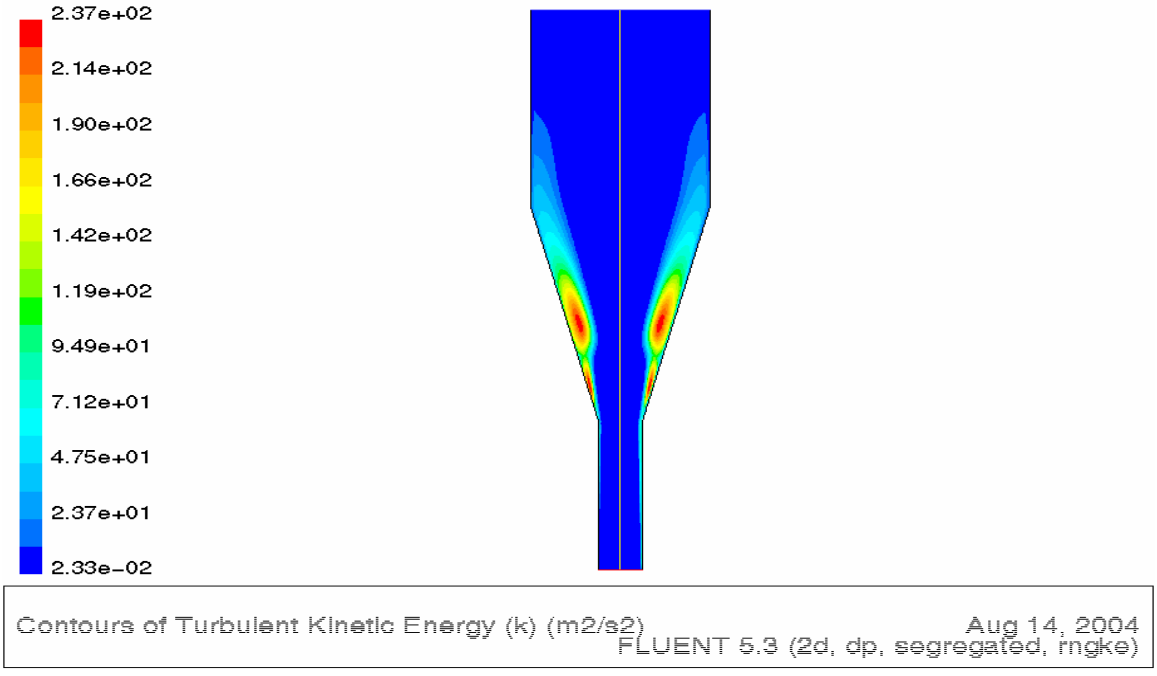

Figure F.17 Contours of Turbulence Intensity (D1)

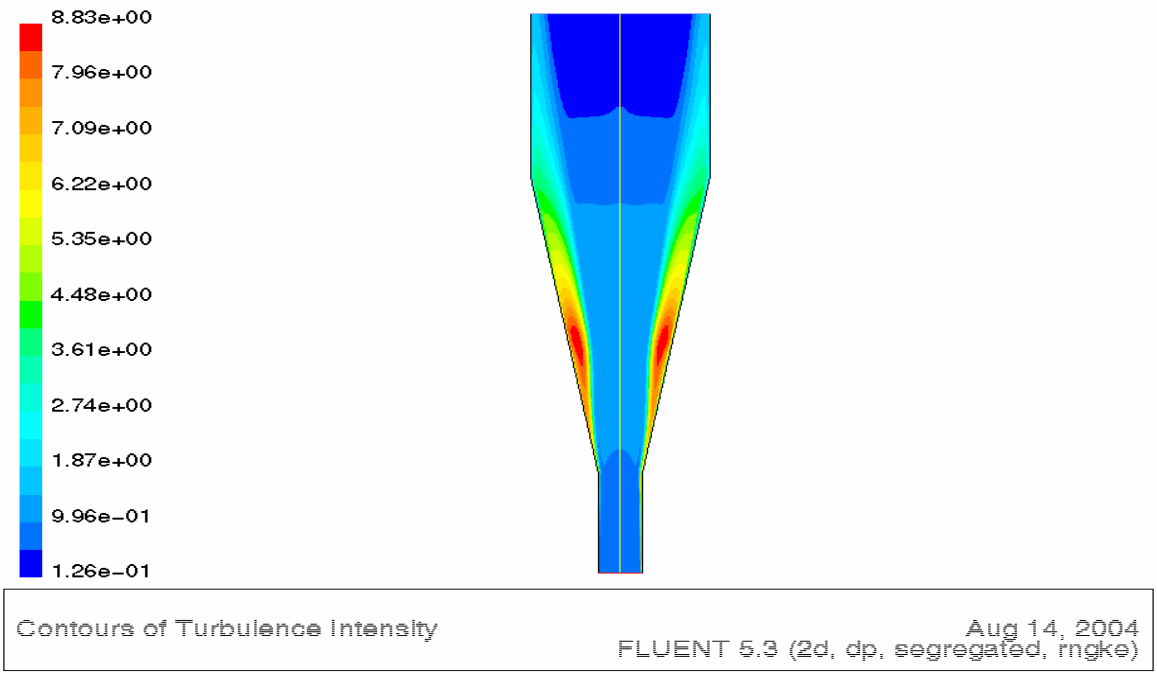


Figure F.18 Contours of Turbulence Intensity (D2)

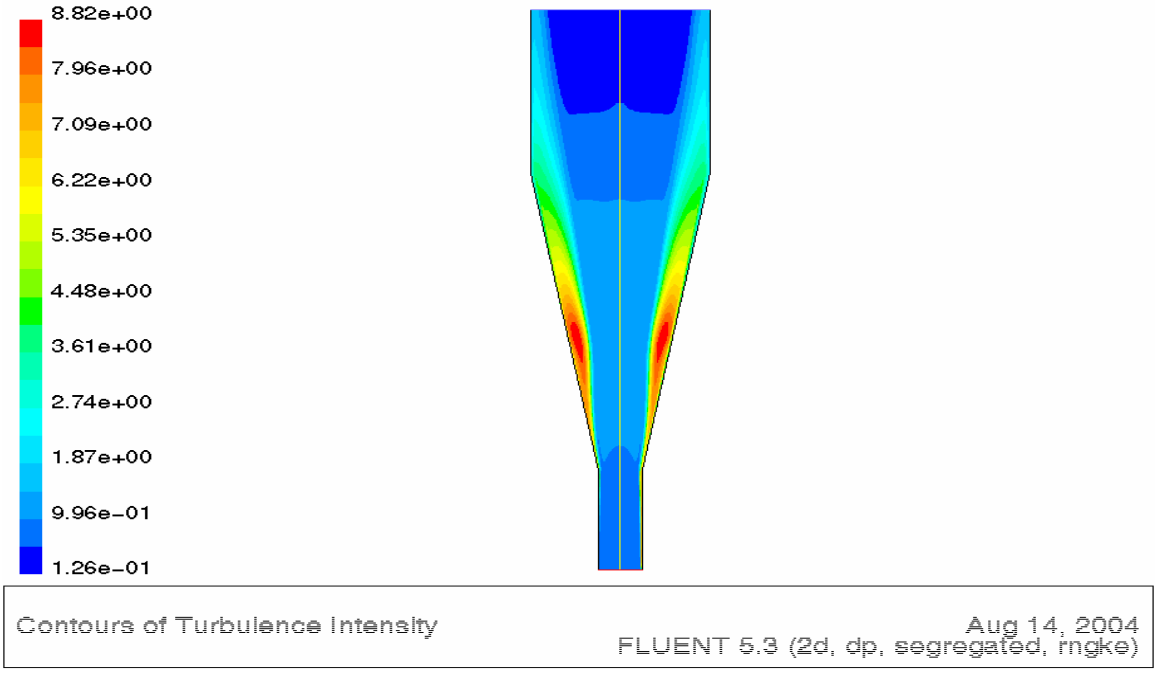

Figure F.19 Contours of Turbulence Intensity (D3)

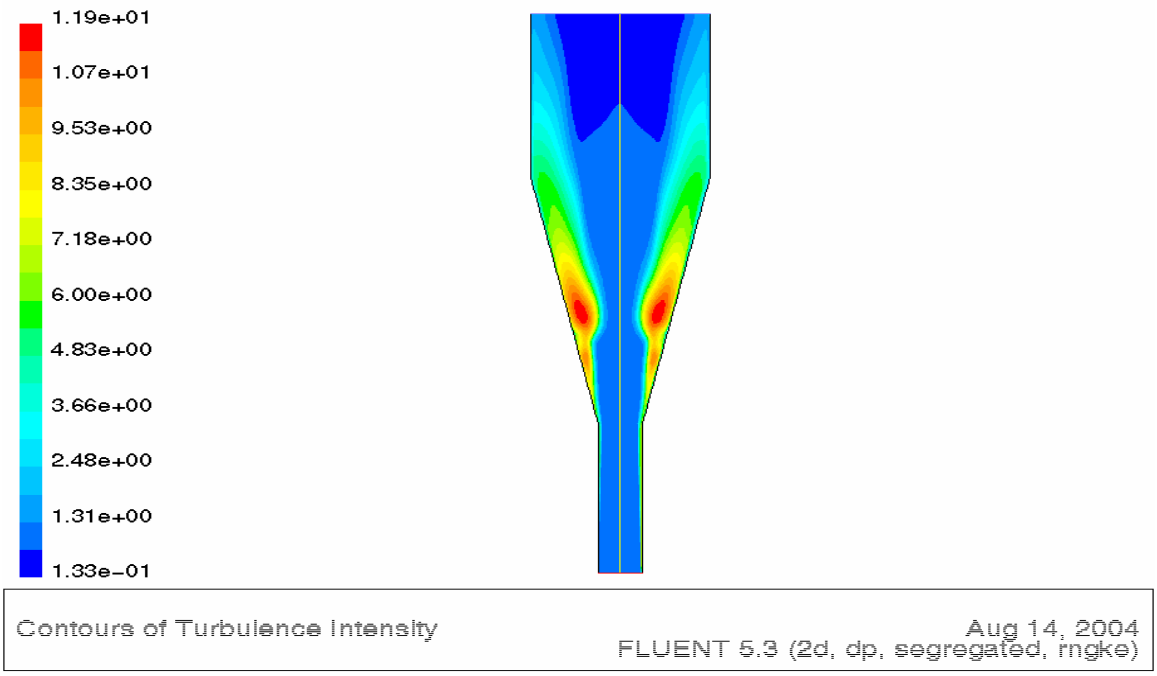


Figure F.20 Contours of Turbulence Intensity (D4)

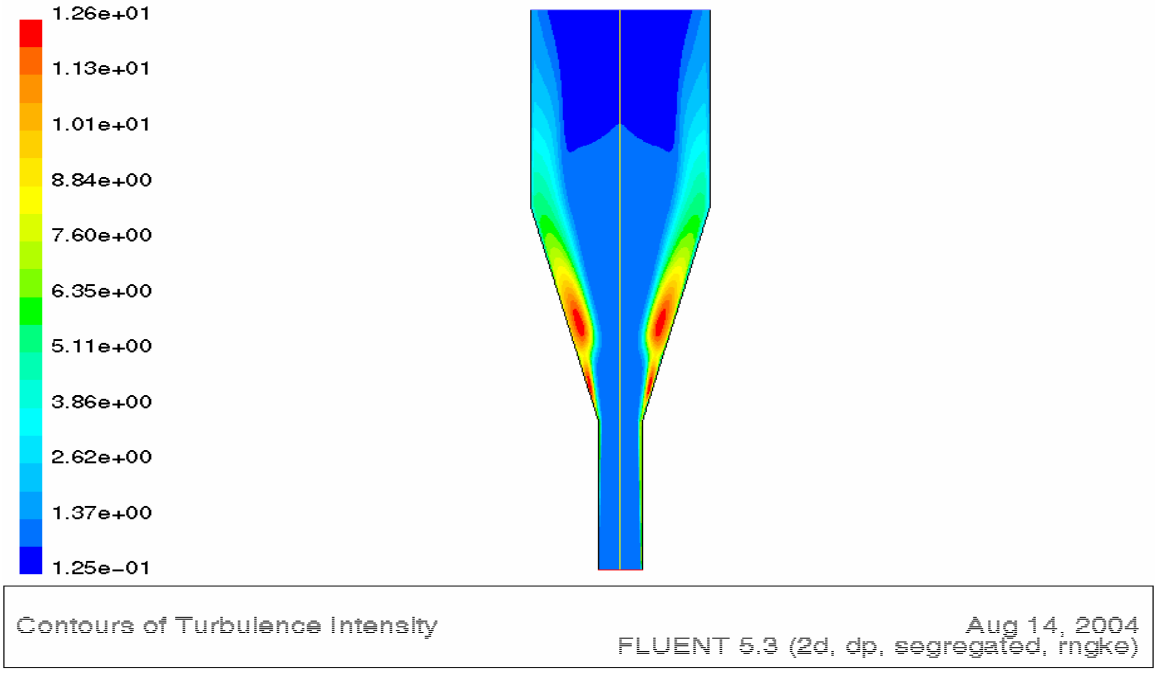

Figure F.21 Contours of Turbulent Viscosity (D1)

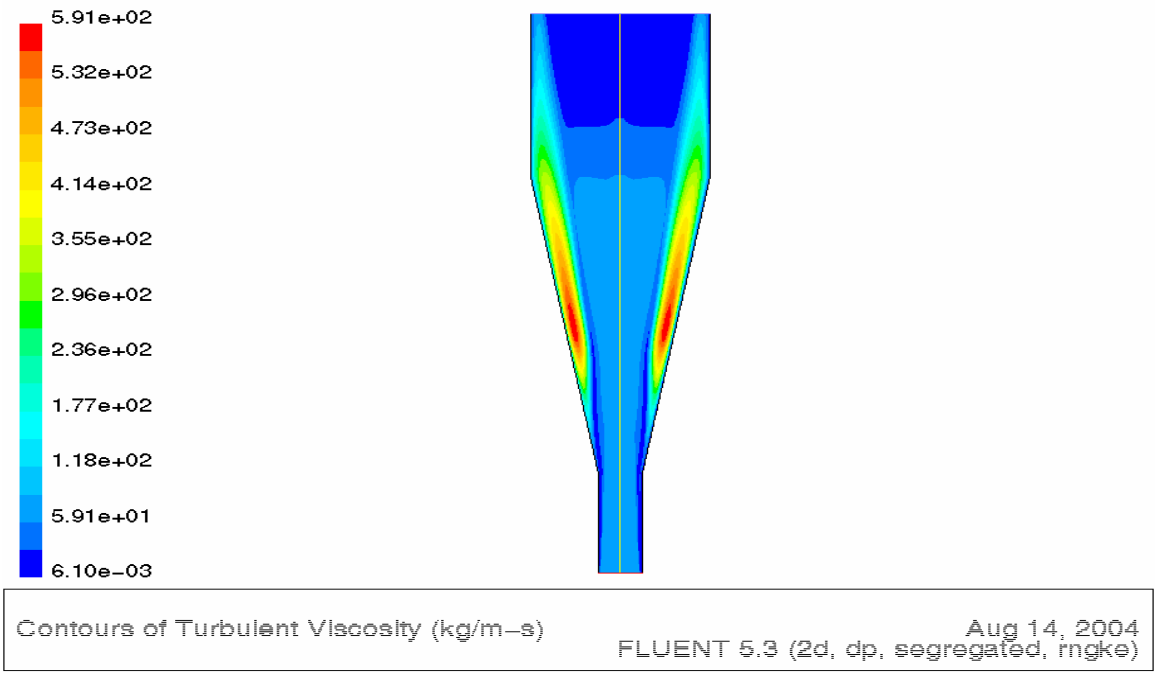


Figure F.22 Contours of Turbulent Viscosity (D2)

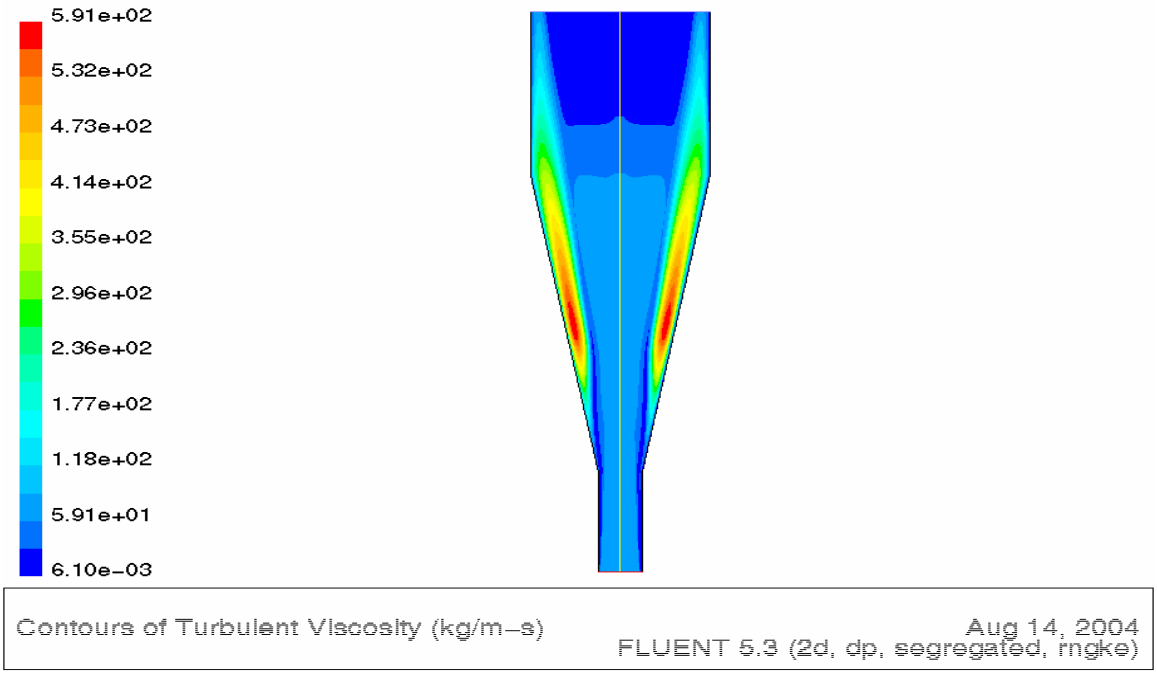

Figure F.23 Contours of Turbulent Viscosity (D3)

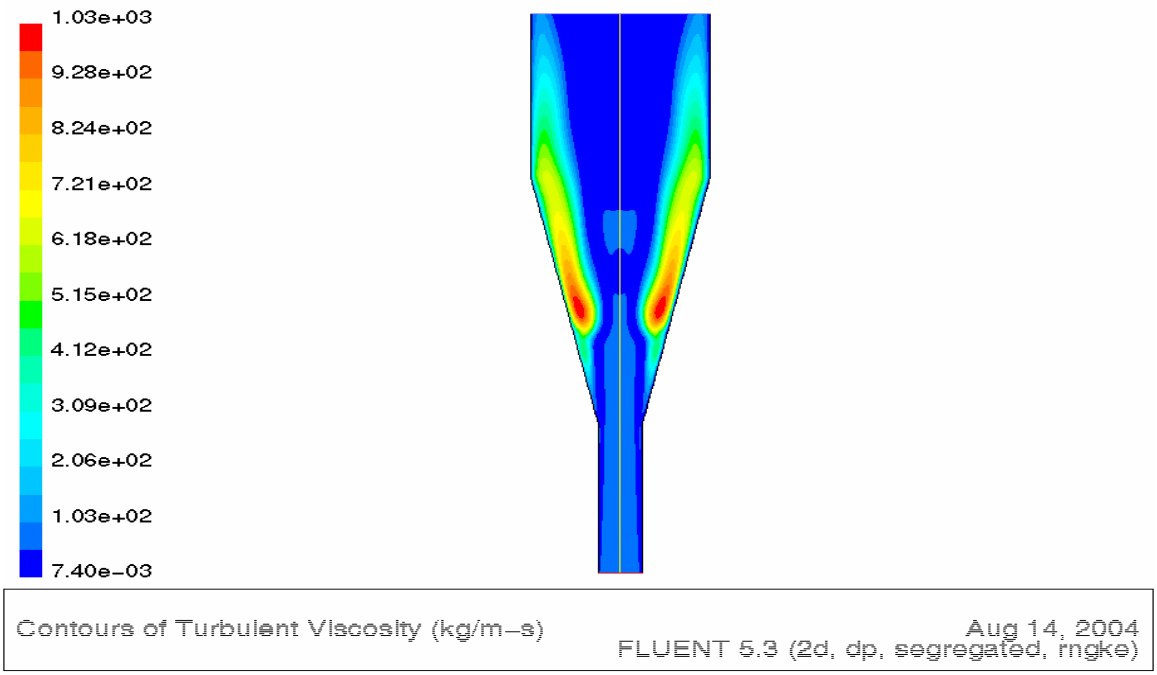


Figure F.24 Contours of Turbulent Viscosity (D4)

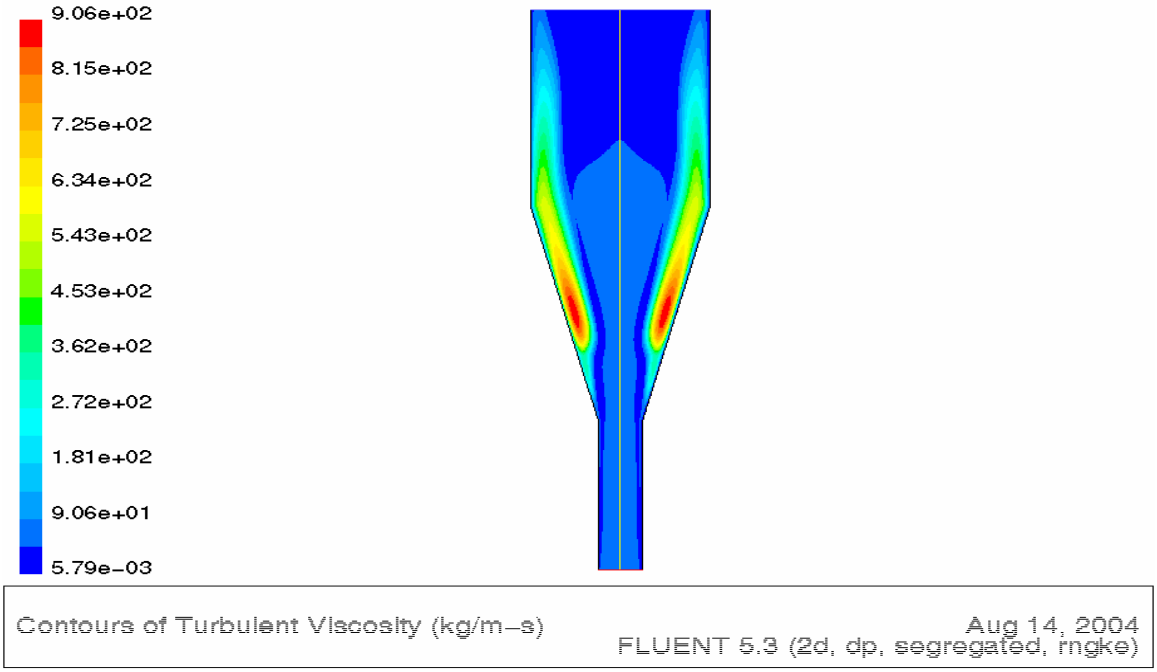

Figure F.25 Velocity Vector of Stream Function (D1)

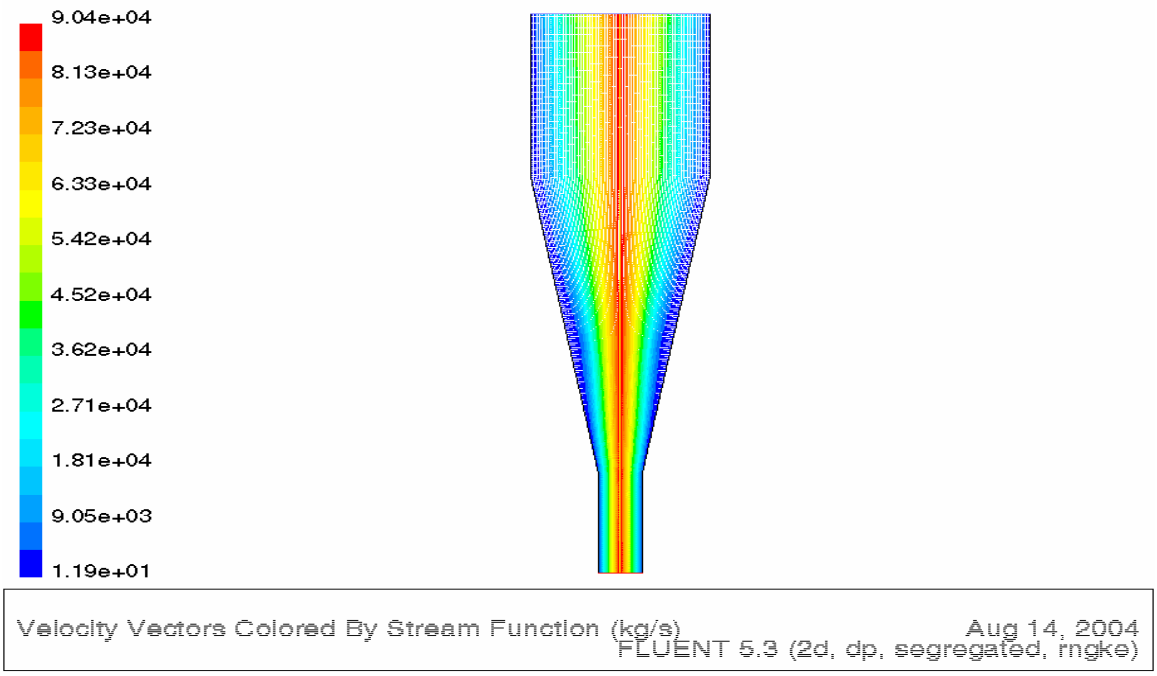


Figure F.26 Velocity Vector of Stream Function (D2)

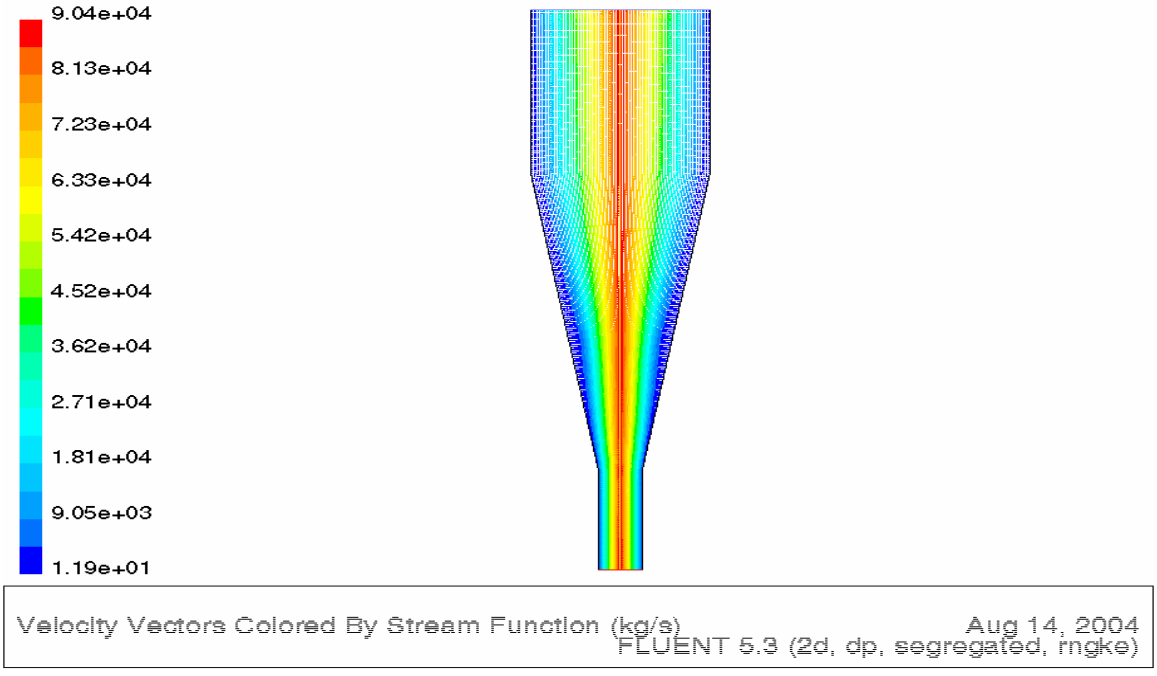

Figure F.27 Velocity Vector of Stream Function (D3)

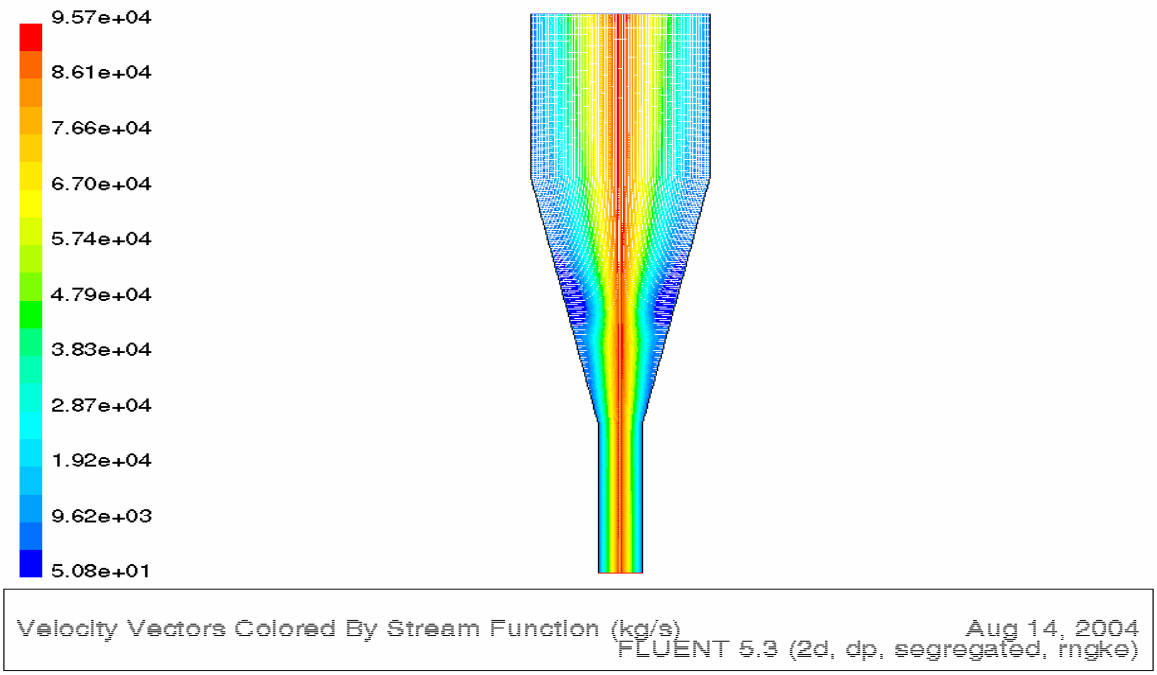


Figure F.28 Velocity Vector of Stream Function (D4)

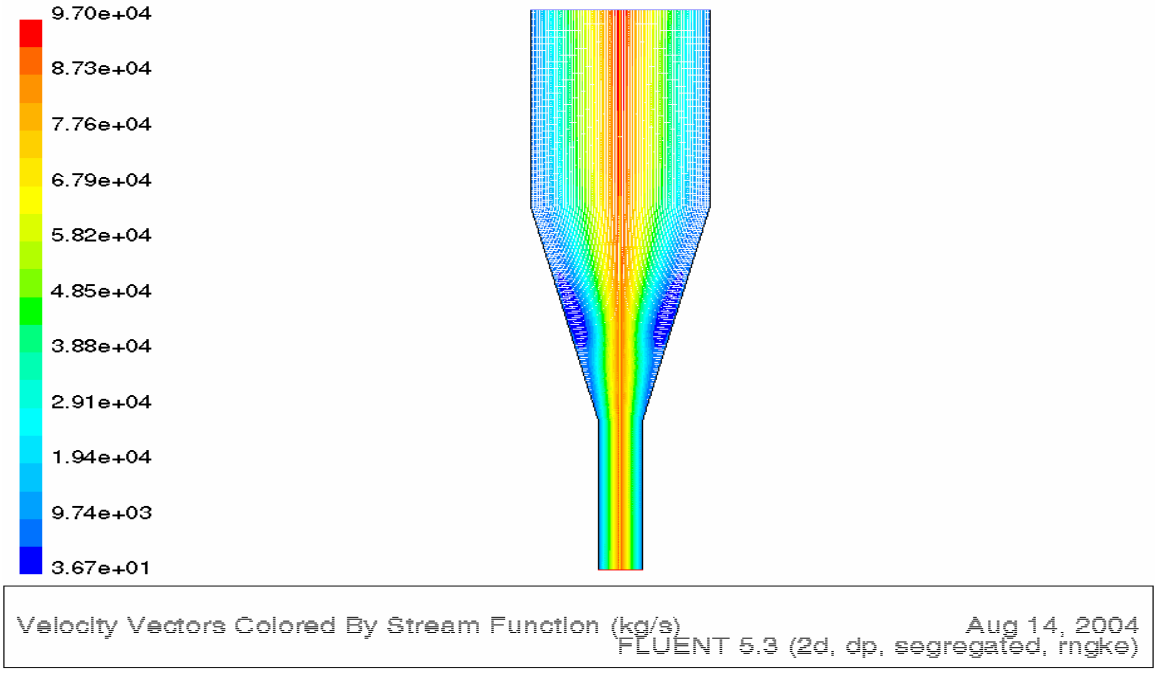

Figure F.29 Graph Total Pressure (D1)

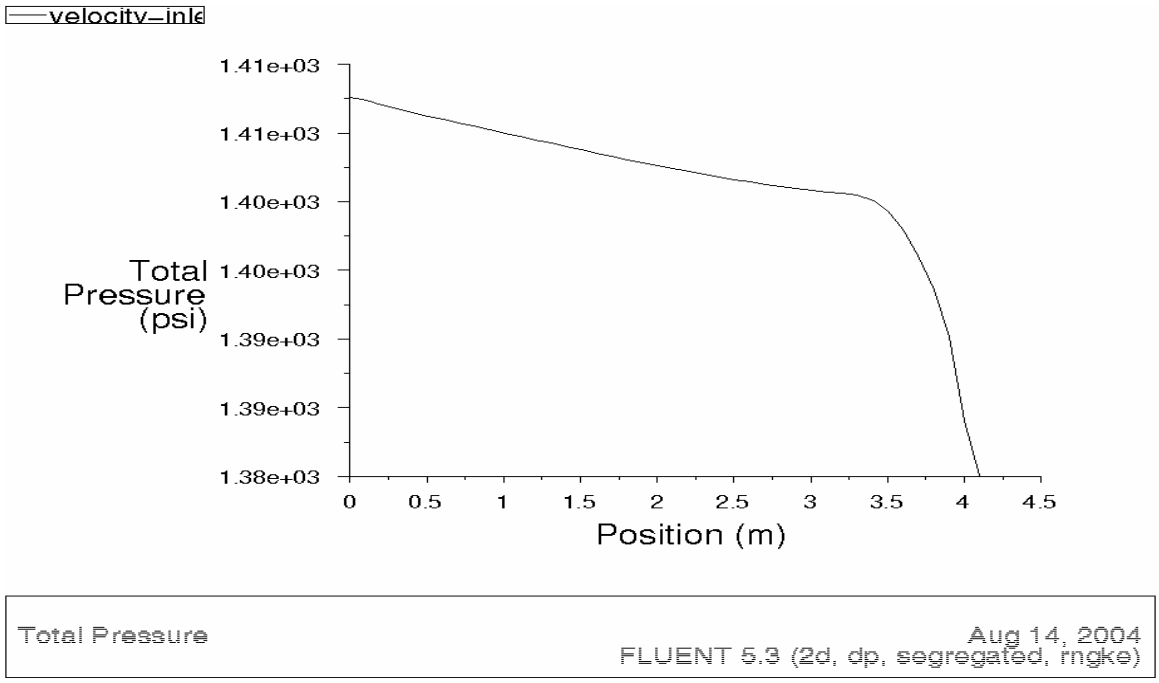


Figure F.30 Graph Total Pressure (D2)

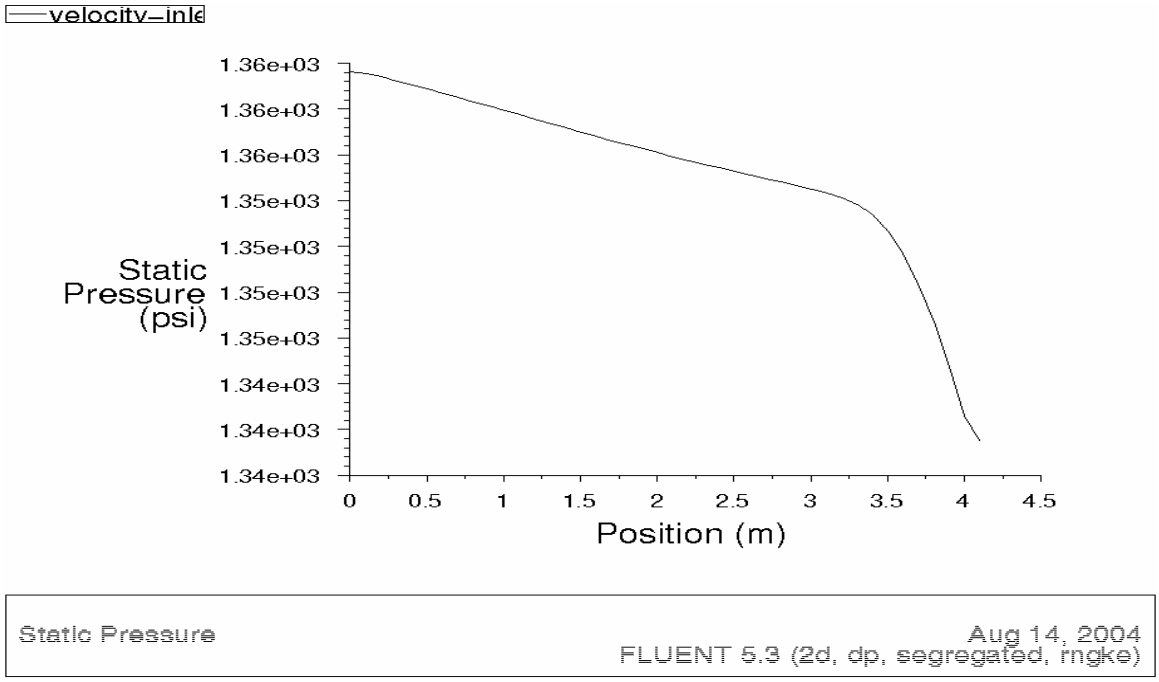

Figure F.31 Graph Total Pressure (D3)

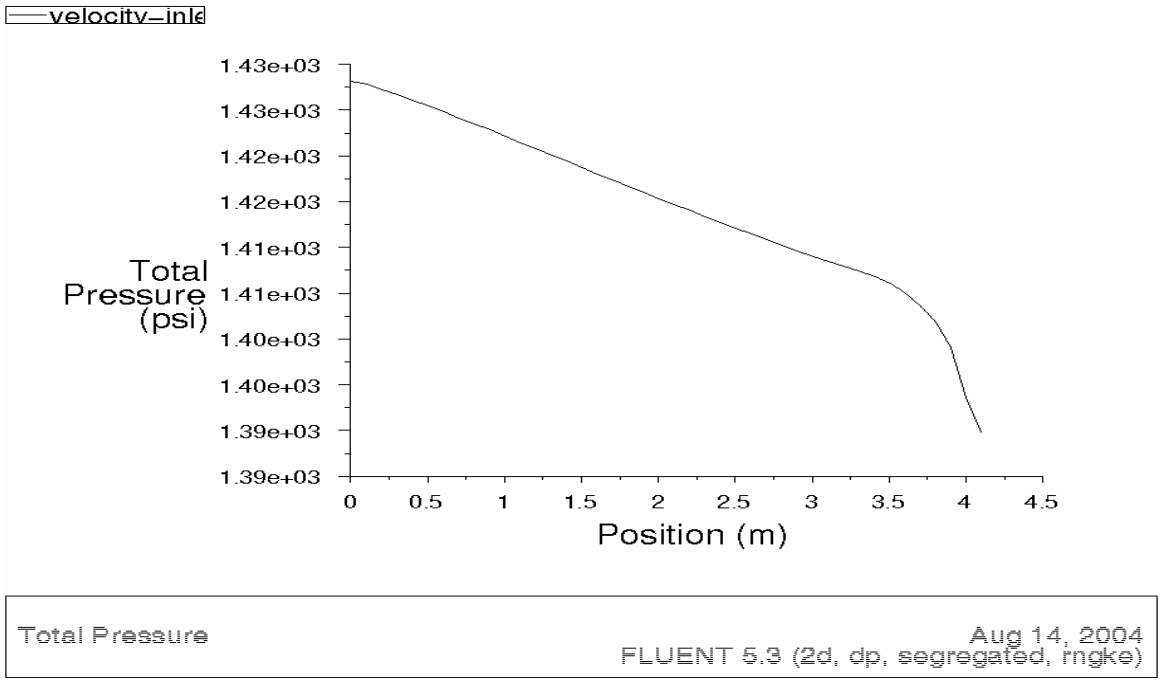


Figure F.32 Graph Total Pressure (D4)

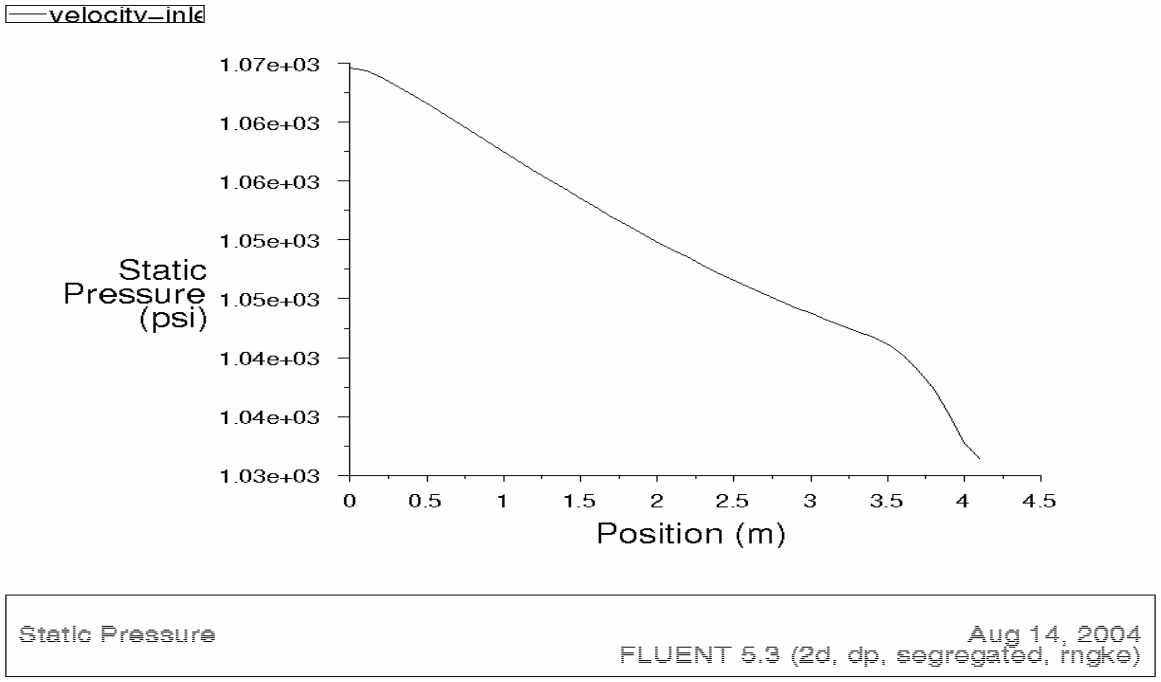

Figure F.33 Graph Turbulence Intensity (D1)

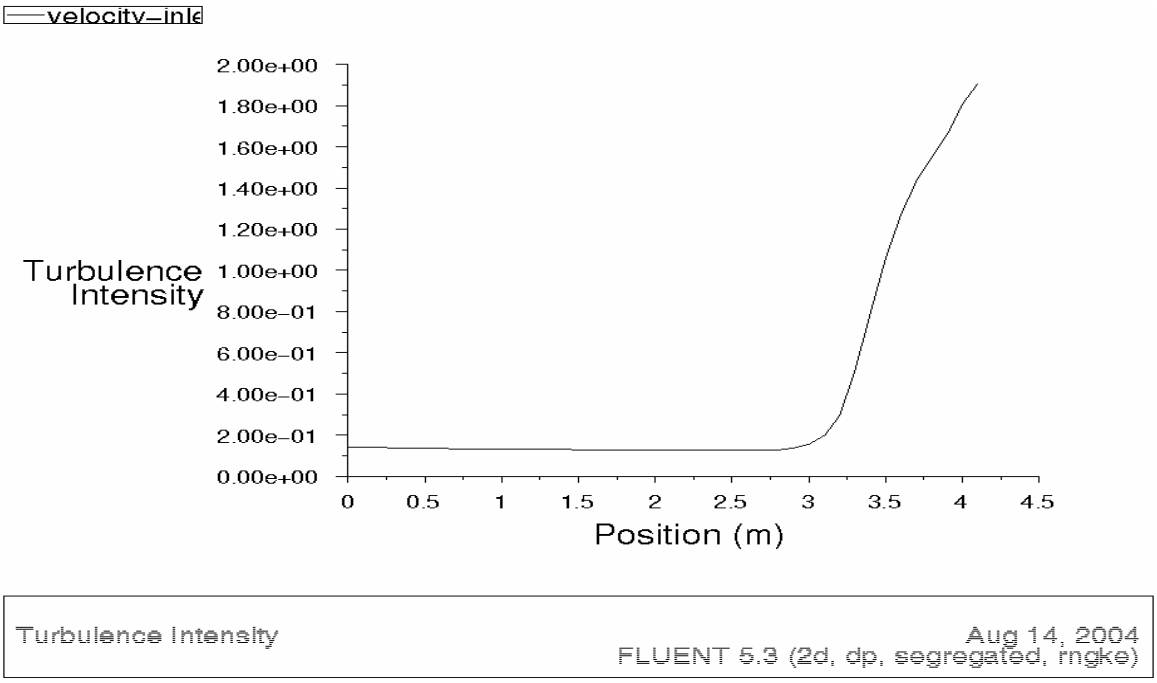


Figure F.34 Graph Turbulence Intensity (D2)

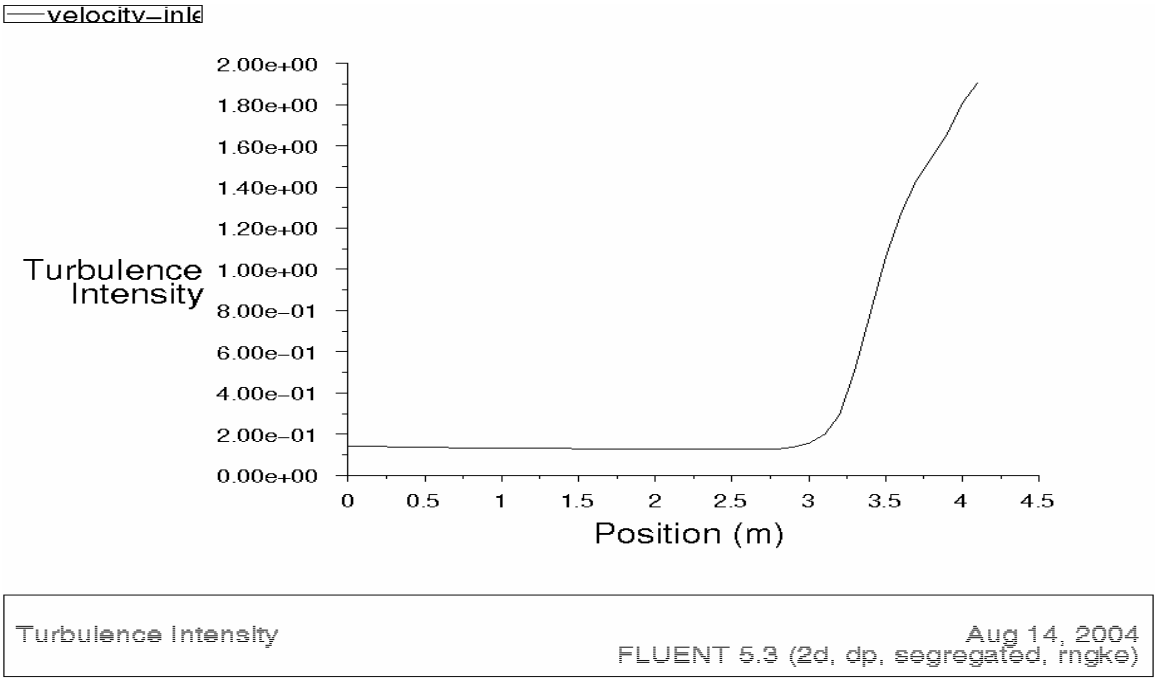

Figure F.35 Graph Turbulence Intensity (D3)

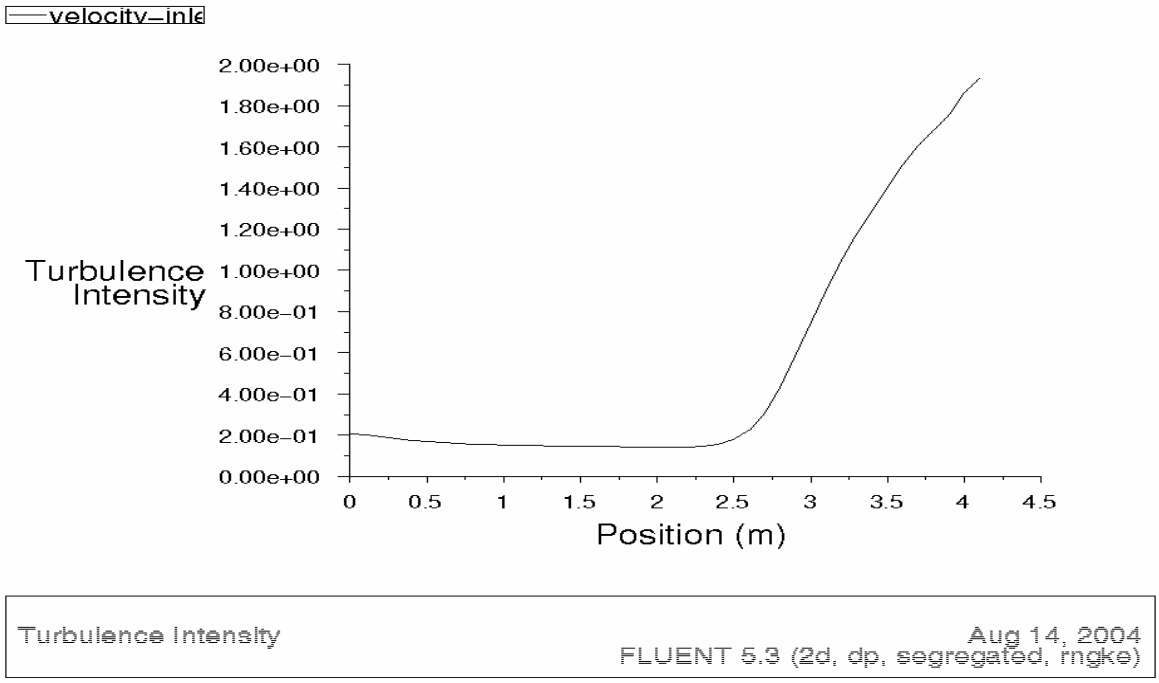


Figure F.36 Graph Turbulence Intensity (D4)

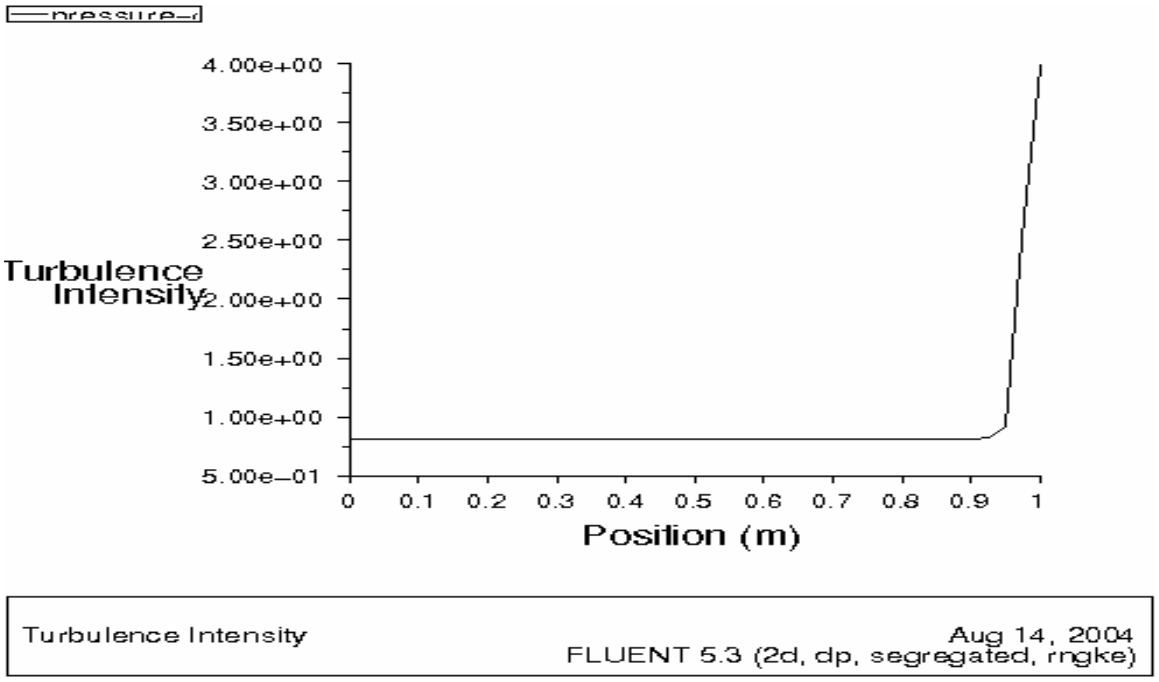

Figure F.37 Graph Turbulent Viscosity (D1)

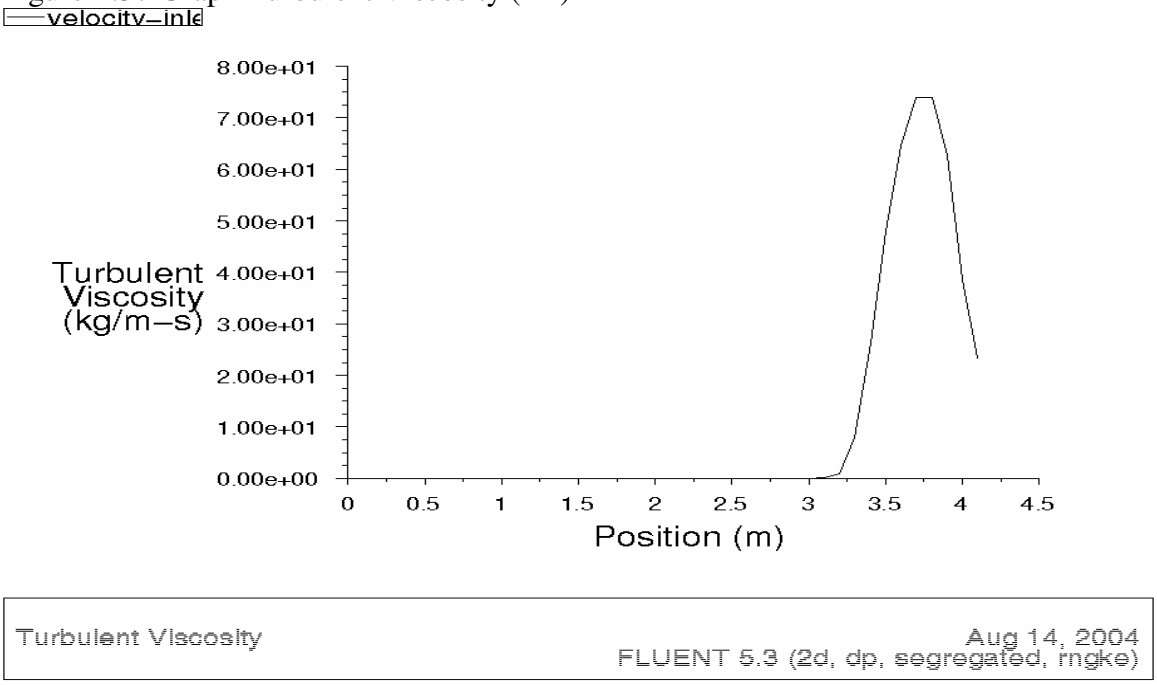


Figure F.38 Graph Turbulent Viscosity (D2)

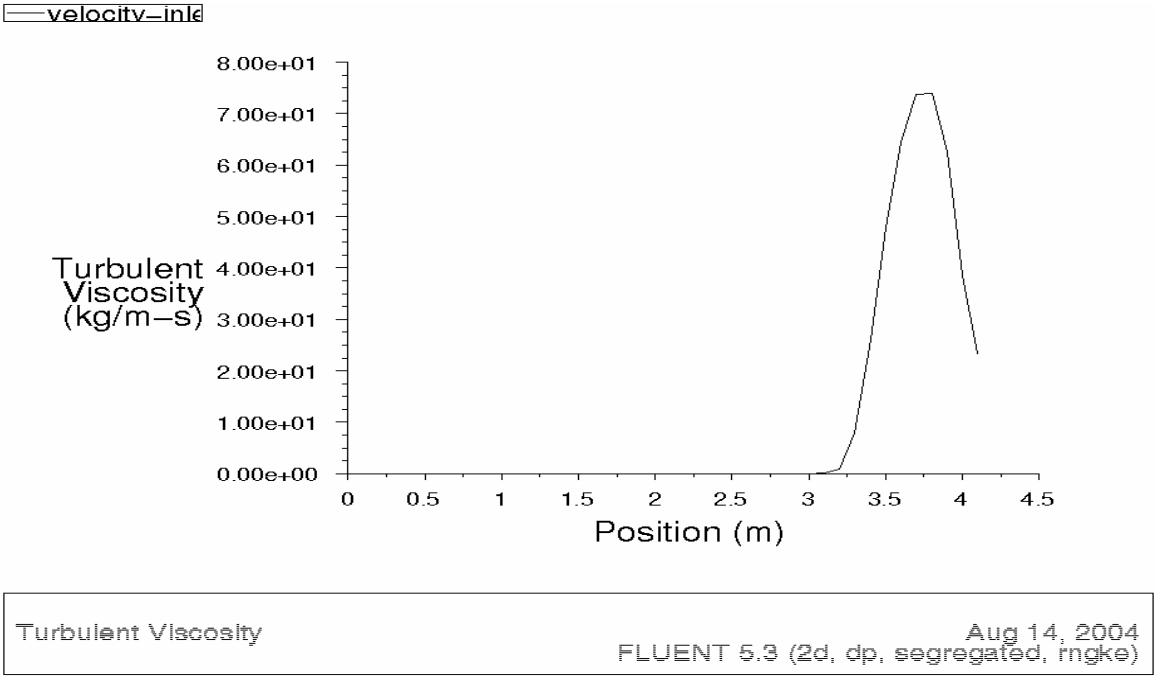

Figure F.39 Graph Turbulent Viscosity (D3)

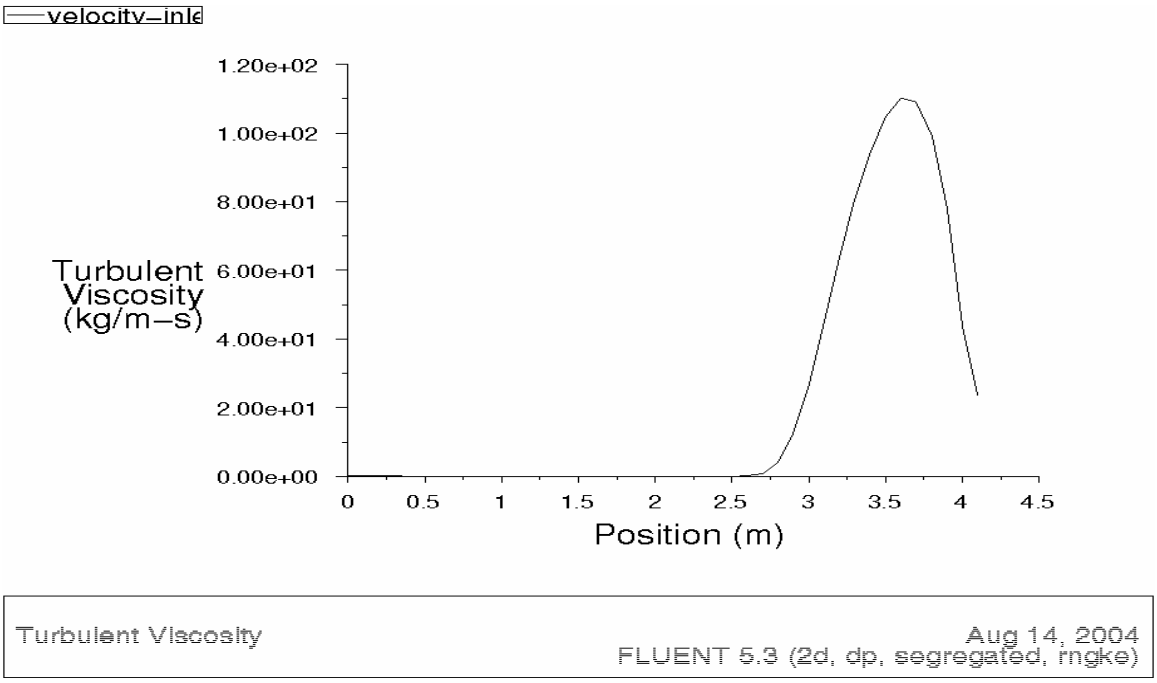


Figure F.40 Graph Turbulent Viscosity (D4)

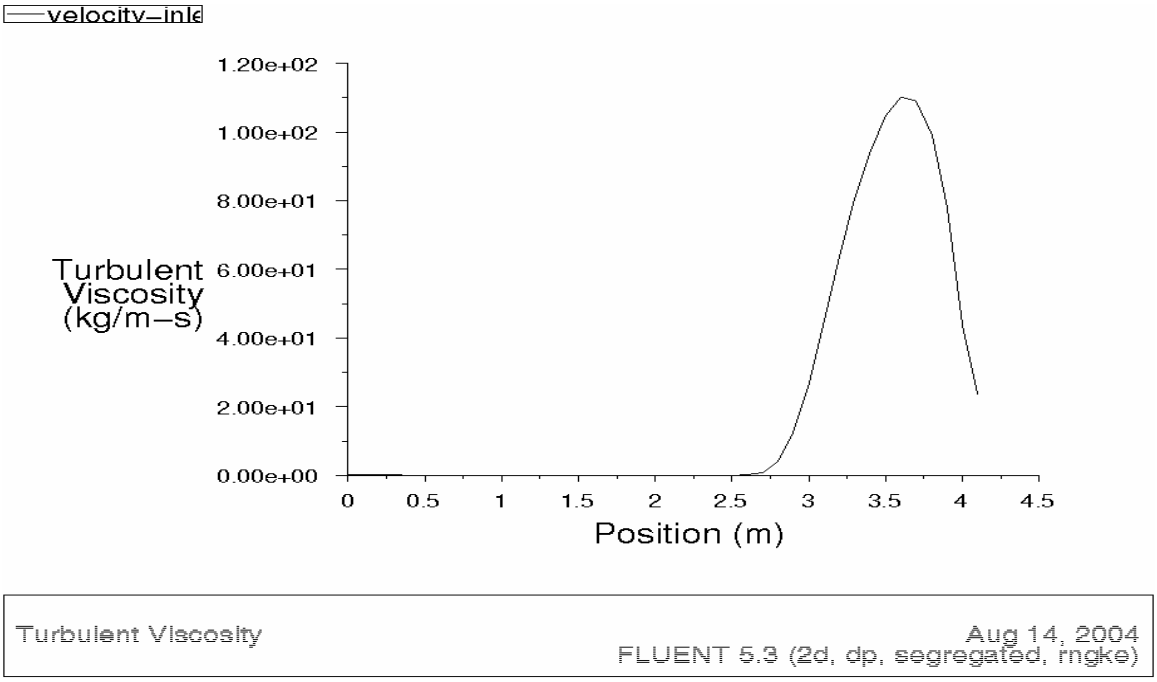

## F.2 3D Model (Sharp Edge with Taper -CDF)

Figure F.41 Contours of Total Pressure

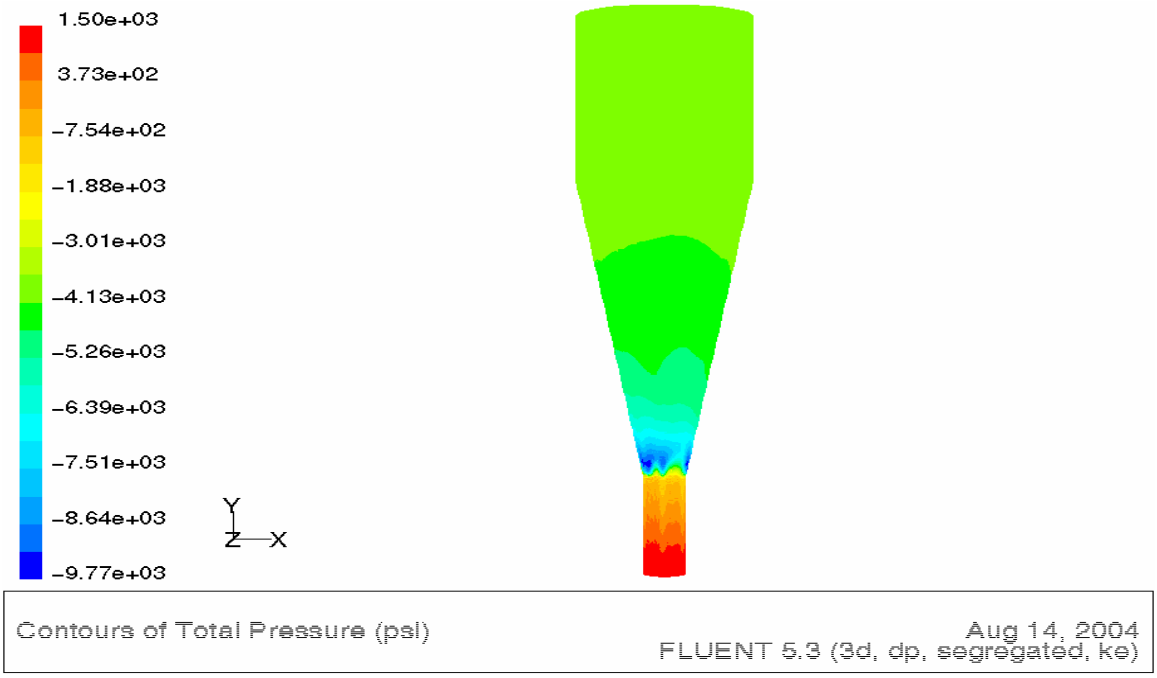


Figure F.42 Velocity Vector by Velocity Magnitude

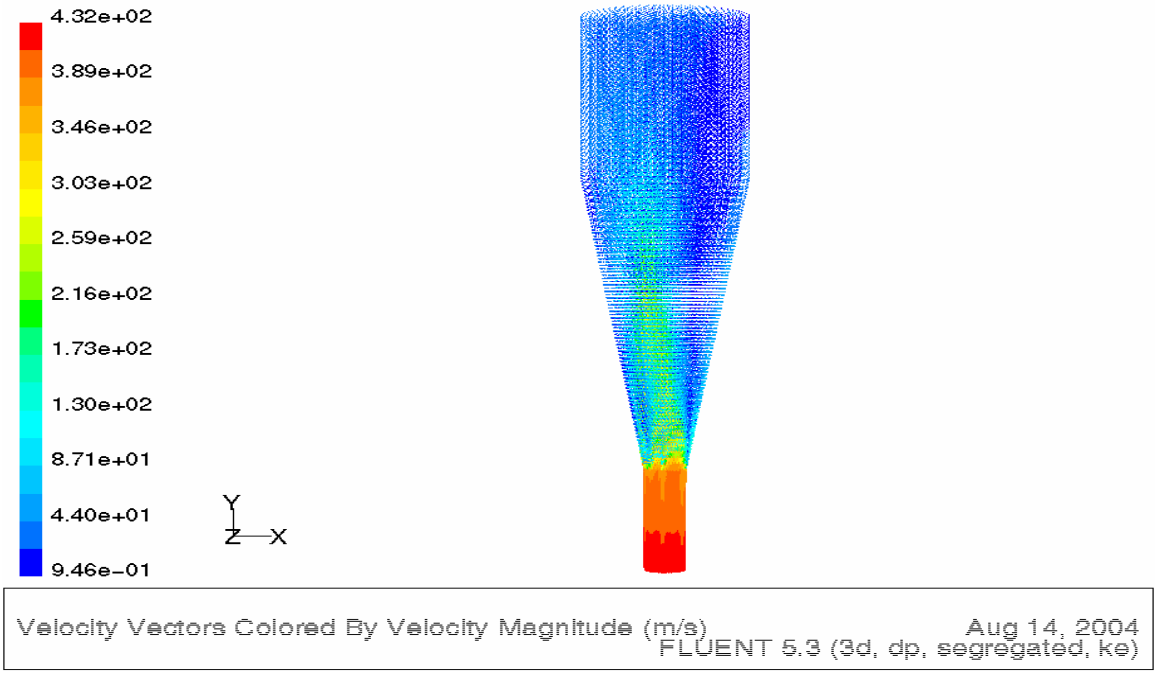

Figure F.43 Velocity Vector by Turbulent Kinetic Energy

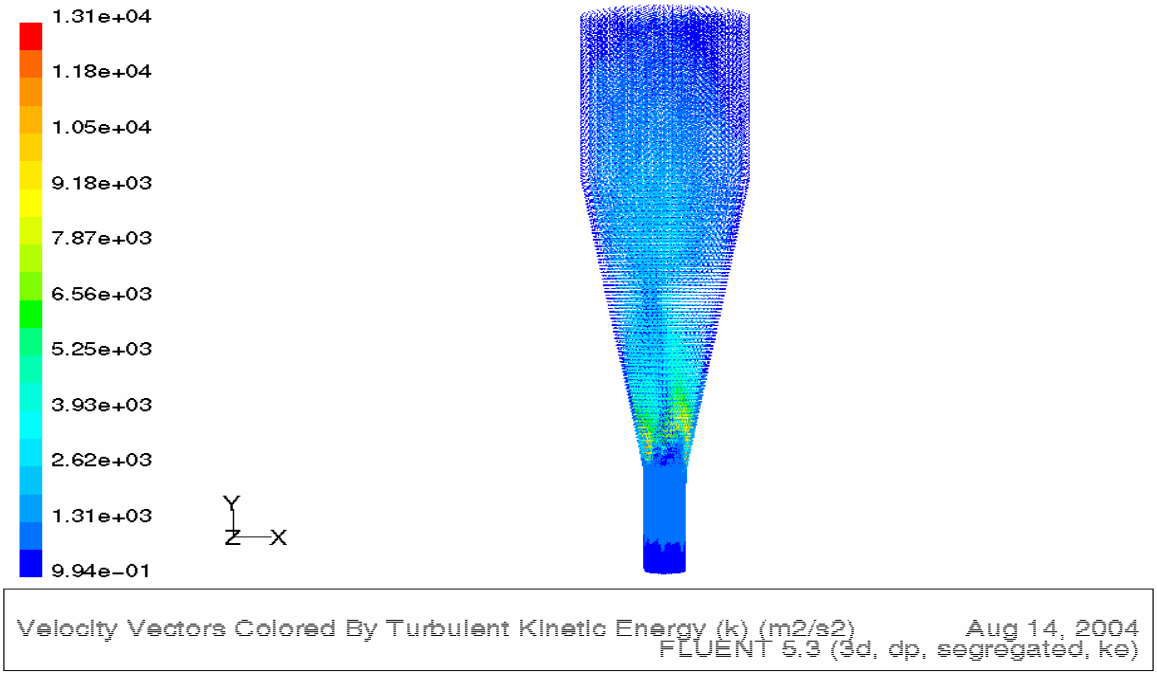


Figure F.44 Velocity Vector by Turbulence Intensity

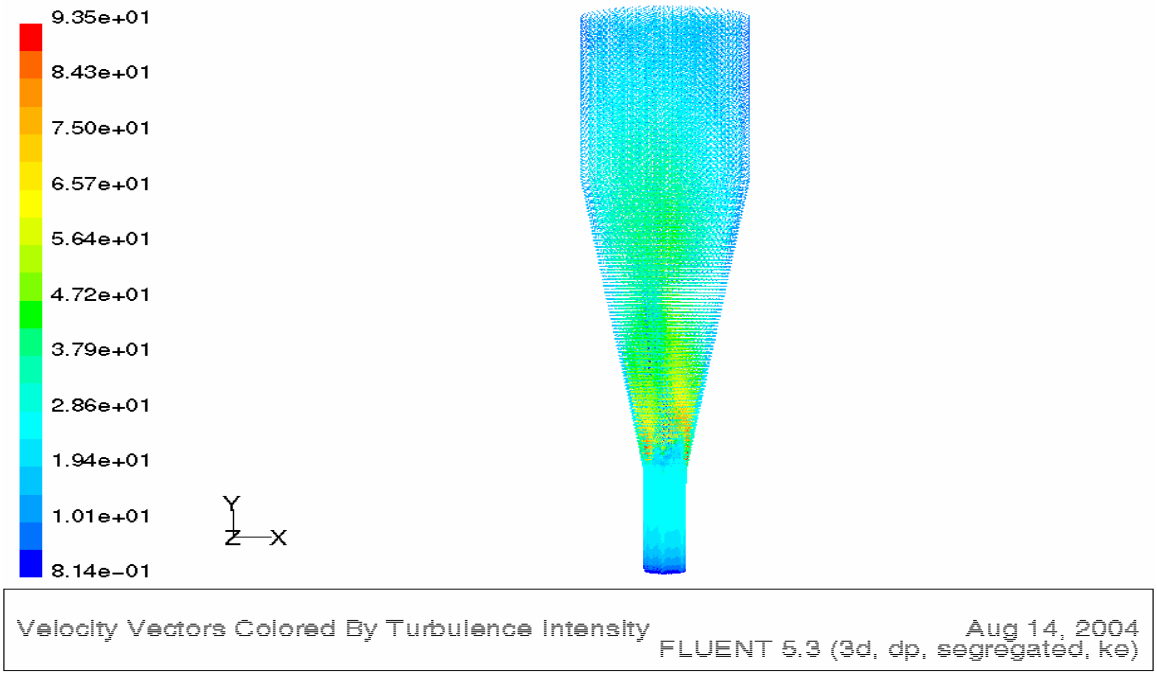

Figure F.45 Velocity Vector by Turbulence Viscosity

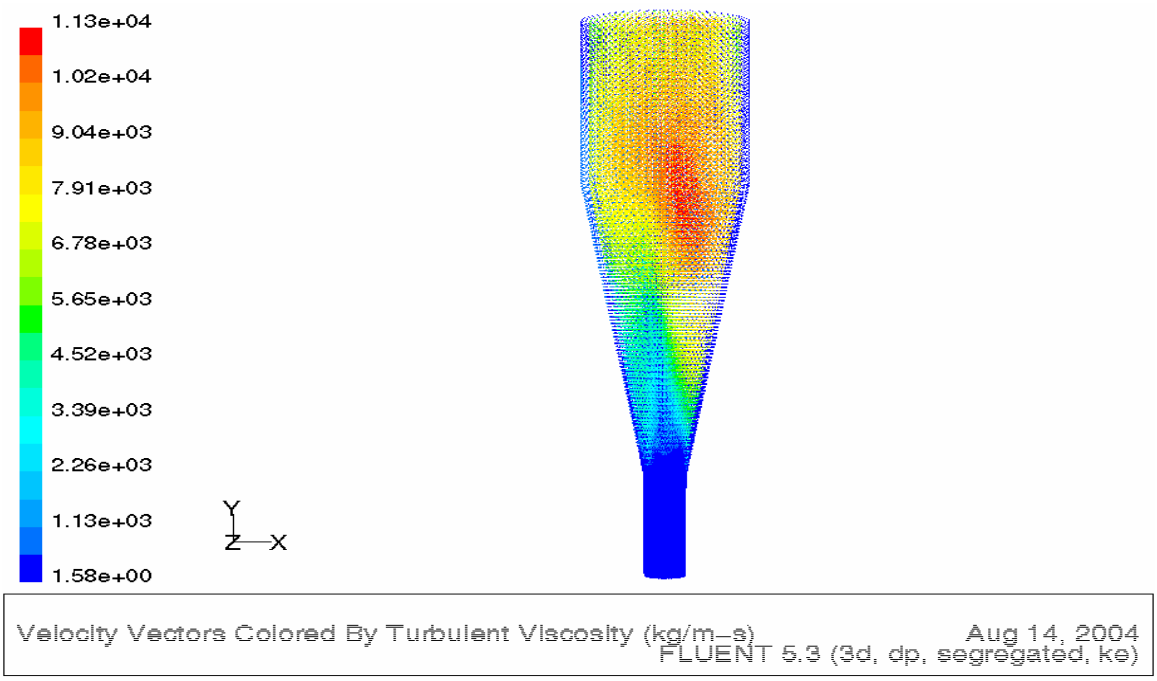


## F.3 3D Model (Rounded -CDF)

Figure F.46 Contours of Total Pressure

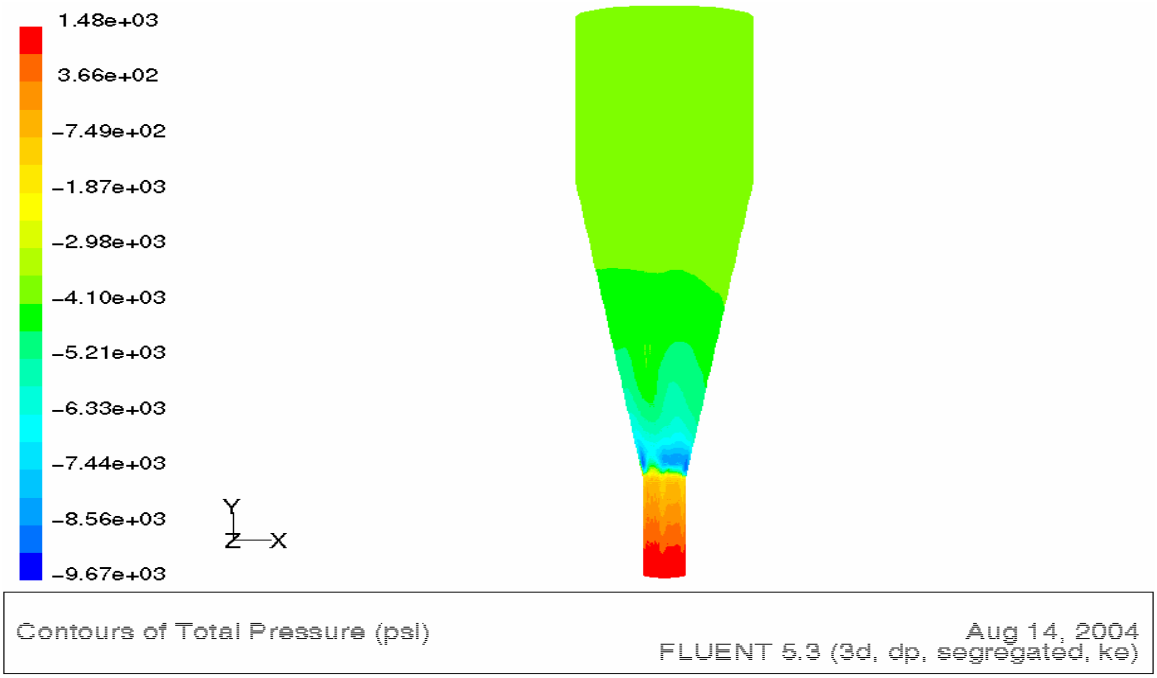

Figure F.47 Velocity Vector by Velocity Magnitude

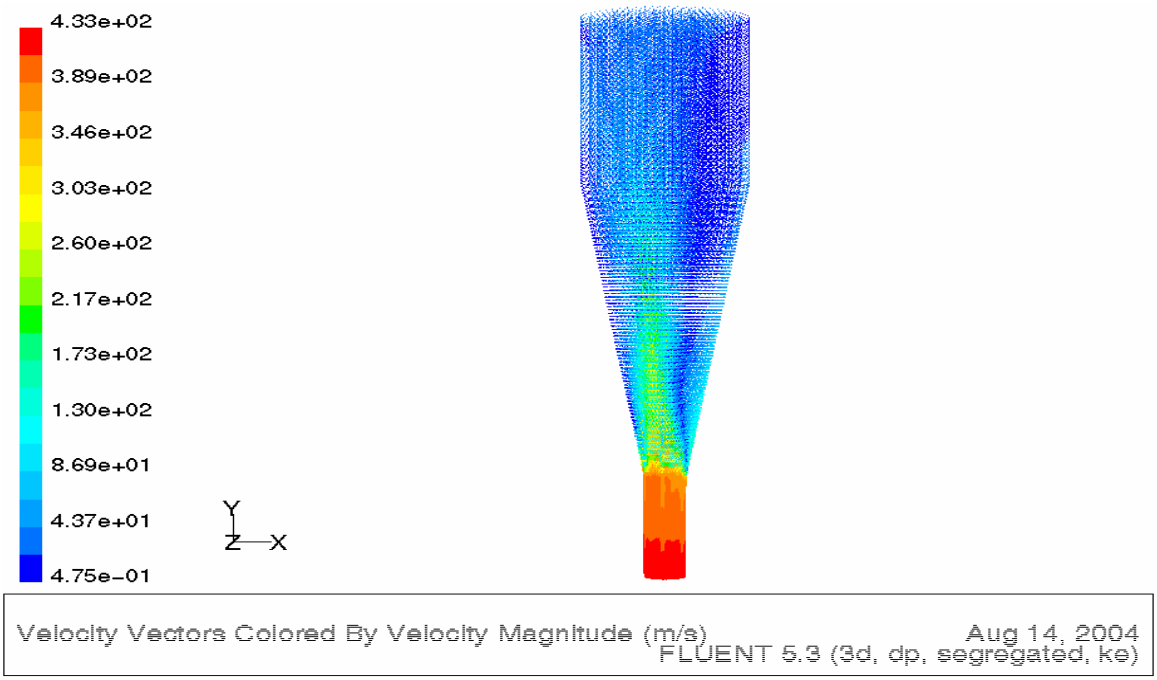


Figure F.48 Velocity Vector by Turbulent Kinetic Energy

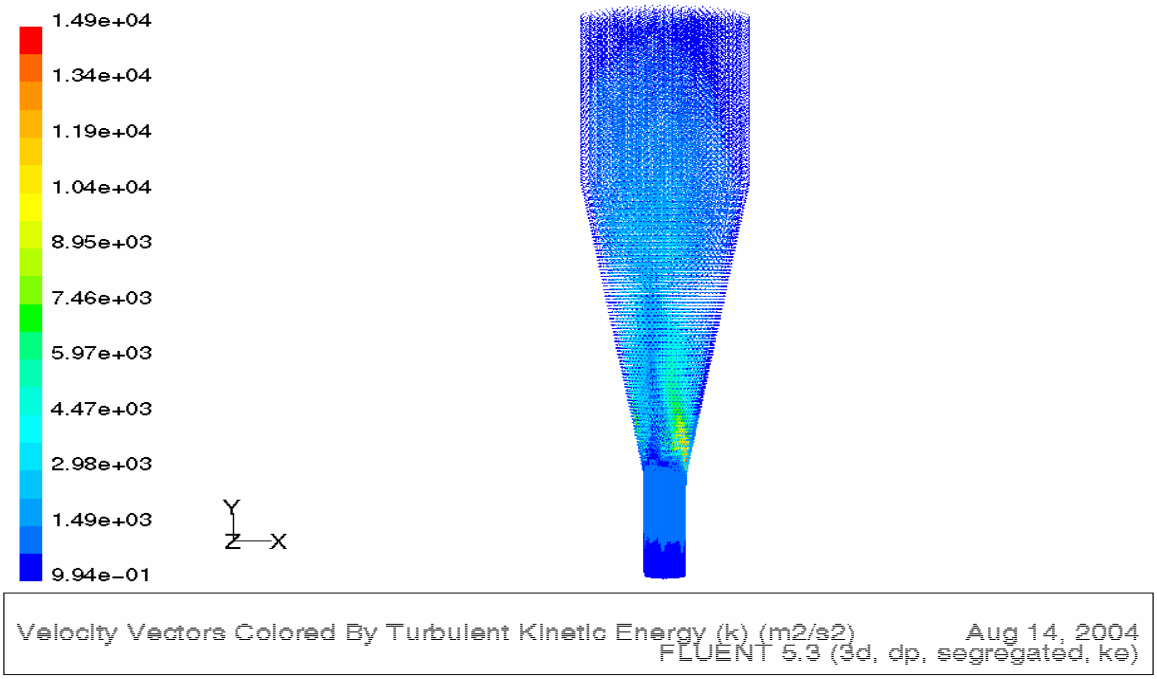

Figure F.49 Velocity Vector by Turbulence Intensity

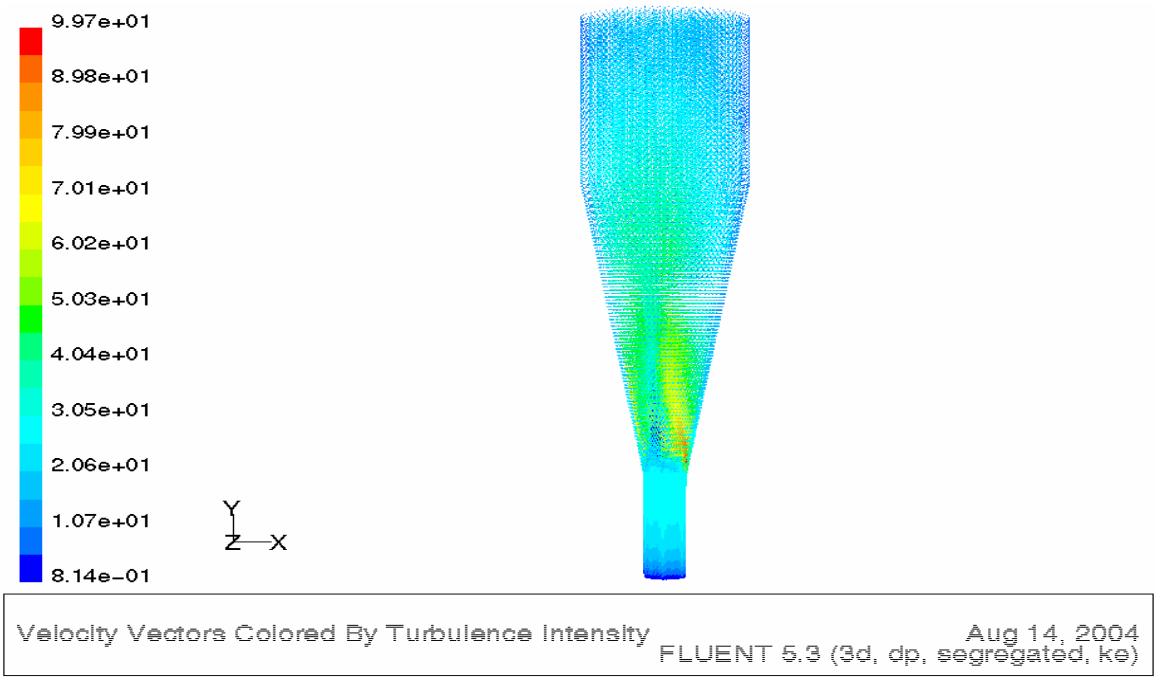


Figure F.50 Velocity Vector by Turbulence Viscosity

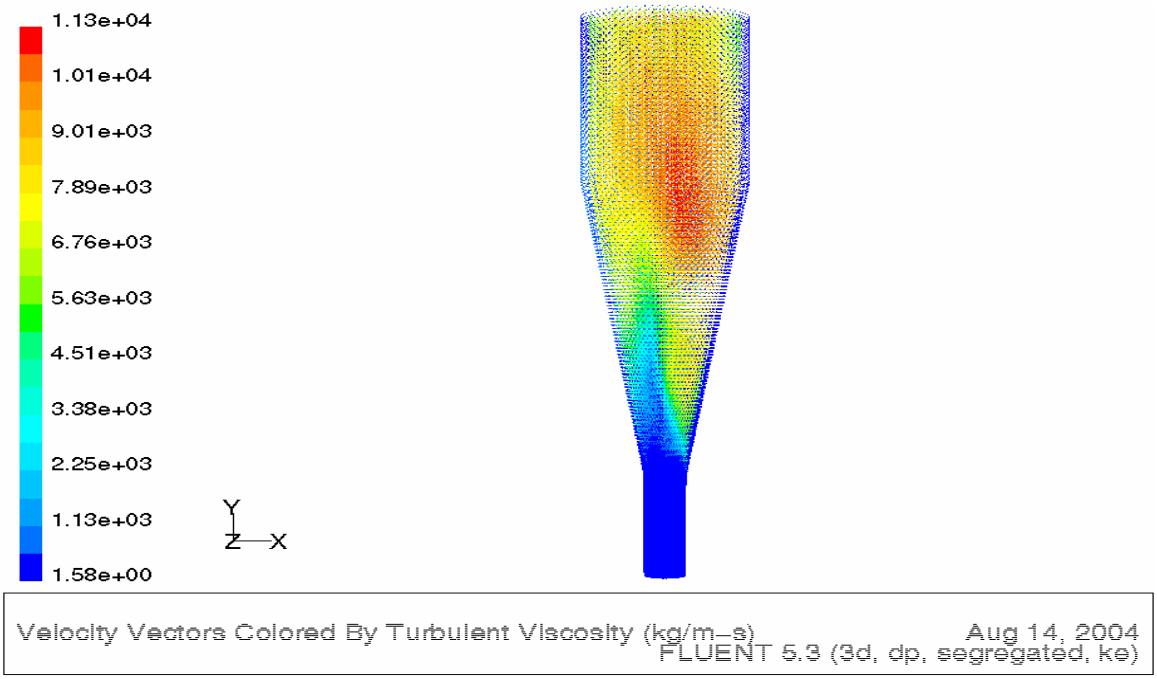

## F.4 2D Model (POME)

Figure F.51 Contours of Total Pressure (D1)

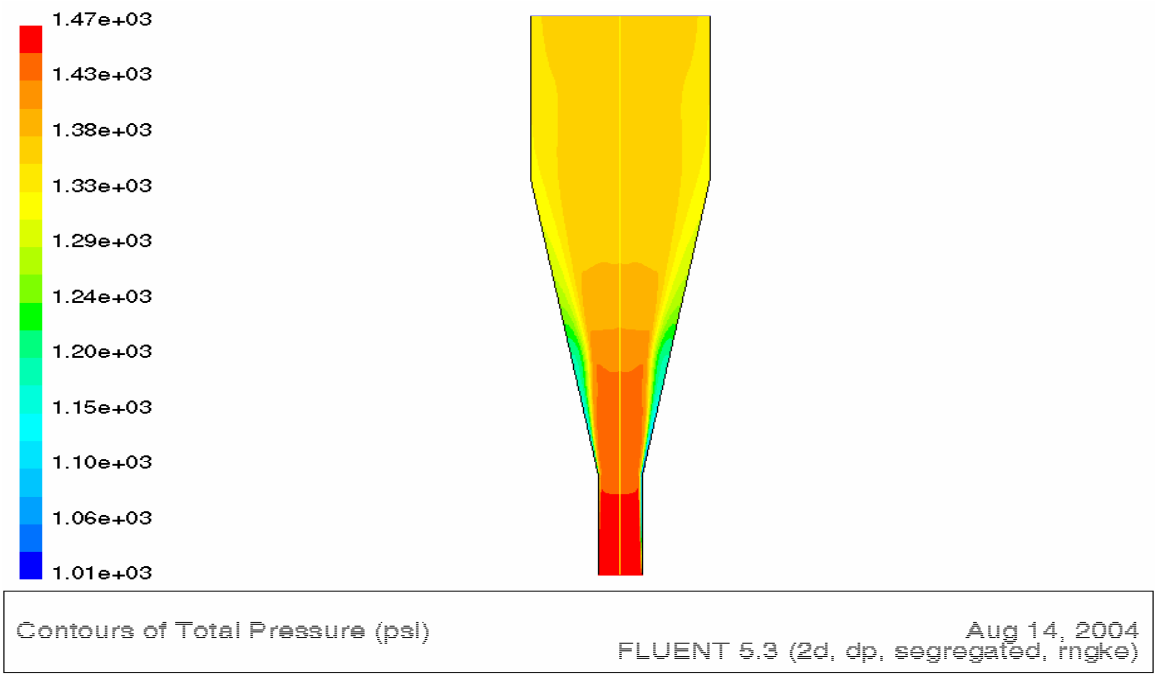


Figure F.52 Contours of Total Pressure (D2)

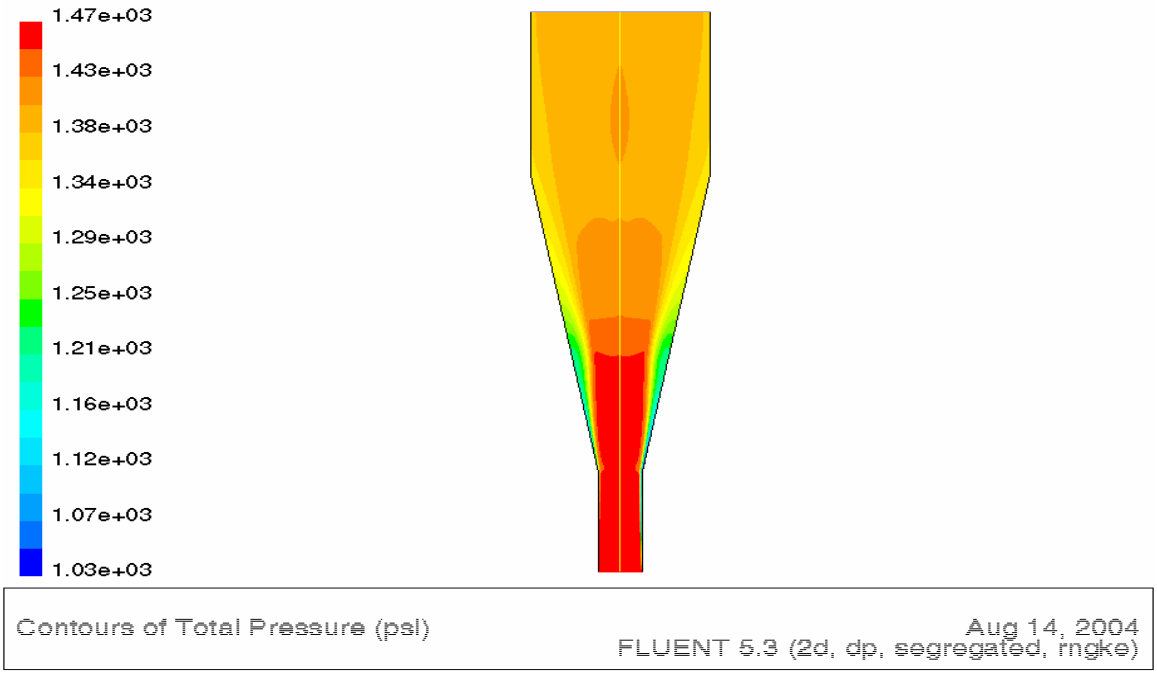

Figure F.53 Contours of Total Pressure (D3)

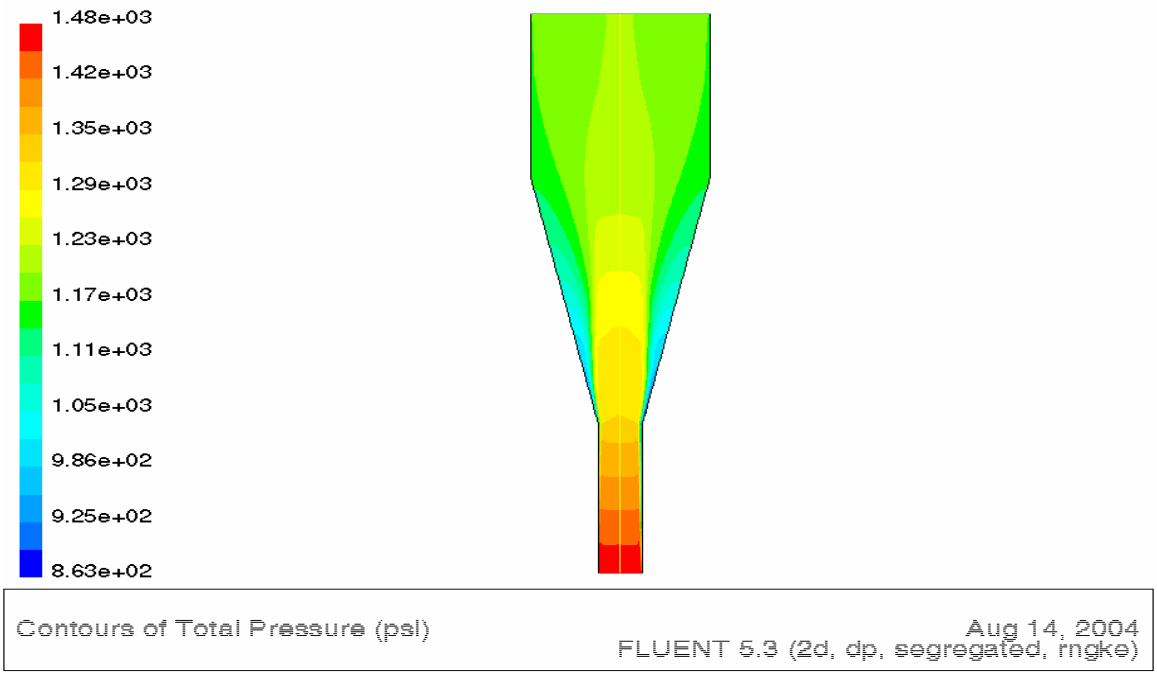


Figure F.54 Contours of Total Pressure (D4)

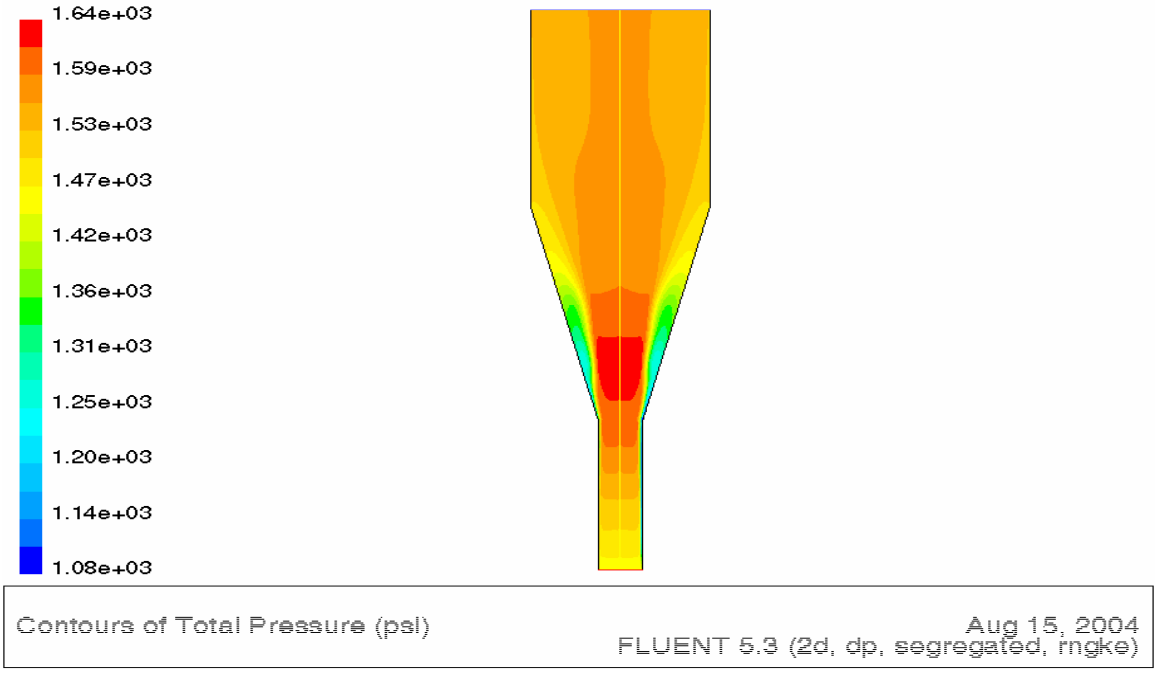

Figure F.55 Contours of Velocity Magnitude (D1)

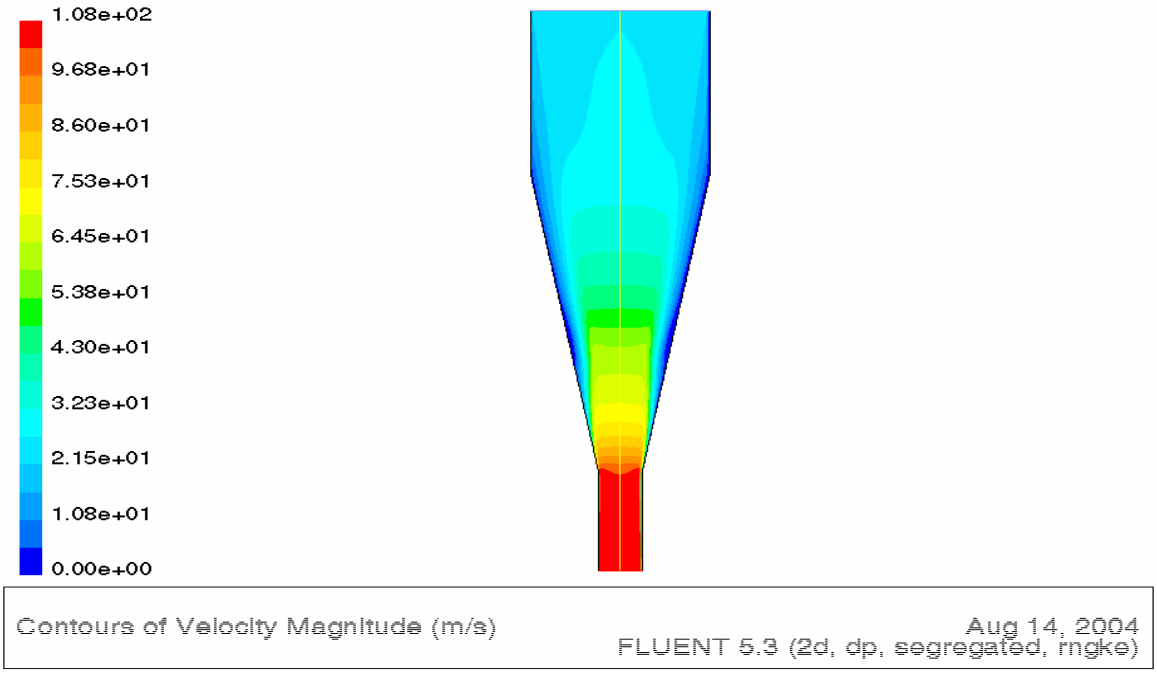


Figure F.56 Contours of Velocity Magnitude (D2)

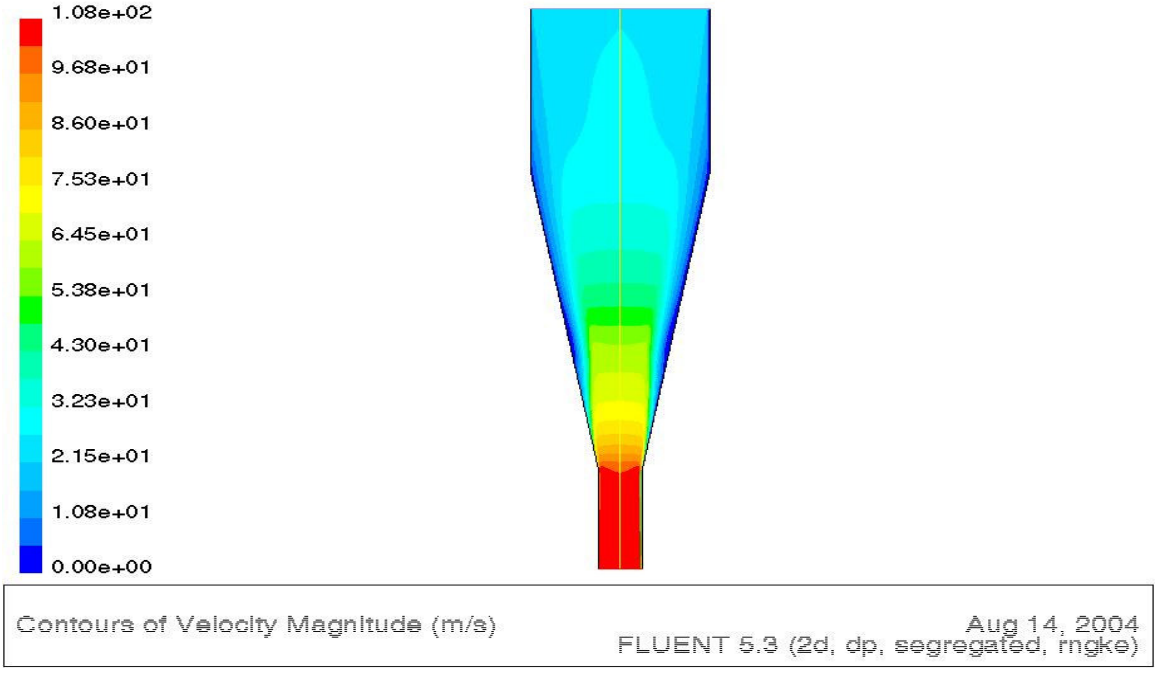

Figure F.57 Contours of Velocity Magnitude (D3)

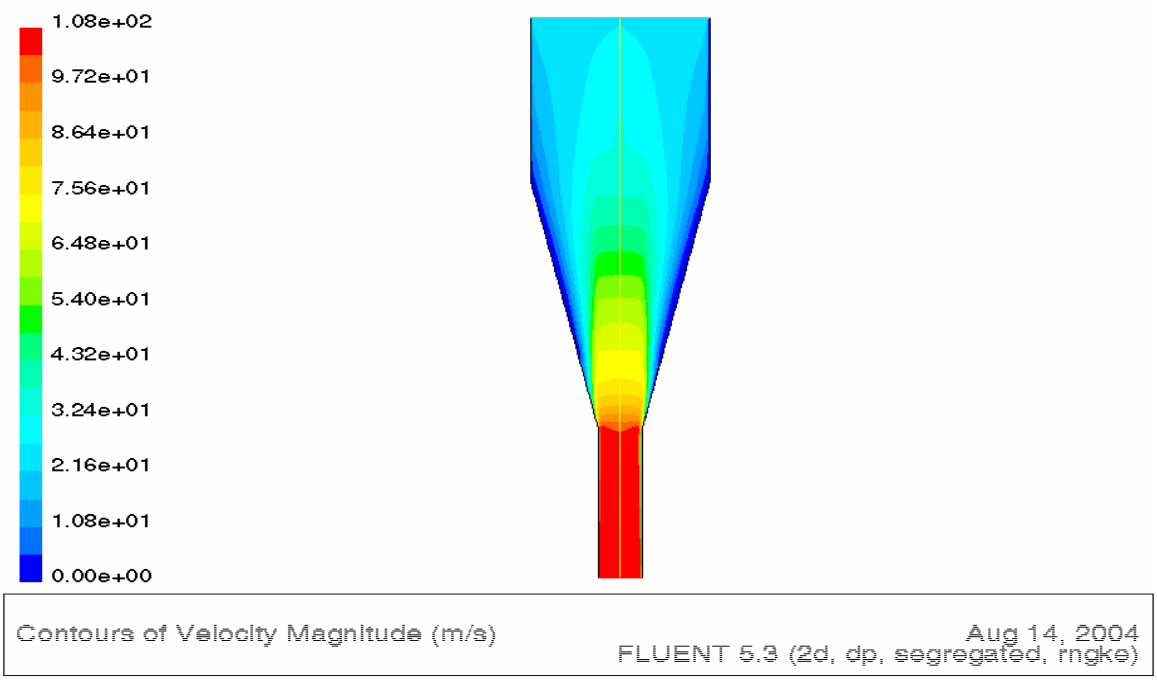


Figure F.58 Contours of Velocity Magnitude (D4)

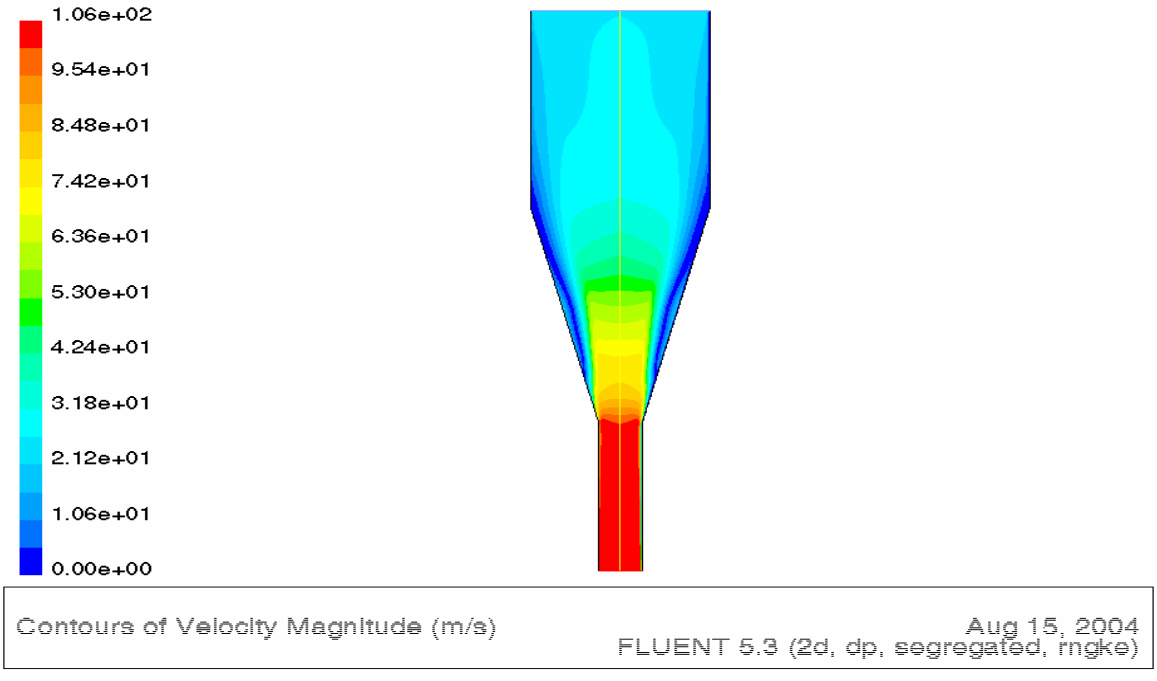

Figure F.59 Contours of Stream Function (D1)

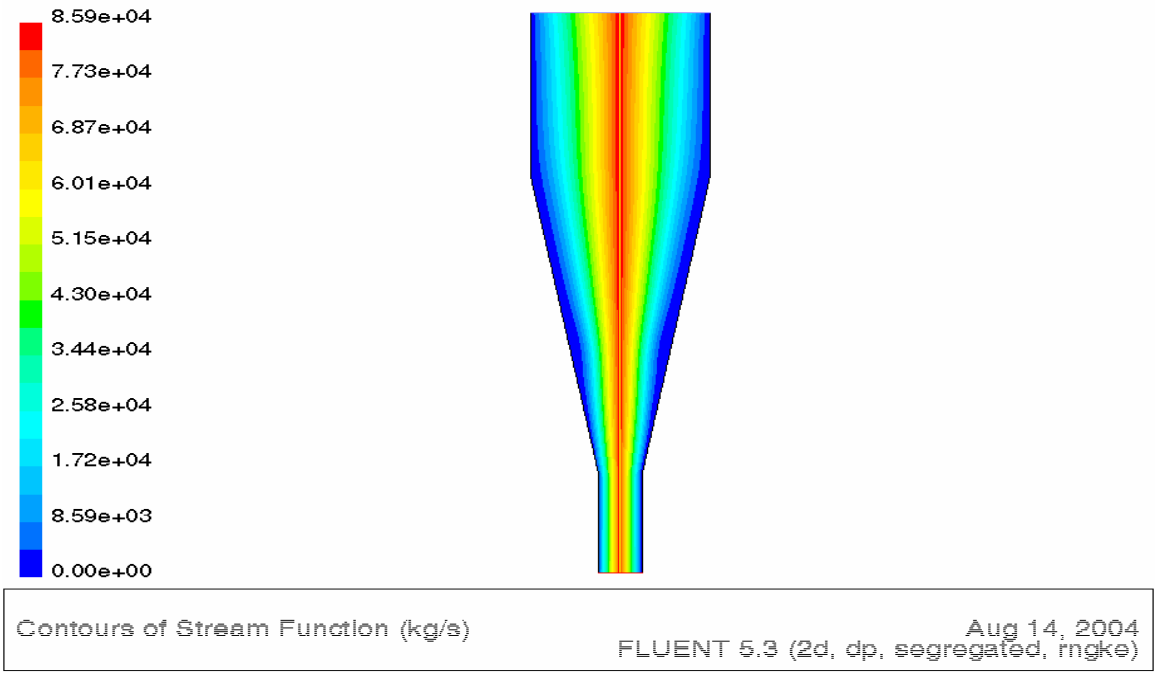


Figure F.60 Contours of Stream Function (D2)

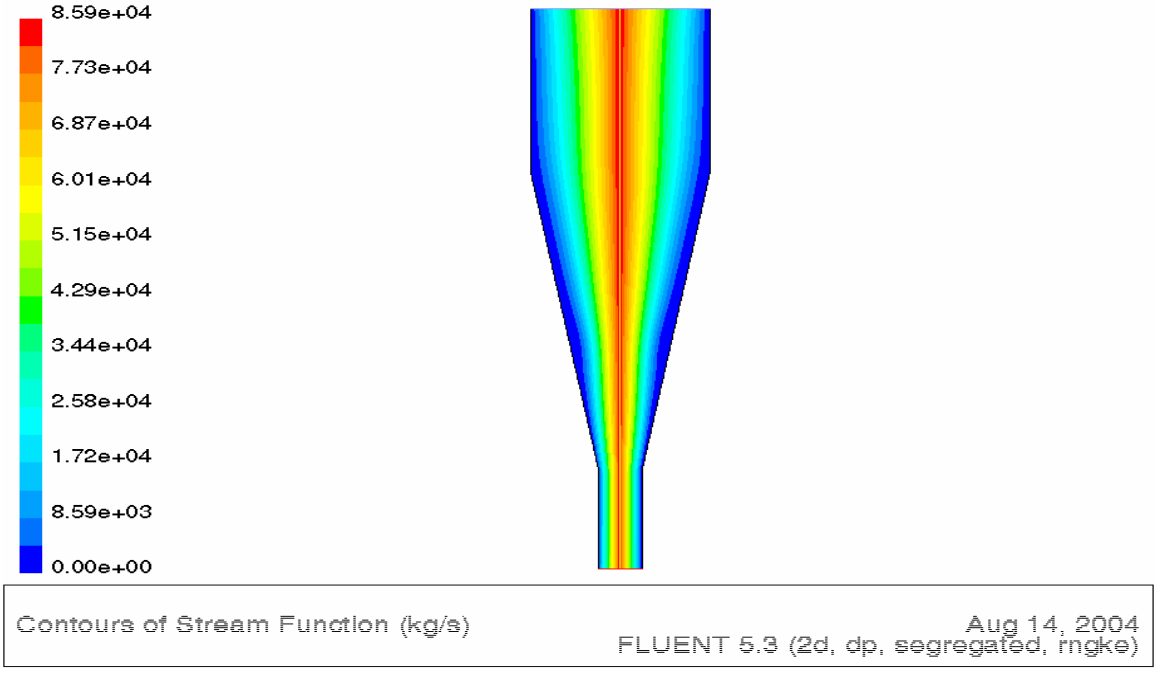

Figure F.61 Contours of Stream Function (D3)

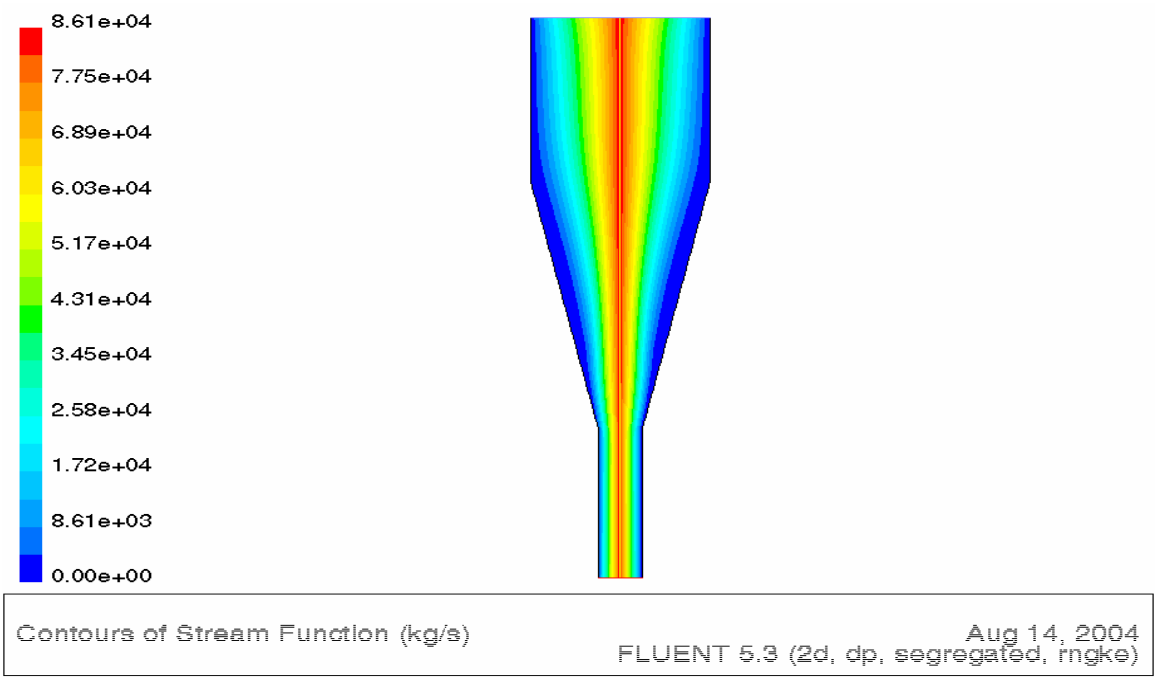


Figure F.62 Contours of Stream Function (D4)

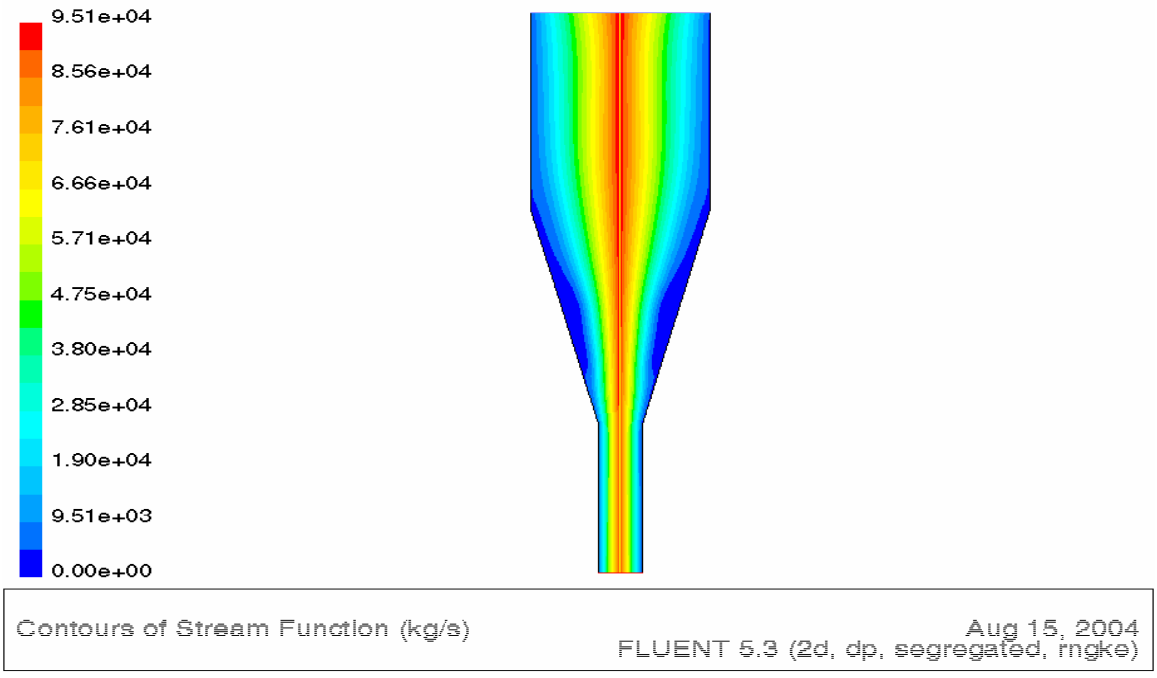

Figure F.63 Contours of Turbulent Kinetic Energy (D1)

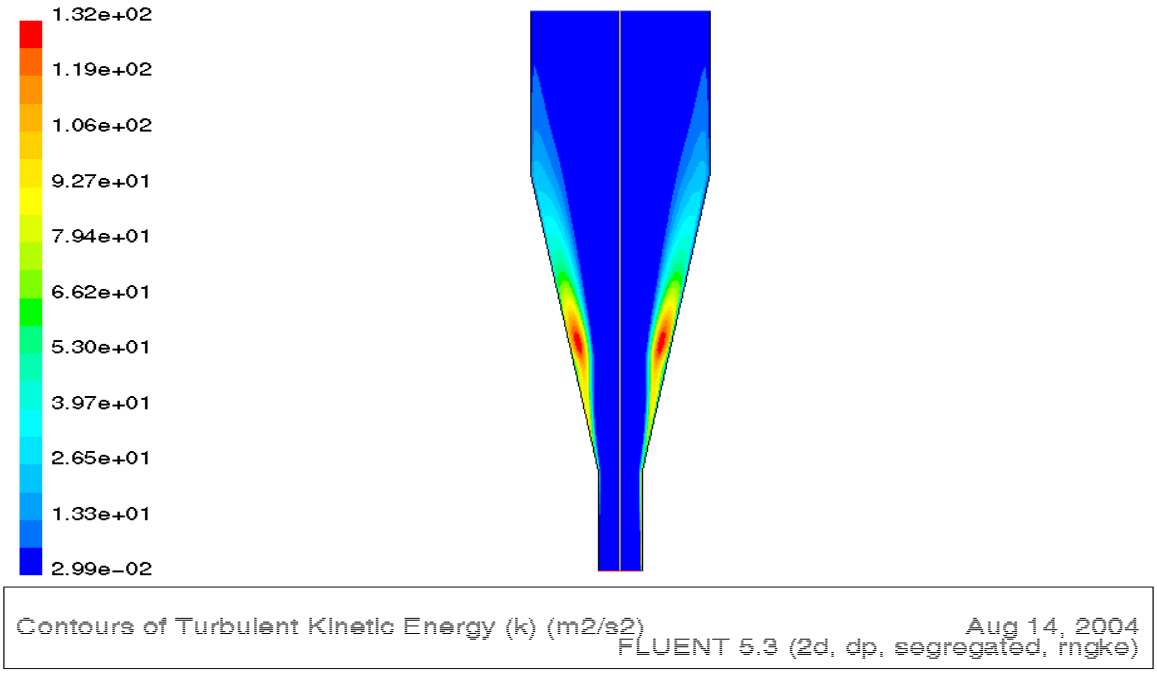


Figure F.64 Contours of Turbulent Kinetic Energy (D2)

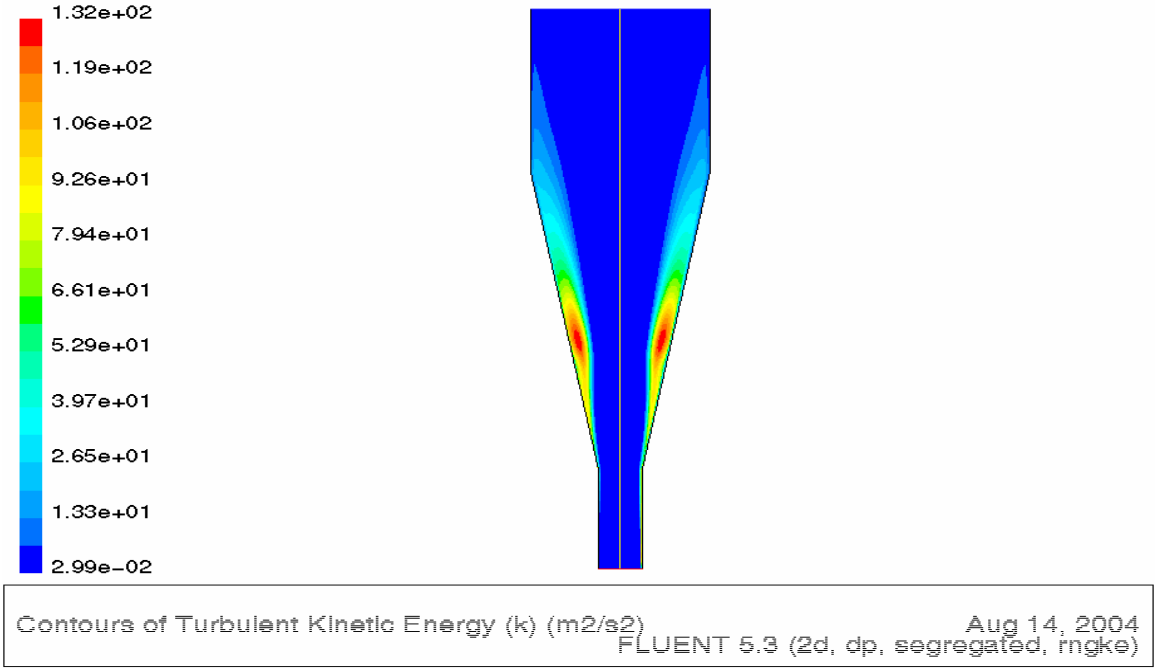

Figure F.65 Contours of Turbulent Kinetic Energy (D3)

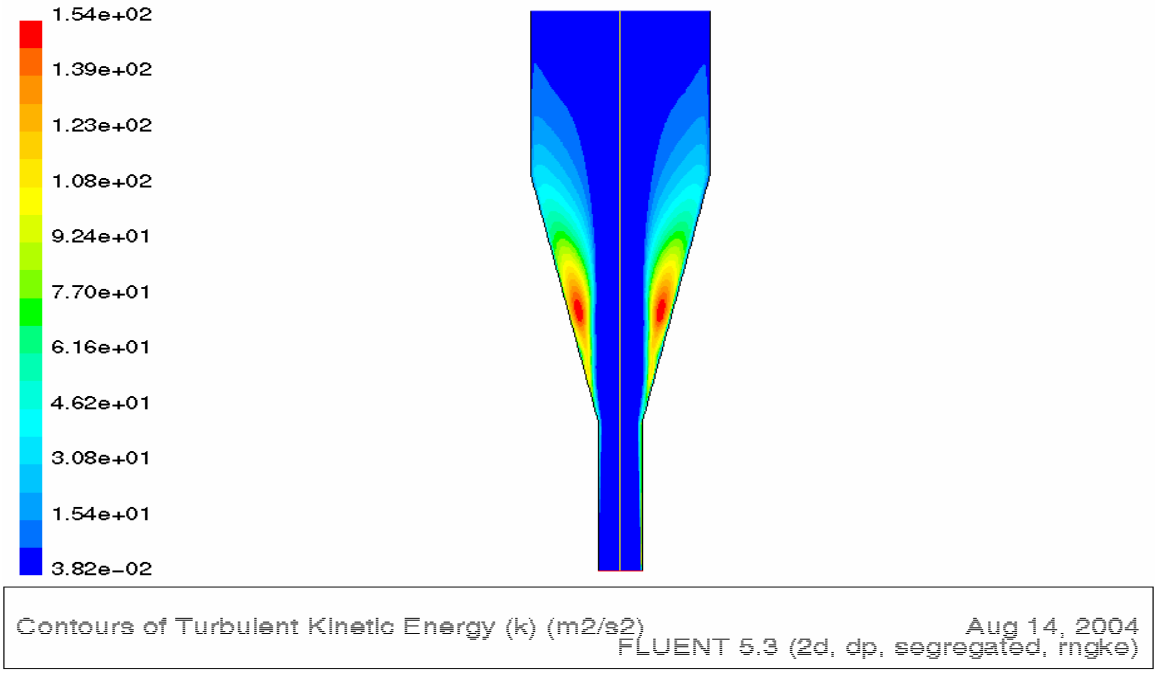


Figure F.66 Contours of Turbulent Kinetic Energy (D4)

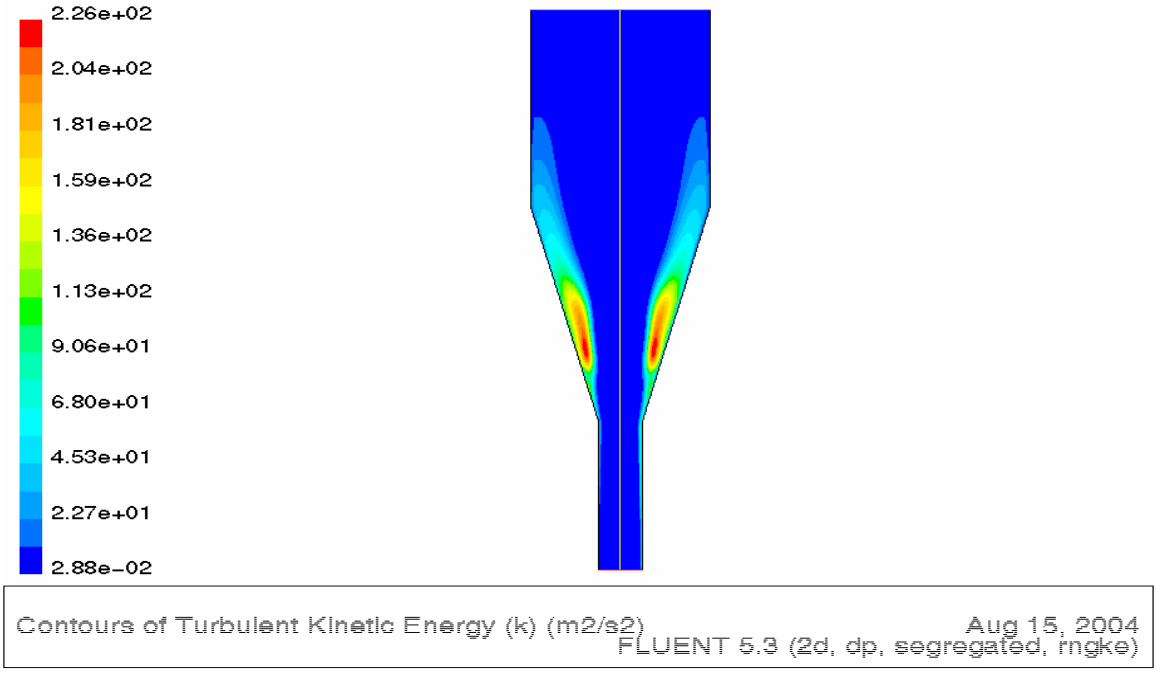

Figure F.67 Contours of Turbulence Intensity (D1)

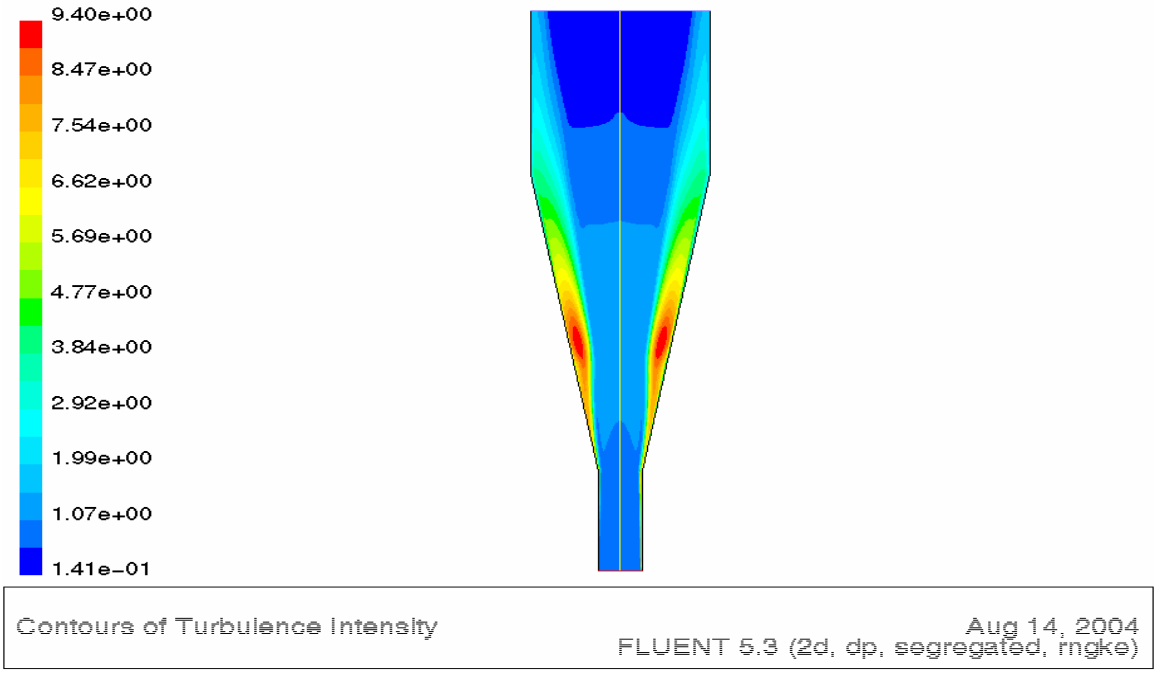


Figure F.68 Contours of Turbulence Intensity (D2)

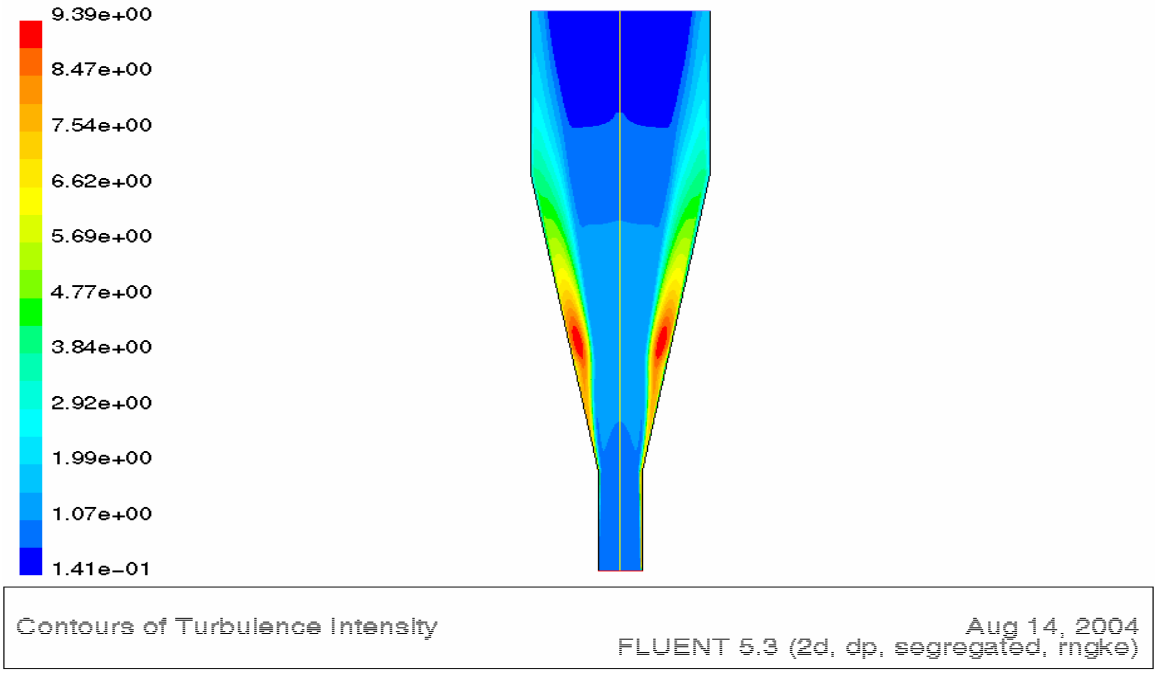

Figure F.69 Contours of Turbulence Intensity (D3)

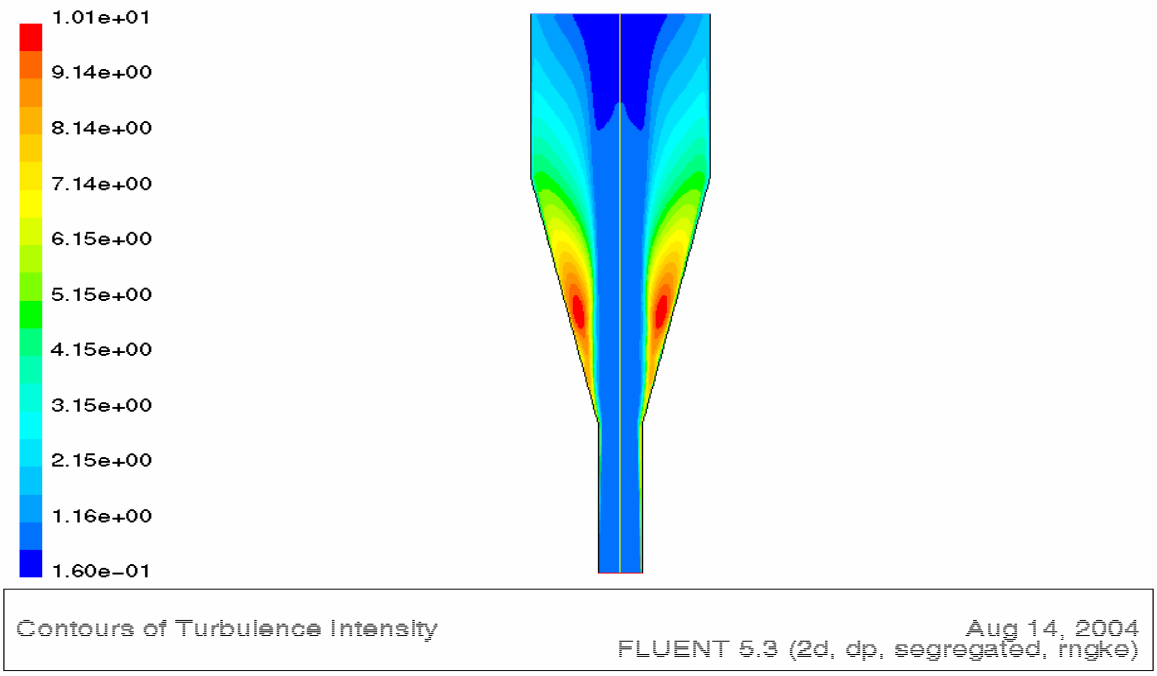


Figure F.70 Contours of Turbulence Intensity (D4)

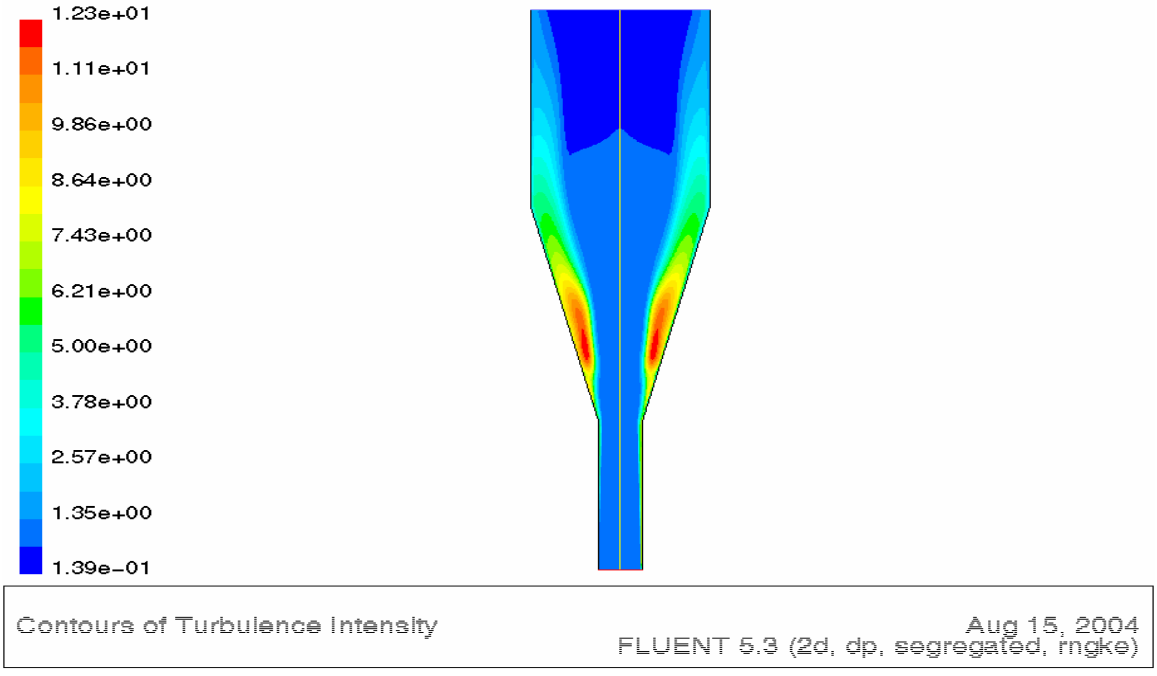

Figure F.71 Contours of Turbulent Viscosity (D1)

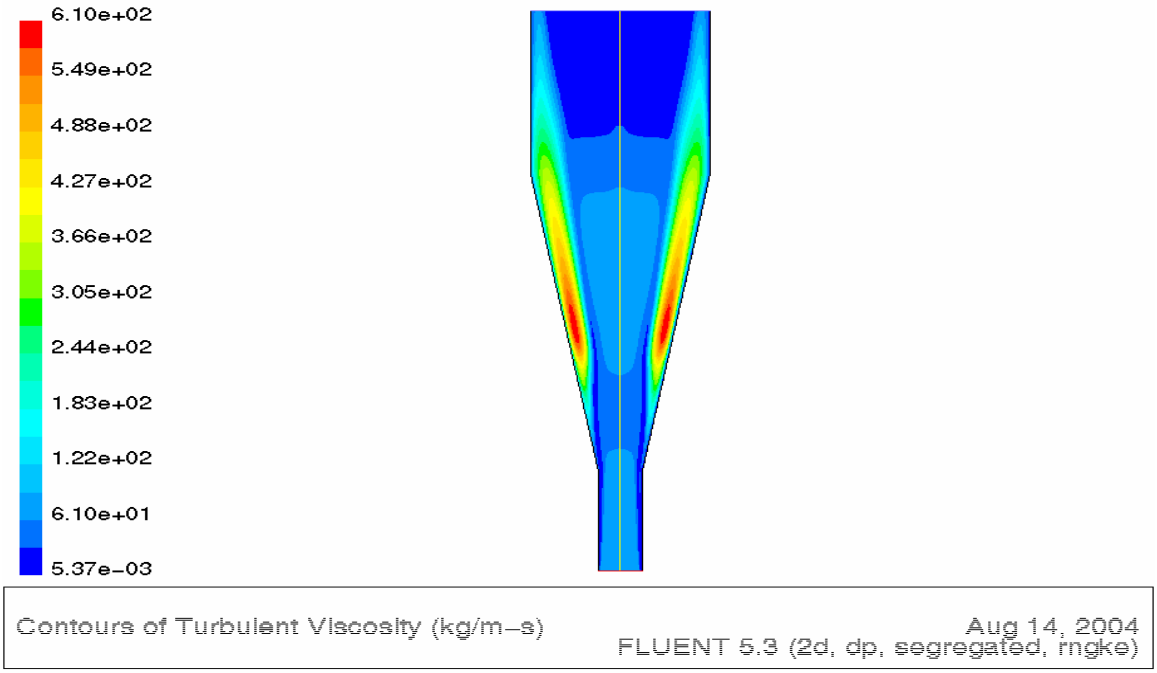


Figure F.72 Contours of Turbulent Viscosity (D2)

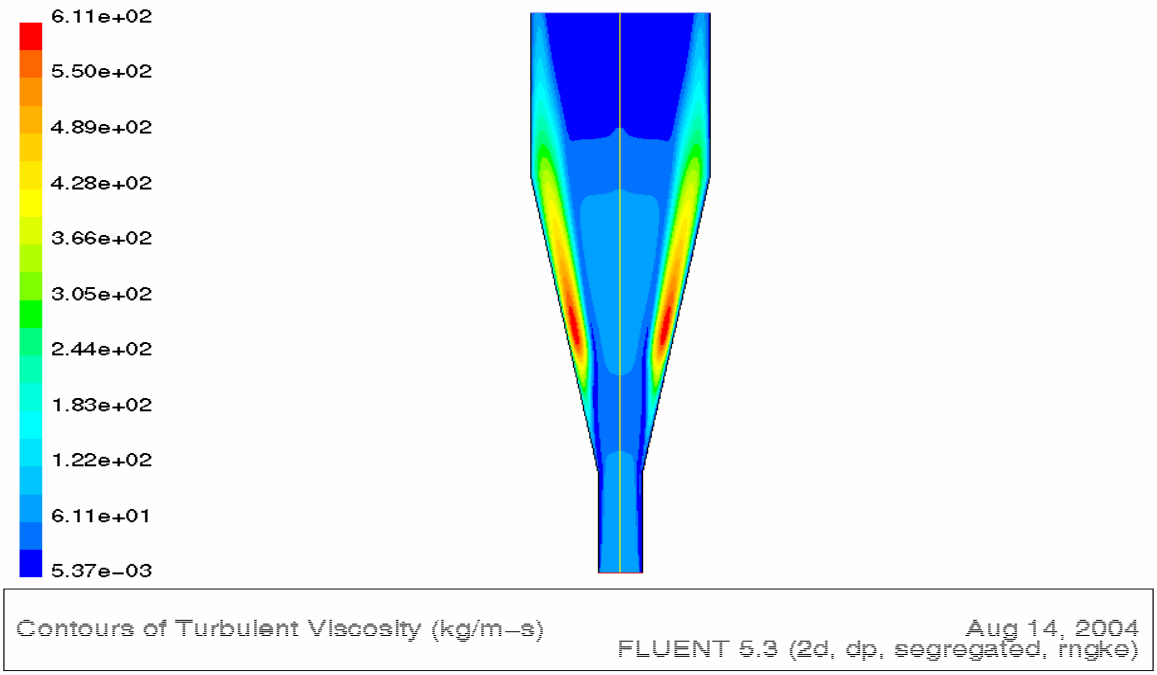

Figure F.73 Contours of Turbulent Viscosity (D3)

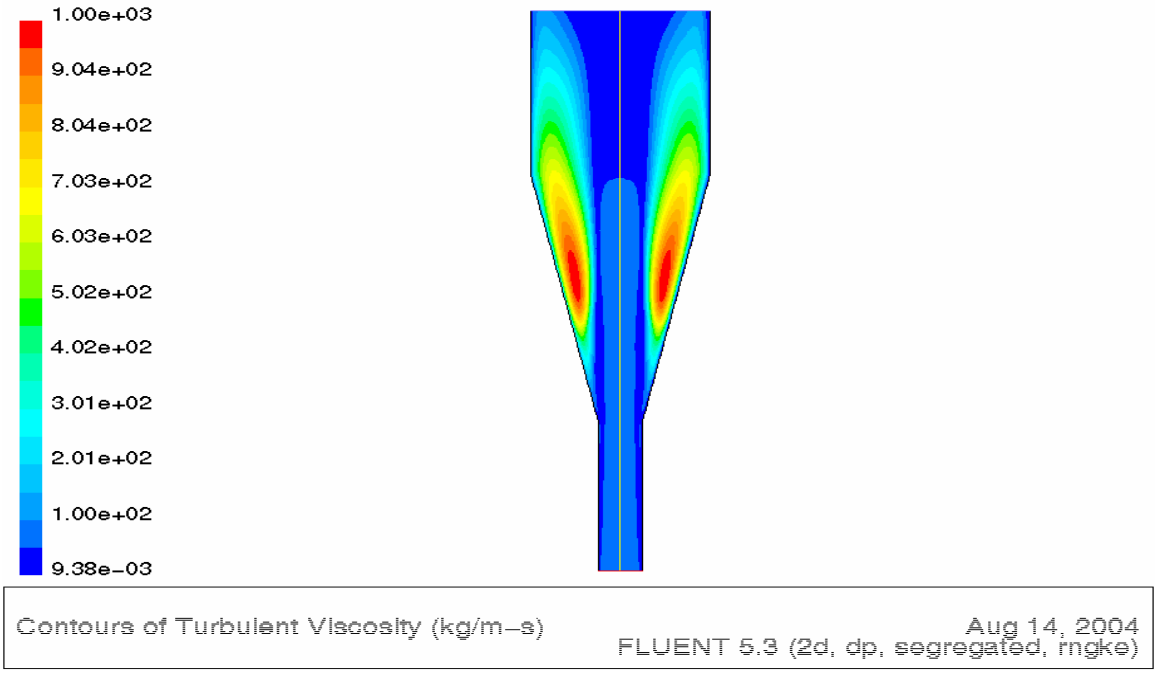


Figure F.74 Contours of Turbulent Viscosity (D4)

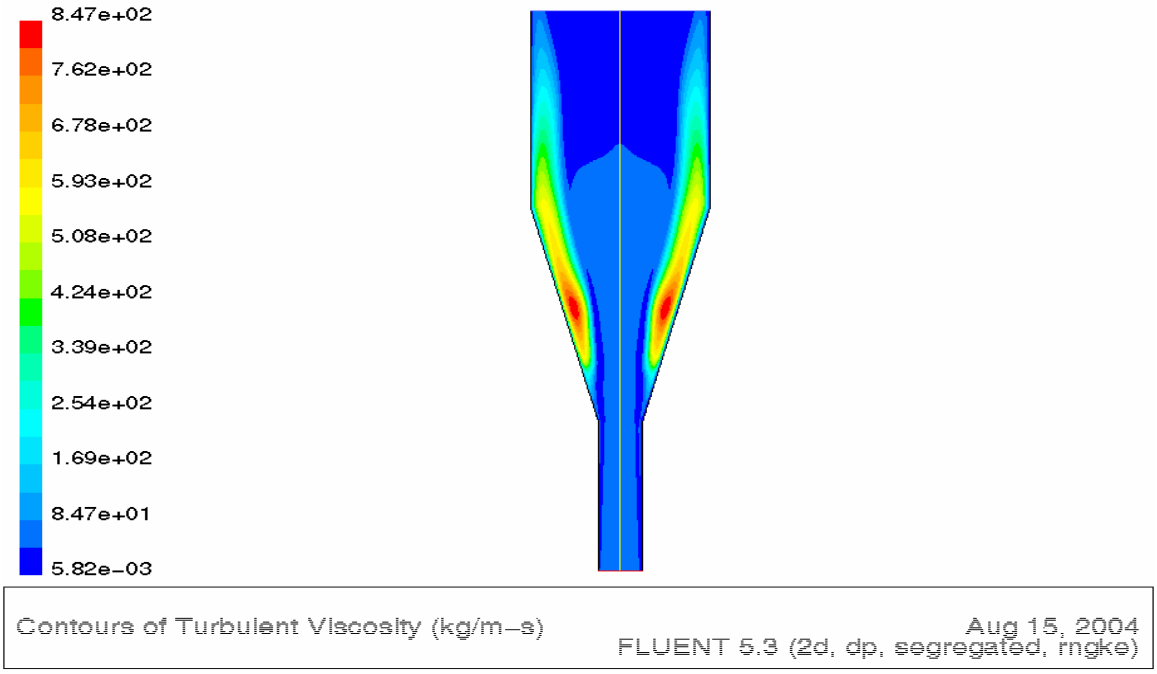

Figure F.75 Velocity Vector by Stream Function (D1)

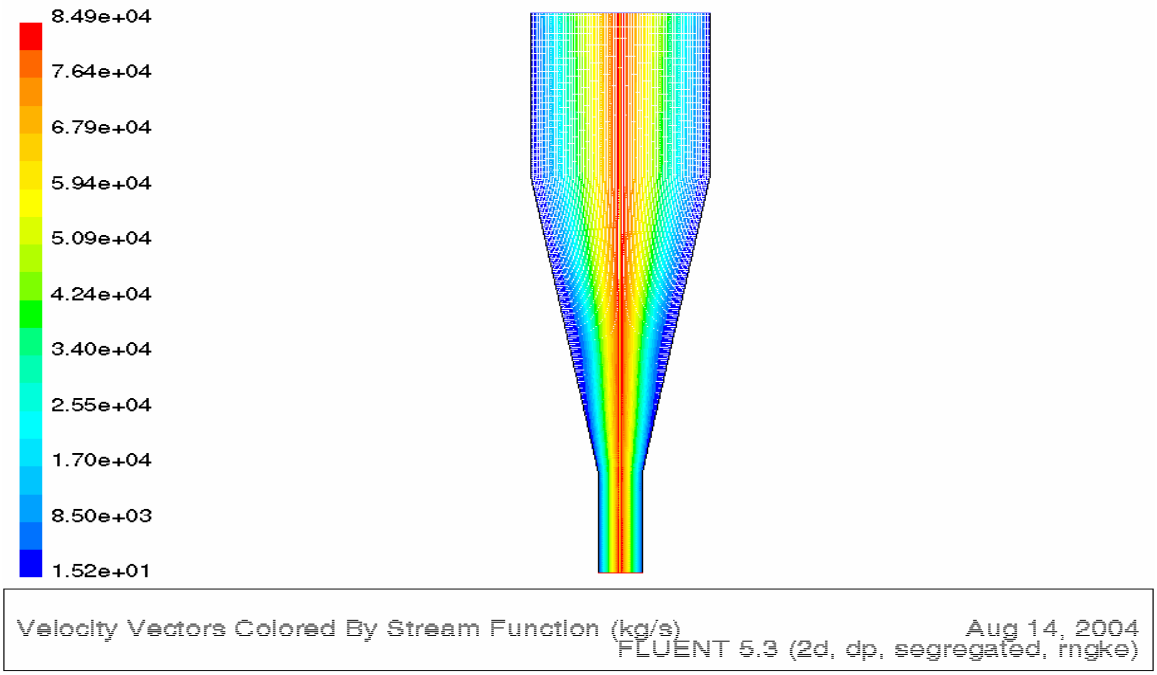


Figure F.76 Velocity Vector by Stream Function (D2)

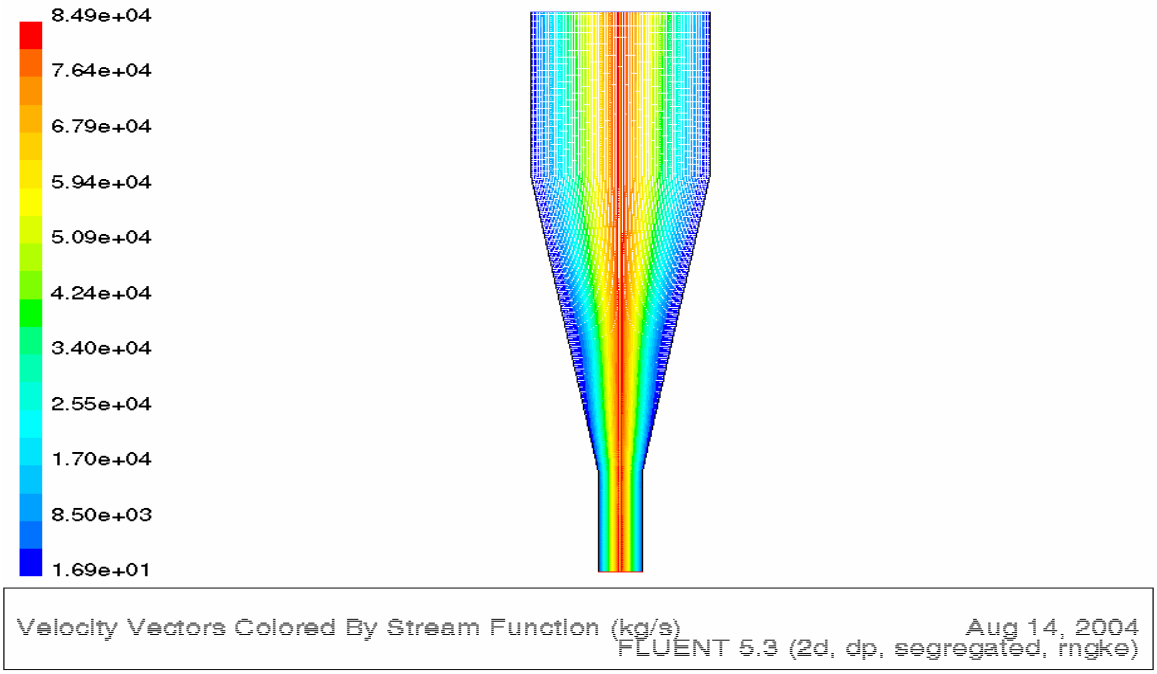

Figure F.77 Velocity Vector by Stream Function (D3)

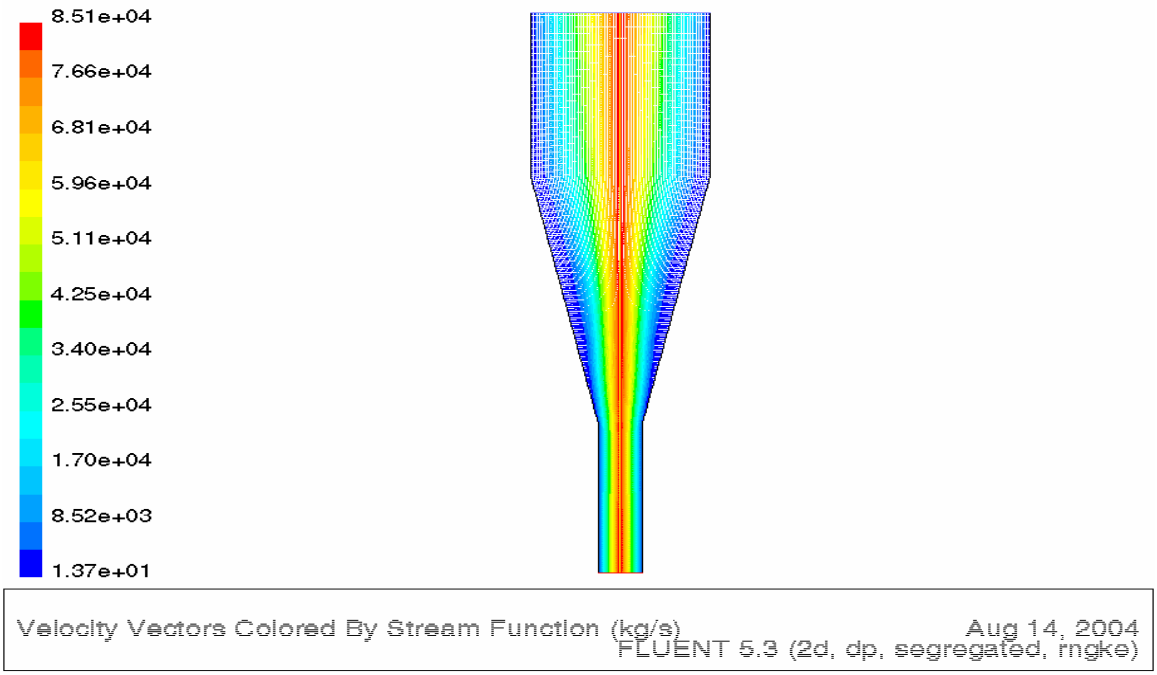


Figure F.78 Velocity Vector by Stream Function (D4)

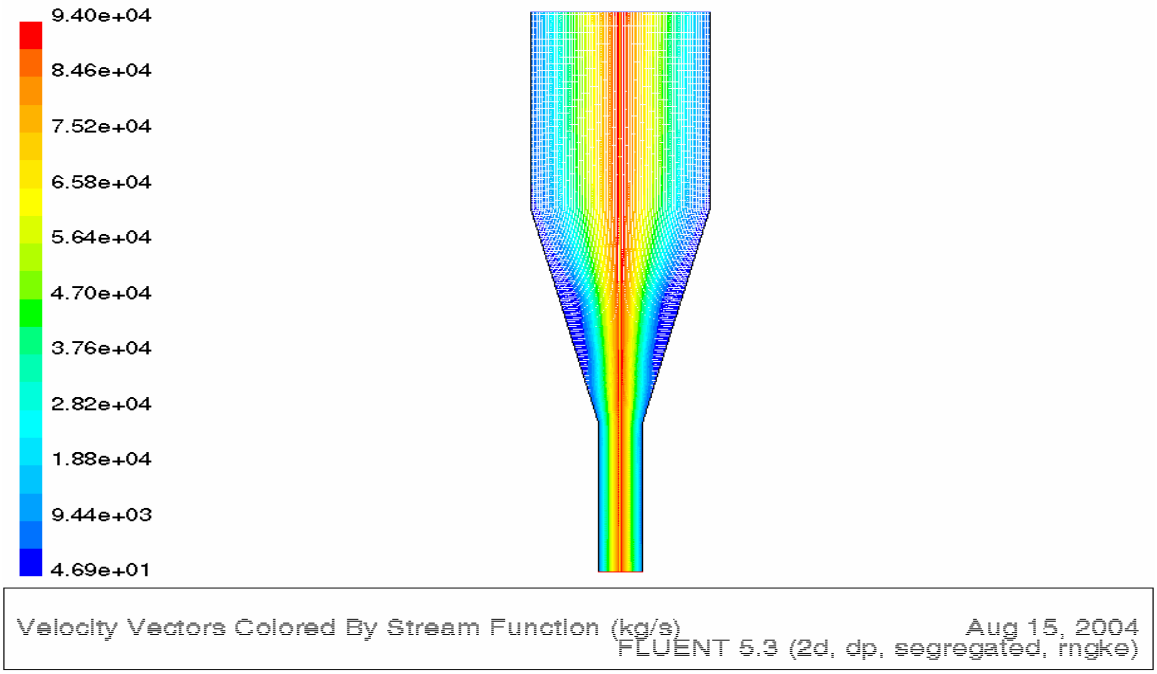

Figure F.79 Graph Total Pressure (D1)

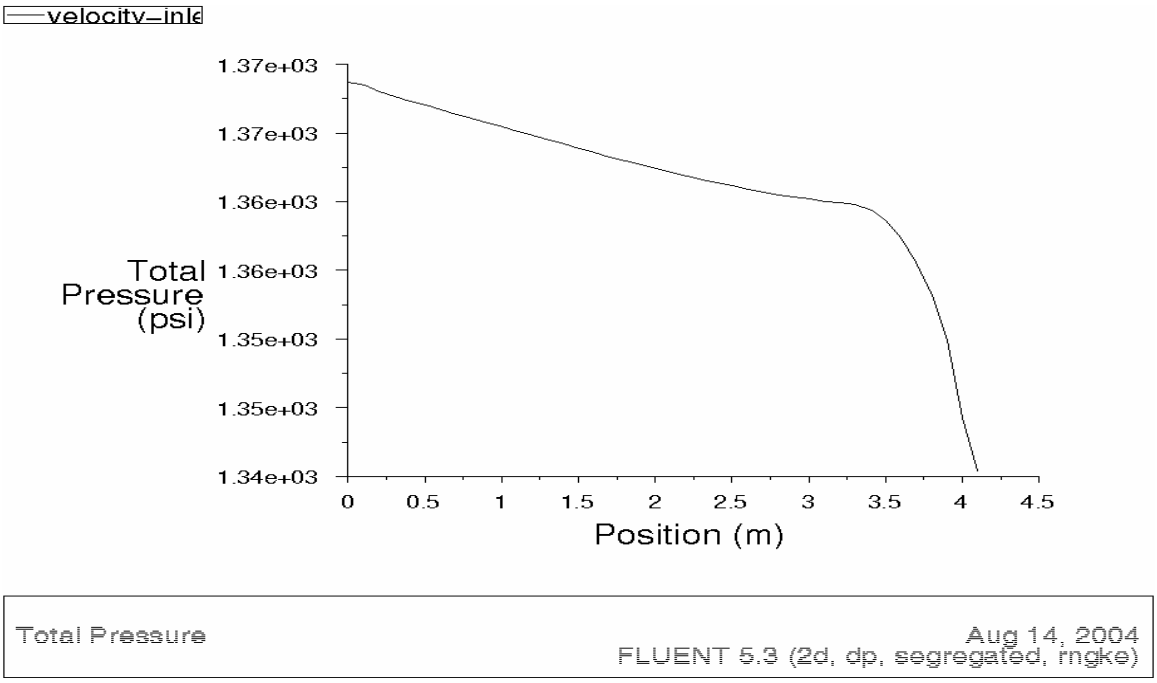


Figure F.80 Graph Total Pressure (D2)

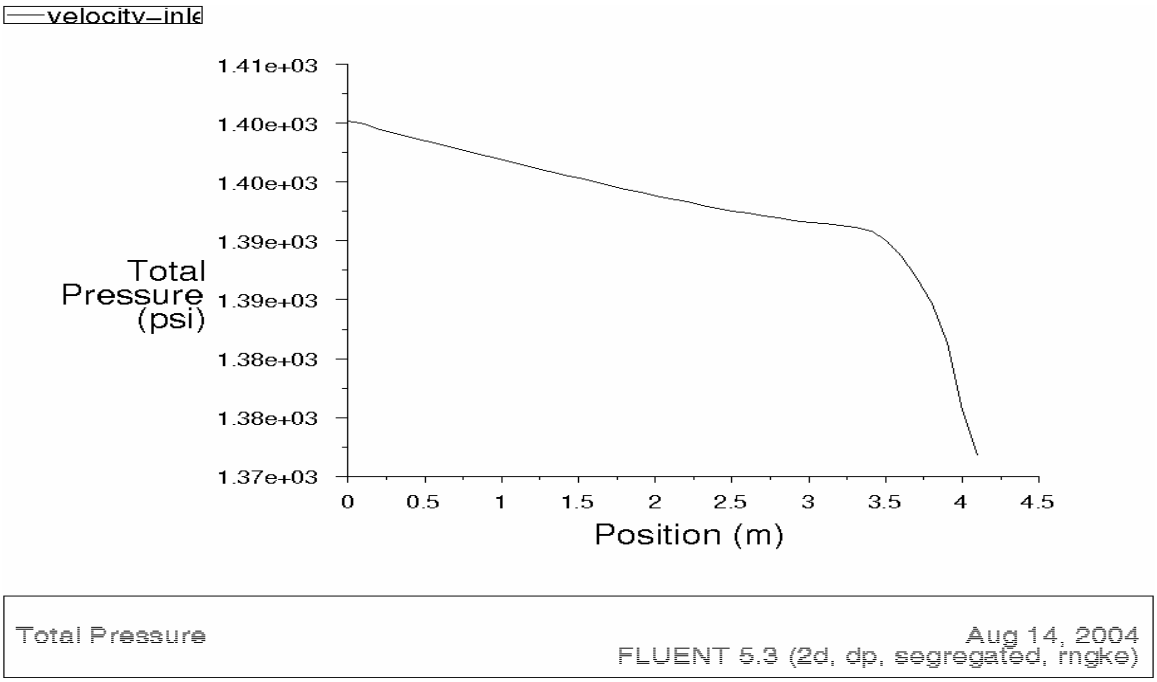

Figure F.81 Graph Total Pressure (D3)

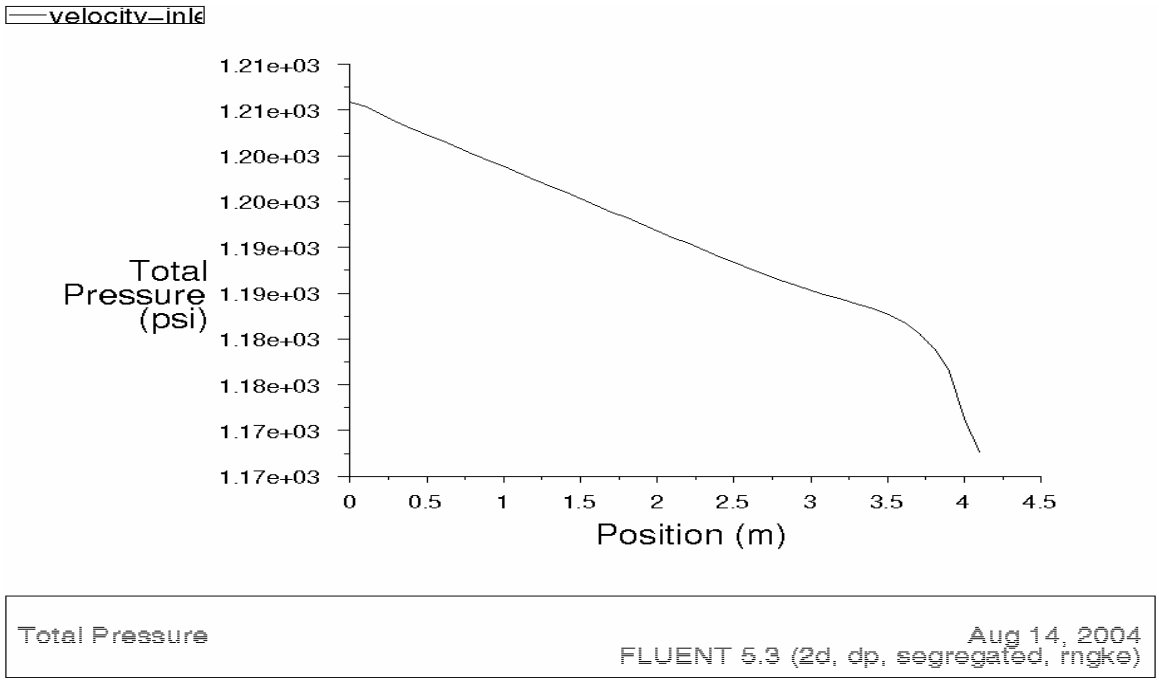


Figure F.82 Graph Total Pressure (D4)

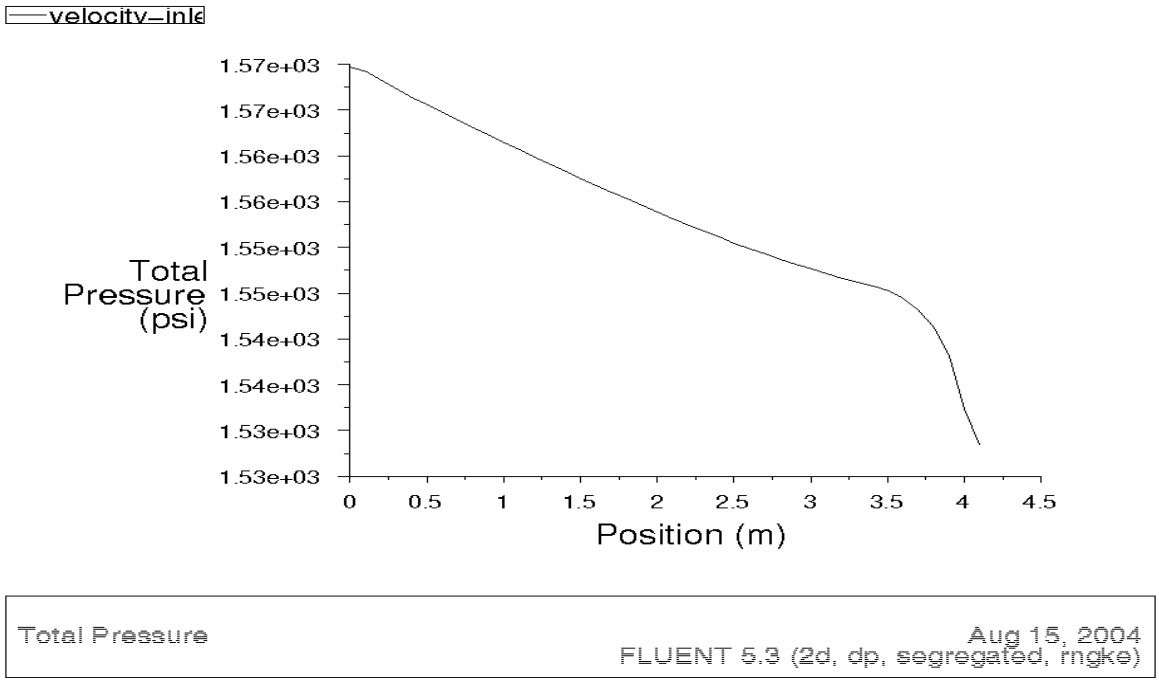

Figure F.83 Graph Turbulent Kinetic Energy (D1)

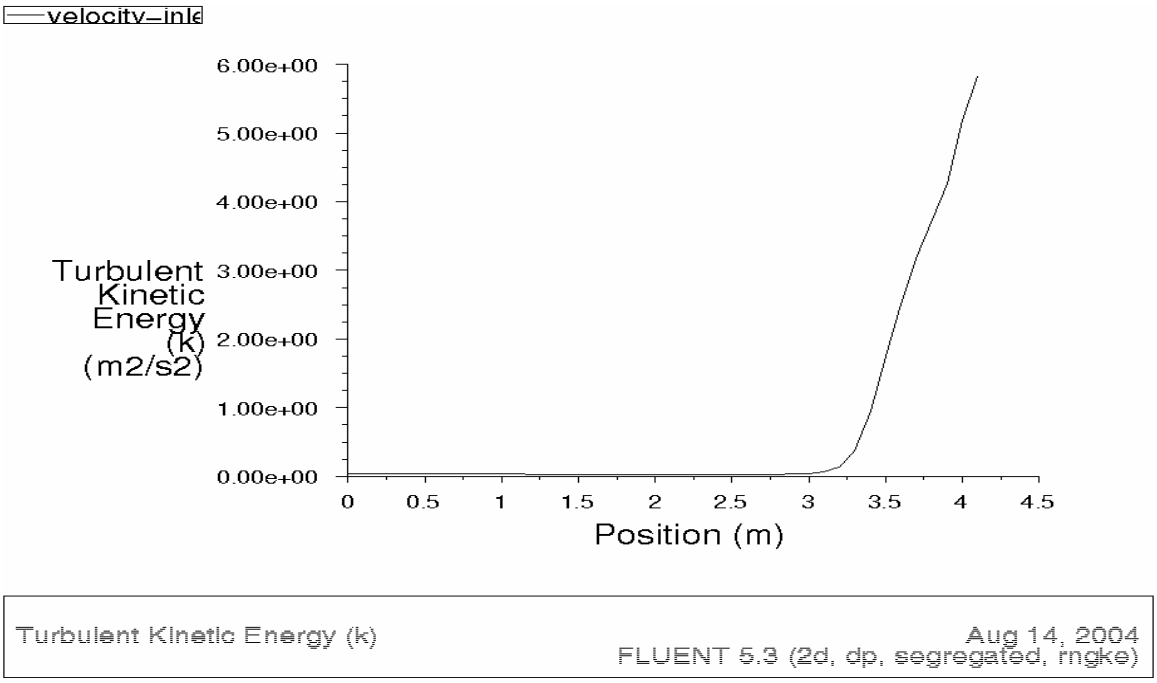


Figure F.84 Graph Turbulent Kinetic Energy (D2)

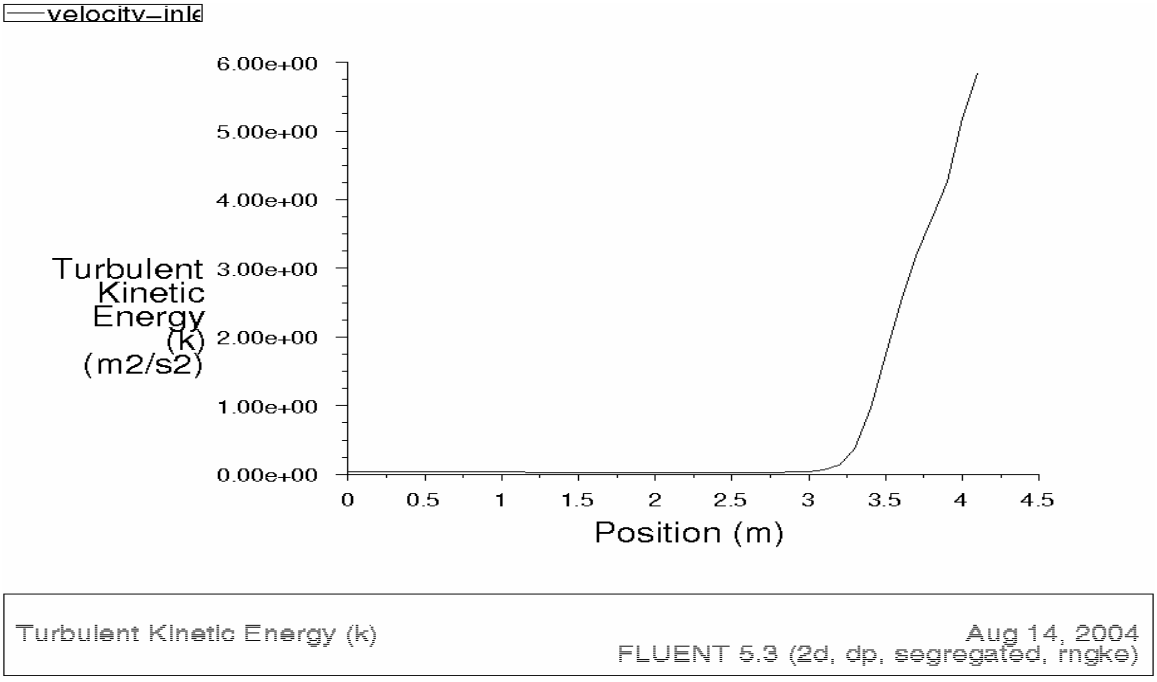

Figure F.85 Graph Turbulent Kinetic Energy (D3)

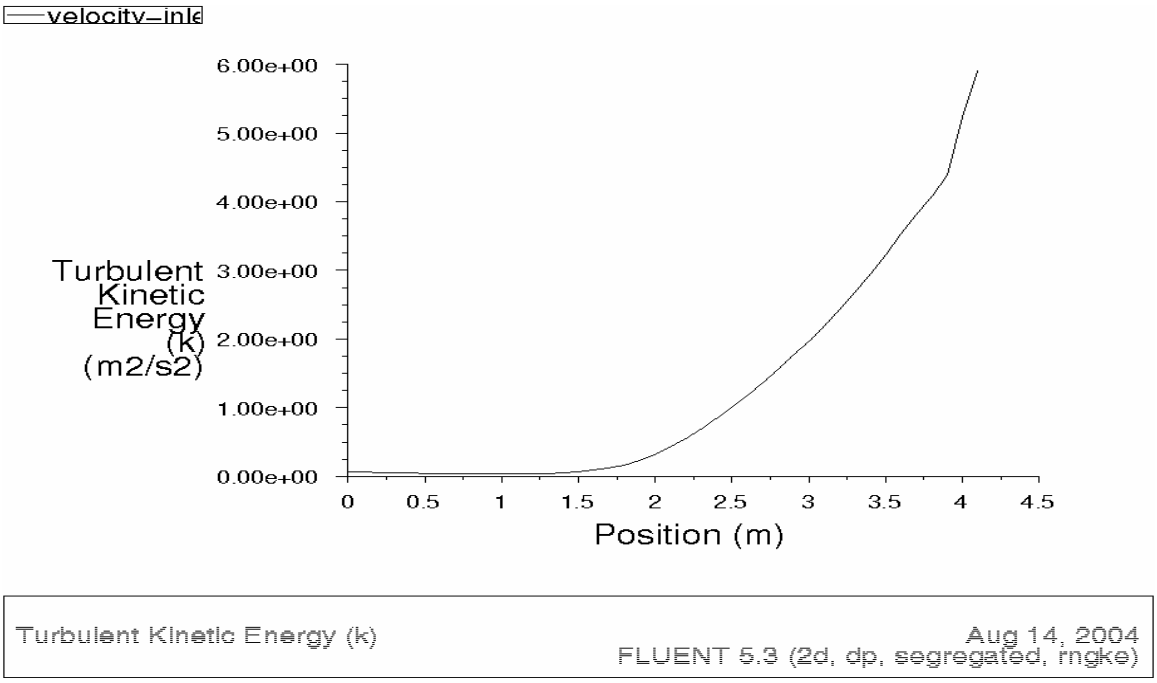


Figure F.86 Graph Turbulent Kinetic Energy (D4)

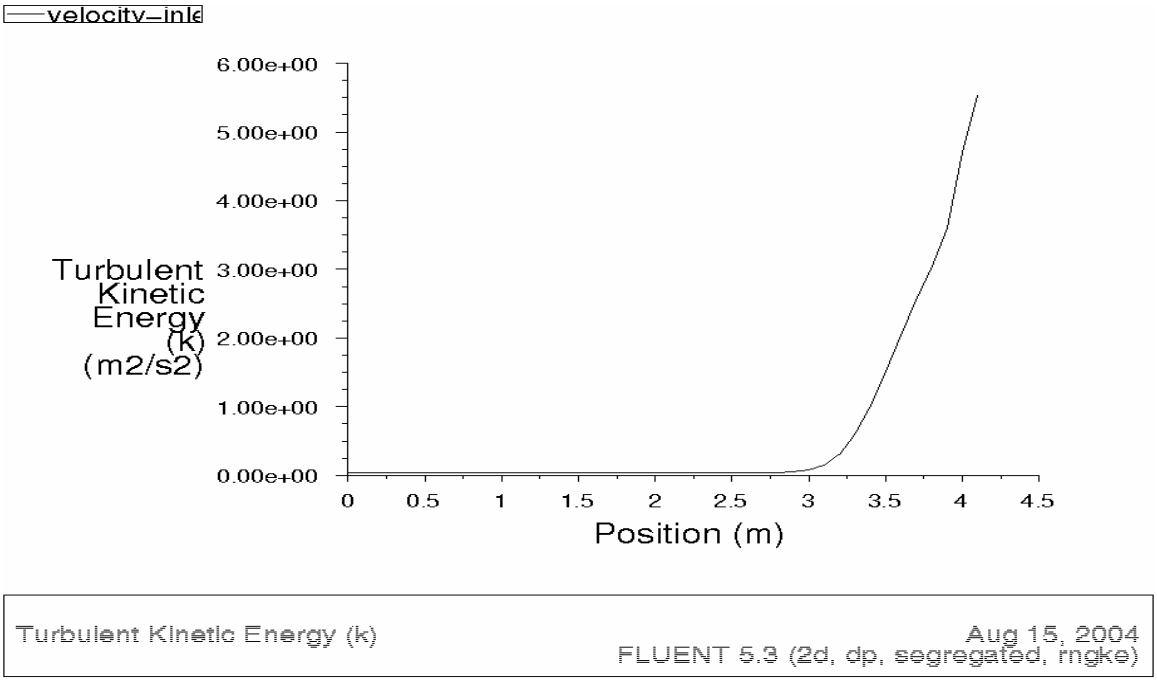

Figure F.87 Graph Turbulence Intensity (D1)

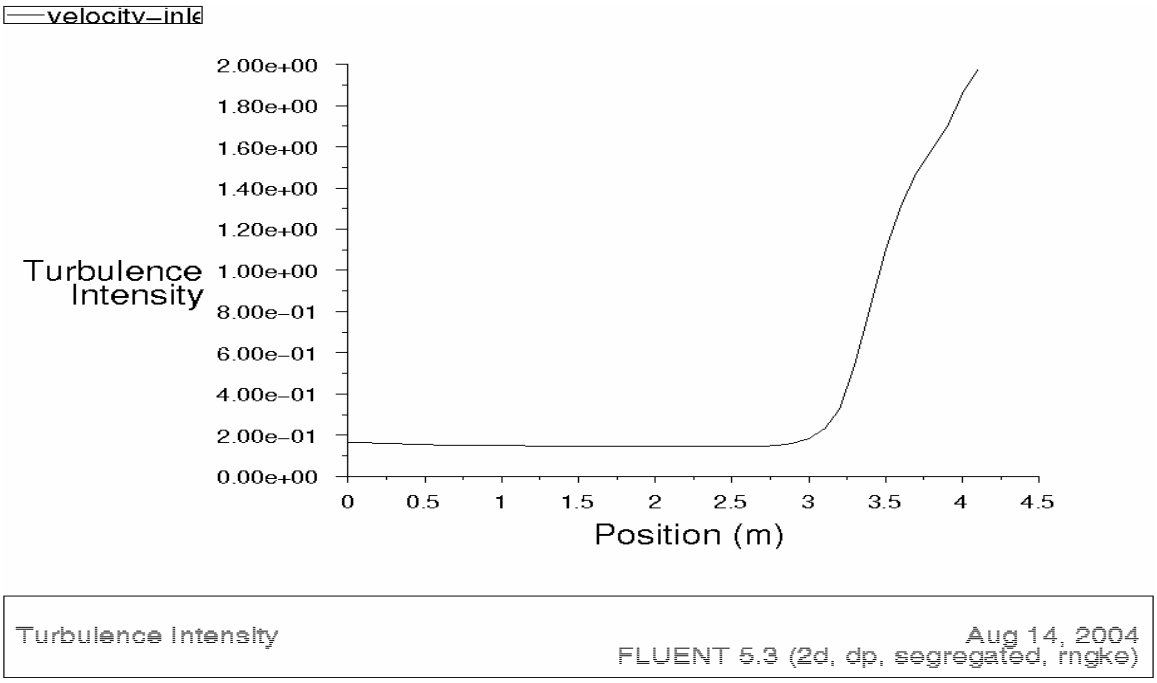


Figure F.88 Graph Turbulence Intensity (D2)

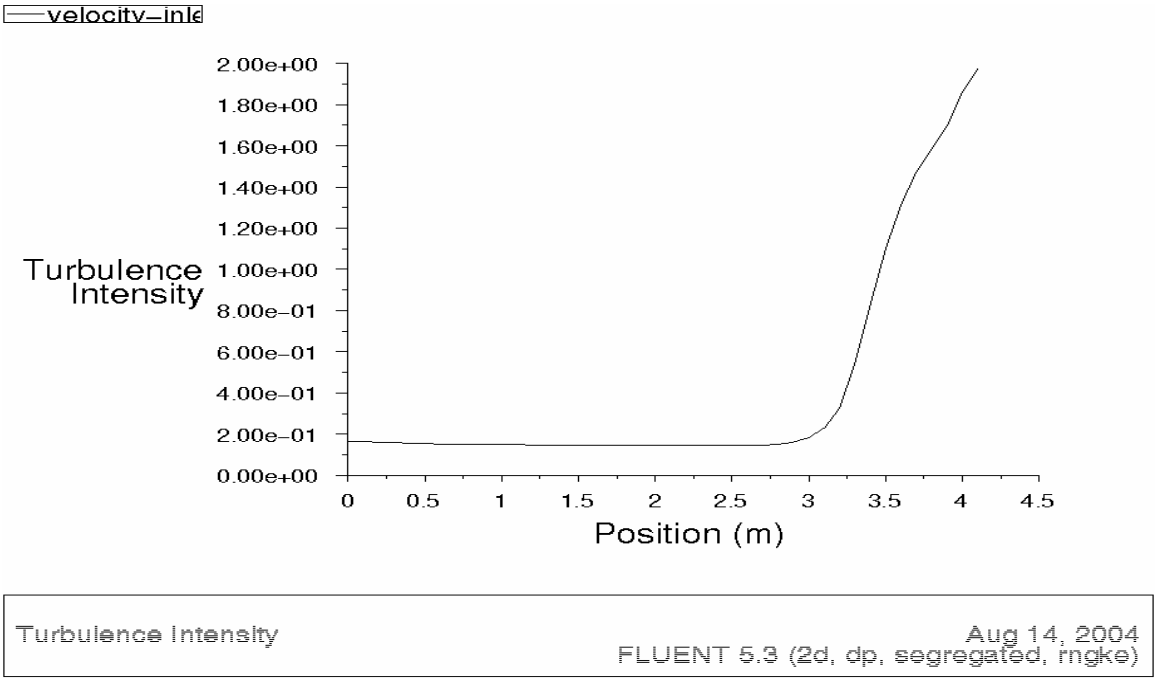

Figure F.89 Graph Turbulence Intensity (D3)

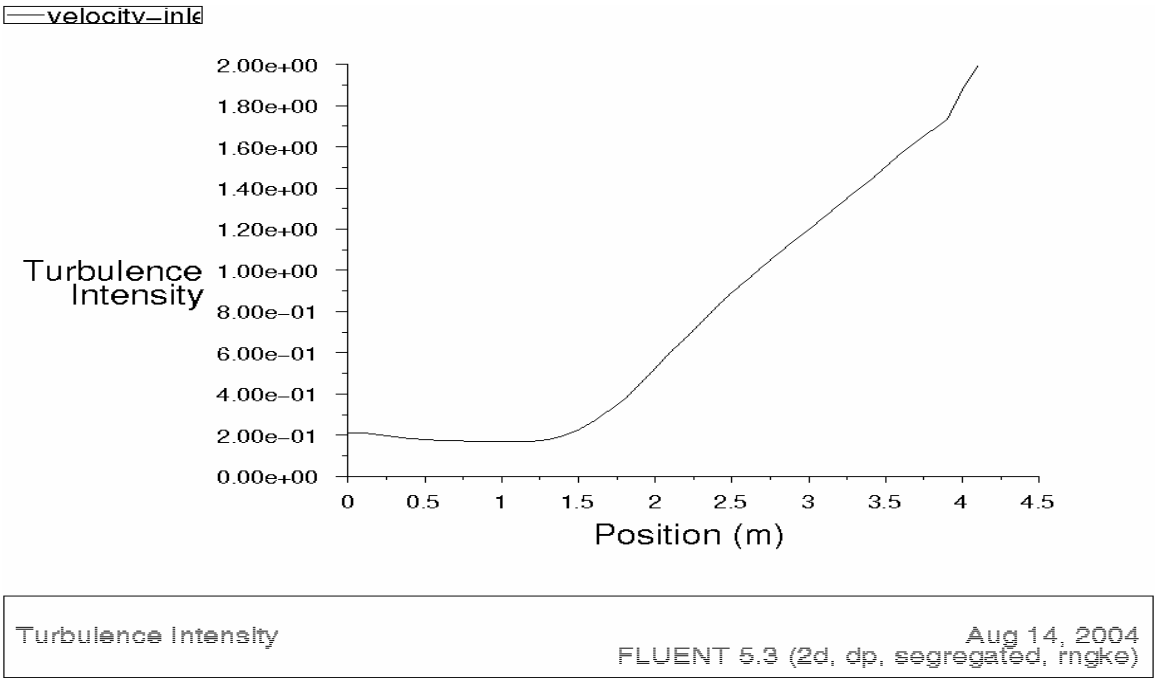


Figure F.90 Graph Turbulence Intensity (D4)

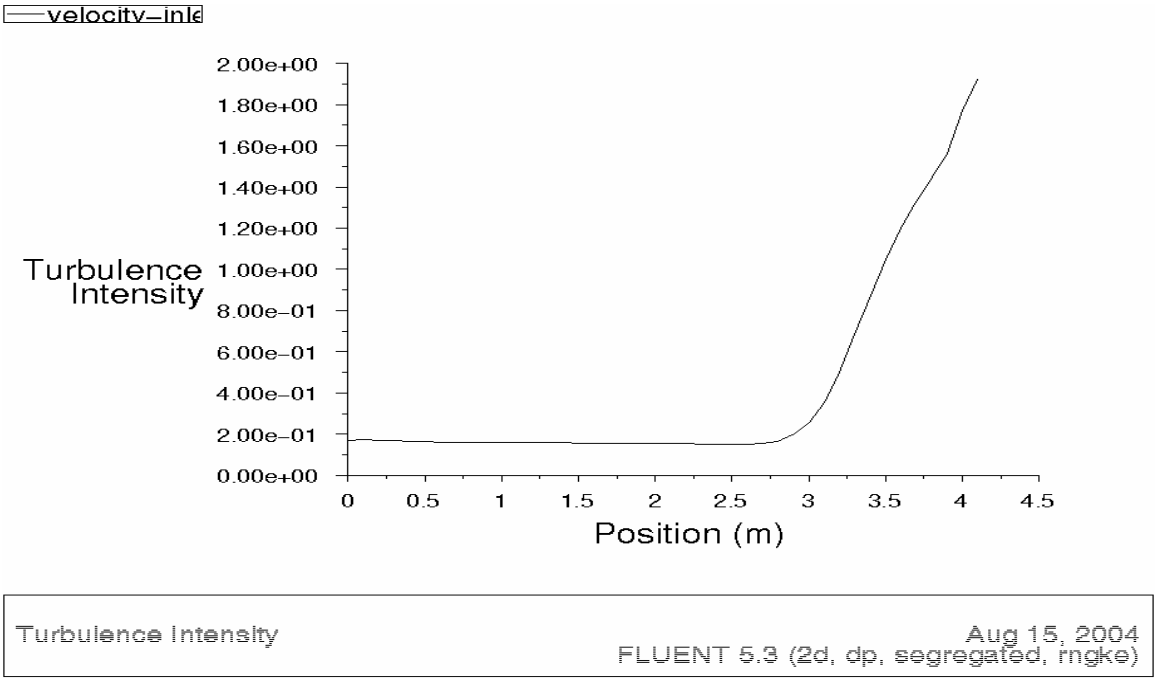

Figure F.91 Graph Turbulent Viscosity (D1)

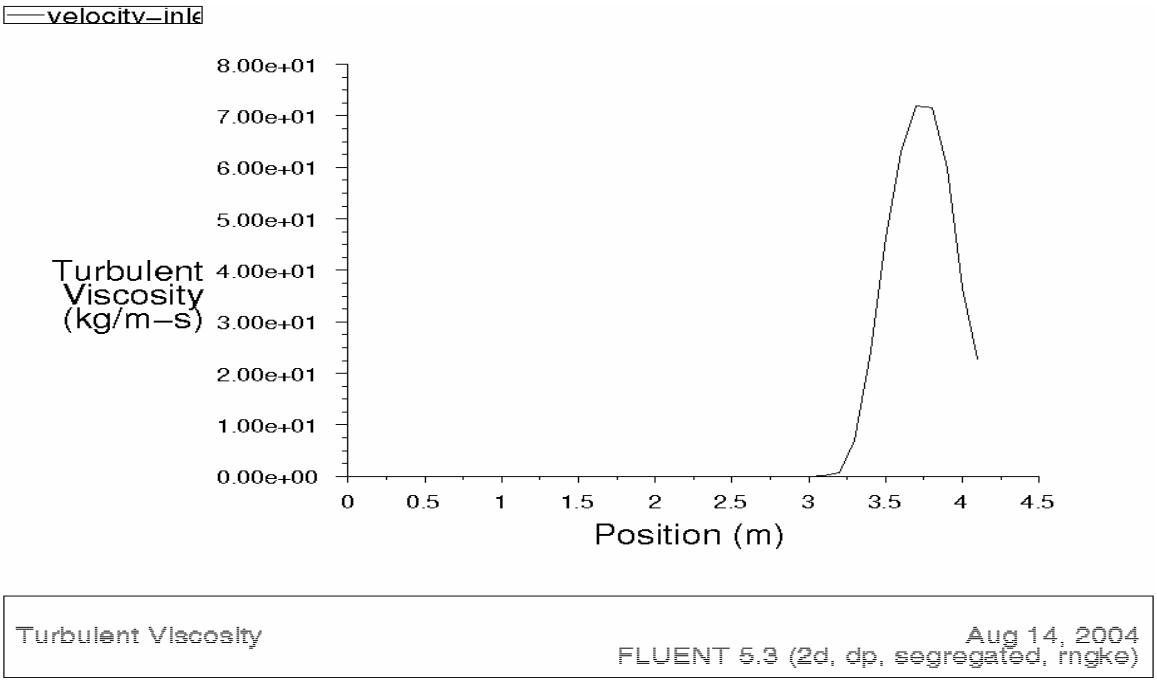


Figure F.92 Graph Turbulent Viscosity (D2)

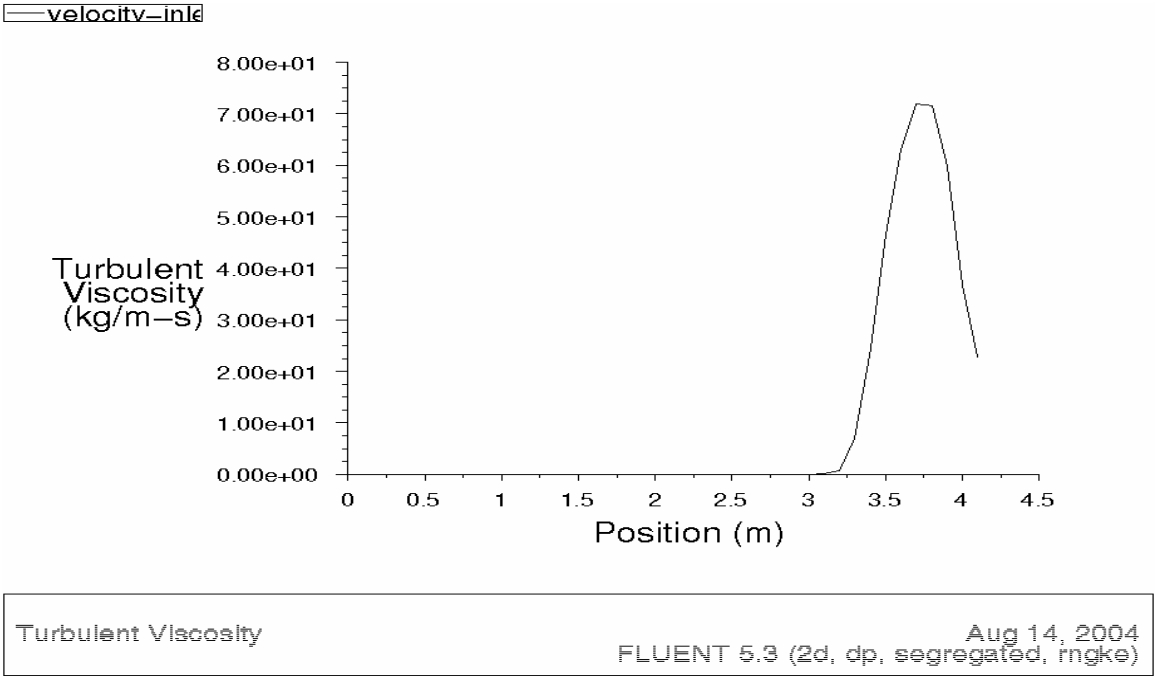

Figure F.93 Graph Turbulent Viscosity (D3)

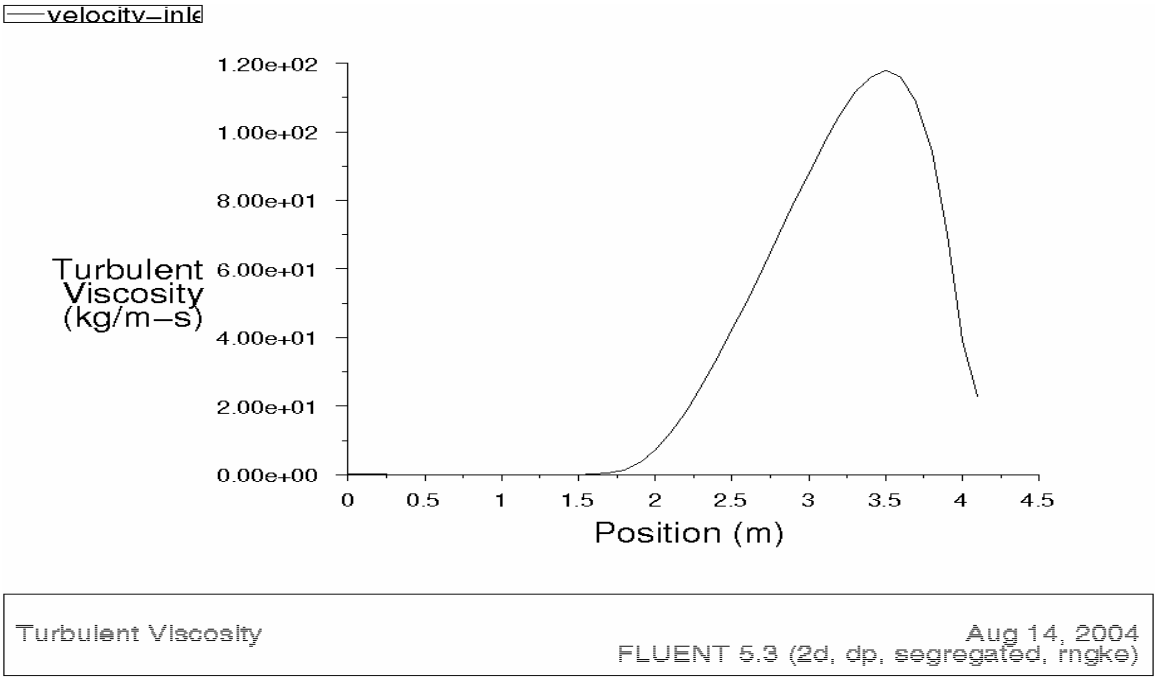


Figure F.94 Graph Turbulent Viscosity (D4)

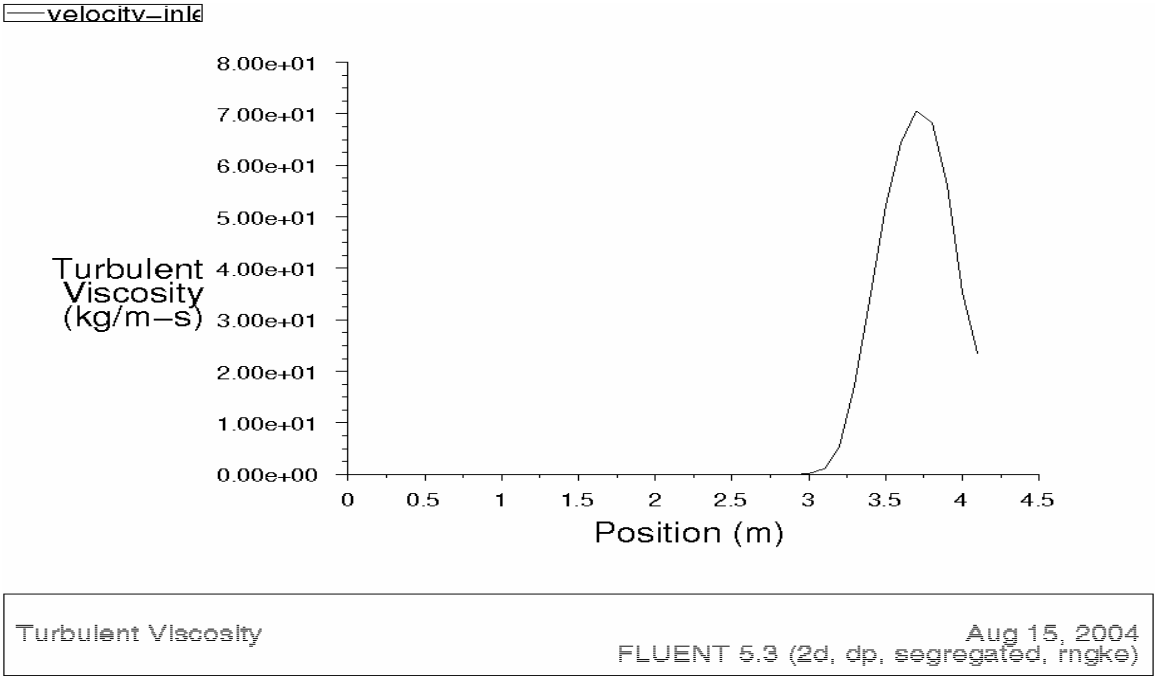

## F.5 3D Model (Sharp Edge with Taper -POME)

Figure F.95 Contours of Total Pressure

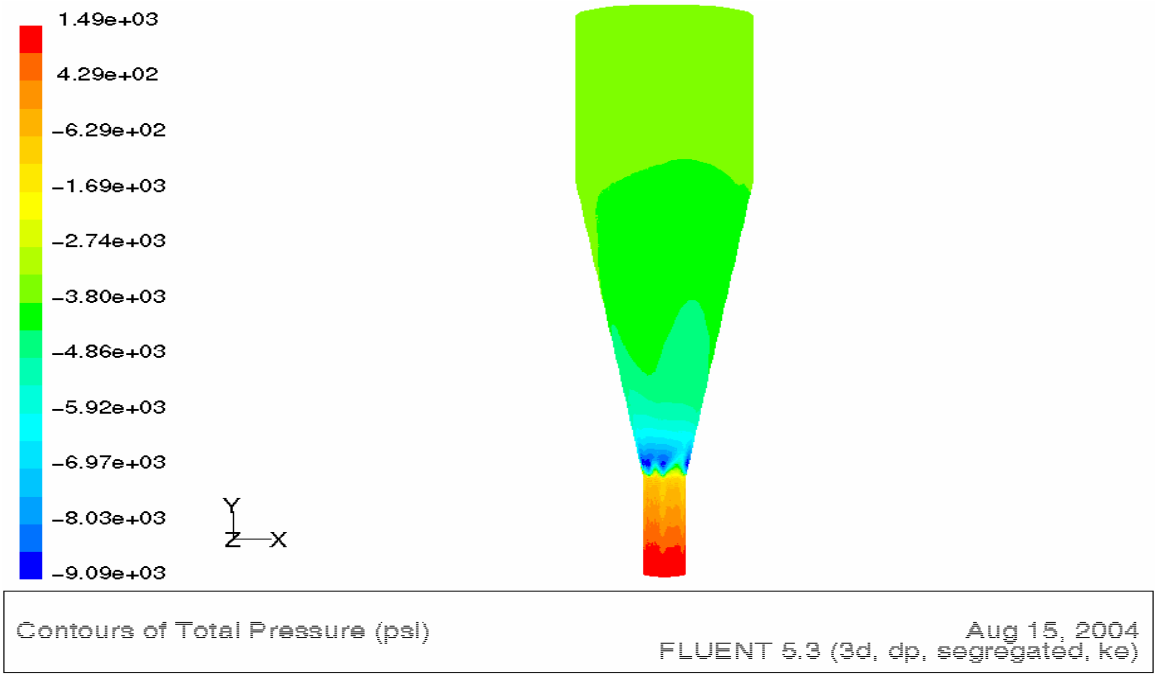


Figure F.96 Contours of Velocity Magnitude

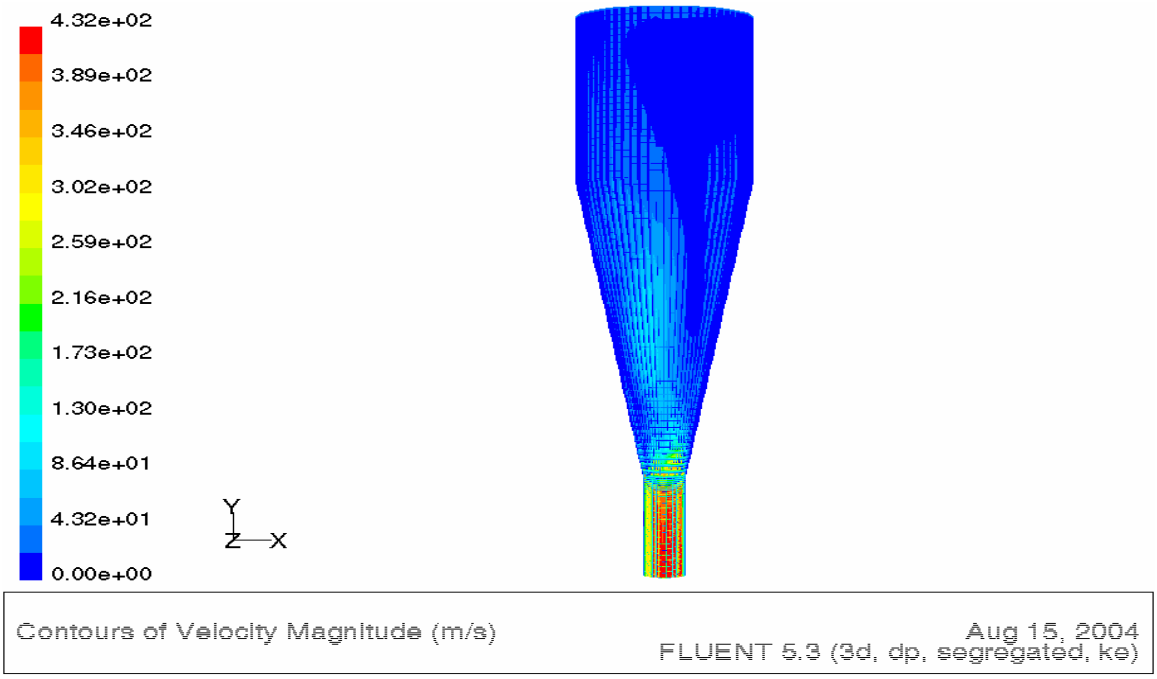

Figure F.97 Contours of Turbulent Kinetic Energy

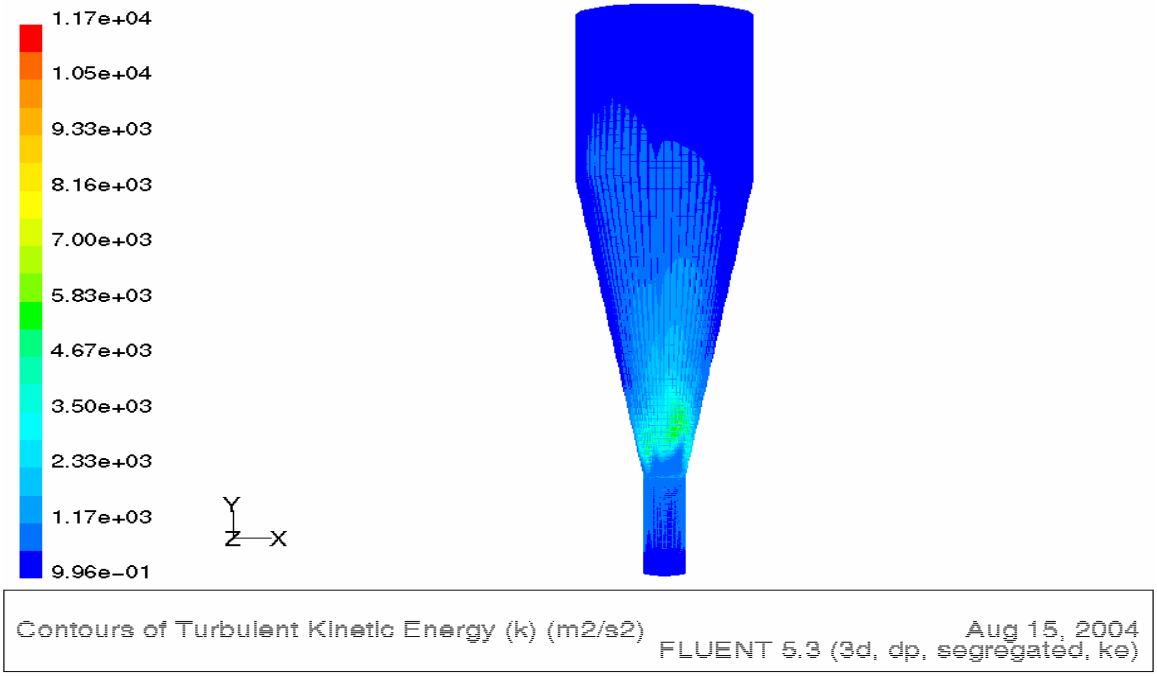


Figure F.98 Contours of Turbulence Intensity

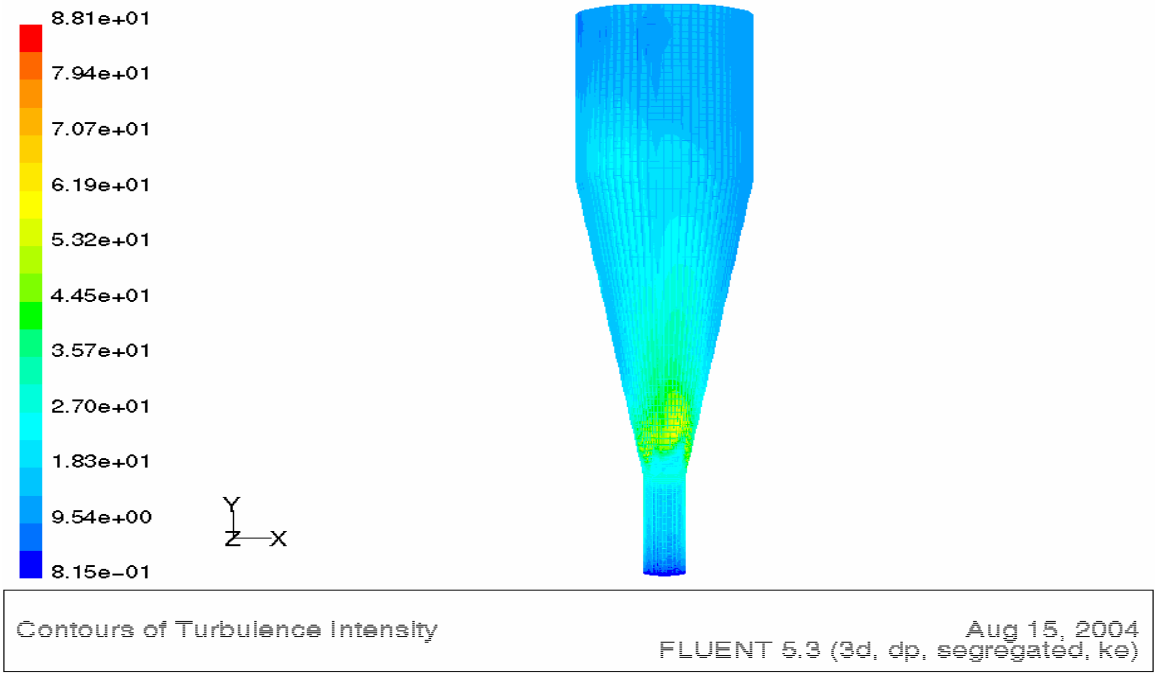

Figure F.99 Contours of Turbulent Viscosity

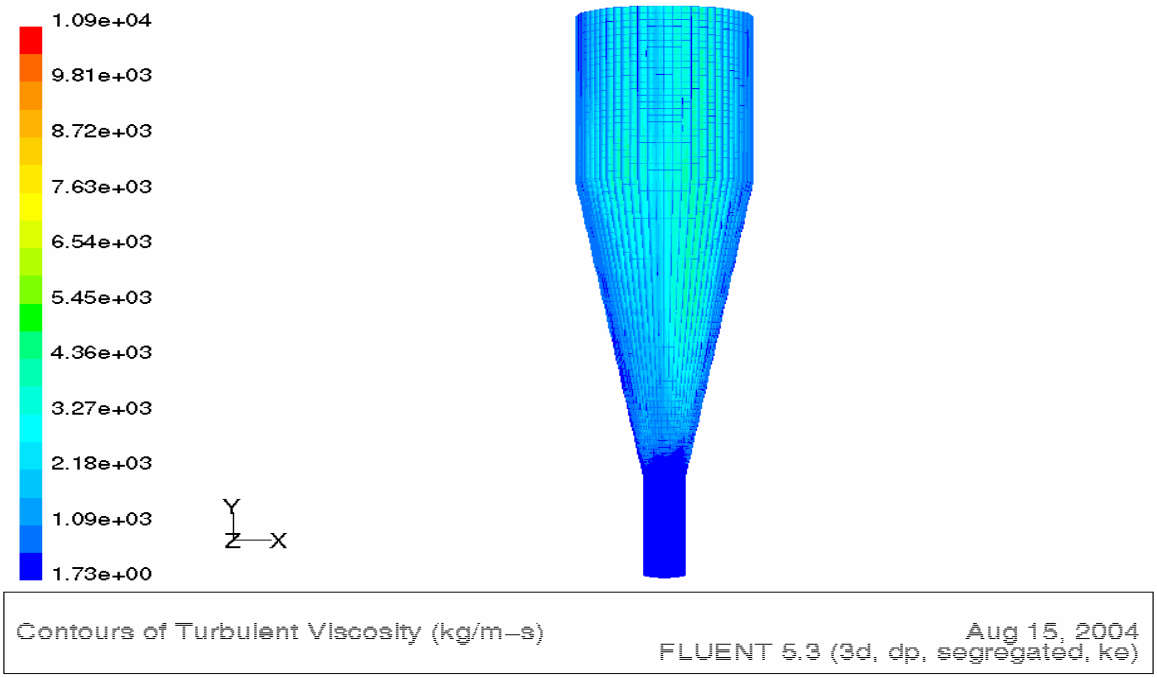


Figure F.100 Velocity Vectors by Velocity Magnitude

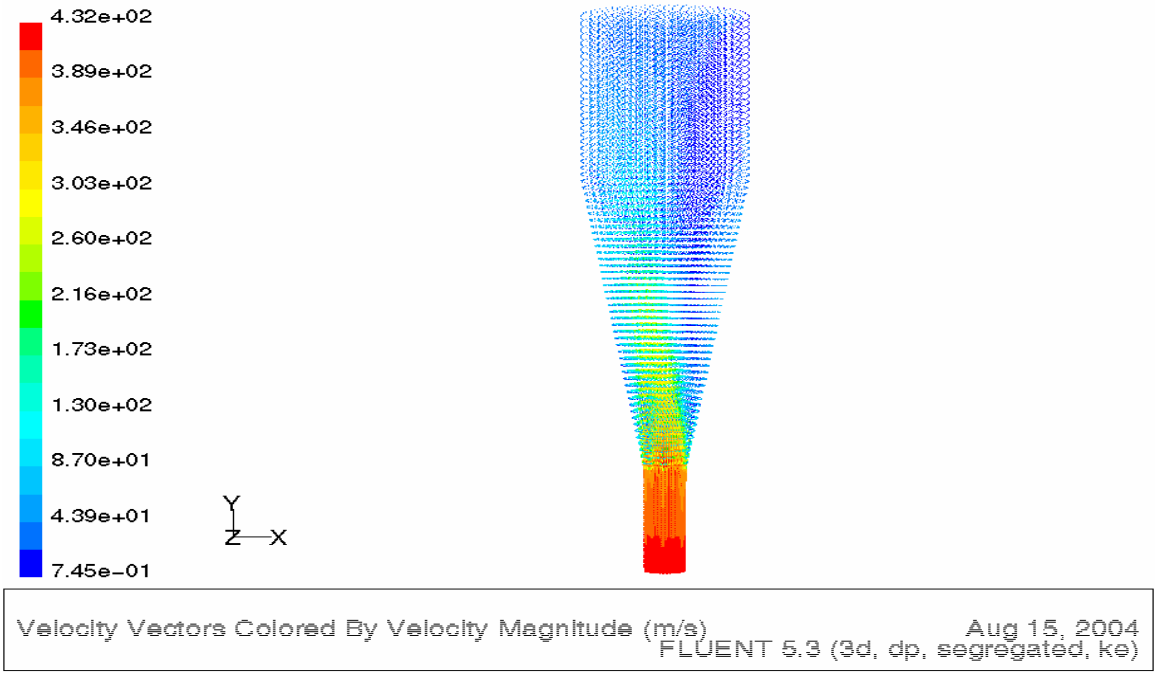

Figure F.101 Velocity Vectors by Turbulent Kinetic Energy

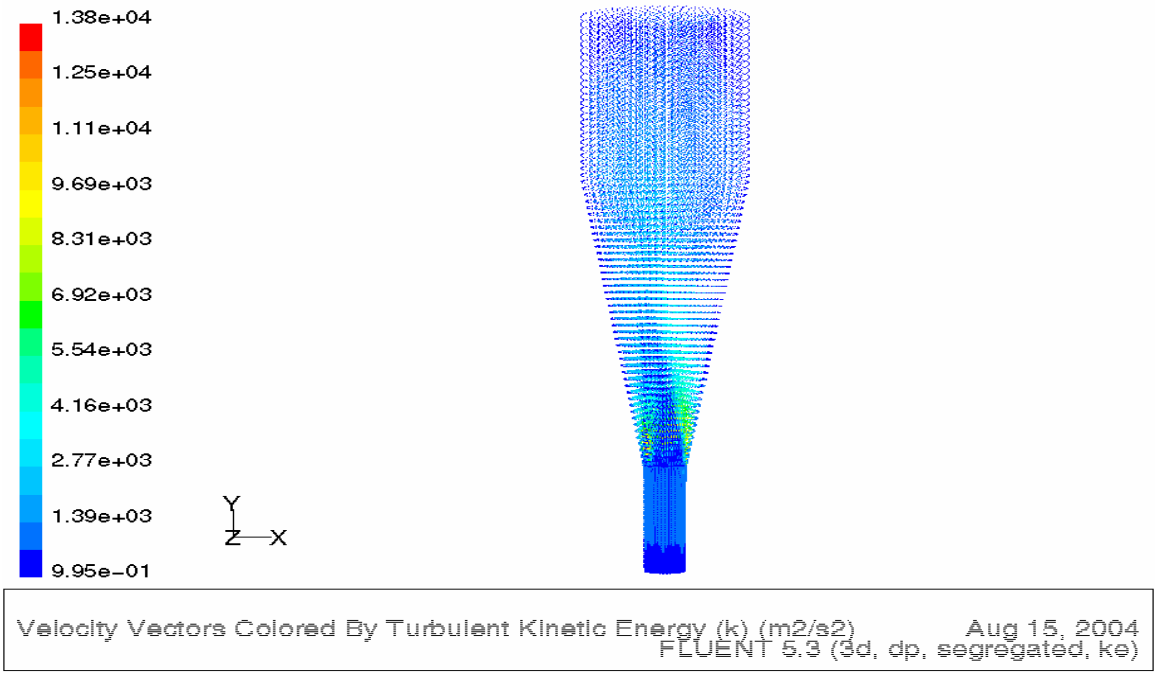


Figure F.102 Velocity Vectors by Turbulence Intensity

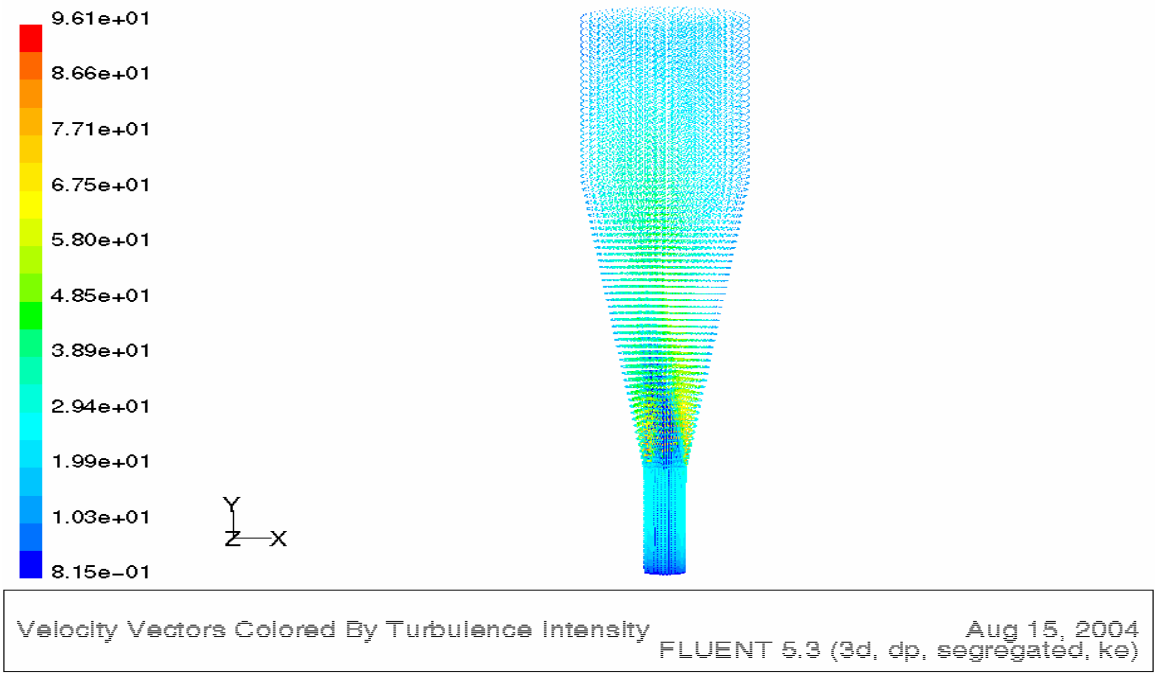

Figure F.103 Velocity Vectors by Turbulent Viscosity

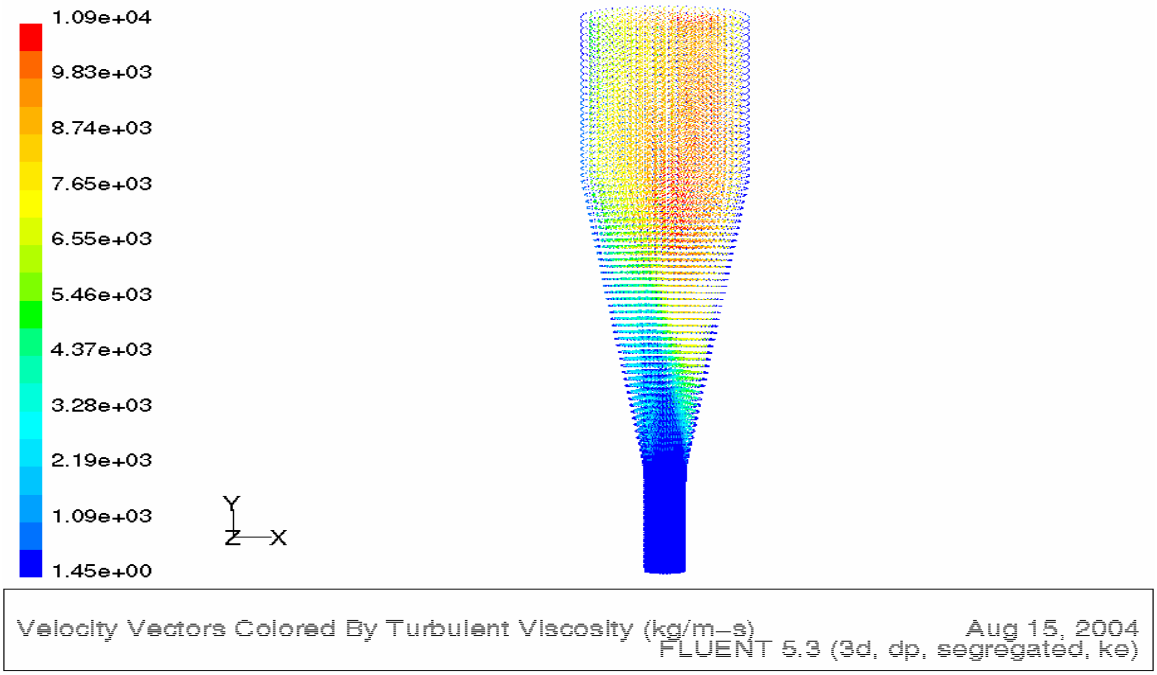


## F.6 3D Model (Rounded -POME)

Figure F.104 Contours of Total Pressure

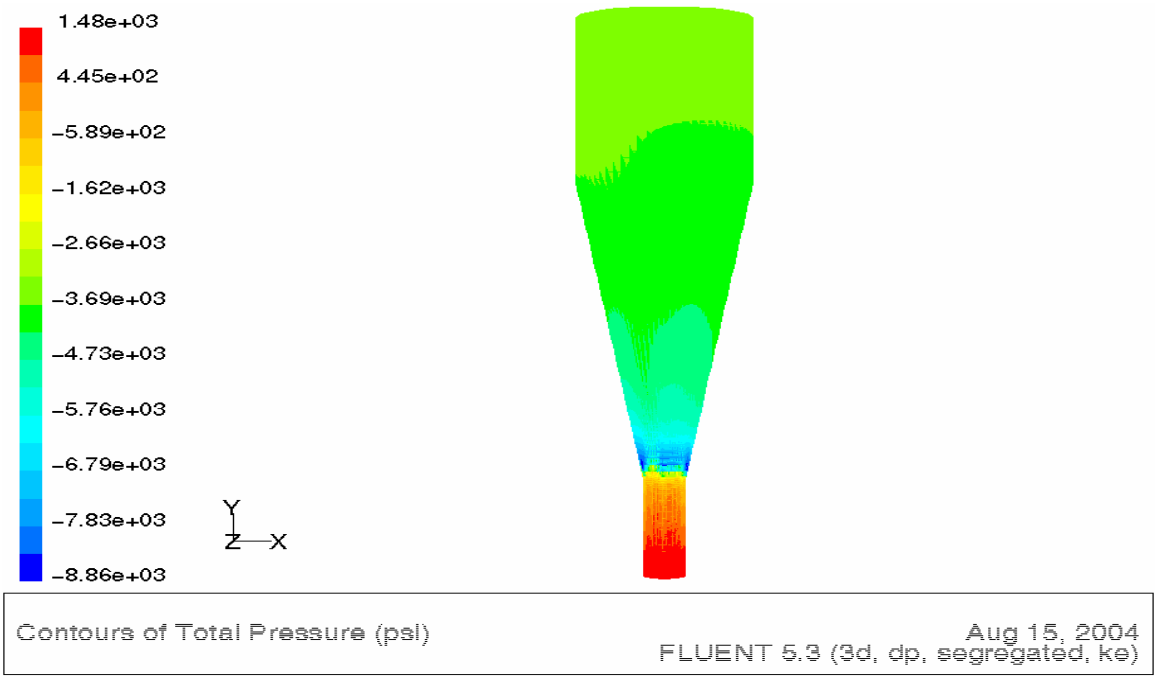

Figure F.105 Contours of Velocity Magnitude

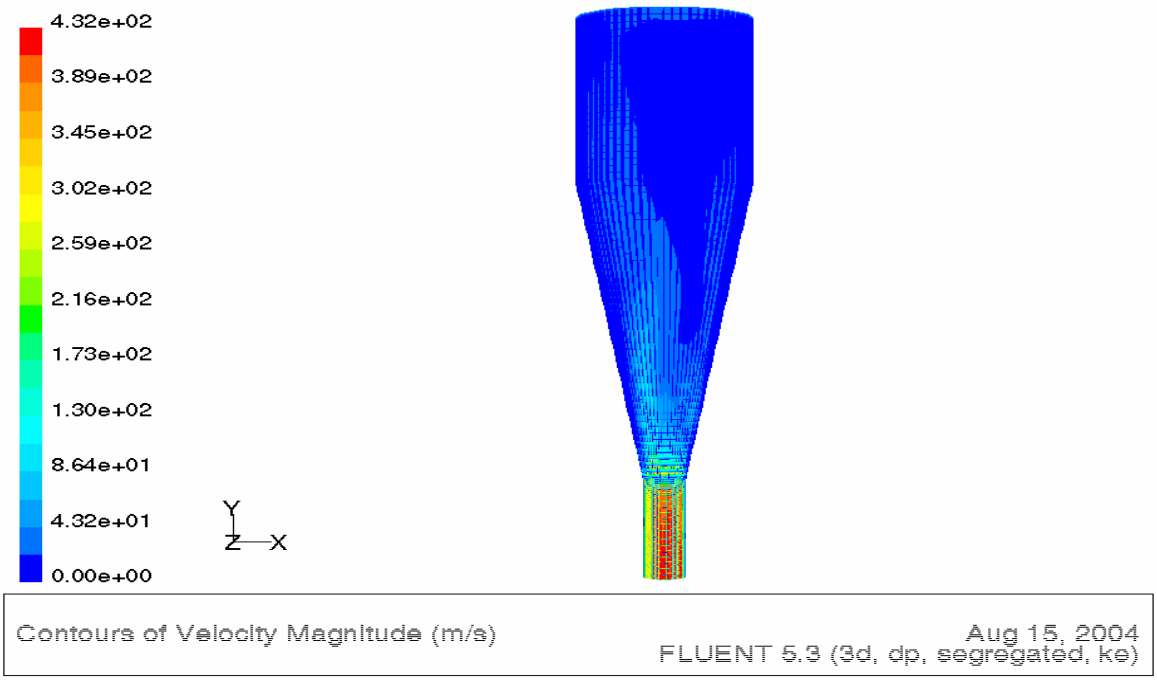


Figure F.106 Contours of Turbulent Kinetic

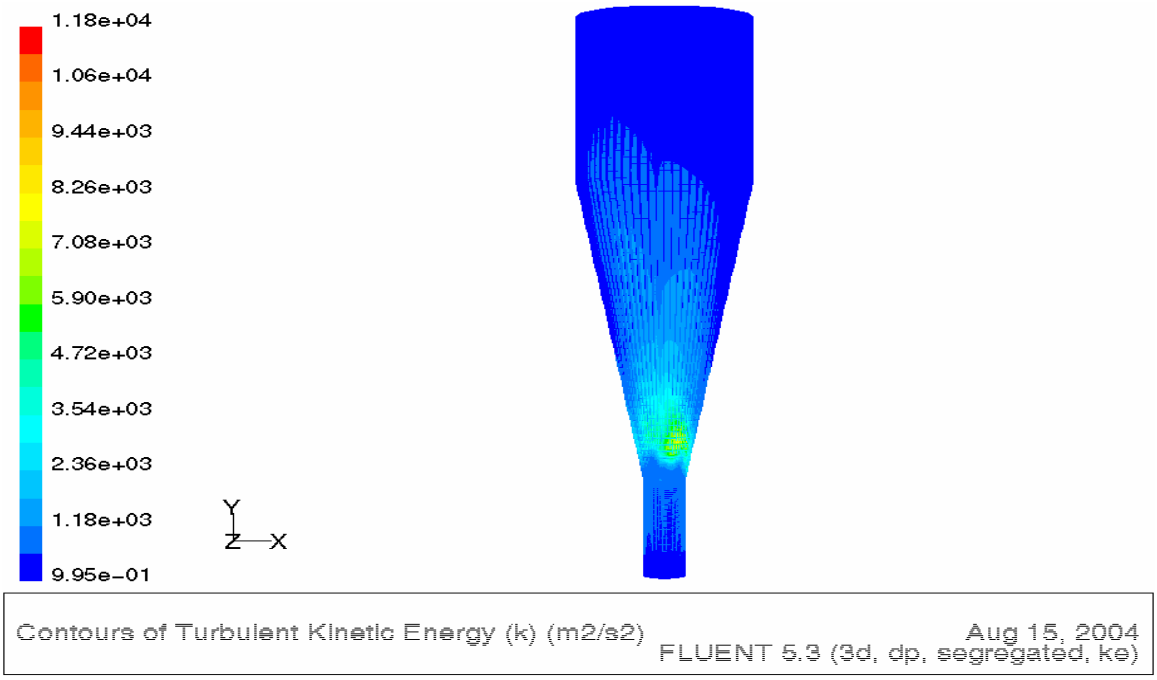

Figure F.107 Contours of Turbulence Intensity

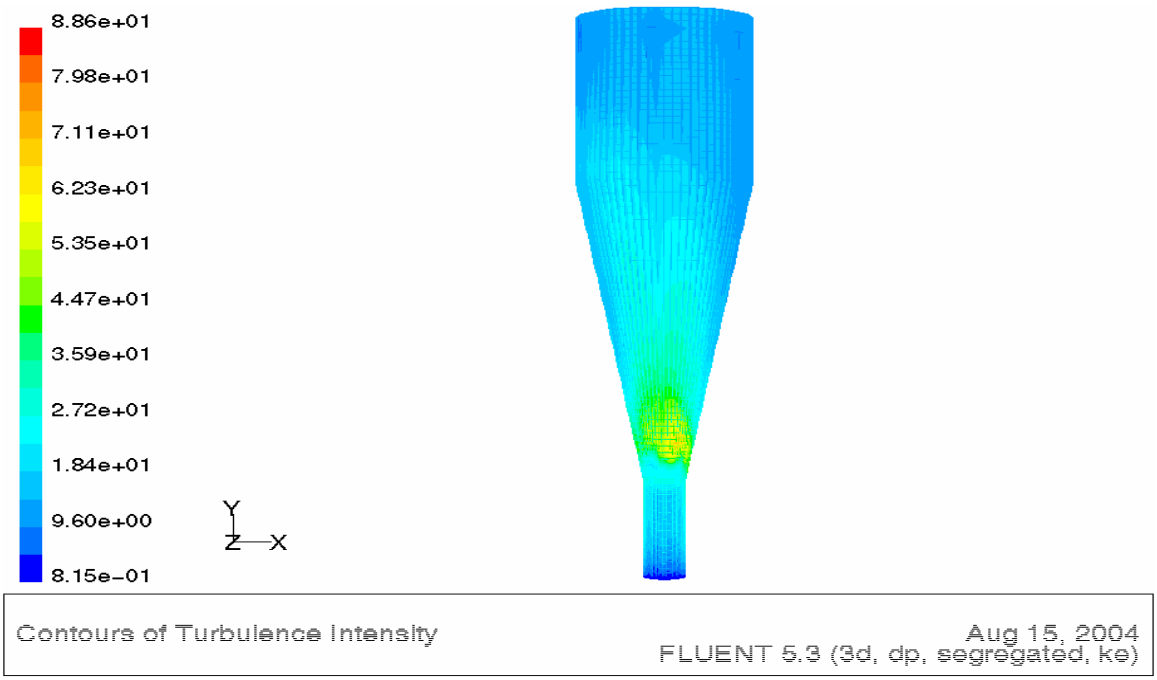


Figure F.108 Contours of Turbulent Viscosity

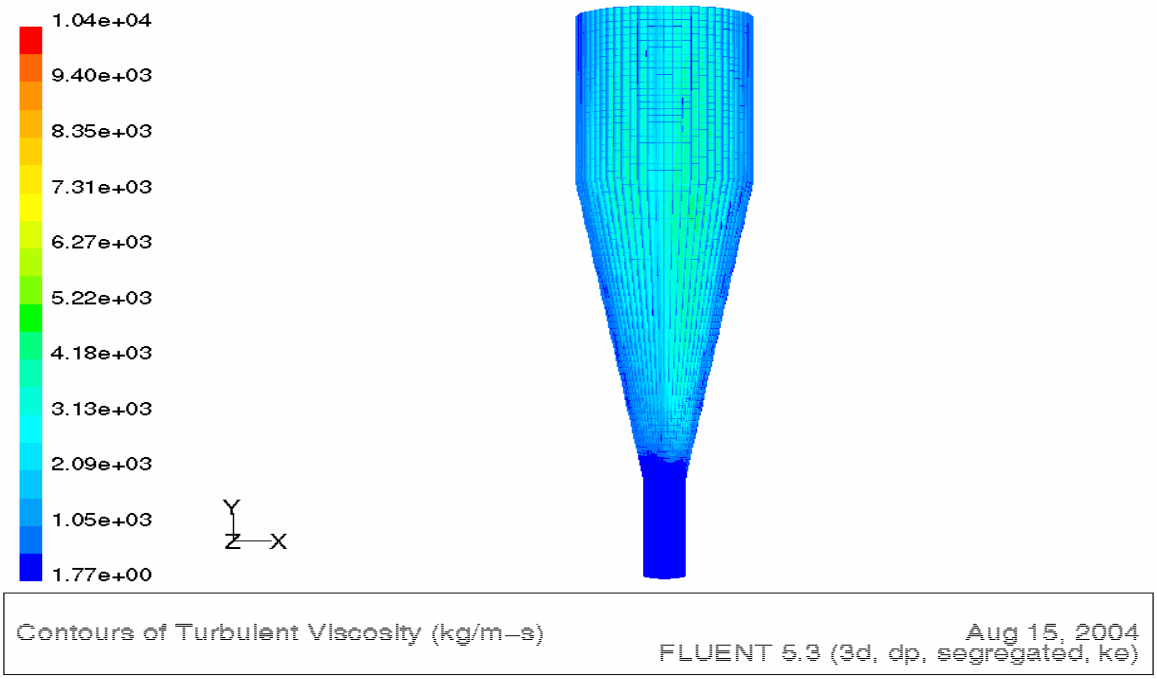

Figure F.109 Velocity Vectors by Velocity Magnitude

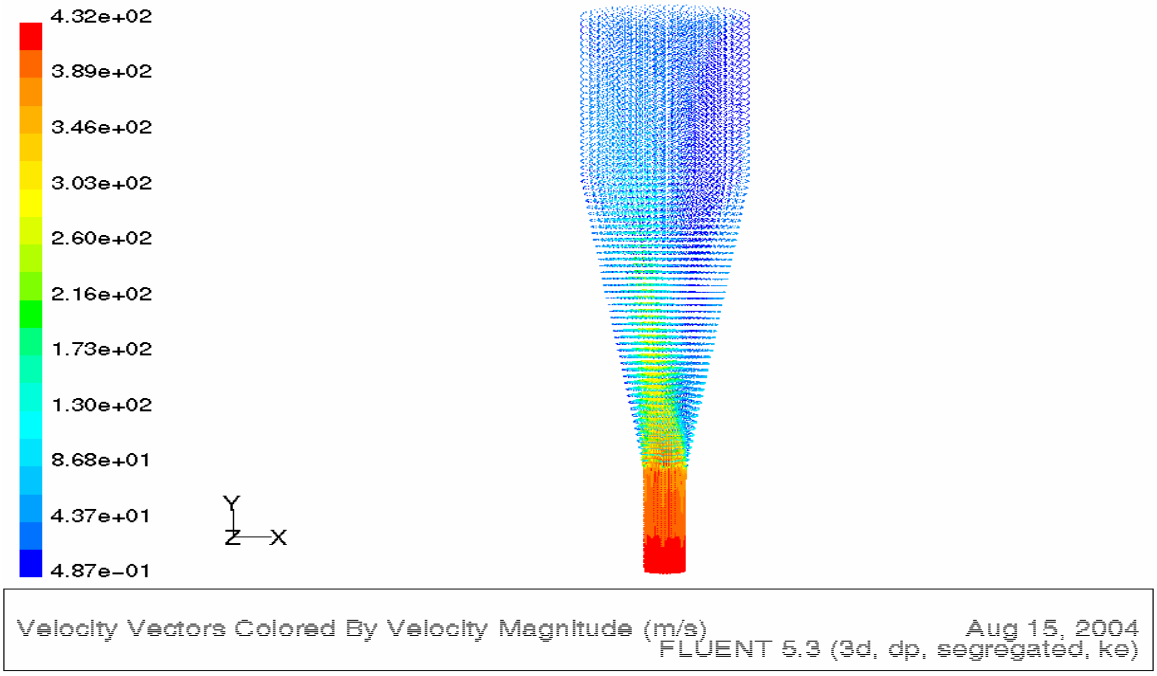


Figure F.110 Velocity Vectors by Turbulent Kinetic Energy

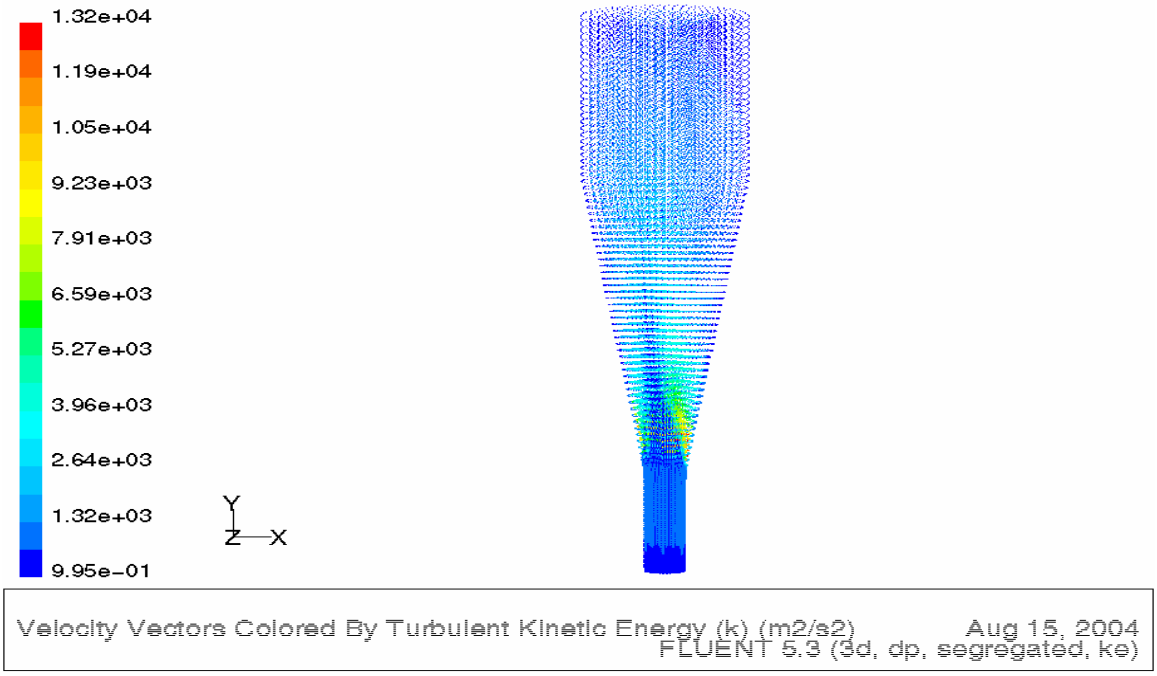

Figure F.111 Velocity Vectors by Turbulence Intensity

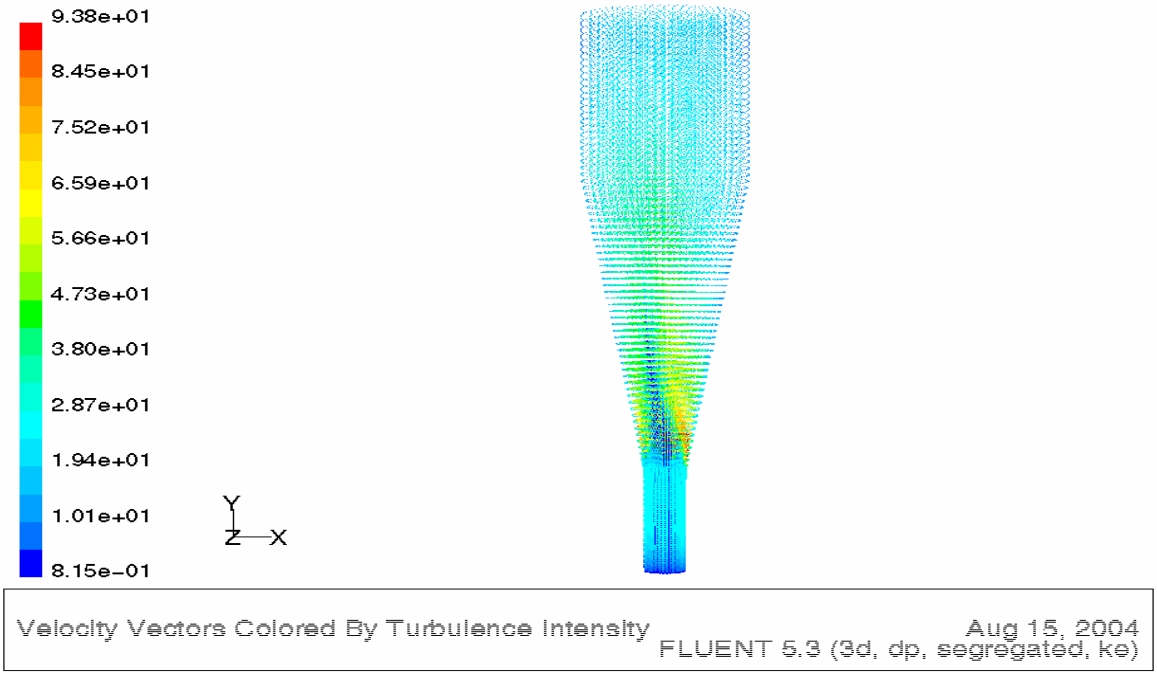


Figure F.112 Velocity Vectors by Turbulent Viscosity